APPLICATION OF NEURAL NETWORK CONTROL TO DISTILLATION

by

PRIYABRATA DUTTA, B.Tech., M.Tech.

A DISSERTATION

IN

CHEMICAL ENGINEERING

Submitted to the Graduate Faculty
of Texas Tech University in
Partial Fulfillment of
the Requirements for
the Degree of

DOCTOR OF PHILOSOPHY

Approved

ACKNOWLEDGMENTS

I wish to take this opportunity to convey my sincere thanks to my research advisor, Dr. Russell Rhinehart. His encouragement, suggestions and guidance in many matters have greatly helped me in achieving my academic goals. What I like most is his unique way of teaching, way of providing hints and making us understand the problem and the direction of solution in a lucid and transparent manner. I acknowledge him for being with me throughout my research. His friendly yet professional attitude towards students has made him a 'superb professor' in my eyes. I feel privileged to get an opportunity to work with an advisor like 'Russ'.

I am thankful to Dr. James B. Riggs for giving me admission to Texas Tech and providing me an opportunity to work in my desired field. I would also like to give my special thanks to Dr. Brian Oldham for opening a door to the Computer Science Department. His calm disposition and brief and to the point answer to all my questions have always been an extra encouragement to me. This dissertation would not have been complete without the corrections by Dr. Robert Bethea. I appreciate his time, effort and interest in the preparation of this dissertation. I also wish to convey my thanks to Dr. Hua Li for his advice, questions and comments as my committee member. Thanks are also extended to the members of the Process Control and Optimization Consortium at Texas Tech University for financial support of this work. Although, I did not get much opportunity to take many chemical engineering courses with the professors in this department, I never felt out of place at any time. For this, my sincere thanks go to Dr. Narayan, Dr. Tock, Dr. Mann, Dr. Heichelheim and Dr. Wiesner.

I acknowledge Mr. Robert Spruill for extending his helping hand during the phase of 'instrumental trouble' of the experimental setup. Tammy and Mary, the two pillars of administration, will always be remembered by me as the best two persons in the Chemical Engineering Department. Thanks are also due to Sandeep Lal, Siva, Ramesh, Mahesh, Ganesh, Abe, Bala, Scott and Joe for their friendship during my stay at Tech.

My last one and a half year stay at Lubbock would not be any better without the assistance of my lovely wife 'Adity'. Besides her moral support and encouragement, her delicious cooking kept me 'going and going' during the last phase of the long experimental runs. Finally, I would like to say that it would not be possible for me to pursue my graduate studies in the US without the support of my mom, my brothers and sisters across the ocean.

TABLE OF CONTENTS

ABSTRACT

Distillation control is challenging due to its coupled, nonlinear, nonstationary, and slow dynamic behavior. Like distillation columns, most chemical processes are usually nonlinear and nonstationary. This nonlinearity greatly limits the effectiveness of linear controllers, especially when the process is operated away from the nominal operating region. Nonlinear controllers, based on phenomenological models, can be developed. However, it is still a very difficult task in real practice, in terms of computational power, to implement these controllers on-line, because the entire model needs to be solved within each control interval. Neural networks give us an alternative approach to model a nonlinear process, and a controller based on this model can overcome the issues of on-line computational problems. Besides nonlinearity, many practical control problems possess constraints on the input, state, and output variables. The ability to handle constraints is essential for any algorithm to be implemented on real processes. Thus strategies for constraint handling within model-based controllers have become one of the more popular research topics.

In this dissertation, a constrained optimization technique for control which uses a neural network gain prediction approach has been developed and implemented on a laboratory distillation column as well as on a dynamic simulator. Here, the neural networks are trained based on a phenomenological model. Also, experimental results have been obtained to confirm the applicability of a neural network model-based controller using an inverse of a state-prediction approach that was developed and simulated earlier

by Ramchandran and Rhinehart (1994). In addition, two separate single-input-single-output (SISO) controllers using the inverse of the state-prediction approach are implemented on the feed and reflux preheaters of the column.

LIST OF TABLES

LIST OF FIGURES

NOMENCLATURE

[DMC]™	Dynamic Matrix Control (with trademark)
GMC	Generic Model Control
HRO	Heuristic Random Optimization
IDCOM	IDentification and COMmand
IMC	Internal Model Control
MAC	Model Algorithmic Control
MIMO	Multi-Input-Multi-Output
MPC	Model Predictive Control
NMPC	Nonlinear Model Predictive Control
NN	Neural Network
PMBC	Process Model-Based Control
RGA	Relative Gain Array
SISO	Single-Input-Single-Output
VLE	Vapor-Liquid Equilibria

CHAPTER I

INTRODUCTION

The increasing stress on 'quality' in process operation and economic performance is placing significant demands on existing control methodologies. One potential means by which to achieve enhanced process control performance is to adopt a model-based strategy. Algorithms which have attracted particular interest are based on the long-range prediction of process outputs commonly known as model predictive control (MPC) (Cutler et al., 1979; Mehra et al., 1985). MPC algorithms have been recognized as effective tools for handling some of the most difficult control problems in industry. MPC has been implemented successfully in several chemical industries in the US (Exxon, TX, Hokanson et al., 1989; Sun Refining, OH, Trans et al., 1989) and in other countries (Sarnia Refinery, Ontario, Canada, Cutler et al., 1987; Pembroke Cracking Company, UK, Park, 1988). MPC schemes derive some of their industrial appeal from their ability to handle input and output constraints, time delays, non-minimum phase behavior and multivariable systems.

Two popular variations of the MPC algorithms are dynamic matrix control [DMC]^{TM} (Cutler et al., 1979, 1987) and model algorithmic control [MAC] (Mehra et al., 1985). The underlying strategy of the MPC algorithms is to use a model to predict the future output trajectory of the process and then to compute a controller action to minimize the difference between the predicted trajectory and a user-specified trajectory.

Despite the commercial success enjoyed by MPC in some industries, there has not been an overwhelming acceptance in general. Whilst a number of reasons for this can be highlighted, one of the main problems is the failure to satisfy robustness, i.e., maintaining control performance without degradation at different operating regions and with changing process conditions. Two of the principal causes of poor robustness are inability to obtain a correct process model and designing a controller structure that is insensitive to process/model mismatch. The process model structure most often assumed is a linear time series. The linear approximation approach can be useful under nominal operating conditions to which the controller is tuned. However, the tuning often shows poor performance under transient upsets in which the process "moves" into another operating region where the original linear model is not a good representation of the process. Under this situation, a globally accurate model proves to be most useful. One possibility is to allow the linear model to adapt to process changes; but, in real process environments, the computational demands placed upon adaptive schemes by everyday process occurrences such as flow, composition, and thermal disturbances can be significant. Furthermore, 'jacketing' code to protect the algorithms from these upsets can be developed, but the difficulty in taking into account all likely occurrences should not be underestimated. In general, the greater the reliance which is placed upon adaptation, the higher is the likelihood of problems. If the reliance upon adaptation is to be avoided, whilst still maintaining a low level of process/model mismatch, then a model which is more capable of describing nonlinearities should be utilized.

Several workers have investigated the use of a nonlinear process representation within a model-based control strategy. Lee and Sullivan (1988) demonstrated the utility of the technique in an application to a forced-circulation single-stage evaporator which is a nonlinear interacting process. Their Generic Model Control (GMC) strategy bears strong similarities to the Nonlinear Internal Model Control (NIMC) approach exhorted by Garcia and Morari (1982) and Economou and Morari (1986). The NIMC method made use of a Newton-type algorithm to provide a tractable solution of the nonlinear model. Recently, Ganguli and Saraf (1993) applied an improved nonlinear model predictive control (NMPC) (Eaton and Rawlings, 1990) to control a distillation column start-up. Due to the need for solving an on-line optimization problem, the computational demand of the control procedure proposed by Ganguli and Saraf (1993) is very high.

Whilst nonlinear system models can provide good process performance, realistic system models are often very difficult and time consuming to derive, and they may be impossible to specify, especially when the basic mechanisms of a process are not completely understood. A desirable objective would therefore be to develop a technique which possesses generality of model structure (facilitating rapid and cheap development), which could also be capable of learning and expressing the process nonlinearities and complexities, and which computes rapidly. One such approach that has recently become popular is the use of artificial neural networks (ANN), or simply neural network (NN) (Bhat and McAvoy, 1990; Bhagat, 1990; Thibault and Grandjean, 1992; MacMurray and Himmelblau, 1993). Though this term, "neural network," originally came from the idea to mimic human neuron activity, it is exclusively used in the scientific and engineering

community to represent a mathematical model for a real system correlating certain input and output data spaces.

The most attractive property of a NN is its ability to represent any arbitrary nonlinear functional mapping between the input and output data. This mapping is achieved through a "training" process that takes place by repeatedly "showing" the input data and the corresponding target outcomes to the net. During the "training" process, an optimizer (or other techniques like back propagation) updates the values of NN weights (starting with random small initial guesses) to minimize the sum of squared (model-predicted minus data) errors. After a sufficient number of training iterations, the optimizer creates an internal approximate process model (i.e., the NN architecture with calculated weights and selected nodal functions) which can correlate the mapping between the desired output and the corresponding inputs.

It is important to note that the NN internal model is not based on any specification of the actual process mechanism; the optimizer generates this approximate model based on the data set given to it. Due to the complete dependence of the neural networks on the data sets, it is usually said that neural networks do not require any *a priori* fundamental understanding of the investigated process. In reality, the above statement is not entirely true. The control engineer has to have some process knowledge for effective implementation of NN model-based controllers. Indeed, the critical point in developing a robust NN model is selecting the most representative process input-output data sets, and this selection can only be achieved through an understanding of the underlying process phenomena.

It is often suggested that these neural network models may be easily obtained from historical plant data, thus solving the problems associated with generating nonlinear process models. But, in reality, gathering enough reliable informative sets of plant data, over a wide enough operating region, for neural network training, is a formidable task. Rather, a phenomenological model can be developed, and the data can often easily be generated using this model for neural network training. In this study, a process simulator of a distillation column is used to generate many sets of steady-state data at different operating conditions. A neural network model is generated off-line based on these steady-state data and subsequently applied to control a laboratory distillation column separating a binary mixture of methanol and water in a dual-composition control mode.

Following successful implementation of steady-state model-based control by the previous researchers at Texas Tech (Pandit, 1991; Gupta, 1994; Ramchandran, 1994), a steady-state modeling approach is taken here. While dynamic models are 'right', steady-state models are often used in process control because they are simple, compute rapidly, and are easy to implement. While both tools have a place, the use of steady-state models, coupled with experience and a general knowledge of distillation-column dynamics, is adequate for many problems and often is more efficient than using dynamic models. Steady-state modeling packages are available commercially from a number of vendors. The models are easily manipulated and provide robust solutions. To make a change to the solution conditions, only a few changes need to be made to the model input data. The input data then are used by the software to find a new solution. Generally, very little time is spent getting converged solutions, which allows us to efficiently generate the large

number of data necessary for the neural network training. One obvious limitation of steady-state modeling, though, is that it tells nothing about the dynamic response, making it difficult to apply to a dynamically ill-behaved system.

The major commercial advanced control approach, MPC, successfully handles constraints and dynamics, but cannot handle nonlinear/nonstationary behavior. There are three major problems for chemical process control: nonlinear/nonstationary behavior, constraints, and ill-behaved dynamics. Often, nonlinearity and constraints are two major problems in many chemical processes where the dynamics are well behaved. In our study, the constraints are implemented on the manipulated variables based on a computationally efficient optimization algorithm, Heuristic Random Optimization (HRO, Li and Rhinehart, 1996). This method along with the neural-network-modeling approach allowed implementation of this controller with a small control interval (1/2 minute compared to 3 minutes in PMBC and DMC) (Pandit, 1991; Gupta, 1994). In many cases, a small control interval offers better control performance. Accordingly, this controller handles the 2-problem combination of nonlinearity and constraints that is very common in control practice.

In summary, MPC handles constraints and ill-behaved dynamics but does not consider the nonlinearity of the process. NMPC requires an extensive computational approach and is still in the stage of theoretical development. Whereas, the controller in this research study based on neural network modeling approach with HRO algorithm, though does not qualify for "ill-behaved dynamics" (e.g., inverse response), takes care of the common control problems of nonlinearities and steady-state constraints.

CHAPTER II

LITERATURE SURVEY

2.1 Distillation Control

2.1.1 Importance

Distillation control has a major impact upon the refining and chemical industries due to its effect upon product uniformity, process throughput, and utility usage. Utility usage for distillation in the US amounts to 3% of the annual US energy consumption. A DOE report (Humphrey et al., 1991) estimated that improved distillation control would reduce the energy consumption for distillation by 15% resulting in an energy savings of 360 trillion BTU/yr (equivalent to $1.6 billion/yr). Moreover, the economic savings associated with improved distillation control for utility savings are, in general, small compared with the value of improved uniformity and increased throughput.

2.1.2 Objectives

Two main facets of distillation controls are

- Product quality control
- Satisfaction of constraints.

The control system for a binary distillation in most cases must maintain the concentration of one component in either the overhead or bottoms at a specified value and maintain the composition at the other end of the column as close as possible to a desired composition. This two-point composition control strategy must function satisfactorily in the face of possible disturbances in (a) feed flowrate, (b) feed

composition, (c) feed temperature, (d) steam supply pressure, (e) condenser water supply temperature, (f) ambient temperature (such as that caused by rainstorms), etc.

2.1.3 Constraints

For safe, satisfactory operation of the column, certain constraints must be observed. For example:

- The column should not flood.
- Column pressure drop should be high enough to maintain effective column operation, that is, to prevent serious weeping or dumping.
- The temperature difference in the reboiler should not exceed the critical temperature difference.
- Column feed rate should not be so high as to overload reboiler or condenser heat-transfer capacity.
- Boilup should not be so high that an increase will cause a decrease in product purity at the top of the column.
- Column pressure should not exceed either a maximum or minimum permissible value.

2.1.4 Distillation Control Literature

The process control literature on distillation column control is vast; and there are so many different types of control methods, algorithms, and control philosophies that it is unrealistic to acknowledge all of them here. This section will limit the discussion strictly to only those references related with this work.

Distillation column control is primarily a multivariable problem. A multi-input-multi-output (MIMO) control can be decomposed into several single-input-single-output (SISO) loops, and in the case of a binary distillation column, four variables, two products, reflux drum level, and reboiler level are controlled using reflux flow, vapor boilup and two product flows. The decomposition into four SISO loops can be made in many ways, giving rise to different control structures.

Morari et al. (1987) provide guidelines for control configuration selection for distillation columns. The paper suggested that the ratio configurations (e.g., reflux/distillate product and boilup/bottom product, i.e., L/D and V/B, respectively) provide improved flow disturbance rejection. The L/D and V/B configuration is recommended (also recommended by Shinskey, 1984) except for very high-purity columns or columns using low reflux (i.e., large relative volatility) which can be sensitive to input uncertainty and flow disturbances.

Morari et al. (1988) present a realistic study of the L-V control of a high-purity distillation column. A single linear controller is developed which gives satisfactory control of the high purity column at widely different operating conditions. Logarithmic transformations of compositions are used to counteract the nonlinearity of the process. Using the composition in the overhead vapor as a controlled output makes the system less sensitive to variations in the condenser holdup. A single diagonal PI controller is compared and is found to be robust with respect to model/plant mismatch. The diagonal PI controller gives a sluggish return to steady-state and the response is improved using a μ-optimal controller.

Haggblom et al. (1990) describe a configuration (disturbance rejection and decoupling configuration, DRD), of a two-point distillation control structure which, in steady-state, simultaneously rejects disturbances in the feed composition and in the feed flowrate and results in implicit decoupling between the two product loops. This structure is tested on a model of a 15-plate ethanol-water pilot-plant distillation column. Experimental results are presented for a 6 wt% ethanol feed-composition disturbance.

While it is acknowledged here that the proper selection of manipulated variable and control variable pairing can make a difference in terms of lower decoupling (i.e., lower relative gain array) of the system, often the L-V configuration (also known as energy-balance configuration) is adopted for its excellent disturbance rejection performance. Throughout our study, the L-V configuration is used for the top and bottom composition control along with the fully coupled multivariable controller.

Another significant difference between Morari and Haggblom's approach and our approach is the selection of the controllers. A complete nonlinear controller is used in our study in contrast to their linear or linearized controllers. In a more recent study, Haggblom (1994) used a nonlinear multivariable control on a distillation column using bilinear modeling approach. A nonlinear model is constructed by letting the parameters of a model (which has the same structure as the linear one) depend linearly on the operating point. This results in a simple bilinear process model, which is fitted to the linear models at the respective operating points. While this method may accommodate some of the nonlinearities of the system, a complete nonlinear modeling approach is obviously the best choice.

Another important aspect of distillation-column control is to take care of the system dynamics. Luyben et al. (1975) has studied the dynamic behavior of high purity (10 ppm) distillation columns via digital simulation. The effects of product purity, relative volatility, composition analyzer sampling time, and magnitude of disturbance have been explored. Results show that systems with low relative volatilities (α = 2) respond slowly enough so that good control can be achieved at very high purity levels, with 5-minute analyzer deadtimes. However, systems with high relative volatility (α = 4) respond so quickly that large deviations in product purities occur before the analyzer can respond. Effective control is obtained by using a composition/temperature cascade system. An intermediate tray temperature is controlled to achieve fast dynamic response to disturbances, and the setpoint of the temperature controller is reset from a product composition controller. The secondary temperature gives better control for feed-composition disturbances when it is proportional only and loosely tuned. The opposite is true for feed rate disturbances.

In this study, the composition is inferred from the tray temperatures and as a result, large delay time of a composition analyzer (e.g., ~5 minutes for a gas chromatograph) is avoided. However, the sensor measurement, analyzer delay (for thermocouples), instrument dynamics (pump, valve), heat transfer dynamics (boiler, heaters) and transportation lag (feed, reflux) create significant pseudo-deadtime in the process. It has been observed that, in our experimental system, the open-loop response for the bottom composition with respect to the boilup change is about 3 hours; whereas, the response time for the top composition with respect to the reflux change is about 1 hour.

Even with this kind of disparity in the system dynamics for the top and the bottom loop of the distillation column, a first-order dynamic assumption on the both control loops performs well and shows no need for any extra dynamic compensation.

There are two relevant publications that deal with methanol/water distillation control and use an experimental setup similar to the one used in this thesis. Wood and Berry (1973) studied the effect of feed-flowrate disturbances on the terminal composition control of an 8-tray pilot-scale binary distillation column operated under the control of an IBM 1800 digital computer. They found that conventional two-point control, whereby the overhead composition is controlled by reflux flowrate and the bottom composition by means of steam rate, was unsatisfactory. Two control systems, namely a noninteracting control system and a ratio control system, were evaluated. The results showed that a very significant improvement in the control of both compositions was achieved by using a noninteracting control or the ratio control scheme compared to the behavior that resulted using conventional two point feedback control. Sanchez et al. (1984) used the same experimental system (as used by Wood and Berry, 1973) to demonstrate their multivariable adaptive predictive control strategy (APCS).

In this study, the fully coupled MIMO controller is able to take care of thecoupling of the system, and the special measures like selecting least interacting configurations is not taken into account.

2.2 Literature on Linear and Nonlinear Control

2.2.1 Linear Model-Based Control

Linear Control theory has been explored extensively by the researchers in the last few decades. Whereas, nonlinear control theory is a relatively new subject. Even nowadays, one finds an effective use of linear controllers in many process control studies. Applications on various advanced types of linear controller are still in the testing stage, and a few of these are discussed below.

Linear model-based control (MBC) methods are based upon linear, empirical process models. Dynamic Matrix Control, DMC (Cutler, 1979), Internal Model Control, IMC (Garcia and Morari, 1982), and IDCOM (Mehra, 1978) are prime examples of linear MBC methods. The model predictive control (MPC) algorithms represented by Dynamic Matrix Control (DMC) (Cutler and Ramaker, 1980) and Model Algorithm Control (MAC) (Rouhani and Mehra, 1982) were based on a discrete convolution model of the process and are basically linear model-based algorithms. Both linear programming (Chang and Seborg, 1983) and quadratic programming (Little and Edgar, 1986) have been applied in MPC for processes with linear constraints. DMC has been used in a number of industrial applications. DMC uses a step response linear model for each input/output pair. DMC is a time horizon controller that uses a hypothetical disturbance level at each step to remove any process/model mismatch and uses the calculated disturbance level for the prediction horizon. The user tunes this controller by selecting the prediction horizon, the control horizon, and the weighting factors for the input moves.

Internal Model Control (IMC) (Garcia and Morari, 1982,1985), as a control framework, is also linear and model-based. Linear programming (Brosilow et al., 1984) and quadratic programming (Richer 1985) were also applied for constraint treatment in a similar manner to that applied for the MPC algorithms. Economou et al. (1986) extended IMC to nonlinear lumped parameter systems by an operator approach. IMC typically uses first order plus deadtime models in a state-space configuration. The controller calculates the control action necessary to return the process to the reference trajectory in one control interval. A filter is applied to the feedback signal in order to improve robustness. The internal model control structure feeds back the process/model mismatch to make adjustments to the setpoint in order to remove offset.

There are two major commercial control packages marketed in the United States known as [DMC]™ (Dynamic Matrix Control) and [IDCOM]™ (IDentification and COMmand). Though these two control strategies can be broadly classified as Model Predictive Control (MPC), significant differences exist between them in terms of control implementation issues. [IDCOM]™ uses an impulse-response model instead of a step-response model (used by [DMC]™). [IDCOM]™ uses a weighted time-series model of the process which is basically a convolution model of the process. This control algorithm assumes that the prediction horizon is equal to the control horizon. [IDCOM]™ uses an impulse-response model instead of a step-response model ([DMC]™). [IDCOM]™ uses a controlled variable (CV) damping approach whereas [DMC]™ uses a manipulated variable (MV) damping approach for tuning the controller. [IDCOM]™ handles the

constraints with a quadratic-programming approach whereas [DMC]™ uses a linear programming approach.

All of the above mentioned controllers can take care of system dynamics and often linear constraints, but cannot accommodate nonlinearity. In this dissertation, a NN-based complete nonlinear controller is developed, and constrained handling capabilities are also demonstrated.

2.2.2 Nonlinear Model-Based Control

Nonlinear control approaches use nonlinear models in order to overcome the limitations of linear fixed-gain controllers (i.e., PI, IMC, MPC, etc.). A nonlinear controller, based upon a model that represents the nonlinearity of the process, has obvious advantages. Moreover, if the nonlinear models used by the controllers are sufficiently detailed and process measurements are available, the nonlinear controller can be able to adapt to gain changes that result from different process operating conditions. The major disadvantages of any nonlinear controller is that an accurate nonlinear model is required, which typically takes a significant amount of highly skilled engineering effort to build. There are a variety of nonlinear controllers that are available with a range of complexity and numerical requirements.

Three of the most significant of the nonlinear controllers available are Generic Model Control (GMC, Lee and Sullivan, 1988), Process Model-Based Control (PMBC, Rhinehart and Riggs, 1988) and nonlinear MPC (Biegler and Rawlings, 1991). GMC uses a single-step-ahead control law, and as a result, is the simplest form of nonlinear control to

implement. GMC has been applied industrially for pH control, for a batch reactor control and for distillation control (Lee, 1993). PMBC is similar to GMC. It uses a simple control objective but adjusts a model parameter for feedback. PMBC has been successfully applied on a commercial basis in Phillips 66 Company at Borger, Texas (Riggs et al., 1991). Pandit experimentally demonstrated dual-composition control on the same laboratory setup as studied in this research using nonlinear PMBC and GMC law (Pandit, 1991). Pandit's nonlinear PMBC model was a nonideal, nonlinear description of the process derived from the fundamental tray-to-tray mass and energy balances and thermodynamic equilibrium considerations. Nonlinear MPC uses dynamic nonlinear models to predict the behavior of the controlled variables into the future, thus selecting the control action that meets a preset performance criteria. Since a high dimensionally constrained nonlinear optimization problem must be solved at each control interval, nonlinear MPC is computationally expensive and computationally more complex than GMC. Nonlinear MPC has been applied for batch reactor control (Biegler, 1991).

Neural Networks (NN) are finding tremendous success in their use as the nonlinear model in nonlinear controllers. NN models offer a significant computational advantage over phenomenological nonlinear models since the NN models are in a highly efficient explicit form. The phenomenological models are typically in a form that is highly implicit and requires numerous iterative loops.

There are also hybrid approaches as well. Neural network models have been used to modify linear MPC model gains on-line in order to improve linear MPC performance

for highly nonlinear system processes (Willis et al., 1991; Turner et al., 1995; Kwaku et al., 1995).

2.3 Neural Network Control

2.3.1 Importance of Neural Networks in Control

Nonlinear models used in nonlinear multi-variable control strategies generally tend to become rigorous and computationally intensive as the process behavior becomes complex. While control success has been demonstrated using rigorous process model-based controllers (PMBC) (Riggs et al., 1993; Pandit and Rhinehart, 1992; Cott et al., 1985), an on-line implementation of this strategy, at times, requires significant computation time.

Neural networks offer an alternate approach to modeling process behavior. They are capable of handling complex and nonlinear problems. And, at the same time, they can compute the process information rapidly. Neural networks are made to "learn" by extracting pre-existing patterns from the data sets that describe the relationship between inputs and outputs of any given process. Thus, NN model can even be formed out of data sets generated from a phenomenological model. The network, once trained on these data sets, will be able to mimic the general behavior of the phenomenological model. In other cases, where detailed process models are not available or are difficult to develop, a neural network model can be generated directly from the raw plant data. However, caution should be taken in selecting reliable data sets to capture the true process behavior. A small

number of available data sets and conflicting data sets are often two major problems in forming a neural network in this way.

2.3.2 Literature on Neural Network Control

Neural networks have been applied successfully to a variety of problems, such as

- process fault diagnosis (Venkatasubramanian et al., 1990; Venkatasubramanian and Chan, 1989),
- modeling of semiconductor manufacturing processes (Himmel and May, 1993; Reitman and Lory, 1993),
- system identification (MacMurray and Himmelblau, 1993; Potman and Seborg, 1992),
- pattern recognition and adaptive control (Hinde and Cooper, 1993; Cooper et al., 1992 a, b),
- process modeling and control (You and Nikolaou, 1993; Nahas et al., 1992; Bhat and McAvoy, 1990; Narendra and Parthesarathy, 1990; Joshi, 1995), and
- statistical time series modeling (Poli and Jones, 1994; Weigand et al.,1990).

In the area of distillation control, neural networks have found application in identification and control of a packed distillation column (MacMurray and Himmelblau, 1993) where a neural network model was used as the model in model predictive control. Neural Network control of distillation in a multi-variable model predictive control framework also include studies on dynamic simulations (Willis et al., 1992). Neural network has also been used in an inverse dynamic model approach (Savkovic et al., 1996).

The papers by Thibault and Grandjean (1992) and Astrom and McAvoy (1992) provide in-depth reviews on neural network applications in chemical process control.

2.3.3 An Introduction to Neural Networks

The structure of neural networks forms the basis for information storage and governs the net's learning process. Neural networks are comprised of interconnected simulated neurons (shown in Figure 2.1). A neuron is an entity capable of receiving and sending signals, and it is simulated by means of software algorithms on a computer. Each simulated neuron (a) receives signals from other neurons, (b) sums these signals, (c) transforms this sum, usually by means of a sigmoidal function, which is a monotonic, continuously differentiable, bounded function [e.g., $f(x) = \tanh(x)$ {bipolar, -1<f(x)<1}, $f(x) = \frac{1}{(1+e^{-x})}$ {unipolar, 0<f(x)<1}], and (d) sends the result to other neurons. A weight that modifies the signal being communicated is associated with each of the connections between neurons. The 'information content" of the net is embodied in the set of all of these weights, which together with the net structure, constitute the model generated by the net. A complete feedforward neural network neuron architecture is shown in Figure 2.2.

2.3.4 Training of Neural Networks

Training is a systematic adjustment of weights to get a chosen neural network to predict a desired output data set (known as a "training set"). Training of a neural network

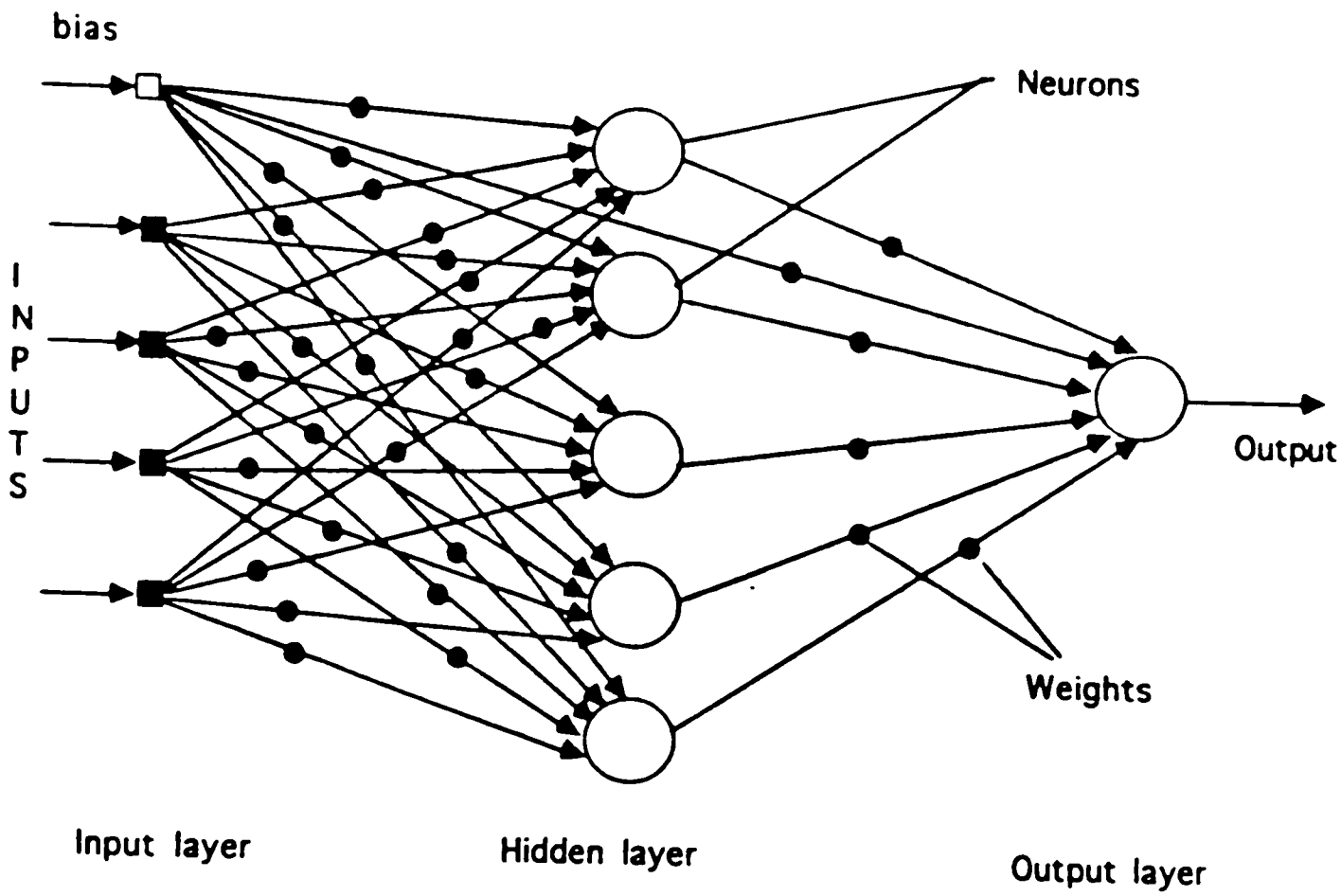

Figure 2.1. Feedforward neural network architecture (4-5-1).

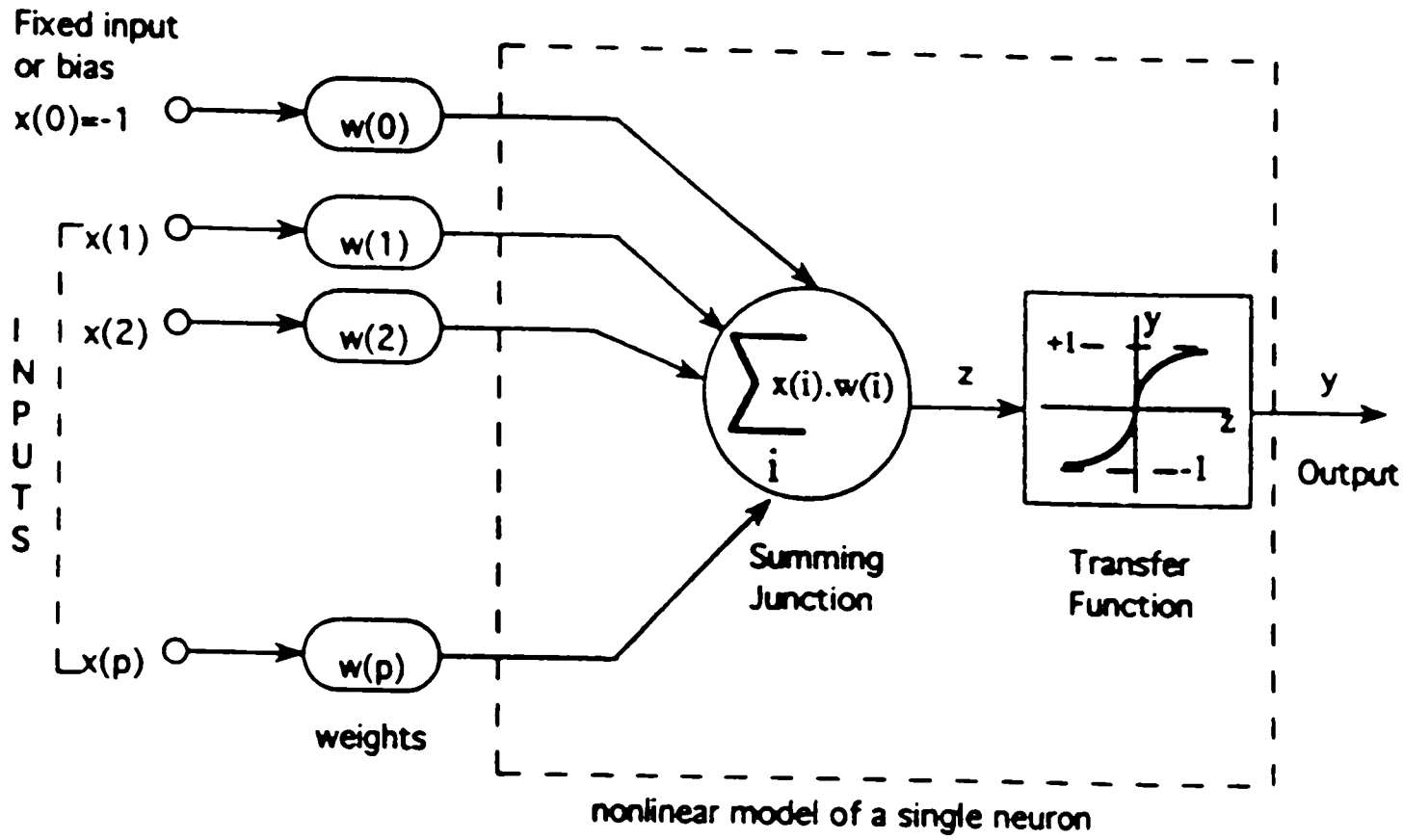

Figure 2.2. Signal Processing within a neuron.

can be either *supervised* or *unsupervised*. In supervised training, the connection weights for each processing element are initially given some random values. As soon as the training starts, the training algorithm (backpropagation/optimizer) begins comparing its predicted outputs to the desired outputs, and any error is used to correct the network. The training method corrects the network by adjusting the set of connection weights of each processing element. The training or the adjustment of weights continues until the algorithm meets the convergence criteria. During the training process, the complete input-output data set is read by the training algorithm at the end of each update of the weights (commonly known as an "epoch" for each exposure of the complete data set). The error between the actual data and the NN model-predicted data continues to get reduced during the training process. A limit on this error may be used as a convergence criterion. Normally, the error on a separate set of data (known as a "validation set") is also calculated along with the error in the training set. After a certain number of iterations, the validation-set error often starts increasing, while the training error may still continue to get smaller and smaller. The training is stopped at this point to avoid any "overfitting" of the network to the training set and to protect network's "generalization" property. Here, "overfitting" implies an equivalent statistical curve-ftting with too many free parameters. "Generalization" means the ability to interpolate and extrapolate by the neural networks in a sensible way. But what is meant by sensible generalization is often not clear. This incremental process of training or updating of weights can sometimes take a considerable amount of time to obtain a resonable fit between the NN model output and the desired output.

2.3.4.1 Backpropagation

One of the conventional methods of training is the backpropagation (or back prop) algorithm. Back prop gets its name from the fact that, during training, the output error is propagated backward to the connections in the previous layers, where it is used to update the connection weights in order to achieve a desired output. Backpropagation uses the Generalized Delta Learning Rule (Rumelhart et al., 1986; Werbos, 1974), and has been used extensively by researchers for neural network training. Classical backpropagation is a gradient approach to optimization which is executed iteratively with implicit bounds on the distance moved in the search direction in the weight space fixed via the *learning rate*, which is equivalent to a step size. The backpropagation technique adjusts each variable (weight) individually according to the step-size along the path of the steepest descent to minimize the objective function. The commonly used optimization function is the "traditional" sum-of-squared-differences of errors defined as:

$$E = \frac{1}{2}\sum_{p=i}^{P} E_p = \frac{1}{2}\sum_{p=1}^{P}\sum_{i=1}^{n_{out}}(D_{pi} - Y_{pi})^2 \tag{2.1}$$

where E is the total sum of squared errors for all P patterns and E_p is the sum of squared errors for the 'p'th pattern. The weight update rule is given by

$$\Delta W_k = -\eta\delta_k \tag{2.2}$$

where W is the weights matrix, η is the learning rate, and δ_k is the gradient of the error function. δ_k is defined as

$$\delta_k = \nabla E_p(W_k). \tag{2.3}$$

This procedure of updating the weights using only the gradient information often requires a very small step-size to attain stability. As a result, the backpropagation method has to be repeated many times to achieve the minimum value of the objective function. The step-size affects the rate at which convergence on a local minimum is achieved. A smaller step-size will help insure convergence, but will greatly increase the number of iterations needed for convergence, which increases the CPU time required for training. A number of trials should be made with different choices of initial values to increase the probability of reaching a global minimum. The choice of initial values for the weights often also affects the convergence pattern. Backpropagation can be very inefficient because of this choice of initial weights (Kramer and Leonard, 1990) and slow convergence.

Despite modifications to the classical backpropagation, such as the addition of a *momentum term* (Rumelhart et al., 1986) to accelerate convergence, it can still be slow and may get stuck in a local minimum. Changing the learning rate and momentum term may allow one to bypass local minima, but convergence to a global minimum can never be guaranteed. An *ad-hoc* procedure used by several researchers to achieve global convergence is to train the neural network with different sets of initial weights (usually initialized randomly to small values). Thus it may require several iterations or initializations before a global minimum is reached. The large amount of training times involved (in terms of CPU time) may be impractical.

The current trend is to use optimization tools and strategies that exhibit distinctly superior performance (Peel et al., 1992; Barnard, 1992; Battiti, 1992; Hsiung et al., 1991)

and, furthermore, are easier to apply because they do not require the choice of critical parameters (such as learning rate and momentum rate) by the user.

2.3.4.2 Optimization Approach

Several researchers (Kramer and Leonard, 1990; Kollias and Anastassious, 1988; Kung and Hwang, 1988; Ricotti et al., 1988; Parker, 1987; Watrous, 1987; White, 1987) have shown that optimization algorithms employing modern unconstrained optimization techniques based on the secant or conjugate gradient methods either alone or together with the backpropagation concept are much better (in terms of faster convergence and lower training time) than classical backpropagation itself.

One of the difficulties in using the steepest descent method is that a one-dimensional minimization in some arbitrary direction "a" followed by a minimization in another direction "b" does not imply that the function is minimized on the subspace generated by "a" and "b". Minimization along direction "b" may in general spoil a previous minimization along direction "a". Therefore, the one-dimensional minimization in general has to be repeated a number of times larger than the number of variables. On the contrary, if the directions were non-interfering and linearly independent, at the end of N steps the process would converge to the minimum of the quadratic function. The concept of non-interfering (conjugate) directions is the basis of the conjugate gradient method for minimization. A major difficulty with the conjugate gradient form is that, for a general function, the obtained directions are not necessarily the descent directions, and numerical instability can result. The use of a momentum term to avoid oscillations in the

backpropagation method can be considered as an approximated form of conjugate gradient. In both cases, the gradient direction is modified with a term that takes the previous direction into account, the importance being that the parameter in the conjugate gradient technique is automatically defined by the algorithm, while the momentum rate has to be "guessed" by the user. More details on the conjugate gradient method are found elsewhere (Press et al., 1992; Battiti, 1992; Leonard and Kramer, 1990a).

An alternative to the conjugate gradient method is Newton method, which is a local method using second-order information. It is important to stress that its practical applicability to multi-layered neural networks is hampered by the fact that it requires calculation of the Hessian matrix, a complex and expensive task. If the Hessian matrix is positive definite (i.e., all eigenvalues > 0) and the quadratic model is correct, *one* iteration is sufficient to reach the minimum. Assuming that the Hessian can be obtained in reasonable computing times, the main practical difficulties in applying the "pure" Newton's method arise when the Hessian is not positive definite, or when it is singular and ill-conditioned. Battiti (1992) has reviewed in detail Newton's method and some modifications to deal with global convergence, indefinite Hessian, and iterative approximations for Hessian itself. Modifications of Newton's method have been used by Poli and Jones (1994) and White (1989) for training feedforward neural networks.

When the Hessian is not available analytically, secant methods are widely used techniques for approximating the Hessian in an iterative way using information only about the gradient. The secant methods are also known as *quasi-Newton* methods. The suggested strategy is to update a previously available approximation instead of

determining a new approximation. The Broyden-Fletcher-Goldfarb-Shanno (BFGS) method (Broyden et al., 1973) uses a positive definite secant update which has proven to be successful in a number of studies. For an 'N' dimensional problem, the complexity for BFGS is of the order 'N^2' (i.e., O(N^2)), which is clearly a problem in terms of computational storage for very large 'N'. However, the method can still remain very competitive if the number of examples is very large, so that the computation of the error function dominates. Secant methods for learning in multi-layer neural networks have been used by Watrous (1987). Modifications of the secant method were used by Hsiung et al. (1991) and Parker (1987).

One drawback of the BFGS method is that it requires storage for a matrix of size NxN and a number of calculations of order O(N^2). A secant approximation with O(N) computing that uses second-order information in methods can be used and is known as the *one-step secant* (OSS) method (Battiti, 1989). But, if the error function that is to be minimized is the one described in Equation 2.1, learning a set of examples is reduced to solving a nonlinear least-squares problem for which special methods have been devised.

The Levenberg-Marquardt method (also known as the Marquardt method, Marquardt, 1963) is a popular technique to solve the nonlinear least-squares problem. The Marquardt method searches for the minimum by starting out with a gradient search method, then switches smoothly to a Newton method as the minimum is approached. Thus, the advantages of both techniques are incorporated into one method, which has the stability of the gradient procedure with respect to poor starting values, and at the same time, possesses the speed of convergence of the Newton method when close to the final

solution. This combination of the gradient search and the Netwon Method increases the computational efficiency and reduces the CPU time necessary for training the network. The update rule for the weights is given as

$$\Delta W = (J^T J + \mu I)^{-1} J^T e \tag{2.4}$$

where J is the Jacobian matrix of derivatives of each weight, μ is a scalar, and e is an error vector. If the scalar μ is very large, the above expression approximates gradient descent, while if it is small, the above expression reduces to the Gauss-Newton method. The algorithm for the Marquardt method is presented in detail in the original paper by Marquardt (1963) and text by Press et al. (1992). The Marquardt method has also been used by other researchers for neural network training (Ramchandran and Rhinehart, 1995; Turner et al., 1995) and reported to be very effective for feed forward neural network training.

In this research, the Marquardt method is used for training of all feedforward neural networks. The entire set of weights are adjusted at once instead of adjusting them sequentially from the output layer to the input layer. The weight adjustment is done at the end of each epoch (one exposure of the entire training set to the network), and the sum of squares of all errors for all patterns is used as the objective function for the optimization problem.

2.4 Self-Tuning Filter

Most chemical and measurement processes are influenced by many small, random, independent environmental disturbances. Accordingly, measured process values respond

with an inherent variability, even when the manipulated process inputs are unchanged. These process variations may indeed be classical electronic instrument noise; but they can also be successive, small, short-lived, but real transients in the process output commonly due to flow turbulences or imperfect mixing. Even without control action, such transients will decay and no control action is warranted. In fact, if a controller takes action on such transients, it will unnecessarily induce process upsets and will increase the process variability. One of the perspectives fundamental to statistical process control (SPC) is to accept inherent process variability and to make changes only when there is a high (about 99.7%) statistical confidence that a change is justified. In automatic control, the value of the manipulated variable is calculated from the process variable output. As a result, the controller undesirably responds to normal process variations, i.e., process noise. Therefore, in almost all practical applications, a filter is used on the process variable to reduce this noise effect. The most common filter is a first-order filter which assumes the following form

$$X_{f_i} = (1-\lambda)X_{f_{i-1}} + \lambda X_i \tag{2.5}$$

where X_i is the current measurement and $X_{f_{i-1}}$ is the filtered value at the previous measurement. The filter factor is λ, which can be correlated with the filter time constant and the sampling interval as follows

$$\lambda = e^{-T/\tau_f} \tag{2.6}$$

where T= sampling interval and τ_f = filter time constant.

Such filters average data to reduce the effect of noise, but they also cause an undesirable lag in the filtered variable. Control degrades when automatic controllers

respond to a lagged measurement. An online SPC-based cumulative sum filter (CUSUM) has been developed by Rhinehart (1992) which eliminates unnecessary manipulated variable action, yet remains responsive to 'real' process changes. This method is primarily based on the calculation of the variance of the noise. The greater the amplitude of the noise, the greater the filtering that must be done to reduce the noise effect on the filtered variable. When the process noise level changes, the filter time constant should also be adjusted accordingly. In recent work by Cao and Rhinehart (1996), a new method of filtering noise, known as self-tuning filter, has been developed, which automatically adjusts the filter time constant based on the noise level. In this method, the user defines an error band and the filtered value remains within this band with respect to the mean value of the process measurements with a 95% confidence limit.

A simple FORTRAN code can be written as follows

```
R2F = 0.9*R2F + 0.1 *(X-XOLD)**2

XOLD = X

AMBDA = 1.0/(0.5+1.2411*R2F/E/E)

IF(AMBDA.GT.1.0) THEN AMBDA=1.0

XF=AMBDA*X+(1.0-AMBDA)*XF
```

The user initializes R2F with E*E. The limit of AMBDA=1.0 is necessary. If the sensor fails or if the measurement noise drops to zero, then AMBDA would increase to a high value (~2) and would amplify the noise in its attempt to keep 5% of the data outside of the E band. An upper bound of AMBDA to 1.0 avoids this amplification problem. The

detailed mathematical analysis and the application benefits of this self tuning filter can be found in the work of Cao and Rhinehart (1996).

CHAPTER III

EXPERIMENTAL SETUP AND SIMULATOR

The experimental work presented in this dissertation is performed on a fractional distillation unit in the Department of Chemical Engineering at Texas Tech University. Since the experimental work takes considerable amount of time, uses expensive equipment and consumes methanol as the source of feed, all control performances are studied first on a dynamic simulator representing the experimental system.

3.1 Experimental Setup

3.1.1 Distillation Unit

The distillation unit is a Technovate Model 9079 fractional distillation system designed for a variety of experimental investigations to evaluate heat-transfer and mass-transfer processes as they pertain to fractional-distillation column performance. Figure 3.1 shows the schematic flow diagram of the setup.

The plate column consists of 6 sieve-plate sections, each assembled from a 0.13-m (5-in.)-long, 0.08-m (3-in.)-I.D. glass pipe section. Each section contains process fittings for feed and liquid/vapor sampling and weir downcomer adjustment. When assembled, the column is approximately 0.76 m (30 in.) in height and is bolted to the reboiler at its bottom and to the vapor feed line at its upper end by means of a bell reducing-coupling section and a flexible Teflon expansion joint, respectively. The sieve plates are 0.0031-m

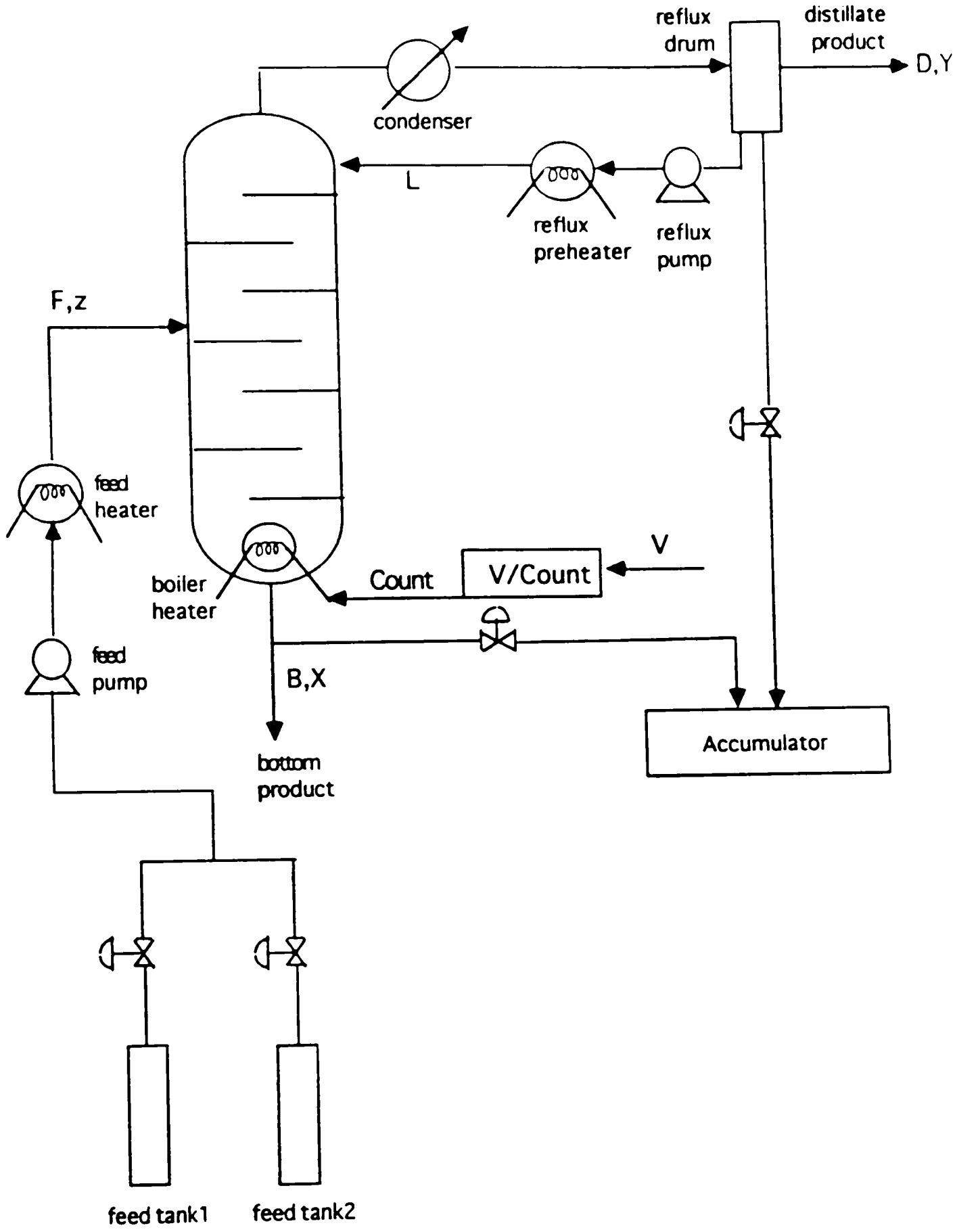

Figure 3.1. Schematic flow diagram of the setup.

(1/8-in.)-thick with 36, 0.0038 m (0.15 in.) holes each and have weirs and downcomers adjusted for 0.0063 m (1/4 in.) liquid holdup on each tray.

The still reboiler is a cylindrical welded, stainless-steel tank with a capacity of approximately 0.019 m^3 (5 gallons). The capacity of the reboiler is reduced to about 0.01 m^3 (10 liters) by filling it with about 700, 0.019-m (3/4-in.) diameter glass marbles. This reduction in liquid volume has made the reboiler respond faster to process changes. The main heating element in the reboiler is a stainless-steel sheathed-bayonet-type cartridge heating element with explosion-proof electrical fittings. This element has a continuously variable control and is rated at 2.5 kW.

A precise liquid-level control is obtained by means of a float-type control element that actuates a solenoid-operated valve which transfers excess liquid from the still boiler to the accumulator. To damp out the on-off effect of the solenoid valve on the continuity of the bottom product flow rate, an online damping element (a first-order lag) in the form of a surge cylinder is installed.

The overhead condenser is a Pyrex and stainless-steel double-pipe heat exchanger which contains the equivalent of 0.14 m^2 (1.5 sq. ft.) of spiral heat exchanger surface. The spiral condensing tube is 3.34 m (132 in.) long and is coiled to a length of 0.46 m (18 in.). The tube is 0.016-m (5/8-in.)-O.D. and has a 0.00048-m (0.019-in.) wall. The distillate receiver is a 0.08-m (3-in.) O.D. by 0.30-m (12-in.)-long Pyrex glass tube, which is flanged at the top and bottom. The top flange also contains a spring-loaded pressure relief valve as an additional safety feature. In our experiment, the column is operated by

keeping the reflux drum open to atmosphere (an unsafe condition, as every time the unit cools off, air is sucked back into the column).

The feed and reflux supply lines have cartridge-type immersion preheaters rated at 0.2 kW each. The heater is interfaced with an IBM-compatible 486 PC via a Keithley Metrabyte Data Acquisition and Control System which uses the 4-20 mA current sent by the computer to change the voltage (0 to 240 volt a.c.) across the heater. The temperature is monitored by K type thermocouples.

3.1.2 Instrumentation

The Technovate unit is installed with instrumentation and a data acquisition and control system (shown in Figure 3.2), but the original manual controls are still in place and can be used as a backup system.

The column is equipped with 12 thermocouples connected at strategic points throughout the system. These include one in the still boiler, six in the column (one for each tray), two on the condenser inlet and outlet coolant lines, one for the distillate line, and one for each preheater (feed and reflux). These thermocouples are of the chromel-alumel type, and each is epoxy-sealed within a stainless steel tube.

There are seven differential pressure (DP) cells used to measure the top and bottoms product flowrates, water flowrate through the overhead condenser, liquid level in the overhead accumulator, sixth tray pressure, reboiler pressure, and pressure in the overhead accumulator.

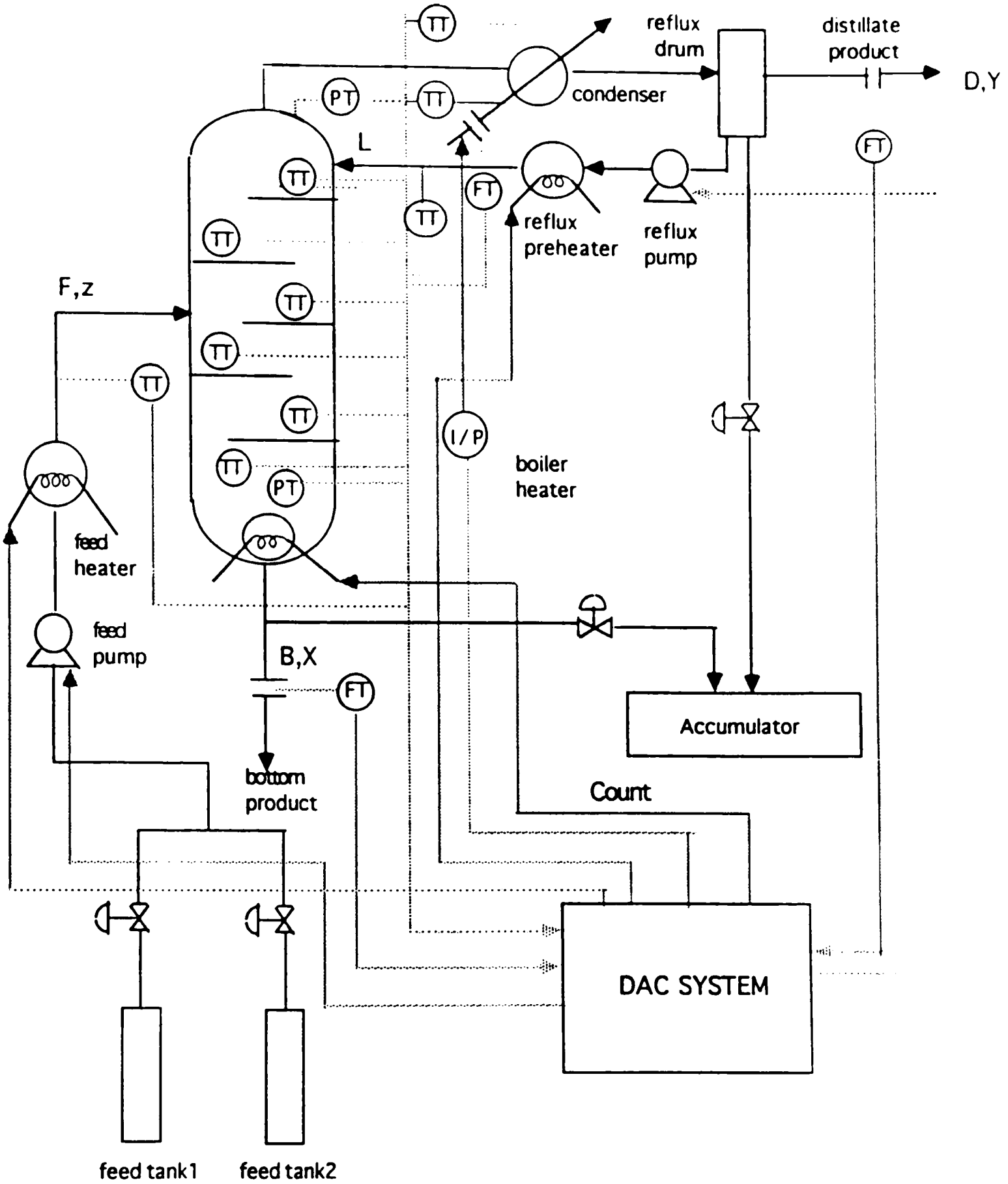

Figure 3.2. Instrumentation and KDAC system.

The feed and reflux are pumped to the column by Durcometer Diatube II pumps driven by adjustable-frequency motor drives. The Diatube pumps are precise metering pumps and controlled by Allen-Bradley Bulletin 1330 state-of-the-art adjustable frequency motor drives.

The feed and reflux immersion preheaters, and the reboiler heater are operated by solid-state controllers. The feed and the reflux preheaters are controlled at the desired temperature setpoints using two separate neural network model-based controllers.

Water through the overhead condenser can be controlled at a desired flowrate setpoint using an air-actuated control valve. A tuned PI controller can be used to control the water flowrate. At present, the air-actuated control valve for the cooling water flow does not work; and therefore, the cooling water is controlled manually.

The feed and reflux pumps and the DP cells on the top and bottoms product flowrates are calibrated off-line prior to the experiment. The calibration procedures are described in the Ph.D. dissertation of Pandit (1992), and the results are reevaluated and updated for the current study. The overall material and component balances in general remain within the errors of 5% and 15%, respectively. For example, in Figure 5.18, the mass balance is evaluated using the data obtained during the experiment for the last 1 hour of steady-state operation. For a feed flowrate of 220 gmole/hr of 20 mole % feed composition, the average distillate flowrate and the bottom product flowrate are 34 gmole/hr and 180 gmole/hr (an error of 2.7%). The top and bottom composition are 91 mole % and 5 mole %, respectively, so the component material balance for methanol gives an error of 9.2%.

3.1.3 Data Acquisition and Control System

The system is equipped with a Keithley Series 500 data acquisition and control system. The data logging and control is done using a Gateway 2000 (486 DX/50 MHz) personal computer which collects twelve temperatures measured by thermocouples and three flow rates, three pressures, and one level signal measured by DP cells. The Keithley Series 500 is a complete measurement and control system with the hardware and software integrated together. The detailed description of the theory of operation of Series 500 can be found in KDAC (Keithley Data Acquisition and Control) manual supplied by the manufacturer. Series 500 is supported by KDAC 500, a powerful software package for the KDAC System. KDAC 500 provides foreground /background architecture, multi-tasking, array management, memory management, disk access and storage, and a library of input and output commands. KDAC 500 commands set up real-time acquisition routines, establish input triggers that make execution of one routine dependent on another, and create and manage KDAC 500 data arrays.

3.1.4 Interfacing Program development

A Borland C version of KDAC 500 software is installed to support the programming language used in this study. The entire coding is done using 'C' for this process control application. The KDAC system is programmed to receive and send signals to the process every 5 seconds and to save the data collected to the hard disk of the computer every half minute. Various library routine functions (e.g., bgread, bgwrite, arput, armake, arget, etc.) along with the initialization routines (kdinit, softinit) provide

the key resource for the real-time interfacing. The background function of the KDAC 500 package stores all the 19 readings collected every 5 seconds over the half minute period, filters out the noise using KDAC 500 routines, and transfers the filtered data to the designated drive. The C program that executes the KDAC 500 commands also sets up the operator interface screens, so that the operator gets all the relevant information regarding the column operation. The operator can also provide his/her inputs on-line whenever needed without stopping the main program. The screen is set up like a window to the whole process and refreshes every 5 seconds.

The interfacing software, with the help of the KDAC system, collects a total of 19 data points (12 temperatures, 3 flowrates, 3 pressures, 1 level signal) and sends 4-20 mA signals to operate the feed and reflux metering pumps, the feed and reflux preheaters, the reboiler heater, and the air-actuated control valve on the cooling-water flow line to the overhead condenser. There are 2 single-loop neural network controllers (on feed and reflux preheaters) and a PI controller on the water flow line for the condenser that are operated through the KDAC system. The 4-20 mA signals are sent to the pumps. The signal for the cooling-water flow is converted to pressure signals by an I/P transducer, which, in turn, operates the air-actuated control valve on the condenser water line. The three solid-state controllers on the two preheaters and the reboiler heater convert the mA signals into voltage signals to control the power to the heaters. Appendix C describes the power characteristics of the reboiler.

One of the safety features included in the instrumentation scheme allows the overhead condenser cooling water to flow, even when the KDAC system program fails or

gets aborted. A default value for the cooling water flowrate keeps the water running. The setup also has a stand-by water-supply line (operated manually) if the power to the unit fails. The operating description can be found in the laboratory manual for the distillation column.

3.1.5 Control Difficulties

Several characteristics of the methanol-water system in this experimental setup make it difficult to control the process. Some of those characteristics are couplings, nonlinearities, nonstationary behavior and differences in system dynamics in the top and bottom composition changes. Previous researchers (Gupta, 1994; Pandit, 1991) have tried to quantify these elements through various experimental tests. One of the conventional methods used to analyze the interactions (or couplings) between the various control loops is to find the steady-state relative gain array (RGA) elements. Ideally, for a noninteracting system, the diagonal elements of the RGA matrix should be one, and off-diagonal elements be should be zeros. The steady-state RGA elements with the control configuration (L,V) for this laboratory setup are experimentally determined (Gupta, 1994) and are shown in Table 3.1.

Table 3.1 Relative Gain Array for L-V Scheme

	Top Composition	Bottom Composition
Reflux Rate	1.5	-0.5
Reboiler Heat Input	-0.5	1.5

The nonlinear nature of this distillation system is also very apparent. Gupta (1994) shows that positive and negative changes of the same magnitudes in the reboiler heat input (10%) do not result in the same amount of bottom composition difference. A 10% increase in the reboiler heat input results in an absolute gain of 0.01 in the bottom impurity, whereas a 10% decrease in the reboiler heat input results in an absolute gain of 0.06 in the bottom impurity -- a nonlinearity 1:5 as measured by a gain ratio.

There are unknown, unmeasured disturbances affecting the column leading to nonstationary behavior. Gupta (1994) illustrates, through an experiment, that a decrease in the reflux flow rate from 65 ml/min to 45 ml/min pushes the top impurity from 2% to 16%. However, when the reflux rate is brought back to 65 ml/min, the top impurity does not return to its previous value of 2%, but settles at around 6%. The presence of this nonstationary behavior is also very evident in various experimental runs conducted in this study. Different control studies with the same setpoint changes do not change the manipulated variables (reflux and boilup rates) by the same amount. The changes in the internal reflux, nonideal flow inside the column (e.g., weeping), variability of tray efficiencies, etc. create this unmeasured variability in the process.

It has also been observed that a significant disparity exists between the top and bottom composition dynamics. The open-loop response time (i.e., the average process time constant) for the top composition is approximately 1 hr, whereas for the bottom composition, the response time is about 3 hr.

3.2 Simulator

In order to test the developed control strategy, extensive simulation studies are made on a tray-to-tray dynamic simulator representing the experimental setup (developed by Ramchandran, 1992) before implementation on the actual experimental setup. The broad features of the simulator are discussed below.

3.2.1 Model Equations

The equations describing the time-domain behavior on each tray of the distillation column are comprised essentially of (1) Overall Material Balance, (2) Component Material Balance and (3) Energy Balance.

1. Material Balance for trays in stripping and rectifying sections:

$$\frac{dM_i}{dt} = (L_{i+1} - L_i) + (V_{i-1} - V_i) \tag{3.1}$$

and for the feed tray:

$$\frac{dM_i}{dt} = (L_{i+1} - L_i) + (V_{i-1} - V_i) + (F_i^L + F_{i-1}^V) \tag{3.2}$$

where M_i is the liquid holdup (lbmoles) on the 'i'th stage (starting i=1 for reboiler); L_i and L_{i-1} are the flowrates of the liquid leaving the 'i'th and 'i-1'th stage, respectively; V_i and V_{i-1} are the flowrates of the vapor leaving the 'i'th and 'i-1'th stage, respectively; F_i^L is the flowrate of the liquid fraction of the feed entering on the 'i'th stage; and F_{i-1}^V is the flowrate of the vapor fraction of the feed entering on the 'i-1'th stage.

2. Component Material Balance for trays in the stripping and rectifying sections:

$$\frac{d(M_i X_{i,j})}{dt} = (L_{i+1}.X_{i+1,j} - L_i.X_{i,j}) + (V_{i-1}.Y_{i-1,j} - V_i.Y_{i,j}) \quad (3.3)$$

and for the feed tray:

$$\frac{d(M_i X_{i,j})}{dt} = (L_{i+1}.X_{i+1,j} - L_i.X_{i,j}) + (V_{i-1}.Y_{i-1,j} - V_i.Y_{i,j}) + (F_i^L.X_{i,j}^F + F_{i-1}^V.Y_{i-1,j}^F) \quad (3.4)$$

where $x_{i,j}$ and $x_{i+1,j}$ are the compositions of the 'j'th component in the liquid leaving the 'i'th and 'i+1'th stage, respectively; $y_{i,j}$ and $y_{i-1,j}$ are the compositions of the 'j'th component in the vapor leaving the 'i'th and 'i-1'th stage, respectively; $x_{i,j}^F$ is the composition of the 'j'th component in the liquid fraction of the feed entering the 'i'th stage; and $y_{i-1,j}^F$ is the composition of the 'j'th component in the vapor fraction of the feed entering on the 'i-1'th stage.

3. Energy Balance for trays in the stripping and rectifying sections:

$$\frac{d(M_i H_{i,j})}{dt} = (L_{i+1}.h_{i+1} - L_i.h_i) + (V_{i-1}.H_{i-1,} - V_i.H_i) \quad (3.5)$$

and for the feed tray:

$$\frac{d(M_i H_{i,j})}{dt} = (L_{i+1}.h_{i+1} - L_i.h_i) + (V_{i-1}.H_{i-1,} - V_i.H_i) + (F_i^L.X_i^F + F_{i-1}^V.H_{i-1}^F) \quad (3.6)$$

where h_i and h_{i+1} are the enthalpies of the liquid leaving the 'i'th and 'i+1'th stage, repectively; H_i and H_{i-1} are the enthalpies of the vapor leaving the 'i'th and 'i-1'th stage,

respectively; h_i^F is the enthalpy of the liquid fraction of the feed entering the 'i'th stage; and H_{i-1}^F is the enthalpy of the vapor fraction of the feed entering on the 'i-1'th stage.

3.2.2 Assumptions

Various simplified assumptions are made in the development of the dynamic simulator and are listed as follows.

- One fixed feed plate is used to introduce the vapor and liquid, feed regardless of the feed or operating conditions.
- Coolant and heating media dynamics are negligible in the condenser and the reboiler.
- Pressure is constant and known on each tray.
- The condenser is a total condenser.
- In terms of the dynamic process behavior, the liquid rates throughout the column are not the same. Liquid flowrates are calculated using the Francis Weir Formula (Luyben, 1990) as follows

$$[Q_L = 3.33 L_w (h_{ow})^{1.5}] \tag{3.7}$$

where Q_L is the liquid flowrate over the weir (ft^3/s), L_w is the length of the weir (ft), and h_{ow} is the height of the liquid over the weir (ft).

- Perfect Level control in the reflux drum and the reboiler allows a constant holdup in the reflux drum and reboiler by changing flowrates of the bottoms product, B, and liquid distillate product, D. Mathematically, this implies $\frac{dM_1}{dt} = 0$ and $\frac{dM_{N+1}}{dt} = 0$

for an N-stage column. As a result, the overall material balance in the reboiler becomes an algebraic equation that can be written as

$$L_{i+1} - L_i - V_i = 0 . \tag{3.8}$$

Similarly, for the condenser, the overall material balance gives

$$V_N - L_{N+1} - D = 0 . \tag{3.9}$$

- Dynamic response of the internal energies on the trays are much faster than the composition or total holdup changes, and, therefore, energy balances on each tray are just algebraic. Therefore, for any general stage '*i*' and taking the feed into account, the vapor flowrate can be calculated as

$$V_i = \frac{(L_{i+1}h_{i+1} - L_i h_i) + (F_i^L h_i^F + F_{i-1}^V . H_{i-1}^F) + V_{i-1}H_{i-1}}{H_i} \tag{3.10}$$

- The reflux rate, L, and the boilup rate, V, are used as the manipulated variables.

- Empirically correlated polynomial equations obtained from regressing experimental data sets (Henley and Seader, 1981) are used for thermodynamic vapor-liquid equilibrium (VLE). The VLE is a functional dependence of the vapor composition to the liquid composition at a particular temperature and pressure. The effect of pressure on the VLE is relatively small compared to the temperature effect. To include the nonideality due to pressure on VLE , a fugacity coefficient model for the vapor and an activity coefficient model for the liquid can be used. The fugacity coefficient for the vapor is often assumed to be 1.0 at a "low" pressure (i.e., below a few bars, Reid, Prausnitz and Poling, 1987). The activity coefficient can be calculated from the excess Gibbs free energy using any standard thermodynamic model (e.g., Margules, Van

Laar, Wilson, NRTL, or UNIQUAC). The Gibbs-Duhem equation for binary mixtures correlates the activity coefficient to the excess Gibbs free energy. However, in this simulator, the VLE is obtained directly by correlating the experimental results obtained by Henley and Seader (1981) at 1 atmosphere pressure because the column is open to atmosphere when operated.

- A single value of the Murphree stage efficiency is used for all the stages, except for the partial reboiler which is ideal (efficiency = 1). The Murphree tray efficiency is calculated based on the following equation

$$E_{i,j} = \frac{Y_{i,j} - Y_{i-1,j}}{Y^*_{i,j} - Y_{i-1,j}} \tag{3.11}$$

where $Y_{i,j}$ is the actual composition of the vapor leaving the 'i'th stage; $Y_{i-1,j}$ is the actual composition of the vapor leaving the 'i-1'th stage; $Y^*_{i,j}$ is the equilibrium vapor composition; $E_{i,j}$ is the Murphree vapor efficiency for the 'j'th component in the 'i'th stage.

3.2.3 Design and Operating Conditions

The various design and operating conditions of the simulator are shown below.

Design Condition :

number of stages = 7 (6 real, 1 ideal (partial reboiler))

feed stage = 4

feed quality = 100^0 F (subcooled)

reflux quality = 110^0 F (subcooled)

pressure = 1 atm abs. (approximately 670 mm Hg, abs.)

Murphree stage efficiency = 90%.

The simulator has been tested at different operating conditions by using a series of setpoint changes and disturbances in feed flowrate and feed compositions. However, the nominal operating conditions along with the range of trained operating region (in brackets) are shown below.

Nominal Operating Condition and Range :

feed rate (lbmoles/hr) = 0.4625 (0.4-0.5)

feed composition (mole fraction) = 0.2 (0.1-0.4)

top product composition = 0.9 (0.80-0.95)

bottom product composition = 0.03 (0.01-0.09)

boilup rate (lbmoles/hr) = 0.35 (0.3-0.4)

reflux rate (lbmoles/hr) = 0.18 (0.14-0.24).

CHAPTER IV

CONTROLLER DEVELOPMENT

In the past two decades, many model-based control algorithms have been proposed to achieve better performance and more robust controllers. In-depth reviews on model-based control strategies are presented in the papers by Bequette (1990), Bosley et al. (1992) and Seborg et al. (1986). All these advanced techniques rely heavily on the availability of a mathematical model that is a good representation of the dynamics of the process being controlled. A vast majority of the techniques use linear or nonlinear dynamic empirical models comprised of past values of the inputs and outputs of the process. More recently, neural network dynamic models have been used in place of the conventional empirical dynamic models in model-based control strategies (You and Nikolaou, 1993; Raich et al., 1991; Bhat and McAvoy, 1990).These control strategies fall under a general class known as Model Predictive Control (MPC).

Another model-based control technique developed by Lee and Sullivan (1988), known as Generic Model Control (GMC), uses a controller based on a steady-state "process inverse" model and a reference system synthesis (Bartusiak et al., 1989) based on first-order dynamics.

4.1 Neural Network Model and Inverse of State Prediction

A "process model" refers to a mathematical equation, or a set of equations, that could determine the estimated output of the process when given the process inputs. For instance, in the case of distillation, a process model would predict the compositions of the

overhead and bottom products given the feed flowrate, feed composition, reflux rate, boilup rate (or steam flowrate to the reboiler), the number of ideal stages, the stage efficiency, etc. A "process inverse model" refers to a mathematical equation, or set of equations, that could determine the values of the manipulated variables that would produce the desired process outputs. In the distillation example, a process inverse model would predict the reflux rate and boilup rate required to produce the desired overhead and bottom product compositions, given all other pertinent input data.

Most MPC strategies use both forms of the model: the process model for system identification, and the process inverse model for the control action. If the process model happens to be an empirical model, then the same model can be inverted to obtain the desired control action. If the process model is a neural network model, then a separate neural network model has to be developed to represent the process inverse.

For chemical process control, it is highly desirable to use models that predict directly the manipulated variables in order to keep the process to its set-point. A real process is always subjected to various types of disturbances (flow, composition, heat, etc.), and often the measurement sensors are so noisy and uncertain that a reliable process control calculation cannot be achieved by depending solely on the process data. But, a proper model can be generated based on the phenomenological understanding of the process. This model can capture the general process information (i.e., the degree of dependency of the process variables to the manipulated variables at different operating conditions) and can be used for control calculations without being very sensitive to disturbances or measurement uncertainties. In the past few years, model-based control

strategy has become extremely appealing to the process industries. If the process dynamics can be approximated as first-order, then the process inverse dynamic models can be replaced by process inverse steady-state models to obtain the control action. This approach is commonly known as Generic Model Control (GMC).

Application of this strategy is first tested on two separate SISO systems (feed and reflux preheaters) on our laboratory apparatus. It is desired to keep the exit temperature of the fluid (methanol-water mixture passing through a tube with variable flowrates and surrounded by a heating coil) constant by providing the exact amount of power to the coil. The DAC system accepts the signal from the computer in the form of a raw integer (known as "counts") and converts this signal to current (0-4 mA). Subsequently, this current signal gets amplified through a step-up transformer and provides the power to the coil. In this experiment, a control approach combining an inverse steady-state model and the GMC law has been adopted. For a SISO system, the GMC law can be written as

$$X_{ss} = X + K_1(X_{sp} - X) + \int_0^t K_2(X_{sp} - X)dt \qquad (4.1)$$

where X_{ss} is the steady-state target value, and X_{sp} is the desired setpoint for X. The control law tuning constants are K_1 and K_2. The control block diagram is shown as below

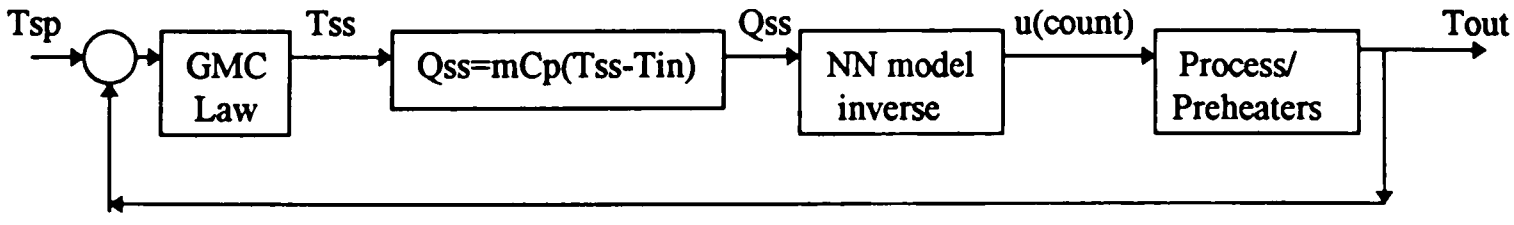

In this approach, the neural network is trained based on the "heating rate" as input and the manipulated variable ("count") as output (a 1-4-1 network). The experimental data was

generated based on a single feed flowrate (40 ml/min) but is made suitable for application at different flowrates by using simple phenomenological models in series. This approach of "hybrid" modeling eliminates the need for extra input (feed flow in this case) to the neural network and, thus, reduces the complexity of the model.

In a multi-input-multi-output system (MIMO) (distillation column in this case), a similar control strategy has been developed and is shown in Figure 4.1. The neural network model is developed here in an inverse model mode taking feed flowrate, F, feed composition, z, overhead composition, X_D, and bottoms composition, X_B as inputs, and the reflux rate, L, and the boilup rate, V as the output. Instead of making a single neural network correlating these 4 inputs and 2 outputs (e.g., 4-5-2), two separate neural networks (4-5-1) are used for the two outputs. While the two networks do not contain extra information compared to a single one, this approach can greatly benefit the neural network training effort. In general, the degree of complexity of training increases with the dimensionality of the problem and the training of two smaller networks can often be easier compared to a single large one. Besides, a different architecture can be adopted for each of these networks (e.g., one 4-5-1 and another 4-7-1) for training ease. This neural network steady-state-inverse modeling is used in conjunction with the Generic Model Control (GMC) law (Lee and Sullivan, 1988). The GMC approach assumes that the process has first-order dynamics and calculates the steady-state target values of the

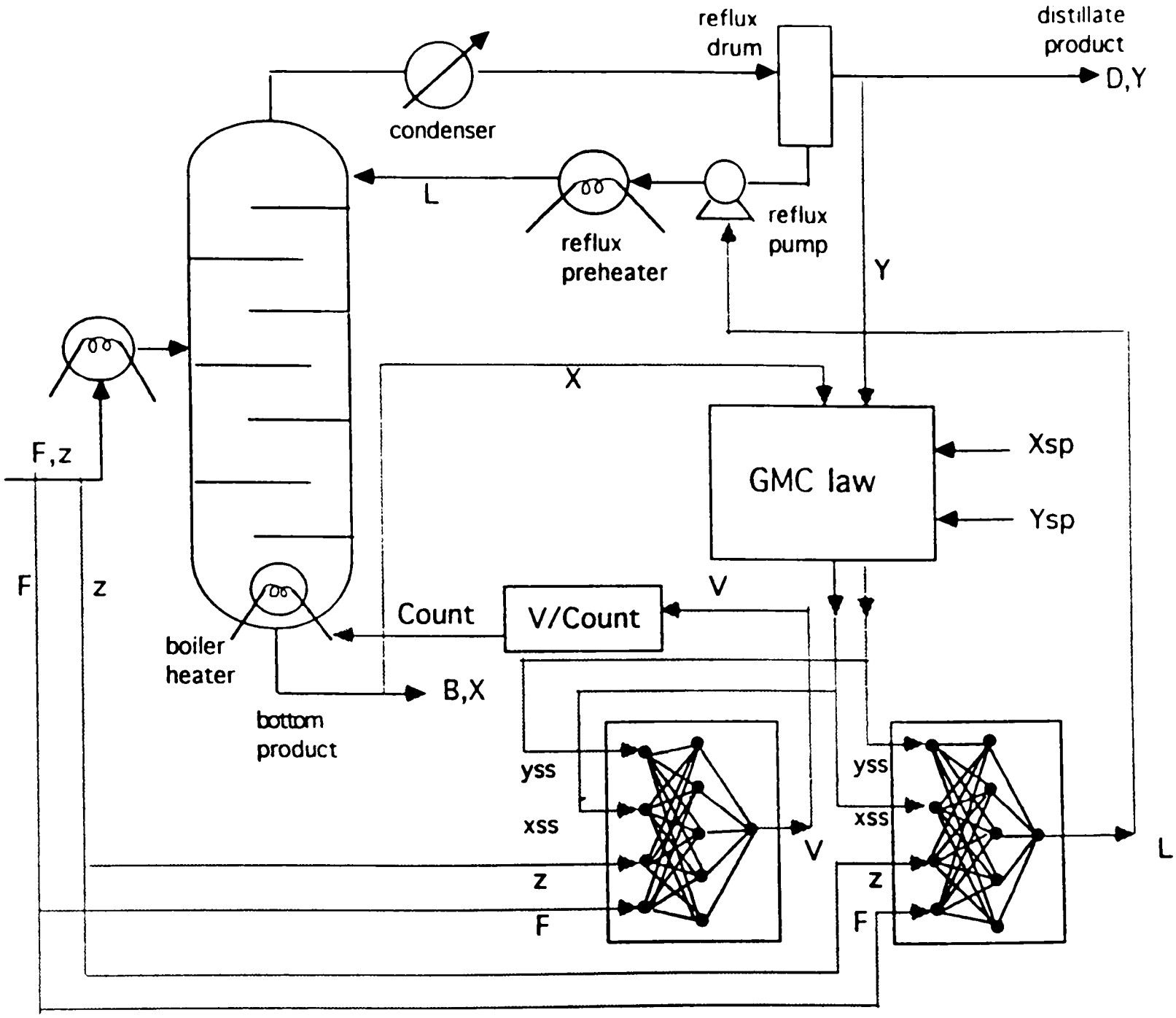

Figure 4.1. Neural network model-based control strategy in inverse of steady-state prediction approach.

controlled output ($X_{D,ss}$ and $X_{B,ss}$) as follows

$$X_{D,ss} = X_D + K_{1D}(X_{D,sp} - X_D) + K_{2D}\int_0^t (X_{D,sp} - X_D)dt \tag{4.2}$$

$$X_{B,ss} = X_B + K_{1B}(X_{B,sp} - X_B) + K_{2B}\int_0^t (X_{B,sp} - X_B)dt \tag{4.3}$$

where $X_{D,sp}$ and $X_{B,sp}$ are the desired setpoints for X_D and X_B, the current values for the overhead and bottom compositions. K_{1D}, K_{2D}, X_{1B} and X_{2B} are the control law tuning constants.

It is important to ensure bumpless transfer at the on-set of control, i.e., at the time of switching the "manual" mode (open loop) to the "automatic" mode (closed loop). Here, the process starts up in an open loop. The initial reflux and boilup rates are calculated, prior to the starting of the experiment, using the neural-network inverse models by providing the desired inputs (i.e., the values of the feed flowrate and composition along with some desired steady-state target values of the compositions, $X_{D,SS}$ and $X_{B,SS}$). The experiment is started with these initial reflux and boilup rates, and the process is allowed to settle down to a near-steady-state condition. At this near-steady-state condition, the values of the process variables (top and bottom compositions, X_D and X_B) may be different from the desired steady-state targets ($X_{D,SS}$ and $X_{B,SS}$) based on which initial manipulated variables are calculated. This deviation depends on the amount of mismatch between the actual process and the neural-network model. When the controller is switched on, it is brought on-line with the intention of maintaining the overhead and bottom product compositions at this near-steady-state condition without producing any upset to the

manipulated variables. At the onset of the automatic mode, the setpoint is assumed to be the same as the last measured values of the process variables. This prevents an old setpoint "bump." Under this condition, $X_{D,SP} \approx X_D$ and $X_{B,SP} \approx X_B$, which implies that the error and the cumulative error terms in Equations 4.2 and 4.3 are all zero. Then a bias can be calculated for each of the controlled variables to accommodate the process-model mismatch as follows:

$$b_{x_D} = X_{D,SS} - X_D \tag{4.4}$$

$$b_{X_b} = X_{B,SS} - X_B \ , \tag{4.5}$$

where b_{x_D} and b_{x_B} are the biases on the overhead and bottom product compositions, respectively.

The initial steady-state target set-points, $X_{D,SS}$ and $X_{B,SS}$, are operator-specified values. For the start-up operation, they are not calculated using the control law in Equations 4.1 and 4.2. The overhead and bottom compositions, X_D and X_B, are measured from the process. The biases represent the mismatch between the process and the neural-network model and are calculated *only once*, whenever the controller is switched to automatic. The control law with the bias term included then reads as follows:

$$X_{D,ss} = b_{x_D} + X_D + K_{1D}(X_{D,sp} - X_D) + K_{2D}\int_0^t (X_{D,sp} - X_D)dt \tag{4.6}$$

$$X_{B,sss} = b_{x_B} + X_B + K_{1B}(X_{B,sp} - X_B) + K_{2B}\int_0^t (X_{B,sp} - X_B)dt \ . \tag{4.7}$$

Figure 4.1 gives a schematic description of this nonlinear control strategy that uses the neural-network inverse of steady-state model. The nonlinear controller reads the process

variable at every controller time interval and calculates target values $X_{D,SS}$ and $X_{B,SS}$ based on the Equations 4.3 and 4.4. The steady-state target values along with the measured values for feed flowrate, F, and feed composition, z, are used as the inputs to the neural-network model of the distillation column. The network then calculates the reflux rate, L, and the boilup rate, V, to drive the process to the temporary steady-state targets, $X_{D,SS}$ and $X_{B,SS}$.

Changes in the disturbances (feed flowrate and feed composition) can be fed directly to the model (when the measurements are available) by allowing the neural network controller to provide a nonlinear feedforward response. Otherwise, these disturbances are taken care of by the controller in a feedback way.

The main advantage of using a neural network model is to speed up the control calculations while capturing the same nonlinear behavior as in any other process model-based control. Since, the neural-network model uses a transfer function whose output is bounded between -1 and +1, the output of the network also becomes bounded. As a result, it always gives an answer within a feasible region.

The inverse of steady-state prediction approach as discussed in the preceeding section has couple of disadvantages. This method cannot handle issues like "integral windup," i.e, when a process variable hits a constraint or a sensor fails to register its change. And, in general, the controller does not consider handling constraints of the manipulated variables or the process variables.

4.2 Neural Network Model and Gain Prediction

While neural network model based controller can be shown to work well in the inverse of steady-state prediction mode, the performance very much depends on the amount of process model mismatch (pmm). In the inverse of the state-prediction mode, a constant bias is used to account for this pmm at a steady-state. If a control transfer is made in the transient, the amount of bias to the process variable becomes large, causing significant shift between the process and the model operating region. Hence, it is always desirable to transfer the control at a steady state. But, achieving or even detecting a steady state is often a difficult task in a real plant because of the various continuous disturbances in the flow, composition, etc., along with the noise and drift in the sensors.

It is the growing conviction of principal investigators at Texas Tech that gain prediction, more than state prediction, that makes model-based control effective. Issues such as achieving a true "steady state," avoiding a "integral windup," and operating the process at the "constraint" can also be properly taken care of by this novel gain-prediction strategy as discussed below. The gain of a process refers directly to the model sensitivity to the manipulated variables. As a result, in this approach, a neural-network model can be trained to predict gains (or inverse gains for direct manipulated variables calculation), given the relevant inputs (for distillation column - feed flowrate, feed composition, top and bottom compositions).

Since gain prediction is the key for control, neural-network models are used to predict the four gains of the distillation process. These gains are used to calculate the change in reflux rate ΔL and the change in boilup rate ΔV from the desired changes in top

and bottom compositions ΔY_D and ΔX_D, respectively. The detailed steps are shown as follows. First, the steady-state targets for top (Y_{ss}) and bottom (X_{ss}) compositions are calculated from the current compositions (Y and X) and the respective setpoints (Y_{sp} and X_{sp}) and are given below.

$$Y_{ss} = Y + K_c^{top}(Y_{sp} - Y) \tag{4.8}$$

$$X_{ss} = X + K_c^{bot}(X_{sp} - X) \tag{4.9}$$

where K_c^{top} and K_c^{bot} are proportional gains for the top and bottom composition targets. Note that Equations 4.8 and 4.9 can be obtained from the Equations 4.2 and 4.3 by omitting the integral terms. Thus, the required changes in the top and bottom compositions to achieve the steady-state can be calculated as follows.

$$\Delta Y_{ss} = Y_{ss} - Y \tag{4.10}$$

$$\Delta X_{ss} = X_{ss} - X \tag{4.11}$$

It is to be noted here that the process has certain response time. The open-loop time constant for the top composition is 1 hr and is 3 hrs for the bottom composition. The manipulated variables calculated to achieve these target composition changes will be implemented many times before the process responds. To avoid this constant integration on the target variables, portions of the last ΔY_{ss} and ΔX_{ss} are subtracted at each control step. The following equation is developed (Rhinehart, 1996) to calculate the desired changes of the process variables (ΔY_D and ΔX_D).

$$\Delta Y_D = \Delta Y_{ss} - \alpha_y(\Delta Y_{ss,old}) \tag{4.12}$$

$$\Delta X_D = \Delta X_{ss} - \alpha_x(\Delta X_{ss,old}) \tag{4.13}$$

where $\Delta Y_{ss,old}$ and $\Delta X_{ss,old}$ are the values of ΔY_{ss} and ΔX_{ss} calculated in the previous control step and α_y and α_x are the two tuning factors for the control. If unconstrained, the changes in reflux rate and the boilup rate from the current state are obtained from the following matrix relationship.

$$\begin{bmatrix} \Delta Y_D \\ \Delta X_D \end{bmatrix} = \begin{bmatrix} K_{yr} & K_{yv} \\ K_{xr} & K_{xv} \end{bmatrix}_{X,Y} \begin{bmatrix} \Delta R \\ \Delta V \end{bmatrix} \tag{4.14}$$

where $K_{yr} = \frac{\partial Y}{\partial R}$, the gain in top composition with respect to reflux change; $K_{yv} = \frac{\partial Y}{\partial V}$, the gain in top composition with respect to boilup change; $K_{xr} = \frac{\partial X}{\partial R}$, the gain in bottom composition with respect to reflux change; and $K_{xv} = \frac{\partial X}{\partial V}$, the gain in bottom composition with respect to boilup change. The local gains of the process are calculated from the simulator by providing a small perturbation in the reflux and the boilup (both in the positive and negative directions) and taking the average.

Four separate neural-network models are developed to predict these four gains at a particular steady-state. A small block diagram of one NN model is shown below.

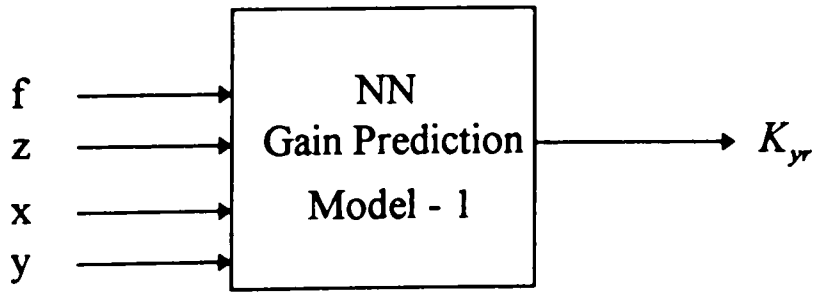

Because constraints can be encountered, the increments in the reflux and boilup rates (ΔR and ΔV) are actually calculated using an optimization program (Li and Rhinehart, 1996), instead of Equation 4.14. Using this optimization method, one can

calculate the manipulated variables based on any cost function (or objective function) and can take care of the constraints. The objective function and the constraints used in this research are as follows.

$$\underset{\Delta R, \Delta V}{Min}\ J = [\frac{(\Delta Y_D - K_{yr}\Delta R - K_{yv}\Delta V)^2}{Eq_1^2} + \frac{(\Delta X_D - K_{xr}\Delta R - K_{xv}\Delta V)^2}{Eq_2^2}] \tag{4.15}$$

subject to $$R_{\min} \le R \le R_{\max} \tag{4.16}$$

$$V_{\min} \le V \le V_{\max} \tag{4.17}$$

where Eq_1 and Eq_2 are known as equal concern factors or weighting factors. Eq_1 and Eq_2 have the same units as the controlled variables. These factors provide different weightings to the corresponding terms in the objective functions and can be determined based on some economic consideration. The current value of reflux R and vapor boilup, V are calculated by simply adding the changes to the previous values of R and V.

$$R = R_{old} + \Delta R \tag{4.18}$$

$$V = V_{old} + \Delta V \tag{4.19}$$

Figure 4.2 shows a detailed block diagram of this control approach.

Several benefits have been observed by this approach compared to the inverse of the state prediction approach.

- There is always a bumpless transfer because the controller determines the changes in the manipulated variables (velocity mode) and not their absolute values.
- Although Equation 4.14 is a linear model, it uses nonlinear gains, which change with the process state.

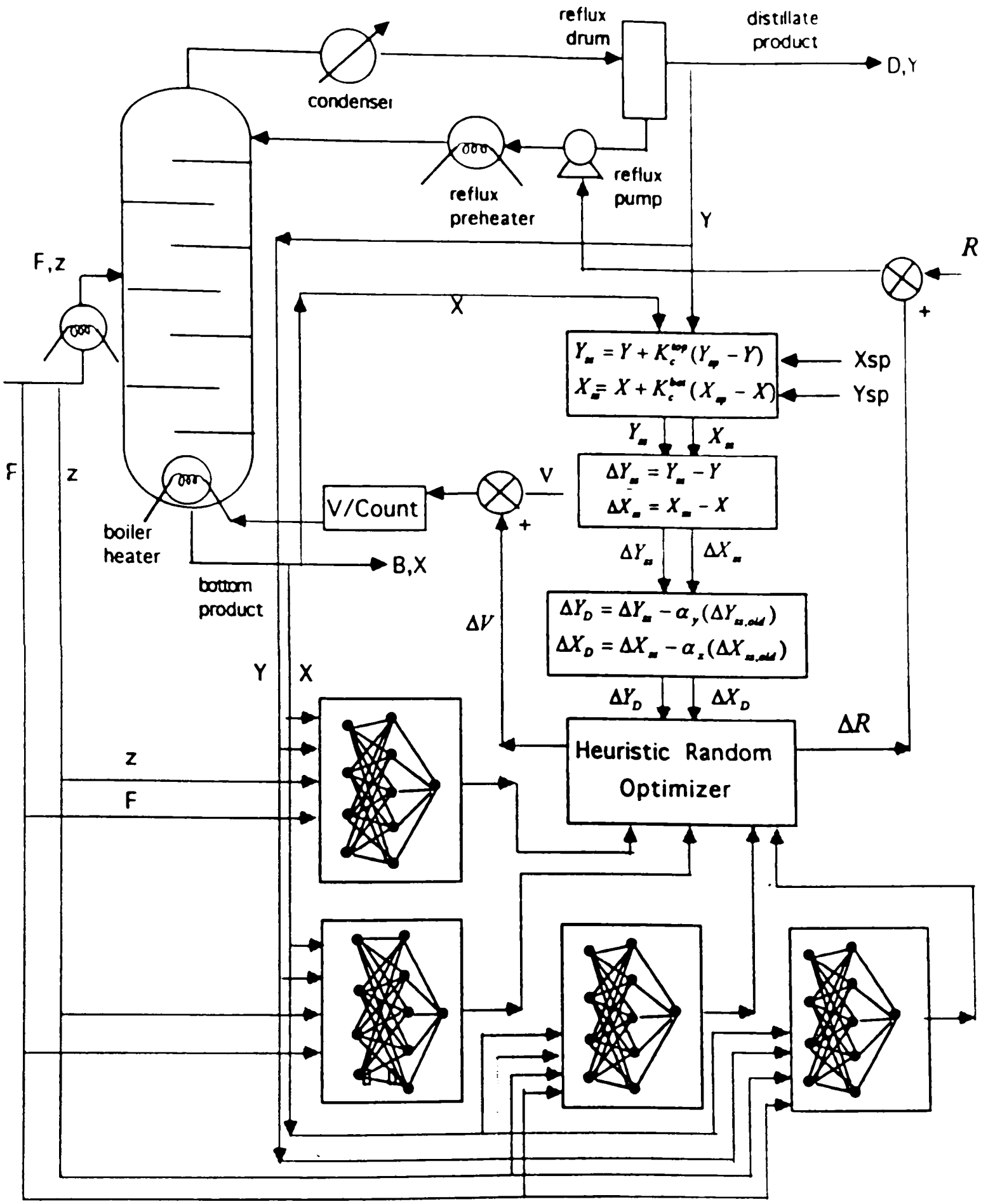

Figure 4.2. Neural network model-based control strategy in gain prediction approach.

- This approach focuses directly on the gain prediction aspect.
- There is no negative effect, such as integral windup, when the process variable is at the constraint.
- The optimizer allows constraint handling.

However, no immediate feedforward action is taken by this controller against feed-flowrate or feed-composition changes. The values of the local gains but not the steady-state target values change immediately with the change of feed flowrate and the feed composition. As a result, the disturbance rejection is achieved primarily by the feedback path. Ongoing simulation studies at TTU are incorporating feedforward, integrating dynamics, and other classes of constraint handling into this control structure.

4.3 Optimization and Constraint Handling (HRO)

Following the work of Li and Rhinehart (1996), this novel Heuristic Random Optimization (HRO) technique is successfully applied here as an online controller to find the optimum change in the manipulated variable, as well as to handle the process constraints. This optimization method has several advantages over other techniques as follows.

- It involves easy computation and is simple to implement. Along with the efficient neural network model prediction, this optimization algorithm allows the flexibility of selecting a smaller control interval.
- The optimizer has the ability to find the global optimality, even in the vicinity of multiple local minima.

- The optimizer can handle constraints without an arbitrary penalty function.
- Stopping criteria convergence is scale independent.
- The optimization algorithm does not involve computationally expensive calculations, such as Hessian matrix inversion, and can handle the situations where the gradient is burdensome or impossible to calculate.
- The optimzer is independent of the choice of the initial guess values of the variables.

Several heuristic principles are used in this optimization search to extract the advantages of the gradient search methods in order to attain a fast convergence. Gradient information is used to 'suggest' but not 'dominate' the generation of the sequence of trials. Heuristic strategies are used to adjust the mean and the standard deviation adaptively according to the gradient information and the history of success or failure of the search trials. The sequence of trials is generated in a random style with a Gaussian distribution with the updated mean and standard deviation. Thus, the influence of the gradient is indirect. The random approach helps to overcome the difficulty of local optima, and enables the gradient to be estimated numerically to save computational effort.

The Gaussian distribution has the following probability density function

$$f_{Gauss}(x) = \frac{1}{\sigma\sqrt{2\pi}} e^{-\frac{1}{2}(\frac{x-\mu}{\sigma})^2} \tag{4.20}$$

where μ and σ signify the mean and standard deviation, respectively.

The gradient-based strategy to update the mean and standard deviation is as follows:

$$\mu_i^{new} = -\frac{df}{dx_i} \cdot \lambda_{\mu,gradient-based} \tag{4.21}$$

$$\sigma_i^{new} = \frac{\phi_{\sigma,gradient-based}}{\left|\frac{df}{dx_i}\right|} \tag{4.22}$$

where λ_μ and ϕ_σ are stepsizes and subscript i denotes the i-th component. The updates of μ and σ are based on reinforcement strategy and are as follows:

$$\mu_i^{new} = \mu_i^{old} + \begin{cases} r_i^{old} \cdot \eta_{\mu,reinforcement} & if \quad \text{the trial is a success} \\ -r_i^{old} \cdot \eta_{\mu,reinforcement} & if \quad \text{the trial is a failure} \end{cases} \tag{4.23}$$

where $\eta_{\mu,reinforcement} > 0$ (recommended value 0.2-0.6).

The trial is a "success" if the trial meets all of the specified constraints and is better than the old trial in its objective function, i.e., the new function value is less than that of the old trial for a minimization problem. Otherwise, the trial is a "failure." σ is updated according to the following rule.

If the trial is "success and wide" or "failure and narrow"

$$\sigma_i^{new} = \sigma_i^{old} f_{ex} \quad . \tag{4.24}$$

If the trial is "success and narrow" or "failure and wide"

$$\sigma_i^{new} = \sigma_i^{old} f_{co} \quad . \tag{4.25}$$

Here, "wide" and "narrow" imply $\left|\frac{r_i - \mu_i^{old}}{\sigma_i^{old}}\right|$ is greater or less than a certain value 'c'. Usually the value of 'c' is between 1 and 2. The "narrow" indicates that the trial is close to the center of emphasis, i.e., μ. The "wide" indicates that the component of the trial is away from the mean value μ. For the update of μ, both gradient-based rule and reinforcement-based rule are used.

For the first stage, the search is done for a feasible initial point, i.e., it satisfies the constraints. In the second stage, a gross search is emphasized to locate the vicinity of the global minimum. In the third stage, the fine search, the global minimum is found with high precision. In our study, the precision is obtained by setting σ a small but constant value in this search. The following termination criterion is used for both the gross and fine search stages.

$$\eta_{trial} \geq \eta_{\max} \tag{4.26}$$

The following values are used in the optimization program in this study.

1. Expansion coefficient for σ update, $f_{ex} = 1.1$,
2. Contraction coefficient for σ update $f_{co} = 1/1.1$,
3. Span constant, c = 2.0,
4. Gradient-based mean update coefficient, $\lambda_{\mu,gradient-based} = 0.1$,
5. Reinforcement-based mean update coefficient, $\eta_{\mu,reinforcement} = 0.4$,
6. Stopping criteria for gross search, $\eta_{\max} = 400$,
7. Stopping criteria for fine search, $\eta_{\max} = 700$,
8. Constant value of σ for the fine search, $\sigma = 0.001$.

The details of the mathematical derivations of this optimization procedure and the results of some test cases can be found in the work of Li and Rhinehart (1996).

CHAPTER V

CONTROL RESULTS

This chapter discusses the experimental control runs carried out on the laboratory distillation column. Experimental verification of the control strategy developed and tested earlier on a simulator by B. Ramchandran is conducted, and the results are included here. In this research, neural-network models are developed based on the steady-state data generated using the simulator and by keeping the same operating condition as that of the experiment. These networks are used for the control purpose of the laboratory column. The results are shown in section 5.2.2.

The neural-network model-based gain-prediction and constraints-handling approach is a novel idea. Therefore, this approach is first studied and developed on the simulator before the implementation on the experimental setup. The simulation results are discussed in sections 5.1.1 and 5.1.2. Section 5.2.3 describes the results obtained using this approach on the actual column. For the purpose of comparison to other control aprroaches, all experimental runs are obtained following the methods of Pandit (1991) and Gupta (1994), as closely as possible.

5.1 Simulator Results

5.1.1. Distillation control with NN gain prediction

Prior to the actual implementation of this novel control strategy on the laboratory distillation column, various controller tests are performed on the simulator by giving

different setpoint changes and disturbances. Table 5.1 gives a description of the controller tests for the simulator in the servo mode (i.e., for the setpoint changes), while Table 5.2 gives a description in the regulatory mode (i.e., for the disturbances). Figures 5.1(a) and 5.1(b) show the results from the controller tests described in Table 5.1. Figure 5.1(a) shows the response of the controlled variables (i.e., the overhead and bottom product compositions) to setpoint changes, as well as the corresponding manipulated variable changes (reflux and boilup rates). Figure 5.1(a) shows that a large setpoint change in the top composition at the 25-hr mark produces a deviation in the bottom composition, which is eliminated quickly by the controller. This deviation can be attributed due to the facts that there is a significant mismatch between the top and bottom composition dynamics and that no special measure is adopted to compensate for this dynamic mismatch. In Figure 5.1(b), the same setpoint changes are given but they are converted to a reference trajectory (i.e., a desired path of the setpoint changes) by providing a first-order lag (filter factor λ=0.01 with the control interval 0.015 hr), and no significant deviation is observed. However, this approach is not used in the actual experiment, and setpoint changes are given without any first-order lag in all the experimental runs.

Figure 5.2 shows the responses of the controlled variables corresponding to the feed-flowrate and feed-composition disturbances as shown in Table 5.2. It can be noted here that the gain-prediction controller eliminates the disturbances exclusively in a feedback path, although the NN accounts for the new feed flowrate and feed compositions as the inputs to the models. One advantage of this feedback-only response is the immediate insensitivity of the manipulated variable changes to the feed-flowrate and

Table 5.1. Tests on Simulator (Servo Mode)

Time (hours)	Description of the Changes
0.0	Open-loop start up with the following nominal values: feed flowrate, F = 0.4625 lbmoles/h; feed composition, z = 0.2 mole fraction methanol; reflux, L = 0.26 lbmoles/h; vapor boilup, V = 0.36 lbmoles/h; efficiency, η=90%
5.0	Controller switch on after bumpless transfer operation $X_{D,SP}$ = 0.92 and $X_{B,SP}$ = 0.032 mole fraction methanol
7.0	Dual Composition Setpoint Change $X_{D,SP}$ = 0.91 and $X_{B,SP}$ = 0.025 mole fraction methanol
25.0	Dual Composition Setpoint Change $X_{D,SP}$ = 0.88 and $X_{B,SP}$ = 0.030 mole fraction methanol
35.0	Single Composition Setpoint Change $X_{D,SP}$ = 0.93 and $X_{B,SP}$ = 0.030 mole fraction methanol
55.0	Single Composition Setpoint Change $X_{D,SP}$ = 0.90 and $X_{B,SP}$ = 0.030 mole fraction methanol
65.0	Single Composition Setpoint Change $X_{D,SP}$ = 0.89 and $X_{B,SP}$ = 0.030 mole fraction methanol
75.0	End of Controller Tests

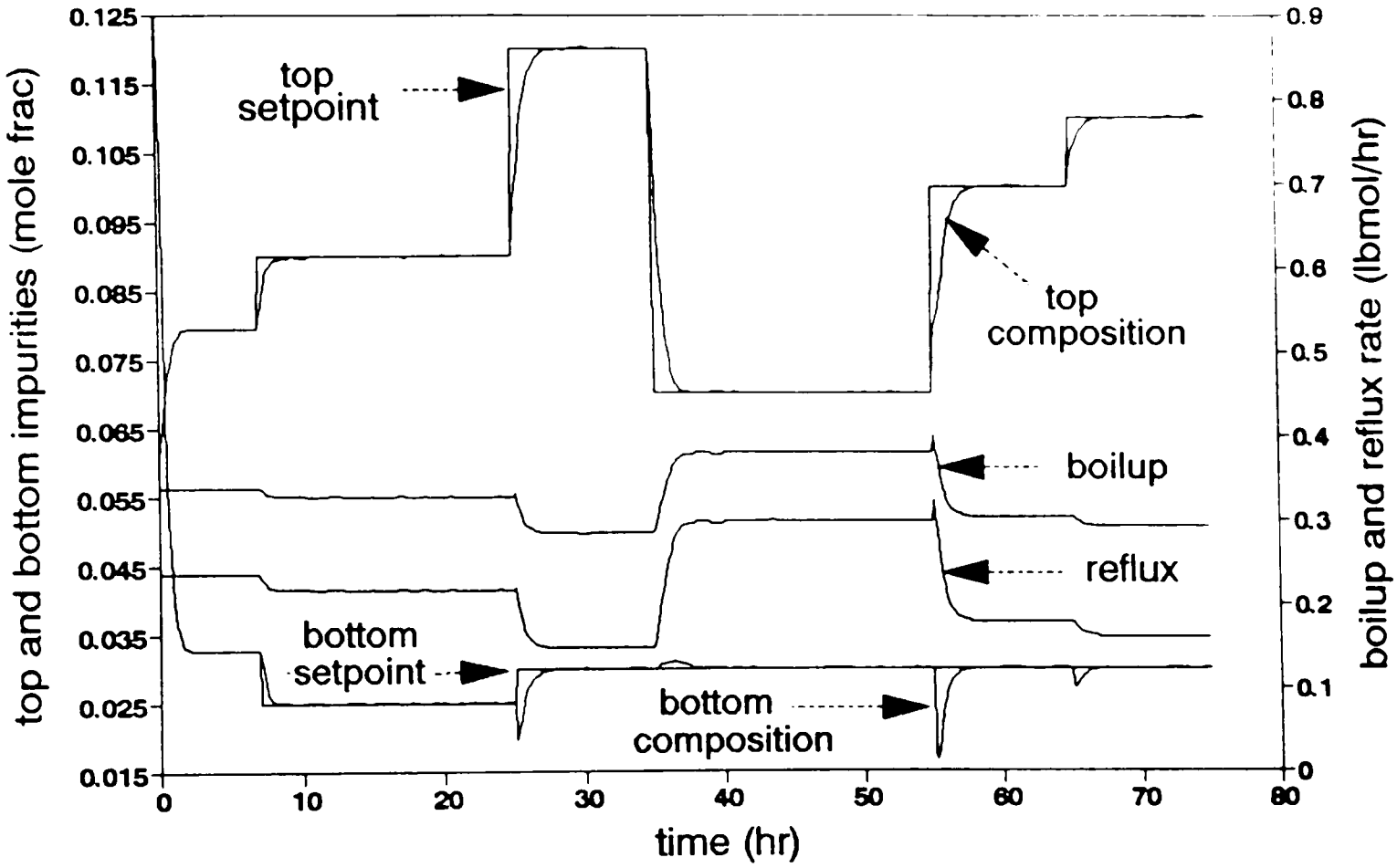

Figure 5.1. Setpoint tracking with neural network gain prediction approach on simulator. (a) Response to unfiltered setpoint changes.

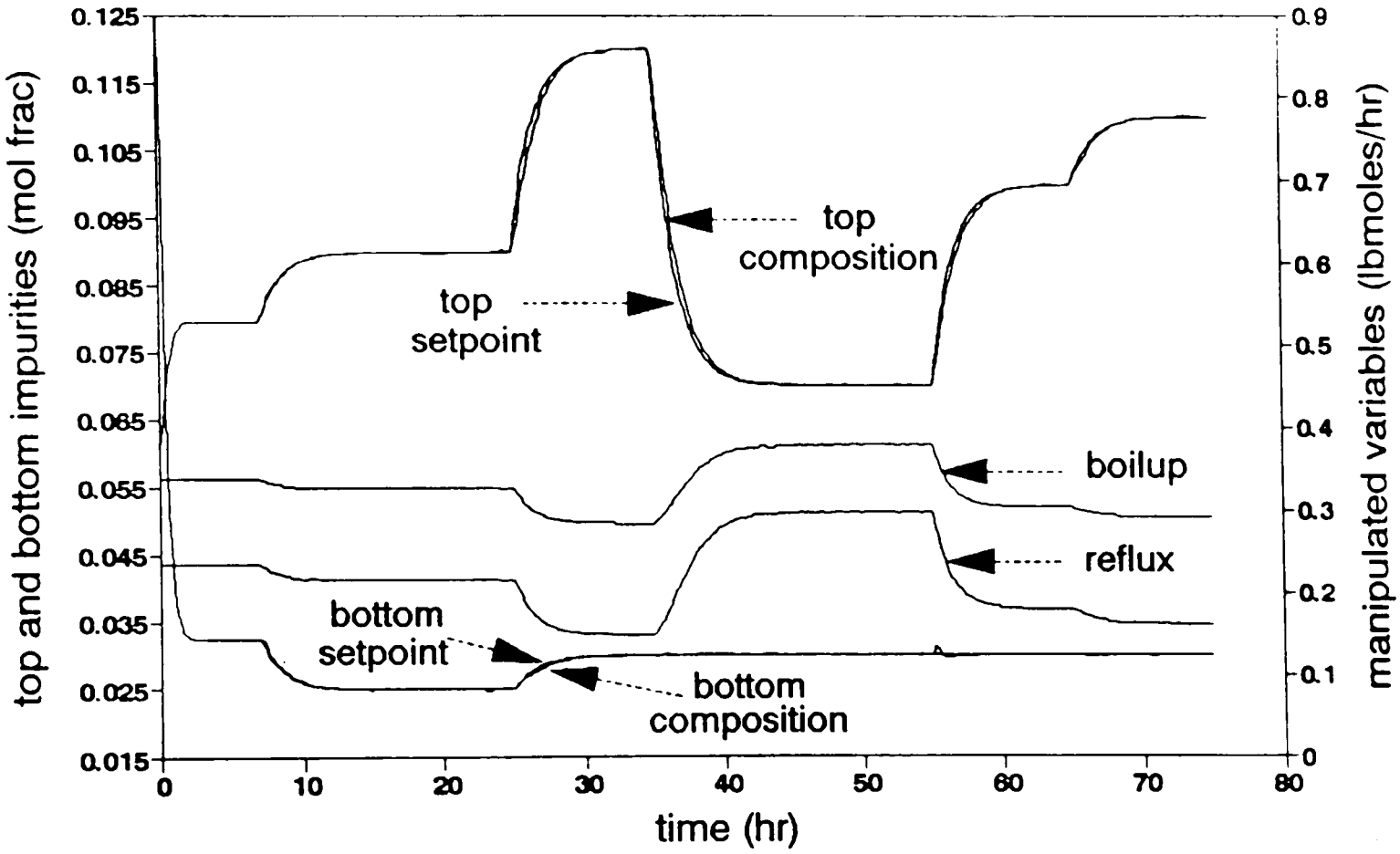

Figure 5.1. Continued. (b) Response to filtered setpoint changes.

Table 5.2. Tests on Simulator (Regulatory Mode)

Time (hours)	Description of the Changes
0.0	Open-loop start up with the following nominal values: feed flowrate, F = 0.4625 lbmoles/h; feed composition, z = 0.2 mole fraction methanol; reflux, L = 0.26 lbmoles/h; vapor boilup,V = 0.36 lbmoles/h; efficiency,η=90%
5.0	Controller switch on after bumpless transfer operation $X_{D,SP}$ = 0.92 and $X_{B,SP}$ = 0.032 mole fraction methanol
7.0	Dual Composition Setpoint Change $X_{D,SP}$ = 0.90 and $X_{B,SP}$ = 0.03 mole fraction methanol
25.0	Feed Flowrate Change F = 0.4162 (-10%) lbmoles/hr
35.0	Feed Flowrate Change F = 0.4625 (+11%) lbmoles/hr
45.0	Feed Flowrate Change F = 0.5080 (+10%) lbmoles/hr
55.0	Feed Flowrate Change F = 0.4625 (-9%) lbmoles/hr
77.0	Feed Composition Change z = 0.18 (-10%) mole fraction
87.0	Feed Composition Change z = 0.20 (+11%) mole fraction
97.0	End of Controller Tests

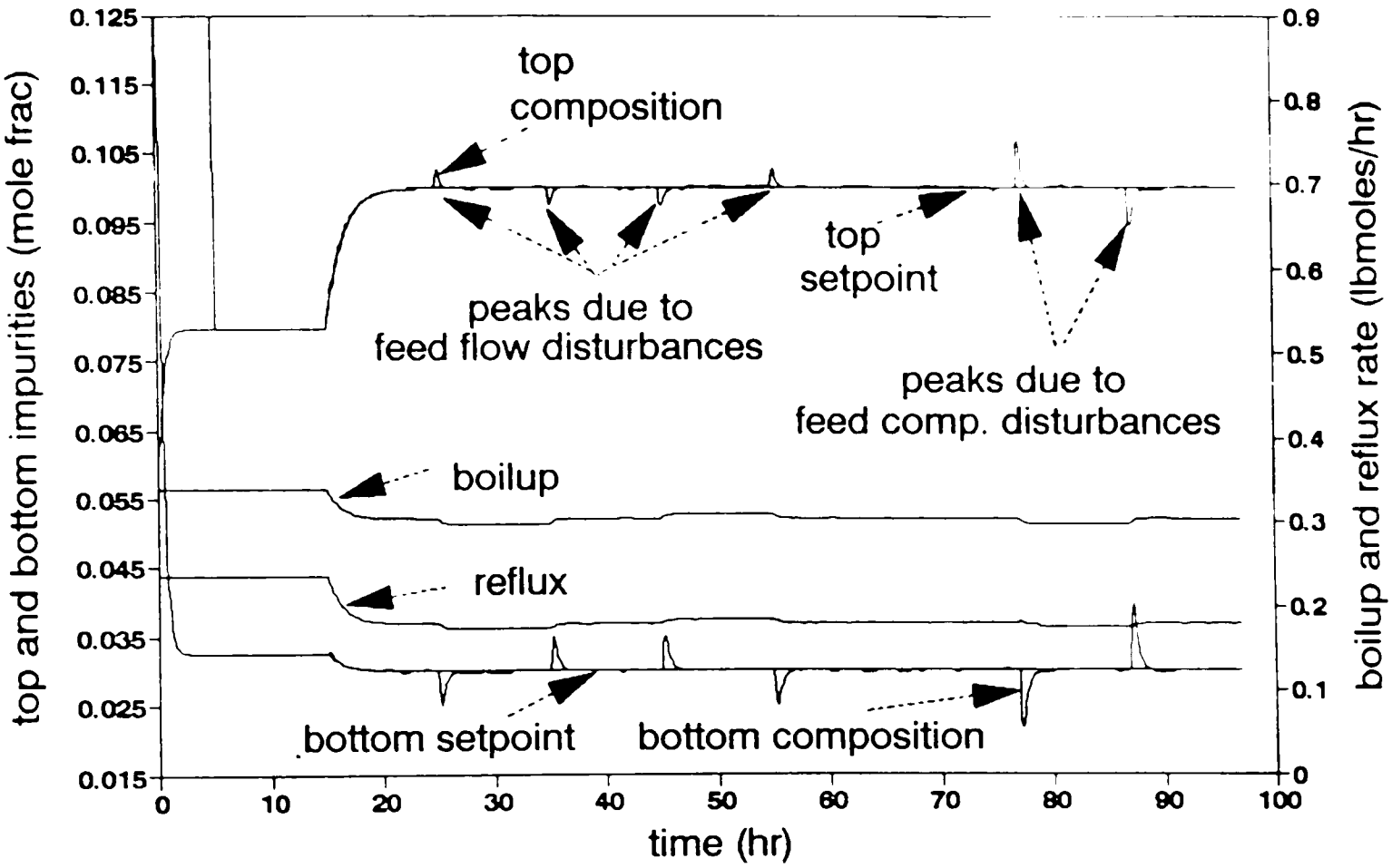

Figure 5.2. Disturbance rejection with NN gain prediction approach on the distillation column simulator.

feed-composition changes. If there is a sudden disturbance in the feed flowrate or feed composition, no major bump occurs in the manipulated variables. The gain changes due to the disturbances remain within the bounded nature of the neural-network output. Unless the process variable deviates from the setpoint, the changes in reflux and vapor boilup calculated from the objective function (Equation 4.15) are always zero. A second advantage is that disturbance measurement sensor faults will not cause a wrong feedforward action. The disadvantage is the delayed response to the upsets. But, as seen in Figure 5.2, the disturbance resulted in small upsets and feedforward action is not necessary.

5.1.2 Distillation Control with Gain Prediction (Constrained Control Mode)

Figures 5.3, 5.4(a) and 5.4(b) describe the controller performance in constraint control mode. In Figure 5.3, the manipulated variables (reflux and vapor boilup rates) are bounded within 0.15 to 0.25 lbmoles/hr and 0.3 to 0.4 lbmoles/hr, respectively. These bounds are characteristic of limits in the experimental process. At the upper bound, the boilup heater uses the maximum power capacity giving rise to a maximum boilup rate (~0.4 lbmoles/hr). If the heating in the boiler falls below certain minimum value (~0.3 lbmoles/hr), the column may be flooded or there may not be enough condensate collected in the reflux drum to maintain the reflux. Similar events happen when the reflux rate goes above a certain value (~0.25 lbmoles/hr) and the corresponding vapor boilup reaches the maximum limit. If the reflux rate falls below a limit (~0.17 lbmoles/hr), the trays in the column become dry, and the separation process stops. It can be observed in Figure 5.3

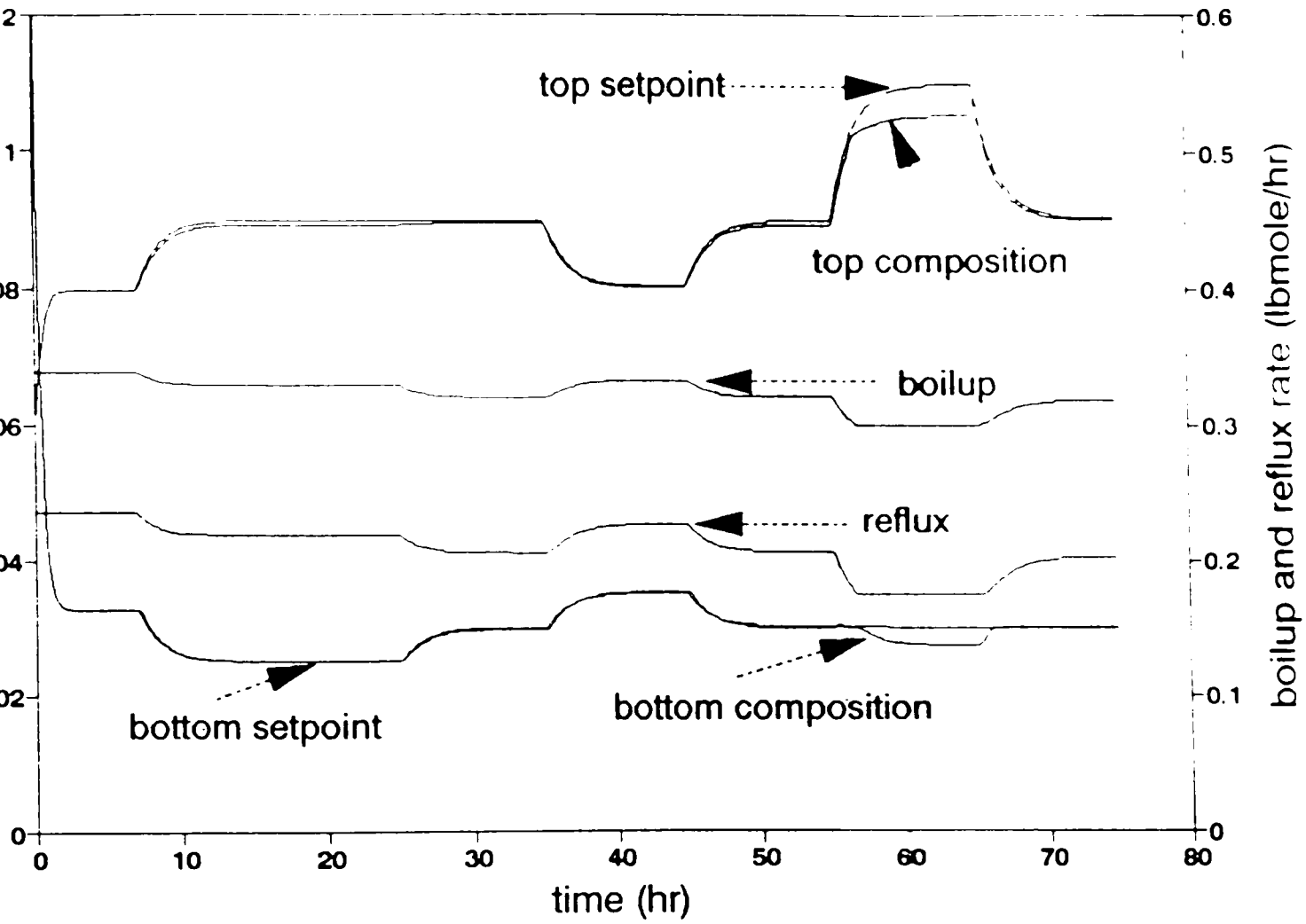

Figure 5.3. Constrained control on simulator with NN gain prediction using setpoint changes.
(0.3<boilup<0.4; 0.15<reflux<0.25).

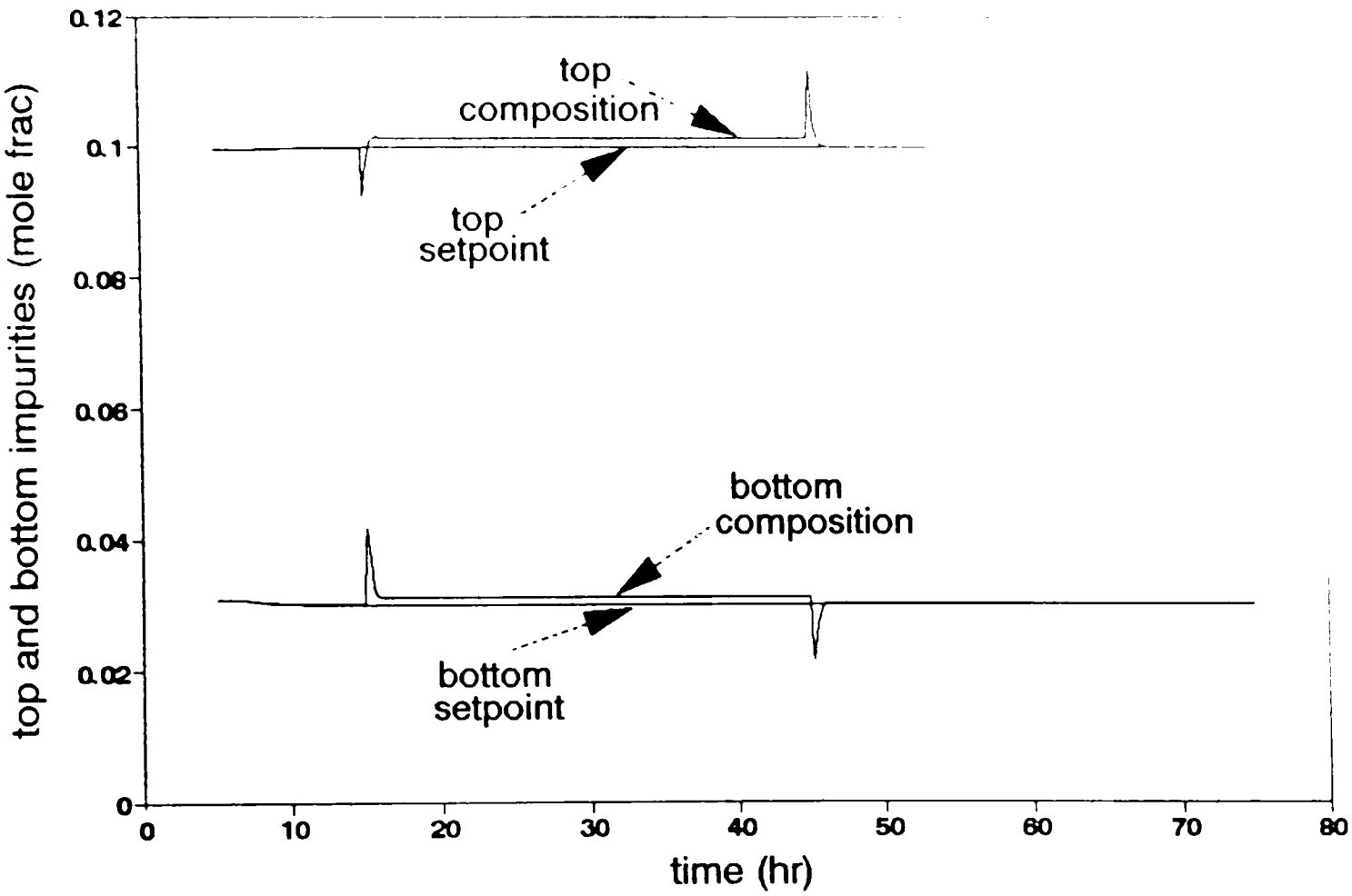

Figure 5.4. Constrained control on simulator with NN gain prediction using feed composition disturbance. (a) Top and bottom compositions.

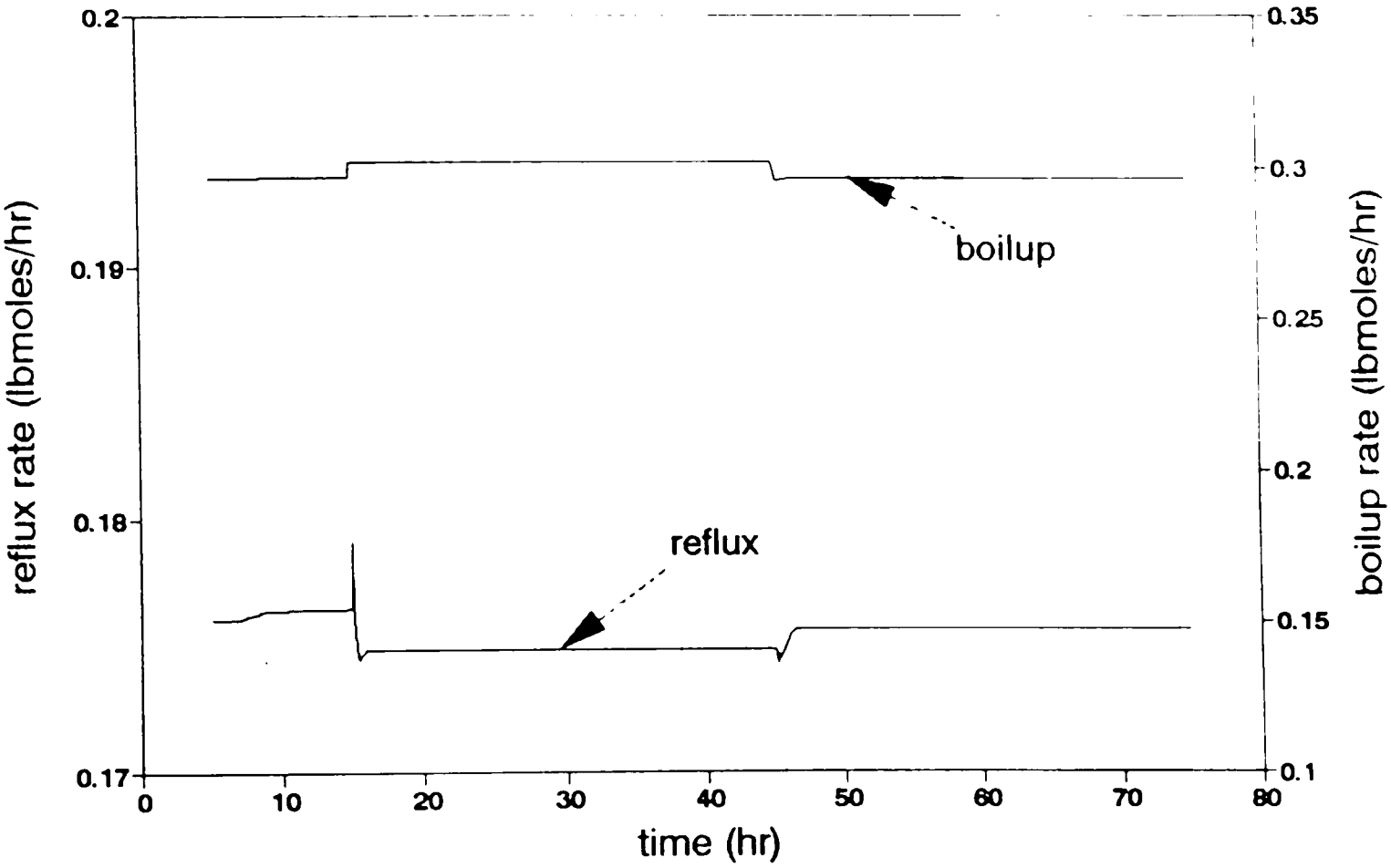

Figure 5.4. Continued. (b) Reflux and boilup rates.
(0.2<boilup<0.3; 0.15<reflux<0.25).

that a large setpoint change is given in the top composition at the 55 hour mark (91 mol% to 89 mol% purity ≈ 9 mol% to 11 mol% impurity). As a result, the reflux rate and the boilup rate start decreasing. Within a couple of hours, the boilup rate hits the minimum constraint. The reflux rate also settles down to about 0.17 lbmoles/hr (well within the bounds) after attaining the minimum of the objective function (Equation 4.15 with Eq_1 and Eq_2 taken as unity). Both the top and the bottom impurities are maintained below their setpoints. These deviations are expected because of the constraint on the boilup rate. At this point, the reflux should decrease to attain the top setpoint. However the control problem is multivariable and the reflux flowrate cannot fall below certain rate because it would decrease further the bottom impurities. Figures 5.4(a) and 5.4(b) show just the reverse trend when the boilup rate is given another bound (0.2-0.3 lbmoles/hr) and allowed to hit the upper constraint. In this case, the boilup rate changes in response to the feed-composition change (20 mol% to 22 mol%). It can be observed in Figures 5.3 and 5.4(a), that the controller is able to respond by coming out of the constraint when the setpoint or the feed composition is set back to its original value. The recovery from the constrained condition is immediate. There is no problem such as integral windup at the constraint.

5.2 Experimental Results

5.2.1 NN Control in State Inverse Mode on SISO Systems (Heaters)

The neural network model-based inverse of steady-state prediction approach is first tested on two separate single-input-single-output (SISO) systems (feed and reflux

preheaters) prior to the implementation on the multi-input-multi-output (MIMO) system (distillation column). The detailed control strategy is discussed in Section 4.1. The performance of this nonlinear NN model-based controller is compared to other linear controllers (e.g., proportional-integral, PI; internal model, IMC; and model predictive controllers, MPC).

In this experiment, a mixture of water and methyl alcohol is passed through a feed preheater at a rate of 40 ml/min. Various steady-state temperatures are then obtained by providing different heating rates (correspond to counts in KDAC system). The process response is a sigmoidal shaped curve, as shown in Figure 5.5. The process gain changes from 0.0014 to 0.176 ^{o}F per count over the entire operating range. Figure 5.6 shows the neural network model prediction on the training data.

Figure 5.7 shows the conventional proportional integral (PI) controller performance. It is interesting to note that the PI controller shows the distinct sluggishness at the setpoint level of 130 and 140^{o}F, but shows much more aggressiveness at the 120^{o}F (even with some overshoot). The control interval is taken as a half-minute in all the experimental runs. The tuning parameters of all the control algorithms are adjusted to give a smooth response for 130-140 ^{o}F without producing excessive oscillations at the 120^{o}F.

An Internal Model Control (IMC) structure (Garcia and Morari, 1985) calculates the control action necessary to keep the process on a desired path to the setpoint. A filter is applied on the feedback signal in order to improve robustness by slowing the desired response. In the experiment, an average first-order-plus-dead-time (FOPDT) model is obtained from the step test data to represent the behavior over the entire operating region.

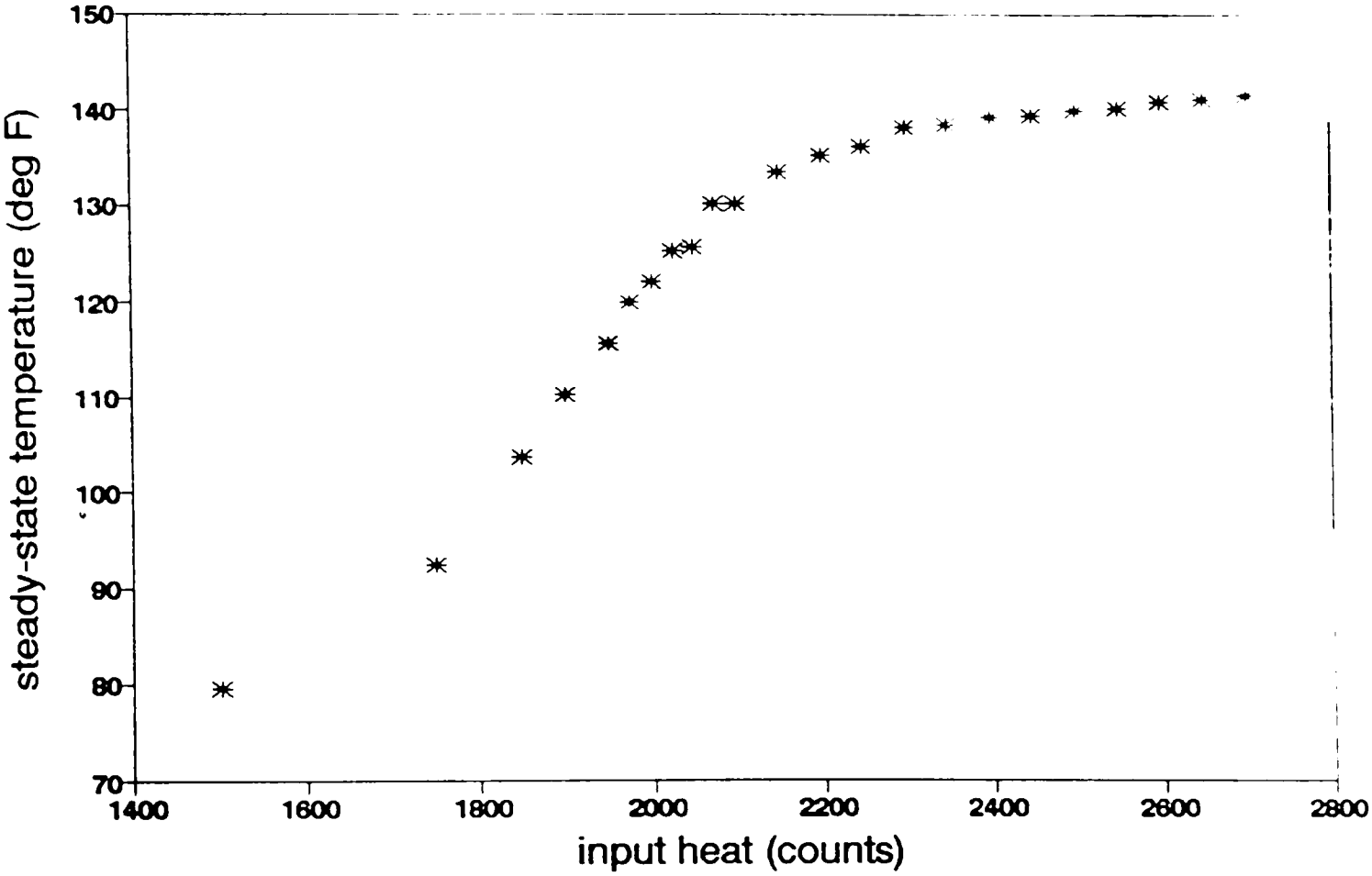

Figure 5.5. Steady-state temperature profile of feed preheater.

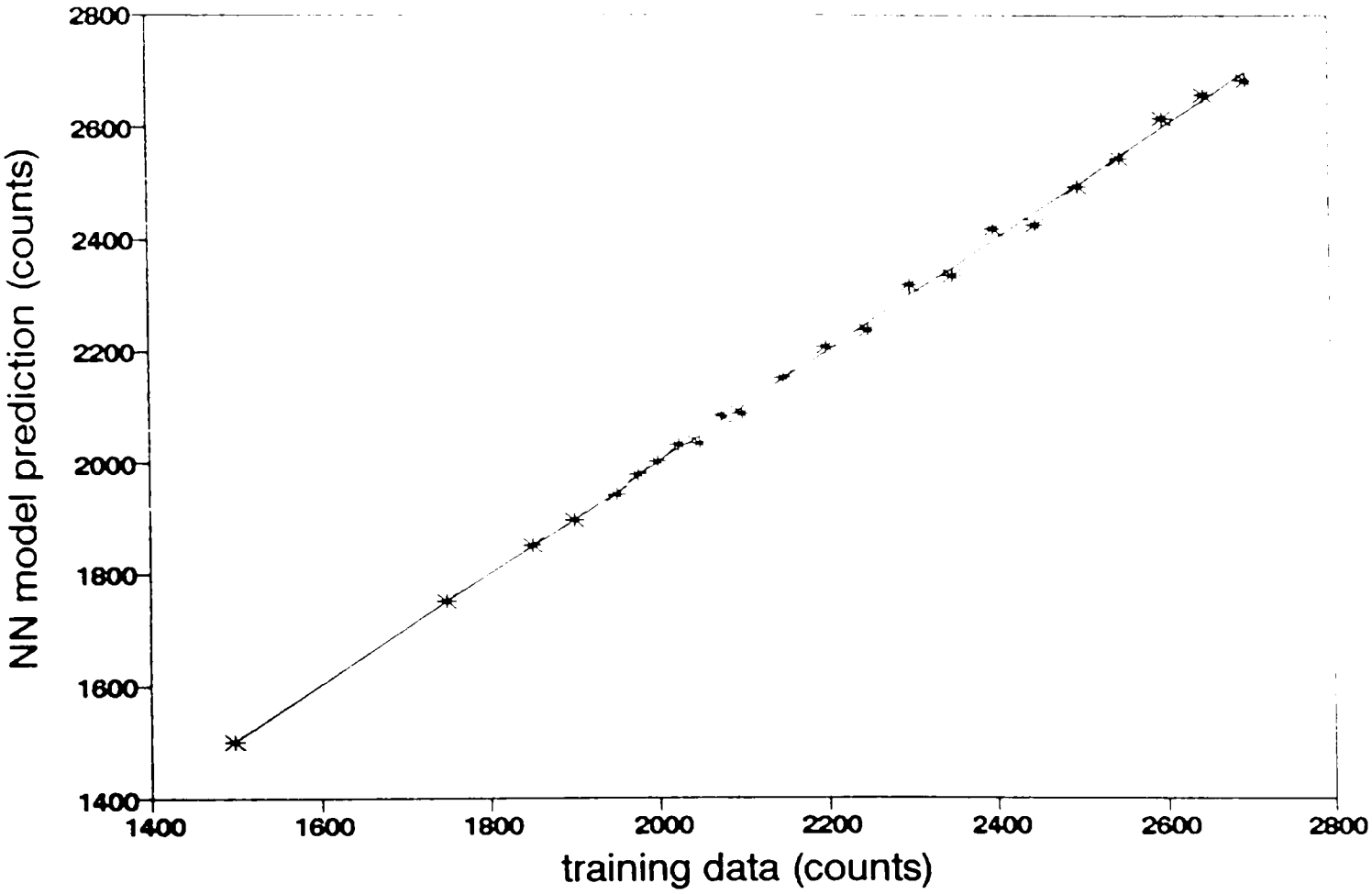

Figure 5.6. Training result on manipulated variable of feed preheater.

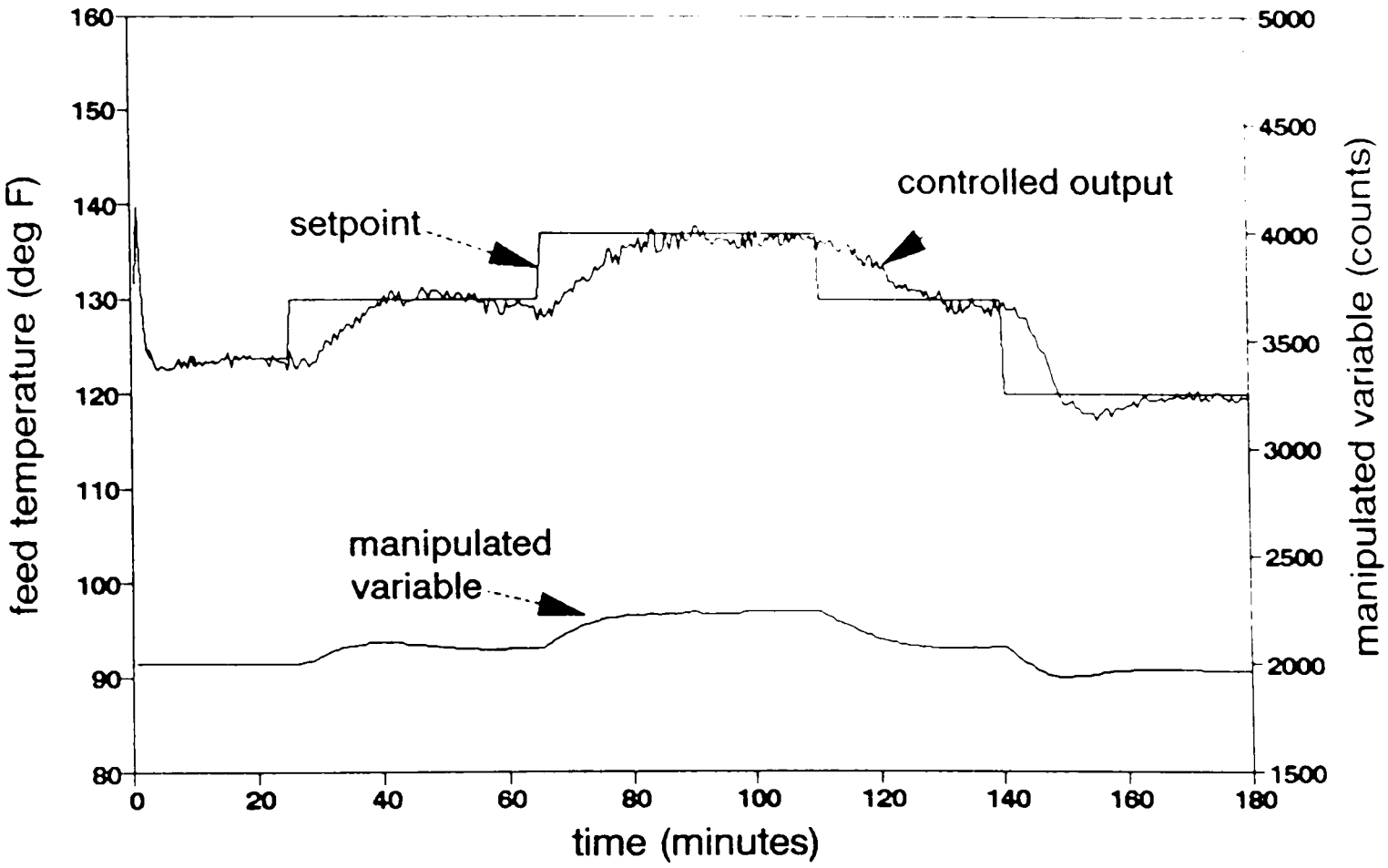

Figure 5.7. PI control of feed preheater.

The Nelder-Mead nonlinear optimization procedure is used to fit the data to the model. The process gain, time constant and dead time are found to be 18.55°F per 1000 count, 4.34 minutes and 2.0 minutes, respectively. The result is shown in Figure 5.8. The tuning constant for IMC, the filter factor, is kept slightly more aggressive than the PI. The presence of nonlinearity in the process is very clear in this case. The IMC controller seems to be doing fairly well at 130 and 140°F, but produces oscillations at 120°F.

The model predictive controller (MPC) follows the work of Cutler and Ramaker (1979). The manipulated variable damping approach is used, and the control objective function is defined as

$$\underset{\Delta u}{\text{Min}}\{\sum^{H} \left|\Delta_{PF}Y - \Delta_{r}Y\right|^{2} + f\sum^{n}(\Delta u_i)^2\} \qquad (5.1)$$

where $\Delta_{PF}Y$ is a vector of predicted future output in the deviation variable for the future Δu's, and $\Delta_{r}Y$ is the desired set point for the deviation variable. The n and H are control and prediction horizon respectively. The control variable output with MPC (Figure 5.9) shows a very similar performance as with IMC and PI. The tuning constant, the move suppression factor 'f', has been tuned for the setpoint change of 130 to 140°F. This tuning produces oscillations at the temperature level of 120°F. The limitation in this control algorithm is the same as in IMC or PI, i.e., the time-series model using the vector coefficients is a linear and stationary model. It failed to accommodate the nonlinearity in the system.

Figure 5.10 shows that the controller, using the GMC law and the NN inverse-steady-state model, produces no oscillations at 120°F. Despite the unmeasured modeling

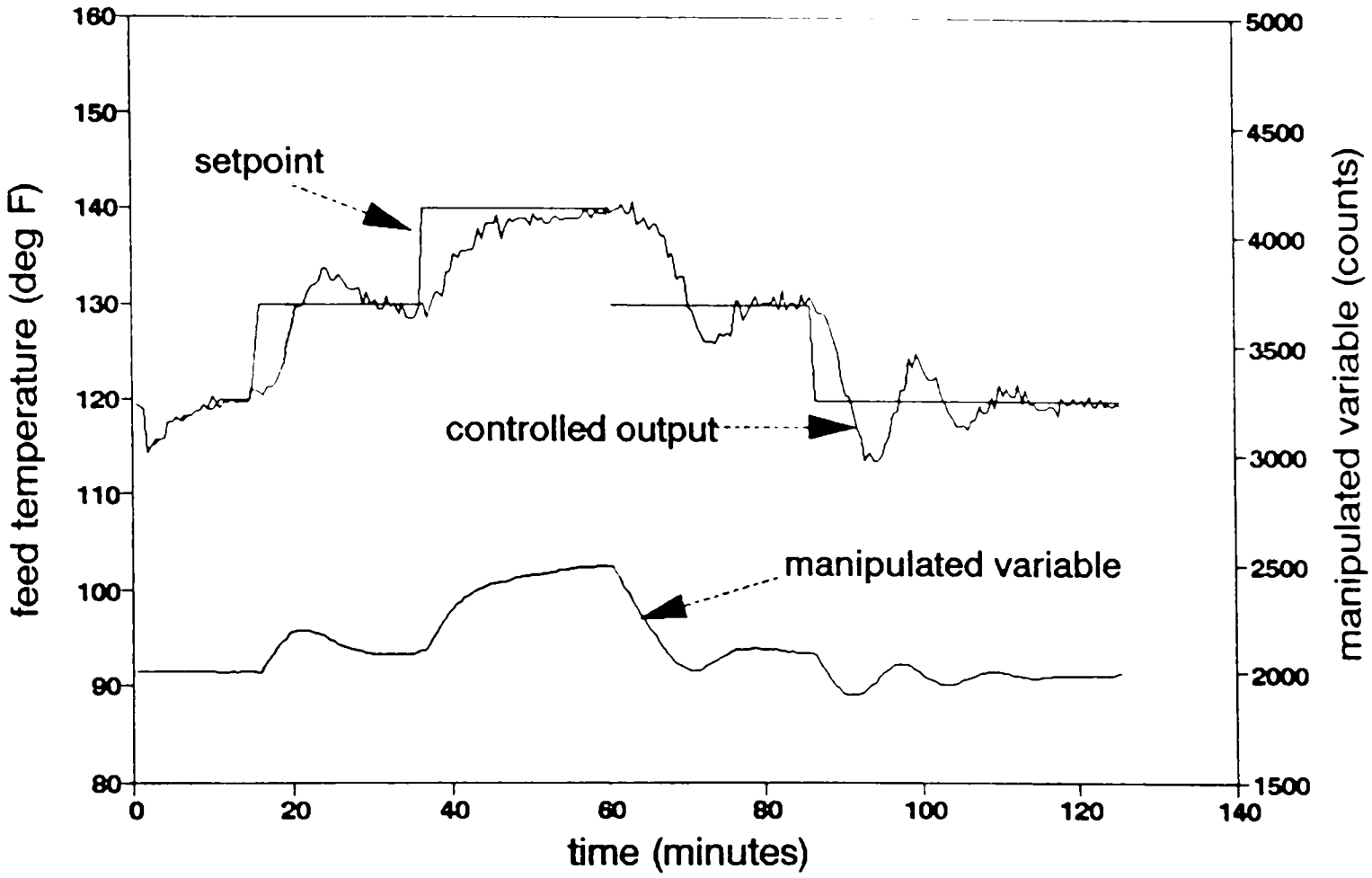

Figure 5.8. Internal model control on feed preheater.

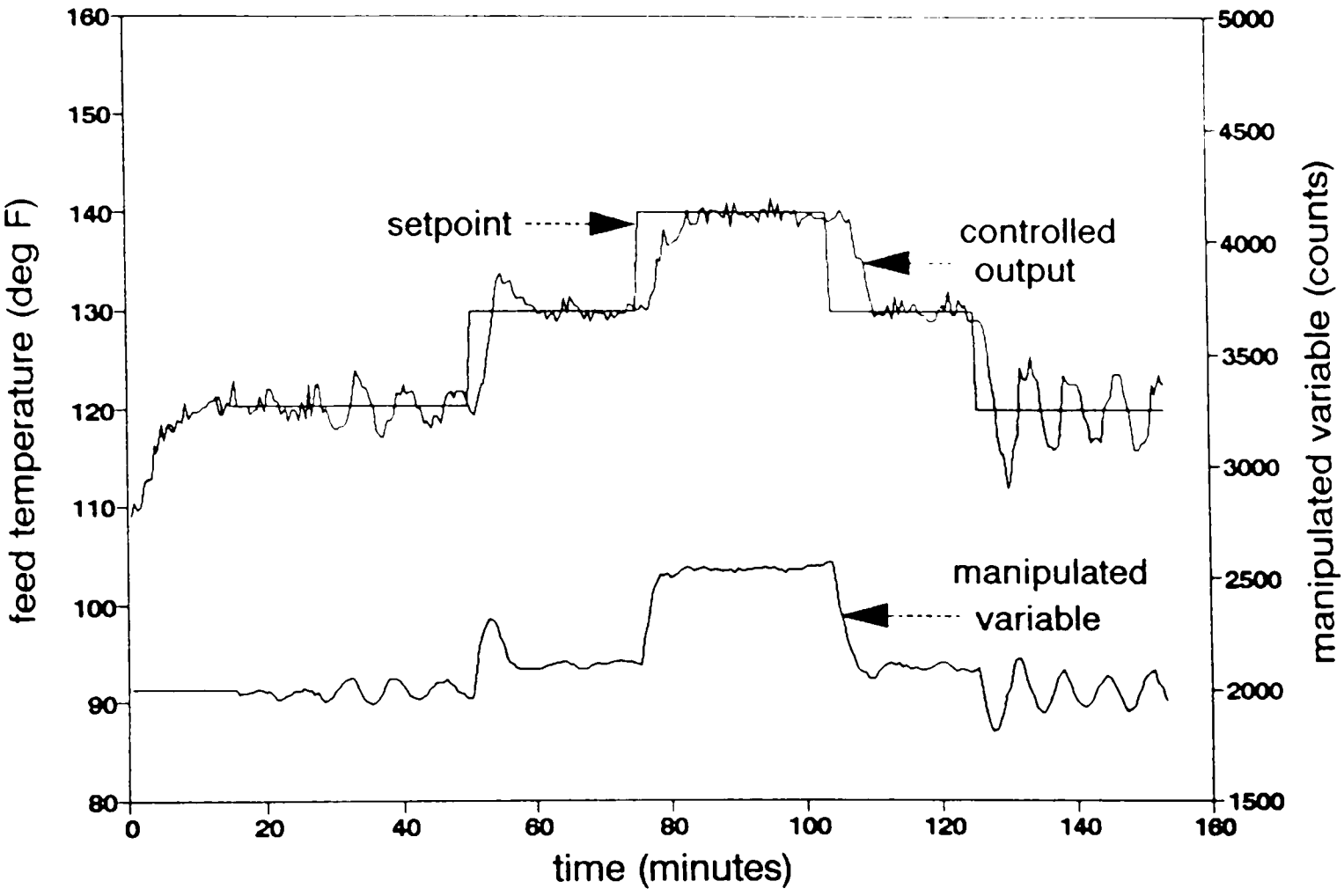

Figure 5.9. Model predictive control on feed preheater.

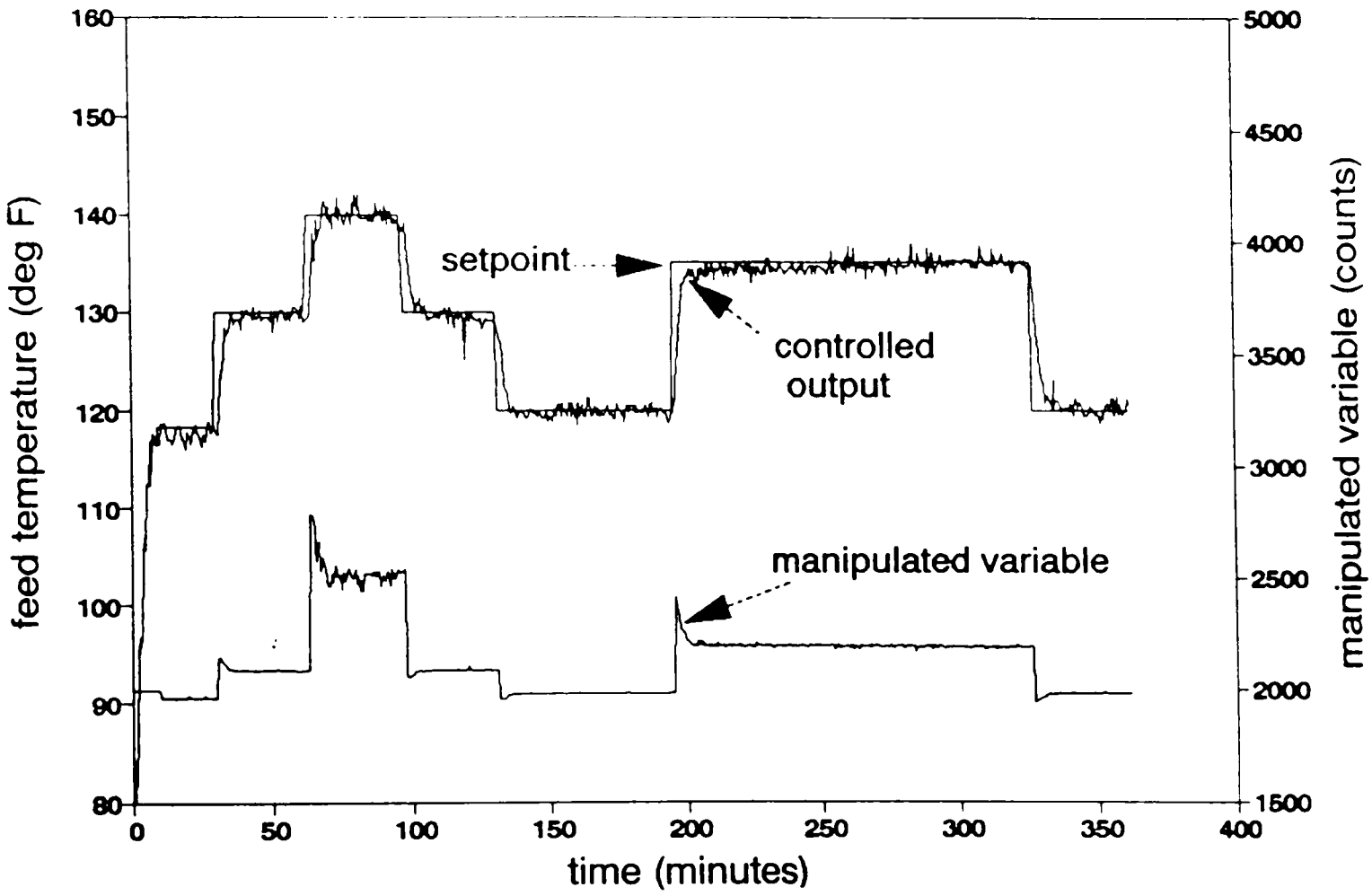

Figure 5.10. Neural network control on feed preheater.

errors or parameter errors, the controller is able to return the process to the setpoint with zero offset in a smooth manner. The manipulated variable moves are much larger at the temperature level of 130 and 140^{o}F in comparison to 120^{o}F. This variation of movements in manipulated variables further illustrates the "gain scheduling" inherent in this controller. A quantitative analysis of the controller performance is shown in Table 5.3. The values of Integral of Square Error (ISE), Integral of the Absolute Error (IAE), Integral of the Time-weighted Absolute Error (ITAE) and total manipulated variable movements are calculated over a time interval of 25 minutes, after the setpoint changes are introduced. This is approximately the maximum time taken by the controller to bring the process to its new setpoint.

Table 5.3 Comparative Study on Feed Preheater Control

	Setpoint Change 130-140^{o}F				Setpoint Change 130-120^{o}F			
	PI	IMC	MPC	NN	PI	IMC	MPC	NN
Rise time (min.)	18.0	23.5	7.5	6.0	9.0	5.0	7.5	4.0
Overshoot ($^{\circ}$F)	0.84	0.9	1.02	1.28	-2.81	-6.27	-1.02	-0.8
ISE ($^{\circ}$F)^2.min	940	840	630	480	910	870	630	290
IAE ($^{\circ}$F) .min	170	140	100	85	155	165	100	60
ITAE ($^{\circ}$F).min^2	1225	845	535	485	1130	1845	535	385
$\sum\lvert\Delta u\rvert$ (counts)	175	395	710	2385	175	1695	710	195

Although the artificial neural network (the steady state form as used) does not take into account time delays that affect the dynamics of the system (i.e., the NN 'believes' that input changes produce an immediate output change), the use of a lower value of the integral gain (K_2) helped in restraining a large overshoot, but still eliminated the offset successfully. As a result, the controlled output is found to be more aggressive, reducing the rise-time, as compared to the linear controller. The neural-network model-based controller is able to produce low ISE (Integral of the Square error), IAE (Integral of the Absolute Error) and ITAE (Integral of the Time-weighted Absolute Error). The neural network controller's success can solely be attributed to its capability to adapt its gain according to the process gain changes. Since the process gains differ significantly (almost 12-14 times) at the 140^{o}F level in comparison to 120^{o}F, the manipulated variable movement also adjusts itself accordingly. As a result, Table 5.3 shows a higher cumulative of absolute manipulated variable movement ($\sum|\Delta u|$) in NN control performance (almost 12 times that of PI). While not shown here, operating experience qualitatively indicates that regulatory performance gives a similar result. A similar NN model-based inverse of a state-prediction controller is implemented on the reflux heater as well. Figure 5.11 shows the neural network training result. The performance of this controller in response to setpoint changes and disturbances is shown in Figure 5.12. In this experiment, reflux flowrate changes are given from 40 to 35 ml/min, 35 to 45 ml/min and 45 to 40 ml/min at time t = 275, 295 and 335 minutes, respectively, along with the various setpoint changes.

The neural network controllers, representing the inverse of a steady-state of the process and generic model control law as the reference system trajectory, show excellent

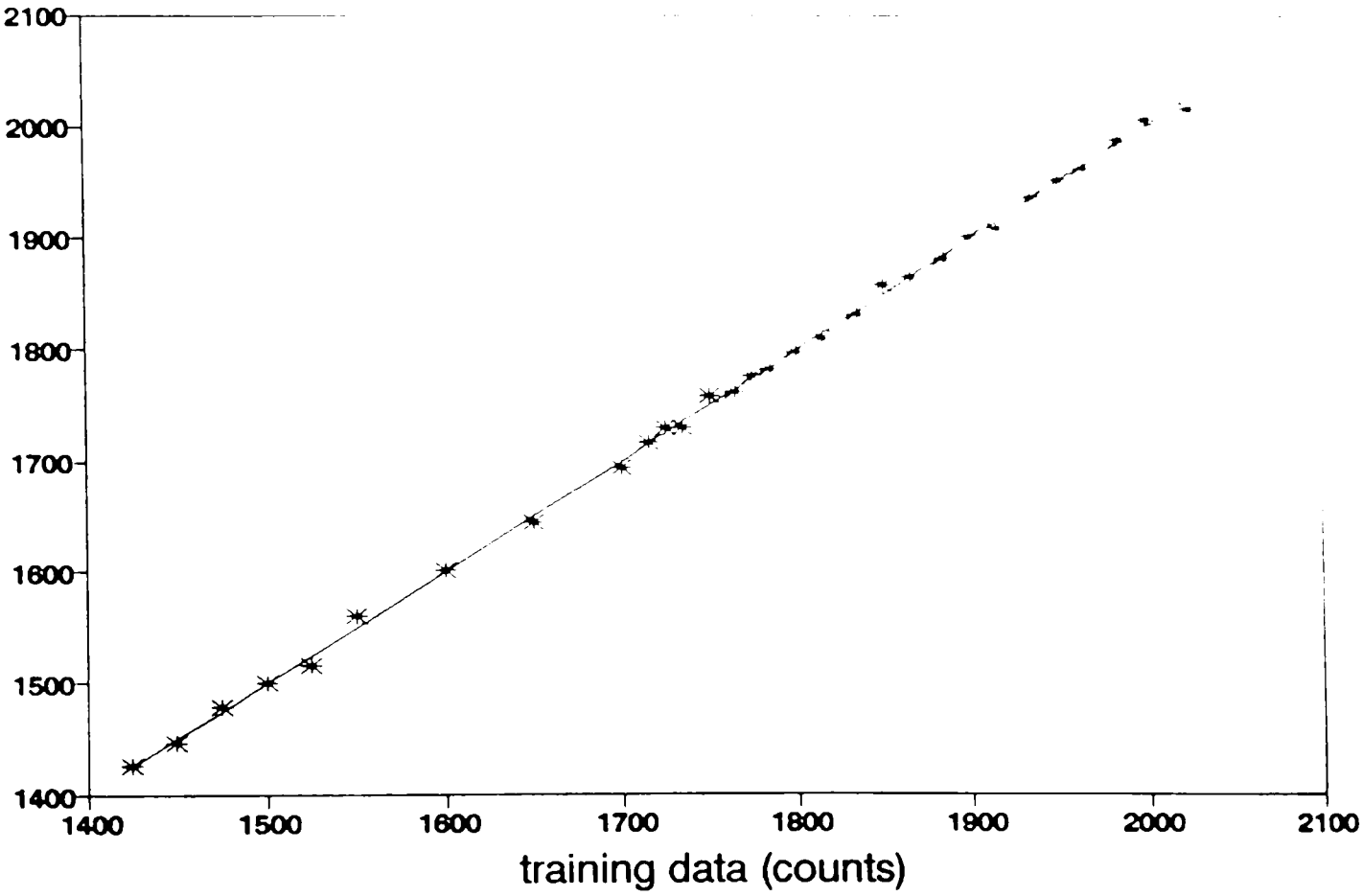

Figure 5.11. Training result on manipulated variable of reflux preheater.

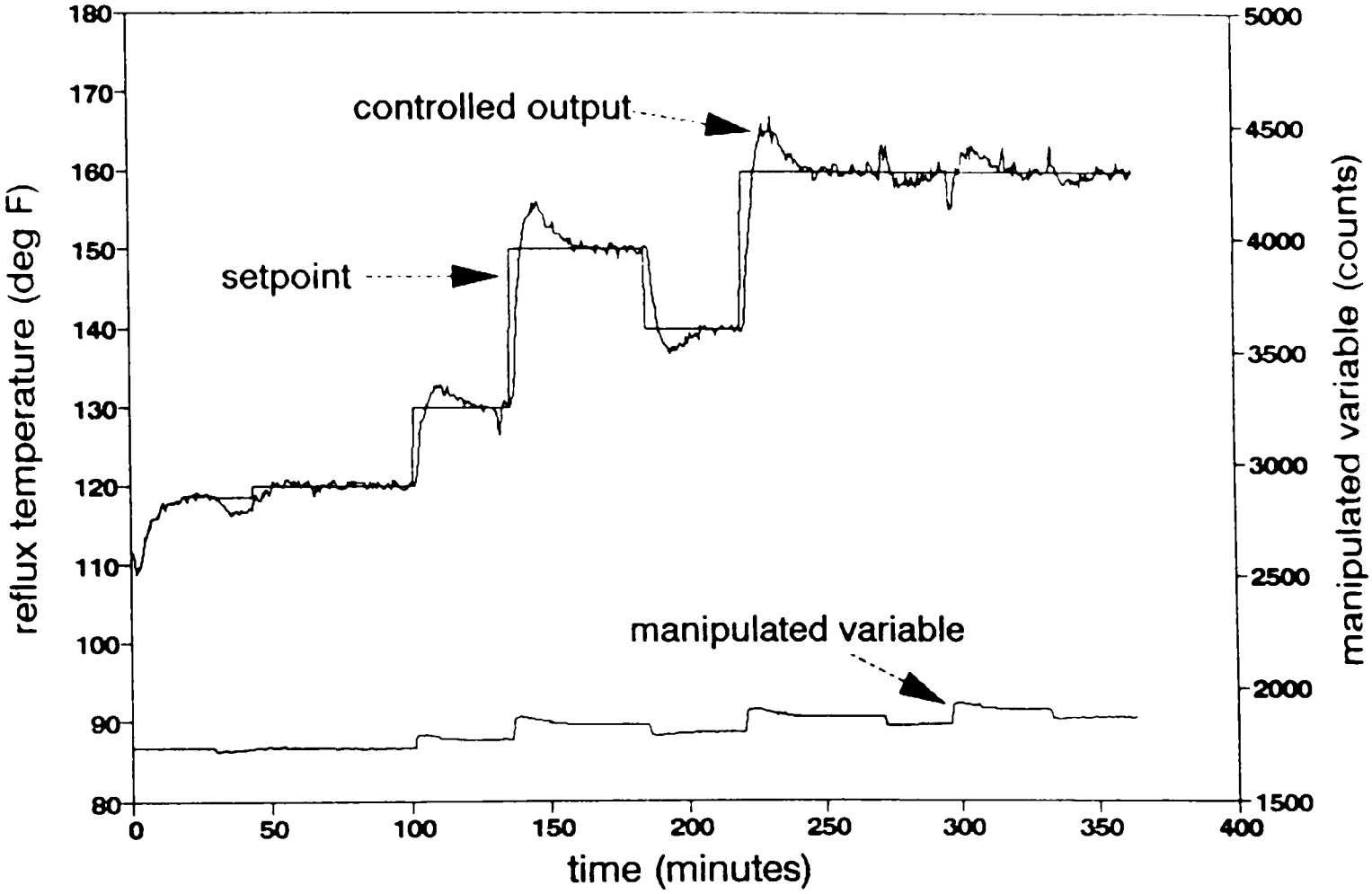

Figure 5.12. Neural network control on reflux preheater.

control on the two electrical preheaters. The linear controllers show poor performance outside the tuned range

5.2.2 NN Control in State Inverse Mode on Distillation Column

This section presents the experimental control results obtained using the neural network model-based inverse of steady-state-prediction approach as discussed in Section 4.1 and following the control strategy as shown in Figure 4.1. The neural network models are developed based on the training of steady-state data sets (209 data sets) generated using the simulator in the operating region of the experiment. Figures 5.13(a) and 5.13(b) show the predicted outputs (vapor boilup rate and reflux rate respectively) by the NN model on the training data sets.

A typical experimental run for dual-composition control is about 7-8 hours. There are three phases in an experimental run.

1. The distillation column is started up in the manual mode by introducing fixed manipulated variables (i.e., fixed reflux and boilup rate), and the process is allowed to settle down to a near-steady-state.
2. The controller is then brought on-line, and the desired setpoints are entered for the top and bottom compositions. The controller controls the column at these conditions, responding to unintentional disturbances, noise, and drifts in the process.
3. After good control is established, either a setpoint change or a disturbance is introduced. The controller controls the column at the desired setpoints of the top and bottom compositions and eliminates any disturbance.

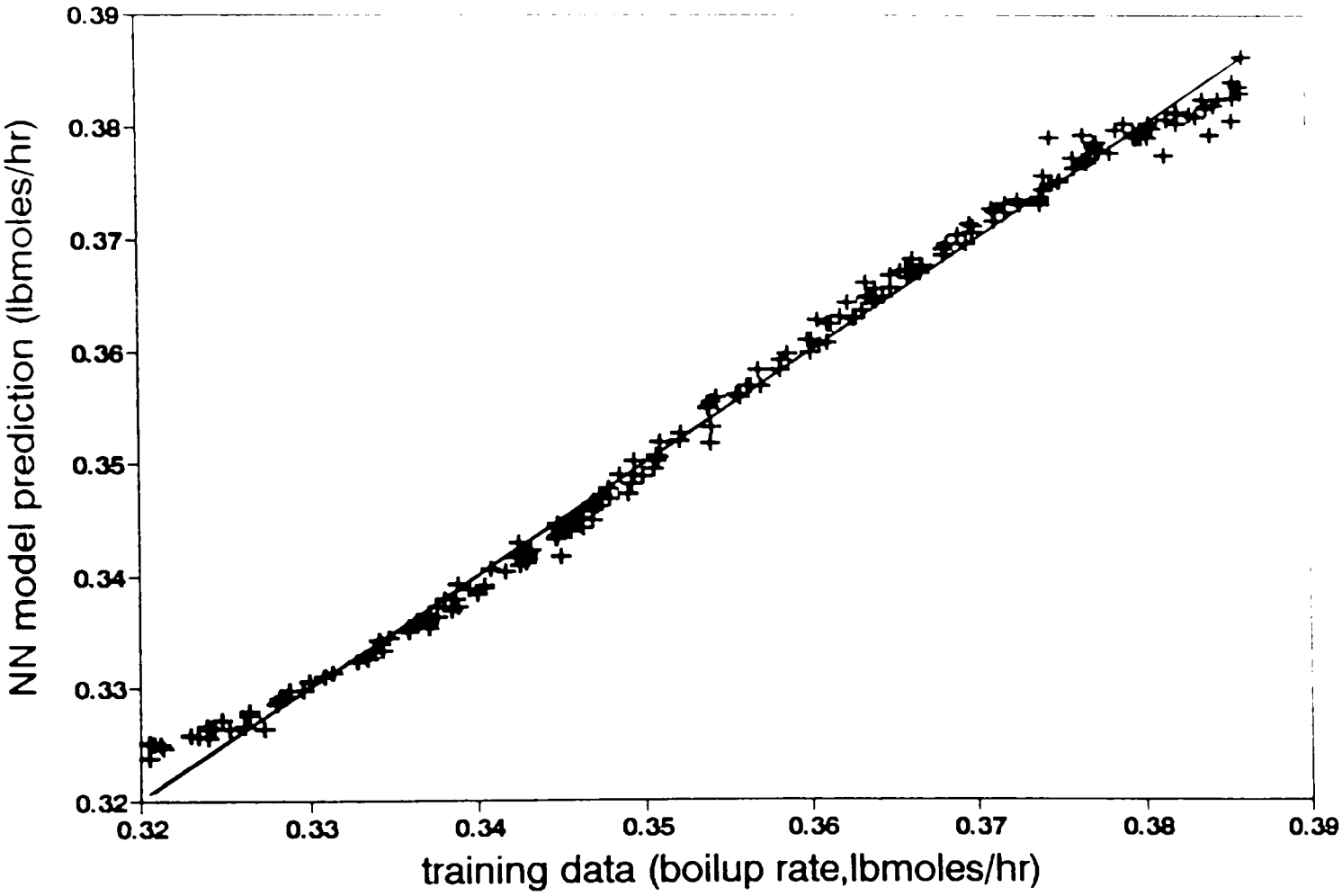

Figure 5.13. Training result on manipulated variables in inverse of steady-state prediction mode. (a) Vapor boilup rate.

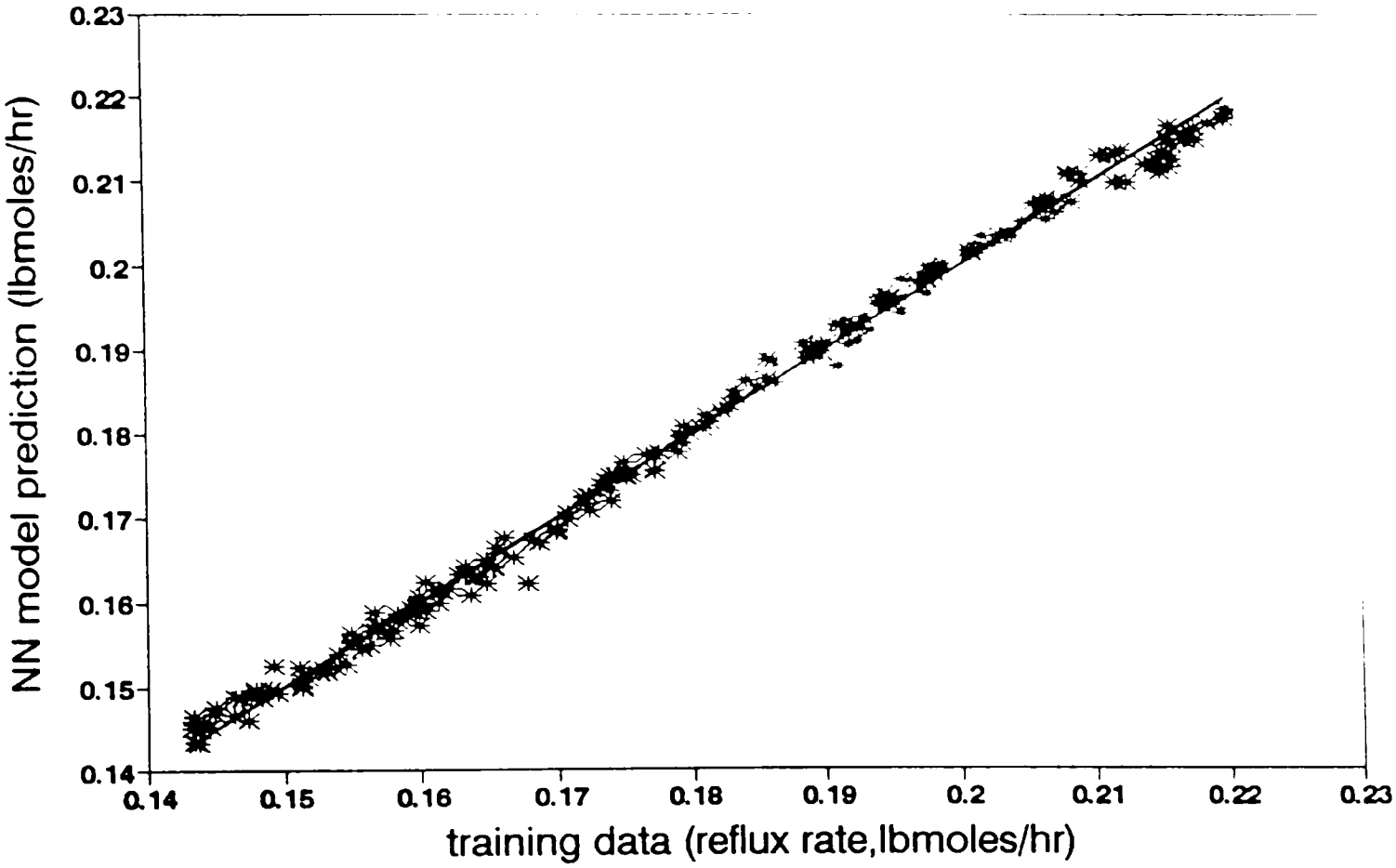

Figure 5.13. Continued. (b) Reflux rate.

For all the runs, the operating conditions are tabulated and the controller performance is presented with the figures of the controlled variables, i.e., the top and bottom compositions and the manipulated variables, i.e., the reflux flow rate and the vapor boilup after converting 'counts' to 'gmoles/hr' using the correlation as described in Appendix C and Appendix D.

Table 5.4 lists the experimental runs discussed in this section. These sets of experiments are done to reproduce Pandit's PMBC (1991) and Gupta's DMC and Advanced Classical Control (ACC) (Gupta, 1994) experimental runs for a one-on-one comparison of control techniques. Both setpoint tracking and disturbance rejection results are discussed below.

5.2.2.1 Setpoint Tracking

Figures 5.14(a), 5.14(b) and 5.14(c) show the column performance for simultaneous setpoint changes in the top and bottom compositions. The conditions are summarized in Table 5.5. As seen in Figure 5.14(a) and 5.14(b), the top composition setpoint is changed from 86.0 mole% to 91.0 mole% methanol, while the bottom composition setpoint is changed from 1.4 mole% to 5.0 mole% methanol. Figure 5.14(c) shows the changes in manipulated variables during the run. The column is started in an open-loop fashion by providing a constant boilup rate of 162 gmoles/hr. Once the vapor starts condensing at the condenser, the reflux pump is started at a constant rate of 78 gmoles/hr. At about 60 minutes, the controllers are put into automatic mode with setpoints of 86 mole% for the top composition and 1.4 mole% for the bottom

Table 5.4. Synopsis of Experimental Runs in Control Performance Study

Objective	Case Number	Changes Made
Setpoint Tracking	1	Top : 86% to 91% Methanol Bottom : 1.4% to 5% Methanol
Disturbance Rejection	2	Feed Composition Disturbance (20% to 35% Methanol (+55% relative)
,,	3	Feed Composition Disturbance (30% to 20% Methanol (-40% relative)

Table 5.5. Setpoint tracking with neural network control in inverse of the state prediction mode (Case 1)

Operating Characteristics	Initial Operating Conditions	Final Operating Conditions
Feed Rate (mols/hr.)	220.0	220.0
Feed Composition (mol % methanol)	20.0	20.0
Feed Temperature (deg F)	100.0	100.0
Reflux Rate (mols/hr.)	73.0	101.0
Reflux Temperature (deg F)	110.0	110.0
Vapor Boilup (mols/hr.)	156.0	168.0
Top Composition (mol % methanol)	86.0	91.0
Bottom Composition (mol % methanol)	1.4	5.0

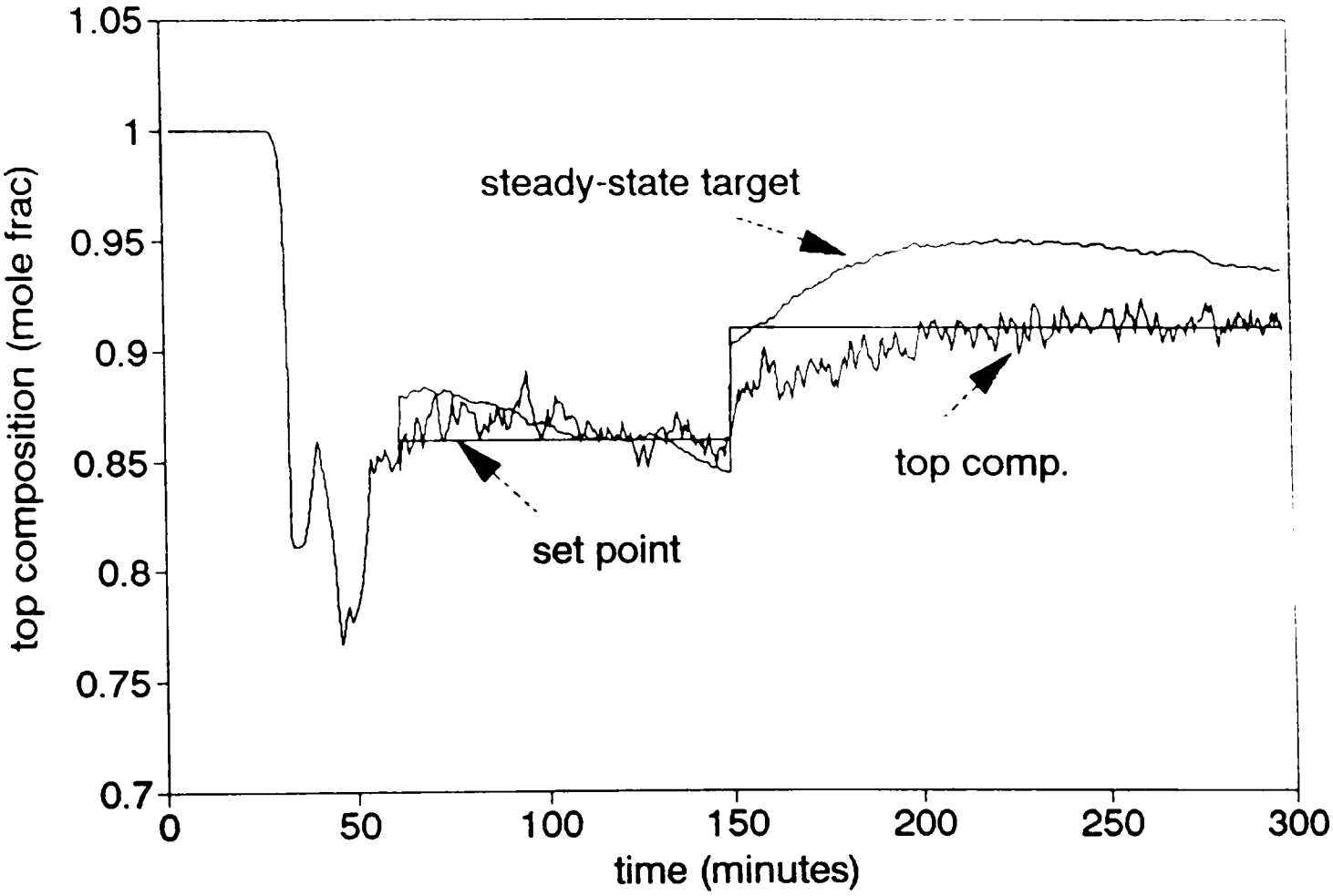

Figure 5.14. Setpoint tracking with neural network control in inverse of steady-state prediction mode (Case 1). (a) Top composition.

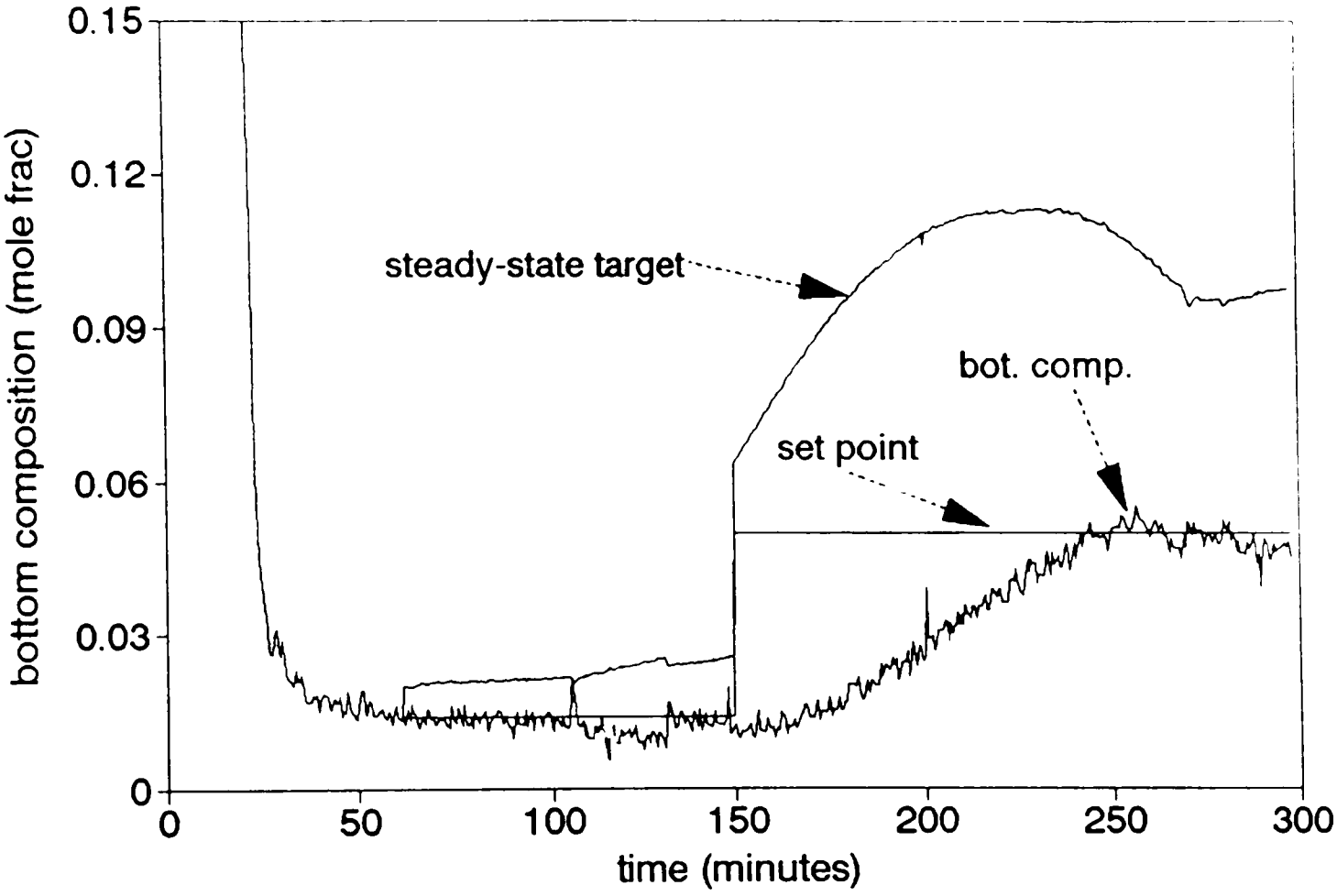

Figure 5.14. Continued. (b) Bottom composition.

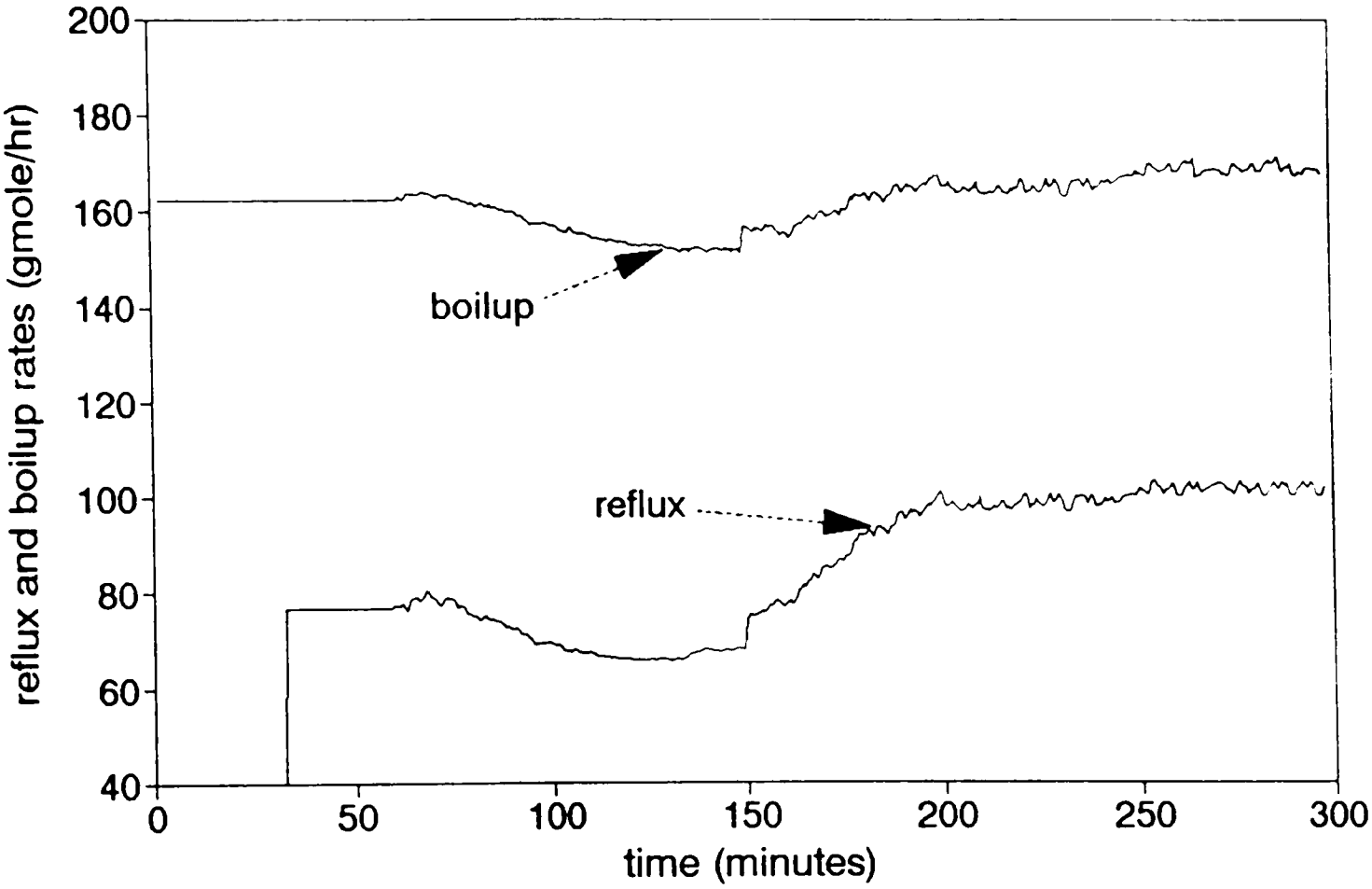

Figure 5.14. Continued. (c) Manipulated variables.

composition. At 150 minutes, simultaneous setpoint changes to 91 mole% and 5 mole% are given for the top and bottom compositions, respectively. After the changes are made, the top composition takes about 50 minutes to settle down to the new setpoint while the bottom composition takes about 100 minutes. The manipulated variable action is shown in Figure 5.14(c). Immediately after the controllers are put into automatic, the manipulated variables start moving to maintain the process at the setpoints. Sharp step changes in the manipulated variables are also expected at the point of simultaneous setpoint changes.

Figures 5.14(a) and 5.14(b) also show the steady-state target values (i.e., the outputs of the GMC law) for the top and bottom compositions. The values of K_{1D}, K_{2D}, K_{1B}, K_{2B} (Equation 4.6 and 4.7) as used in this experimental run are 1.1, 0.028 min^{-1}, 1.1, 0.02 min^{-1}, respectively. These parameter values are achieved by "field tuning" on-line, for good servo control, as an experienced operator would tune conventional decoupled PI controllers. This tuning took a total of 10 runs.

It is observed that the integral values (i.e., K_{2D} and K_{2B}) produce maximum effect in terms of the aggressiveness of the controller and eliminating the offset. The process responds slowly to the changes of the manipulated variables, suggesting that the process is primarily an integrating process. An increase in the proportional values (i.e., K_{1D} and K_{1B}) requires a decrease in the integral values in order to keep the process away from the constraint and to avoid any integral windup. Lower values of the integral terms would result in an offset. It is also observed that because of the relatively faster dynamics of the top composition, the performance of the dual-composition control mode (in terms of rise time, settling time, etc.) depends mainly on the tuning of the bottom

composition control loop. The tuning ranges of K_{1D}, K_{1B}, K_{2D} and K_{2B} explored on the experiment are (0.7 -2.0), (0.7 - 2.0), (0.015-0.05) $\min^{-1}$ and (0.015 - 0.05) $\min^{-1}$, respectively.

The initial deviations in the steady-state target values from the actual compositions at the transfer to the automatic mode, as observed in Figures 5.14(a) and 5.14(b), are due to the process-model mismatch represented by the bias terms of Equation 4.6 and 4.7. The controller has been able to accommodate this process-model mismatch and maintain both the top and bottom compositions successfully at their respective setpoints.

5.2.2.2 Disturbance Rejection

Two types of disturbances were investigated by the previous researchers on this particular column. One is the feed-flowrate disturbance and another is the feed-composition disturbance. It has been observed that a feed flowrate disturbance (+20% or -20%) from 220 gmoles/hr (base value of the present experiment) does not produce significant deviations in the top and bottom compositions compared to the feed-composition disturbance. Therefore, in this research, only feed composition disturbances are introduced and analyzed for the control study.

The feed composition disturbances are introduced according to Case 2 and Case 3 shown in Table 5.4. The detailed operating conditions during these experimental runs are shown in Tables 5.6 and 5.7. Figures 5.15(a) and 5.15(b) show the control results for a feed-composition disturbance from 20 mole% to 35 mole% (+55% relative) methanol, introduced at a time about 70 minutes intto the run. Because of this disturbance, the top

Table 5.6. Disturbance rejection with neural network control in inverse of the state prediction mode (Case 2)

Operating Characteristics	Initial Operating Conditions	Final Operating Conditions
Feed Rate (mols/hr.)	220.0	220.0
Feed Composition (mol % methanol)	20.0	35.0
Feed Temperature (deg F)	100.0	100.0
Reflux Rate (mols/hr.)	73.0	58.0
Reflux Temperature (deg F)	110.0	110.0
Vapor Boilup (mols/hr.)	156.0	160.0
Top Composition (mol % methanol)	90.0	90.0
Bottom Composition (mol % methanol)	2.1	2.1

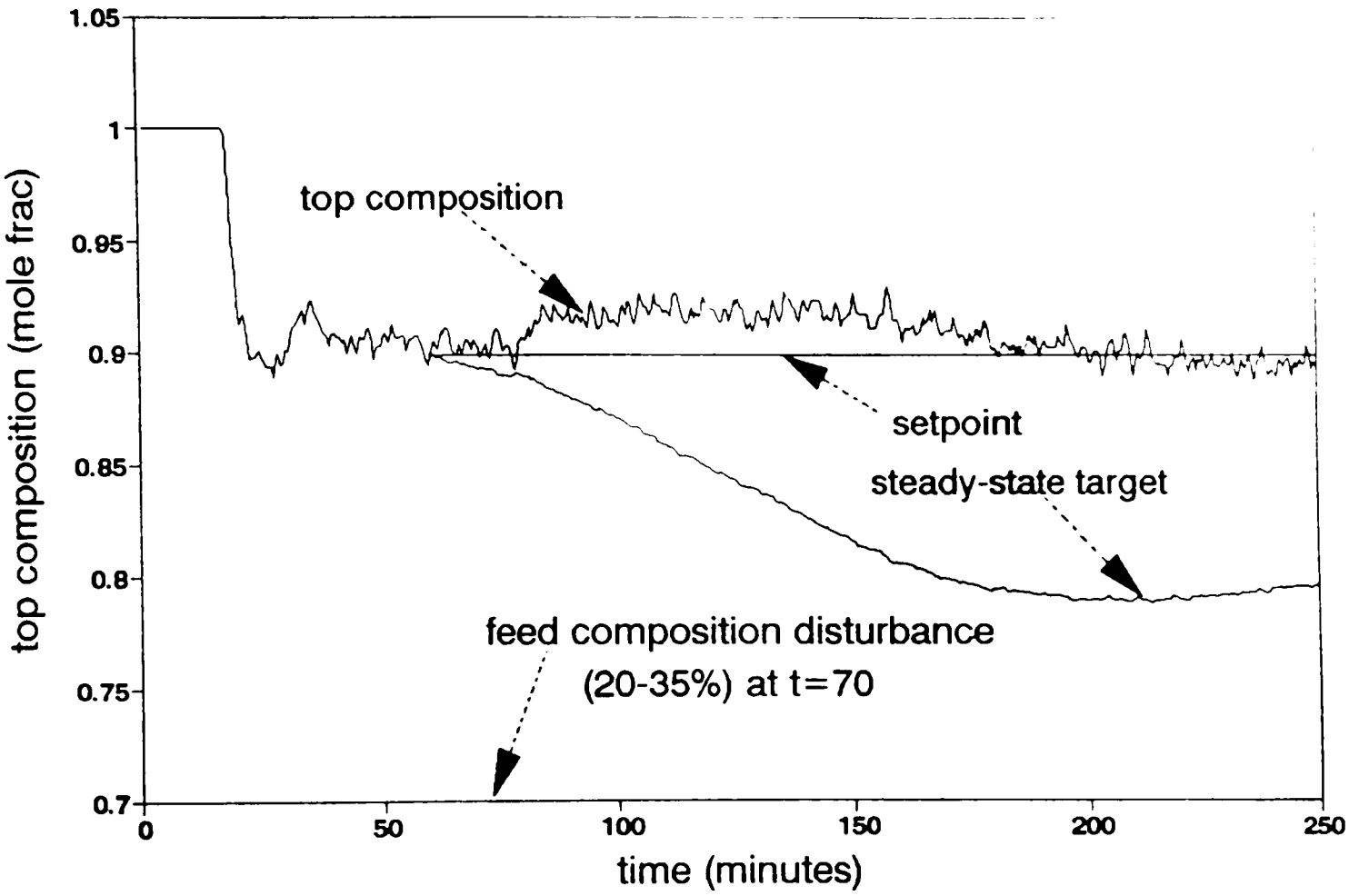

Figure 5.15. Disturbance rejection with neural network control in inverse of steady-state prediction mode (Case 2). (a) Top composition.

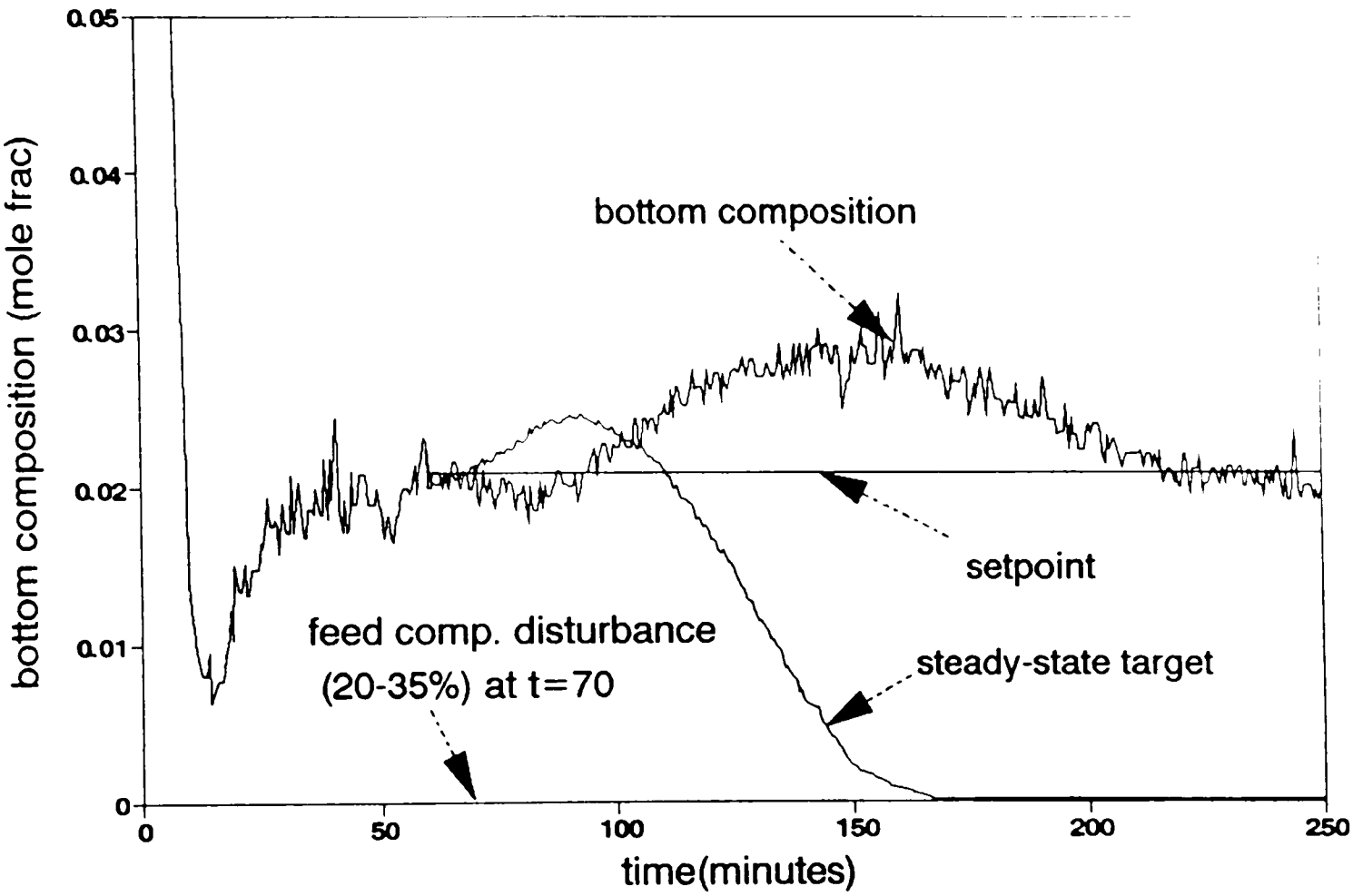

Figure 5.15. Continued. (b) Bottom composition.

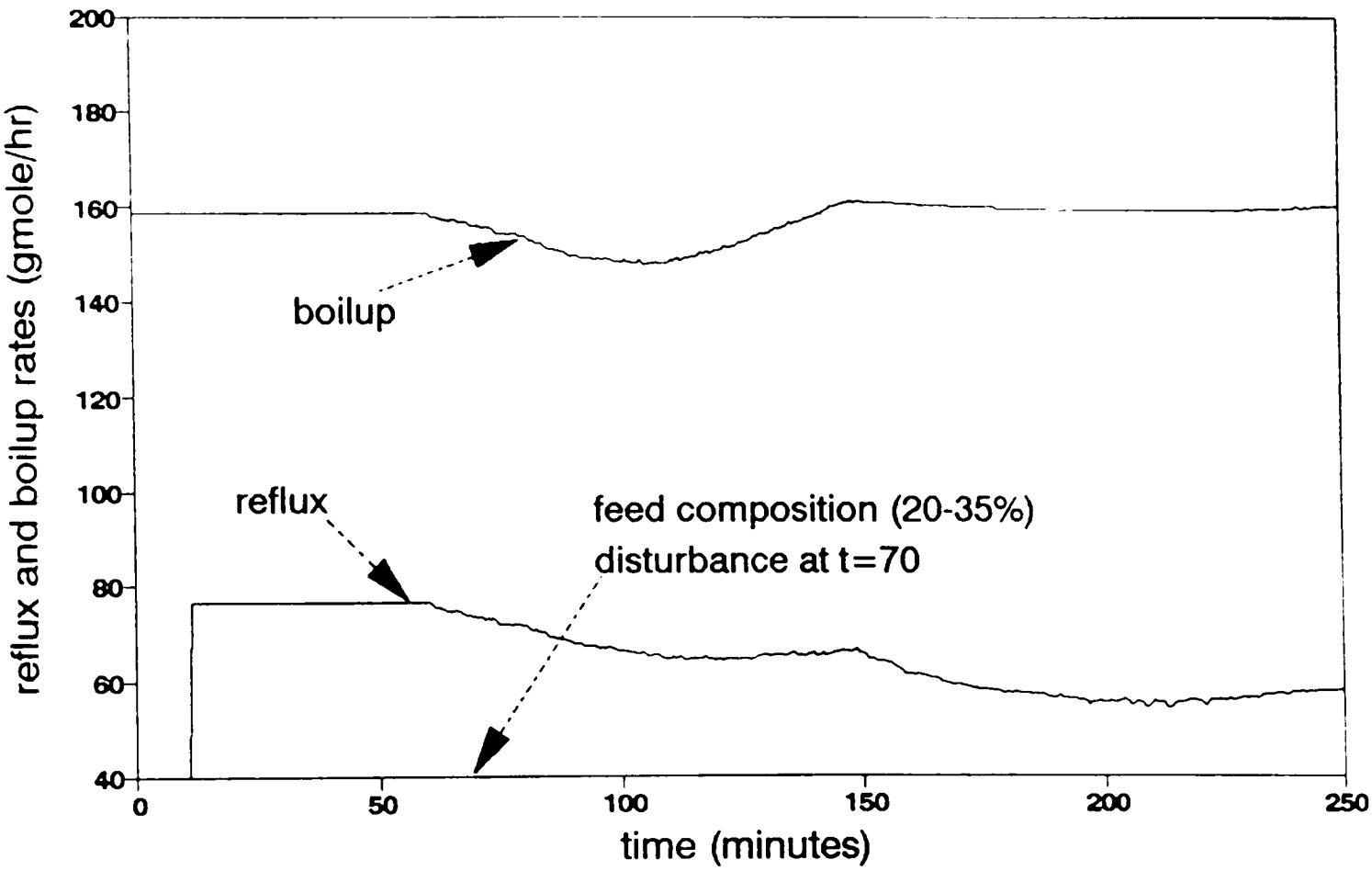

Figure 5.15. Continued. (c) Manipulated variables.

Table 5.7. Disturbance rejection with neural network control in inverse of the state prediction mode (Case 3)

Operating Characteristics	Initial Operating Conditions	Final Operating Conditions
Feed Rate (mols/hr.)	220.0	220.0
Feed Composition (mol % methanol)	30.0	20.0
Feed Temperature (deg F)	100.0	100.0
Reflux Rate (mols/hr.)	76.0	69.0
Reflux Temperature (deg F)	110.0	110.0
Vapor Boilup (mols/hr.)	158.0	148.0
Top Composition (mol % methanol)	90.0	90.0
Bottom Composition (mol % methanol)	2.5	2.5

and bottom compositions start deviating from the setpoints shortly after the introduction of the disturbance. But, the controller is able to bring the compositions back to their setpoints (90 mol% and 2.1 mol%, respectively) within the next 120 minutes. Figure 5.15 (c) shows the response of the manipulated variables. In this experiment, the reflux pump is started at about 10 minutes. Figures 5.16(a) and 5.16(b) show the control results for a feed-composition disturbance from 30 mole% to 20 mole% (-40% relative) methanol, introduced at about 90 minutes. In this case, the controller is able to bring back the compositions to their setpoints (90 mole% and 2.5 mole%) within 100 minutes after the introduction of the disturbance. Figure 5.16(c) shows the corresponding responses of the manipulated variables. Here, the reflux pump is started at about 40 minutes, and the controller is brought to automatic mode at about 80 minutes.

It can be stated here that the constraint-handling capabilities are not explored with this controller. Since this controller has integral terms in the GMC law, the steady-state target would cause 'integral windup' at the constraint. If the manipulated variable hits a constraint and the process variable keeps a sustained offset, the target output of the GMC law would start winding. When the constrained condition is removed, the target output would take a long time to return to its original value.

5.2.3 NN Control of Distillation Column in Gain Prediction Mode

This section presents the experimental control results obtained using the gain-prediction neural-network approach as discussed in Section 4.2. The detailed control strategy is shown in Figure 4.2. The neural-network models are developed based on the

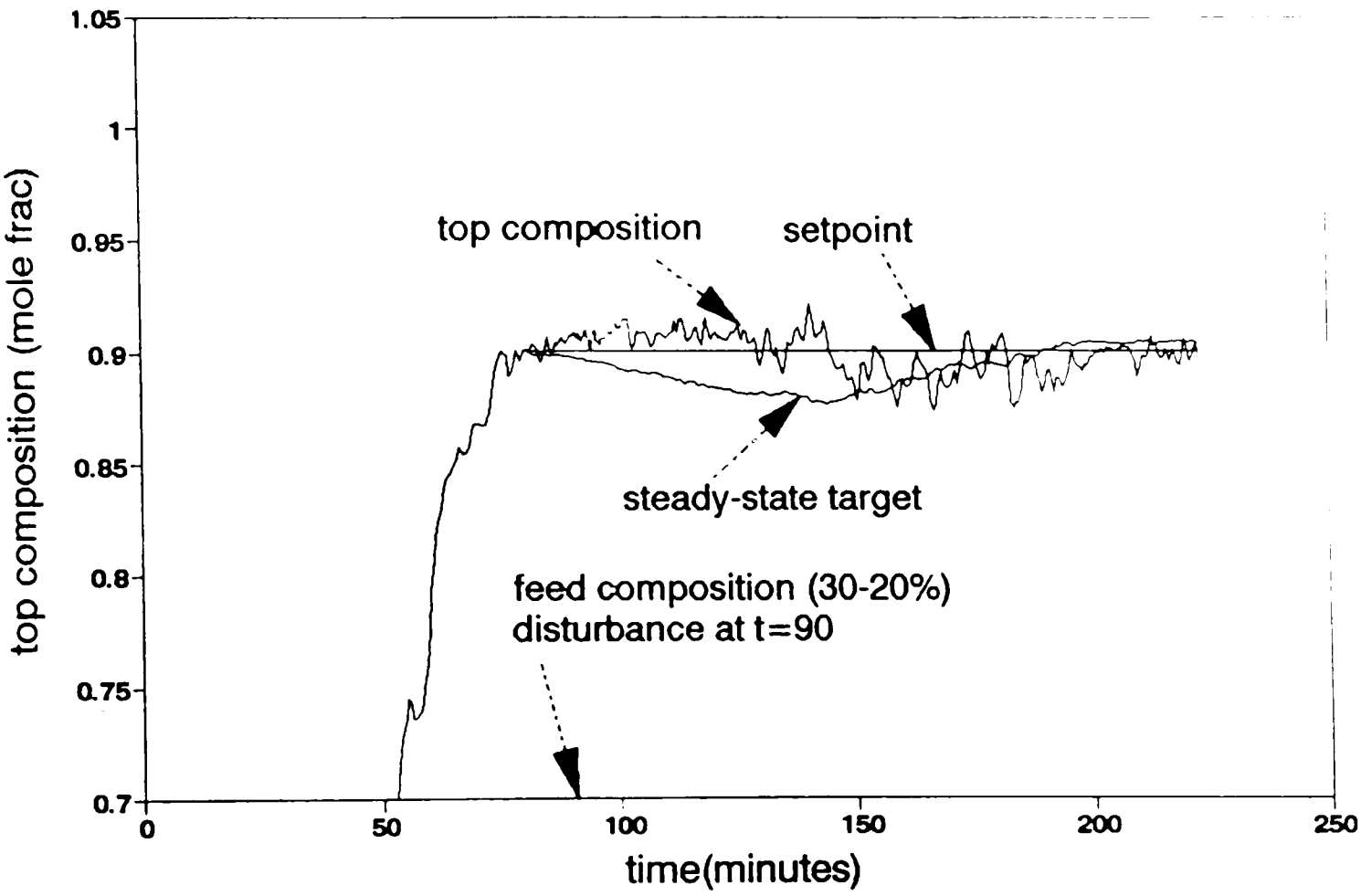

Figure 5.16. Disturbance rejection with neural network control in inverse of steady-state prediction mode (Case 3). (a) Top composition.

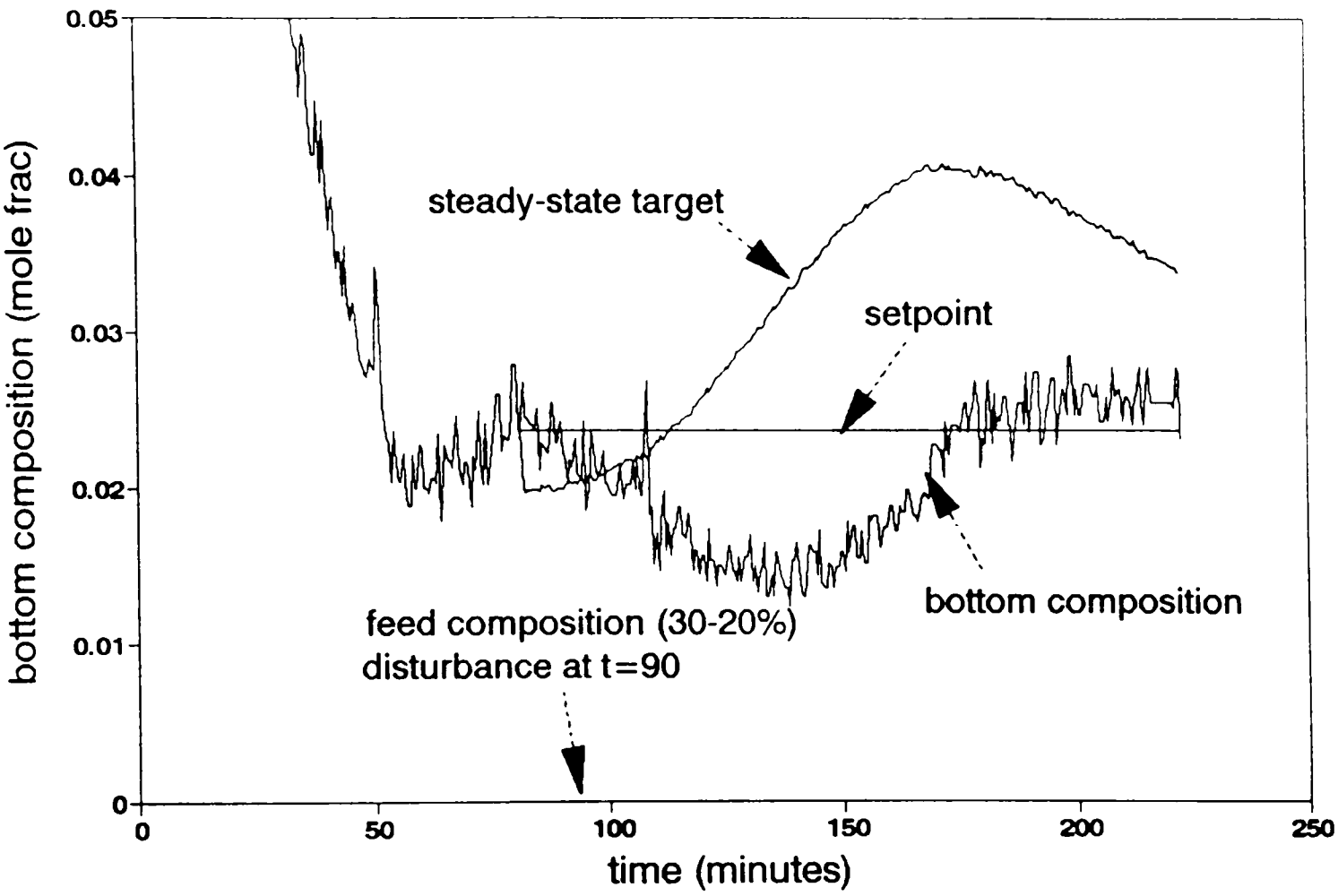

Figure 5.16. Continued. (b) Bottom composition.

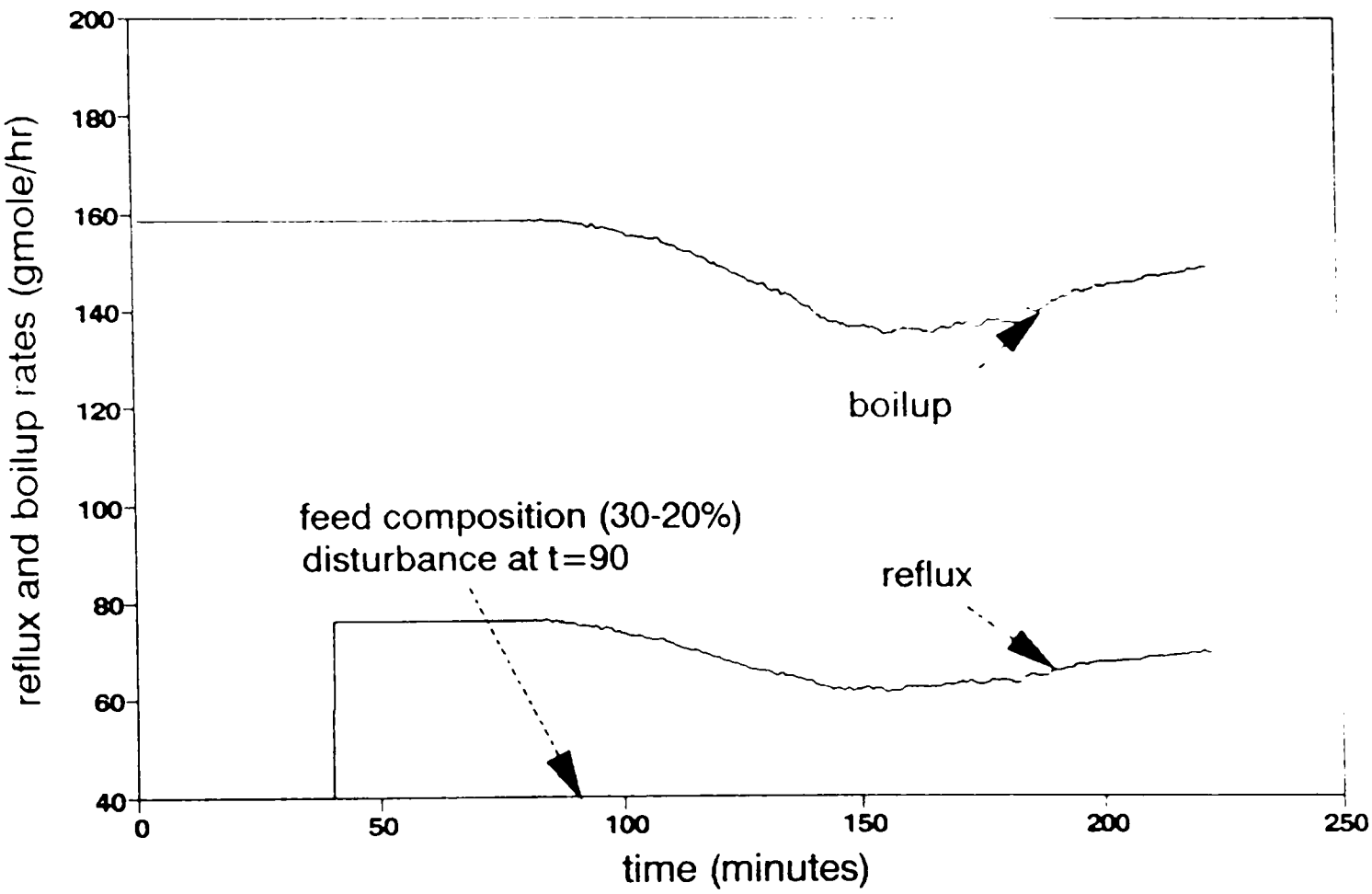

Figure 5.16. Continued. (c) Manipulated variables.

training of local steady-state gains (188 data sets) generated using the simulator in the operating region of the experiment. Figures 5.17(a), (b), (c) and (d) show the predicted outputs (K_{yr}, K_{yv}, K_{xr} and K_{xv}) by the four separate NN models (each 4-5-1) on the training data sets. The predicted outputs closely follow the 45° line suggesting a very good training on the data sets. The gain (K_{yr}) changes in the training region is as much as 0.5 mole fraction/(lbmoles/hr) to 7 mole fraction/(lbmoles/hr), a ratio of 14:1. The controller is tested in a similar manner to the inverse of the steay-state-prediction approach (i.e., for setpoint tracking and feed-composition disturbance rejections) as shown in Table 5.4.

5.2.3.1 Setpoint Tracking

Figures 5.18(a) and 5.18(b) show the column performance for a simultaneous setpoint change in the top and bottom compositions. The conditions are summarized in Table 5.8. As seen in Figures 5.18(a) and 5.18(b), the top composition setpoint is changed from 86.0 mole% to 91.0 mole% methanol, while the bottom composition setpoint is changed from 1.4 mole% to 5.0 mole% methanol. Figure 5.18(c) shows the changes in the manipulated variables during the run. The column is started in the open-loop fashion and after about 100 minutes, the controllers are put into automatic mode with setpoints of 86 mole% for the top and 1.4 mole% for the bottom. At about 175 minutes, step changes in the setpoints of both top and bottom compositions are made. After the change, the top composition takes about 50 minutes to settle down to the new setpoint while the bottom composition takes about 125 minutes.

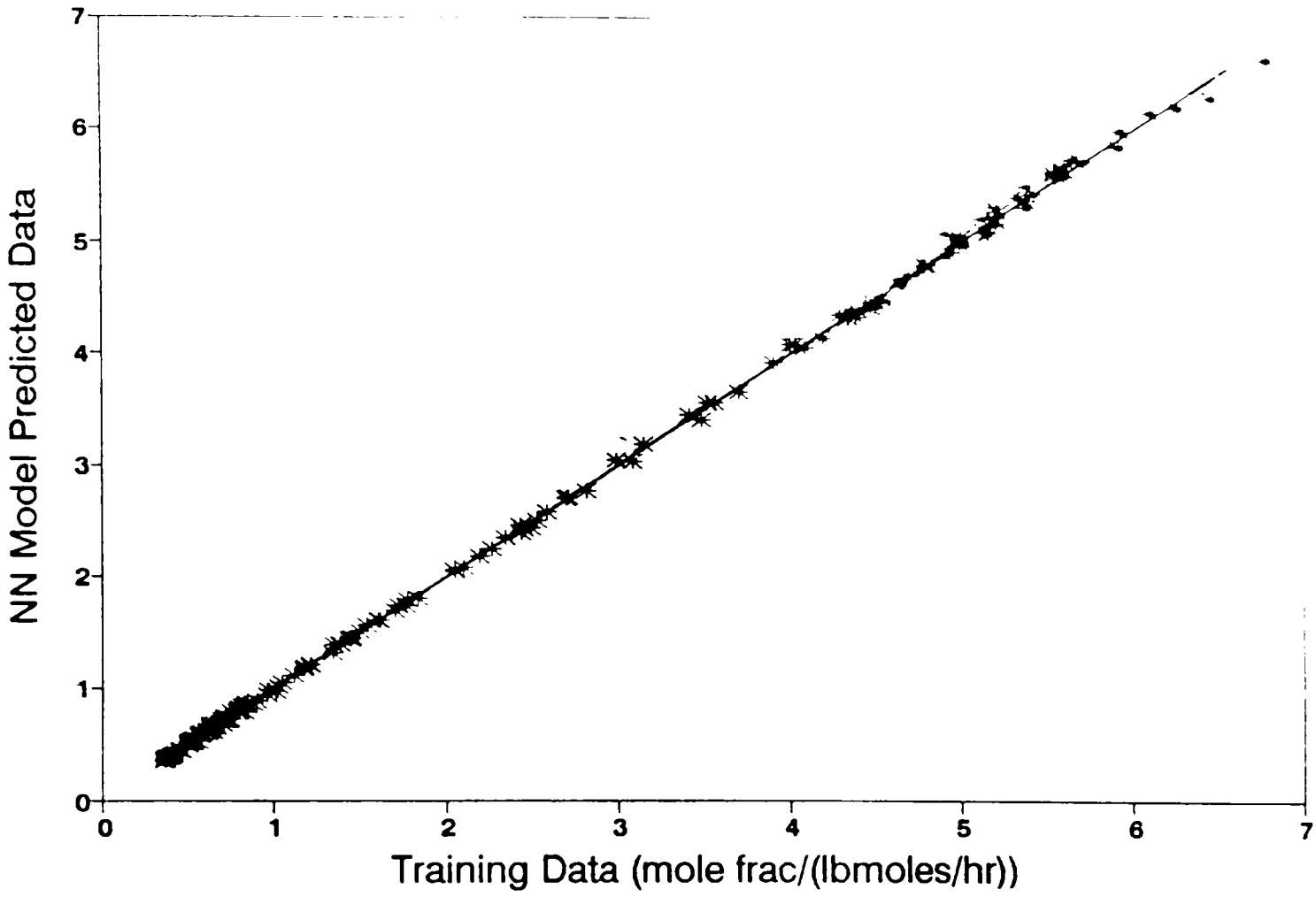

Figure 5.17. Training results on gains in gain prediction approach.
(a) Gain-1 (top composition/reflux), Kyr.

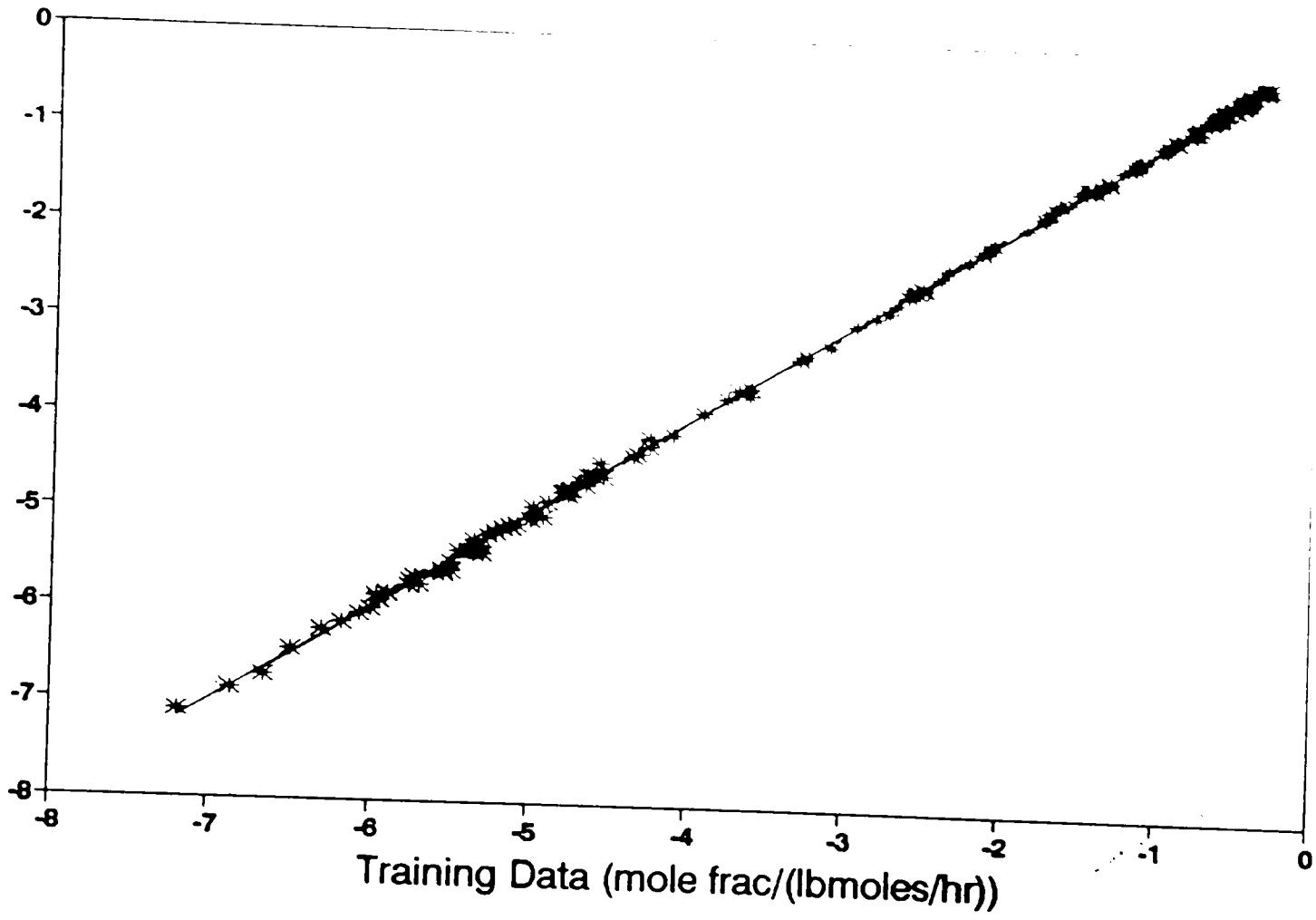

Figure 5.17. Continued. (b) Gain-2 (top composition/boilup), Kyv.

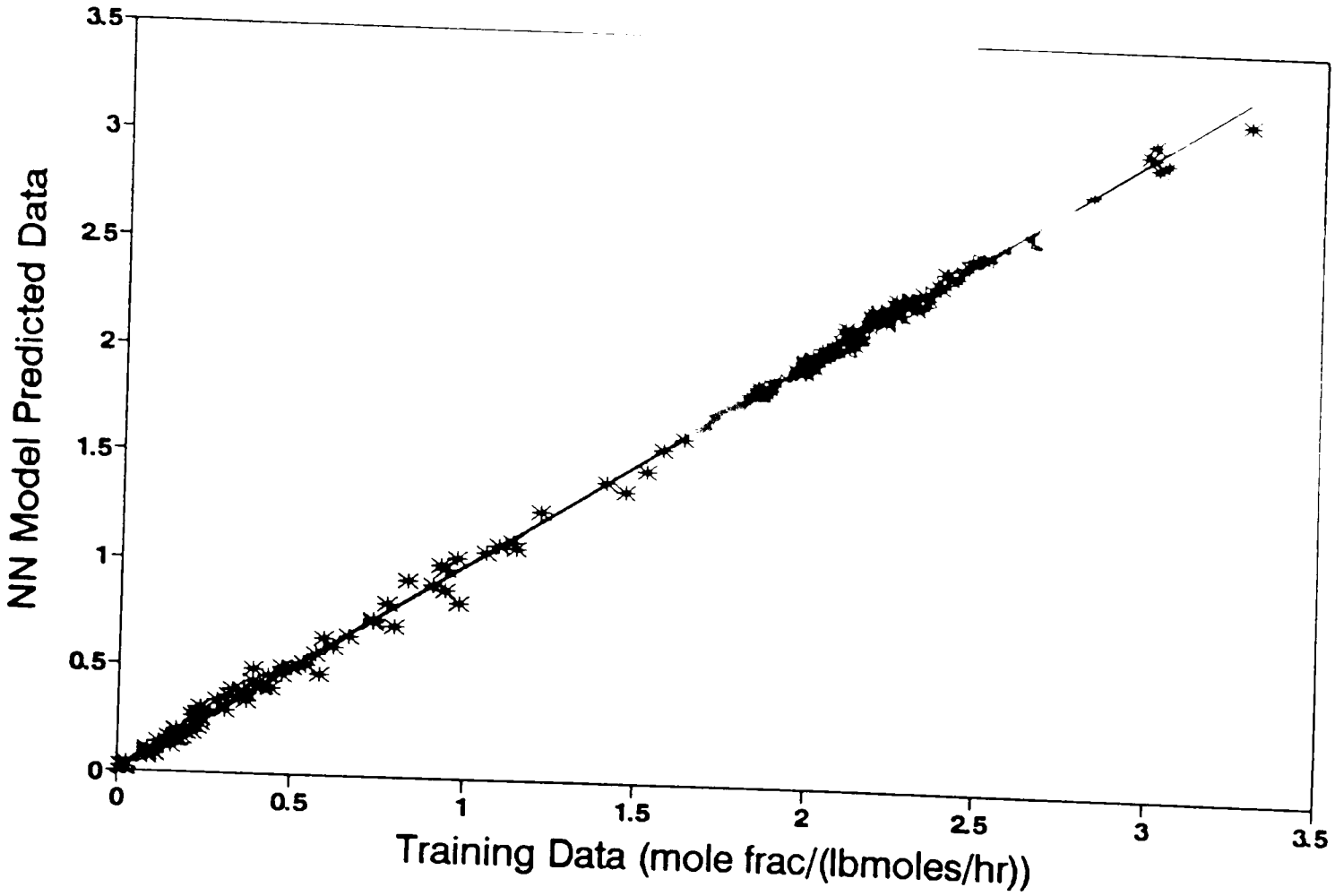

Figure 5.17. Continued. (c) Gain-3 (bottom composition/reflux), Kxr.

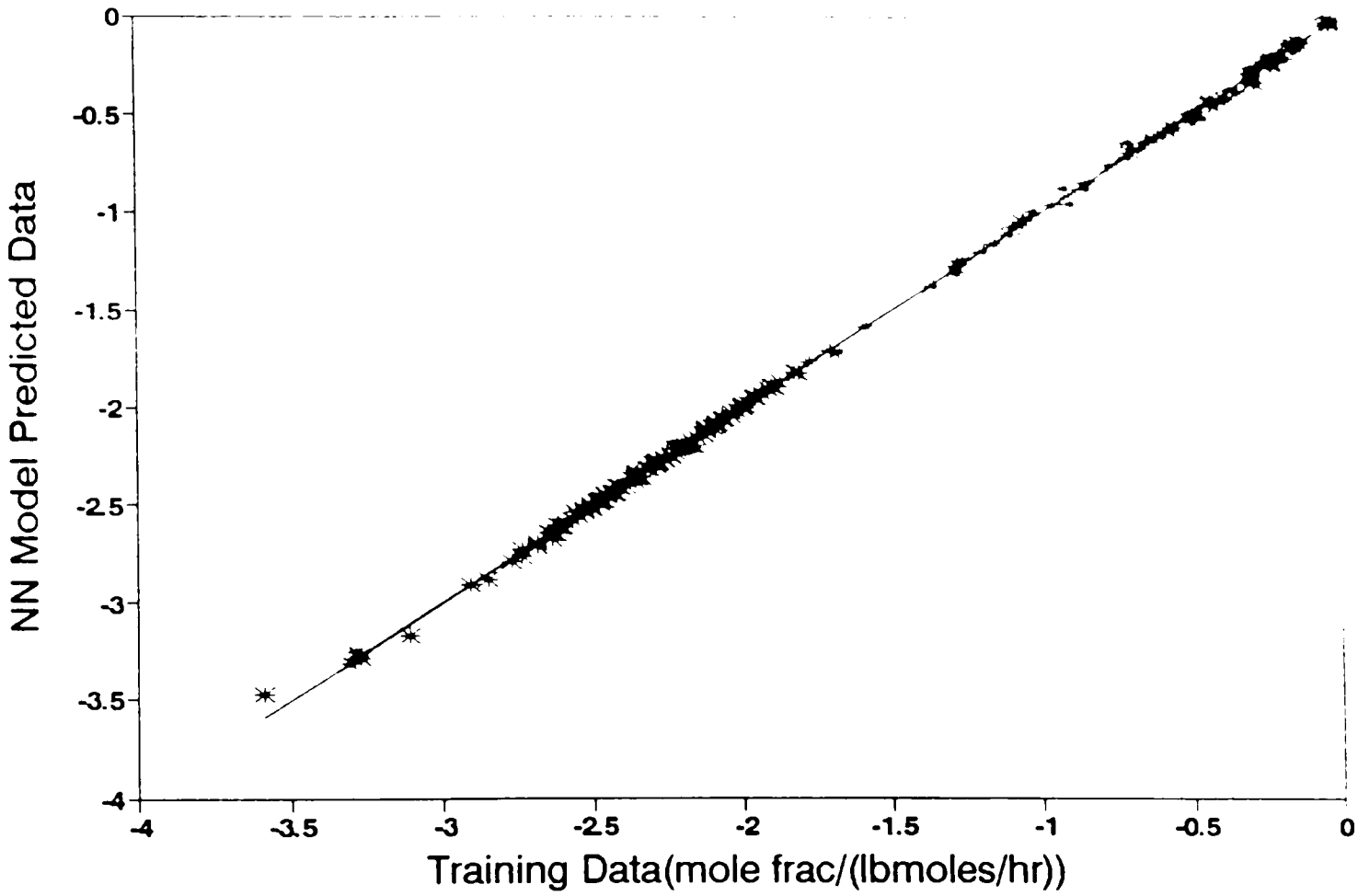

Figure 5.17. Continued. (d) Gain-4 (bottom composition/boilup), Kxv.

Table 5.8. Setpoint tracking with neural network control in gain prediction mode (Case 1)

Operating Characteristics	Initial Operating Conditions	Final Operating Conditions
Feed Rate (mols/hr.)	220.0	220.0
Feed Composition (mol % methanol)	20.0	20.0
Feed Temperature (deg F)	100.0	100.0
Reflux Rate (mols/hr.)	80.0	100.0
Reflux Temperature (deg F)	110.0	110.0
Vapor Boilup (mols/hr.)	170.0	160.0
Top Composition (mol % methanol)	86.0	91.0
Bottom Composition (mol % methanol)	1.4	5.0

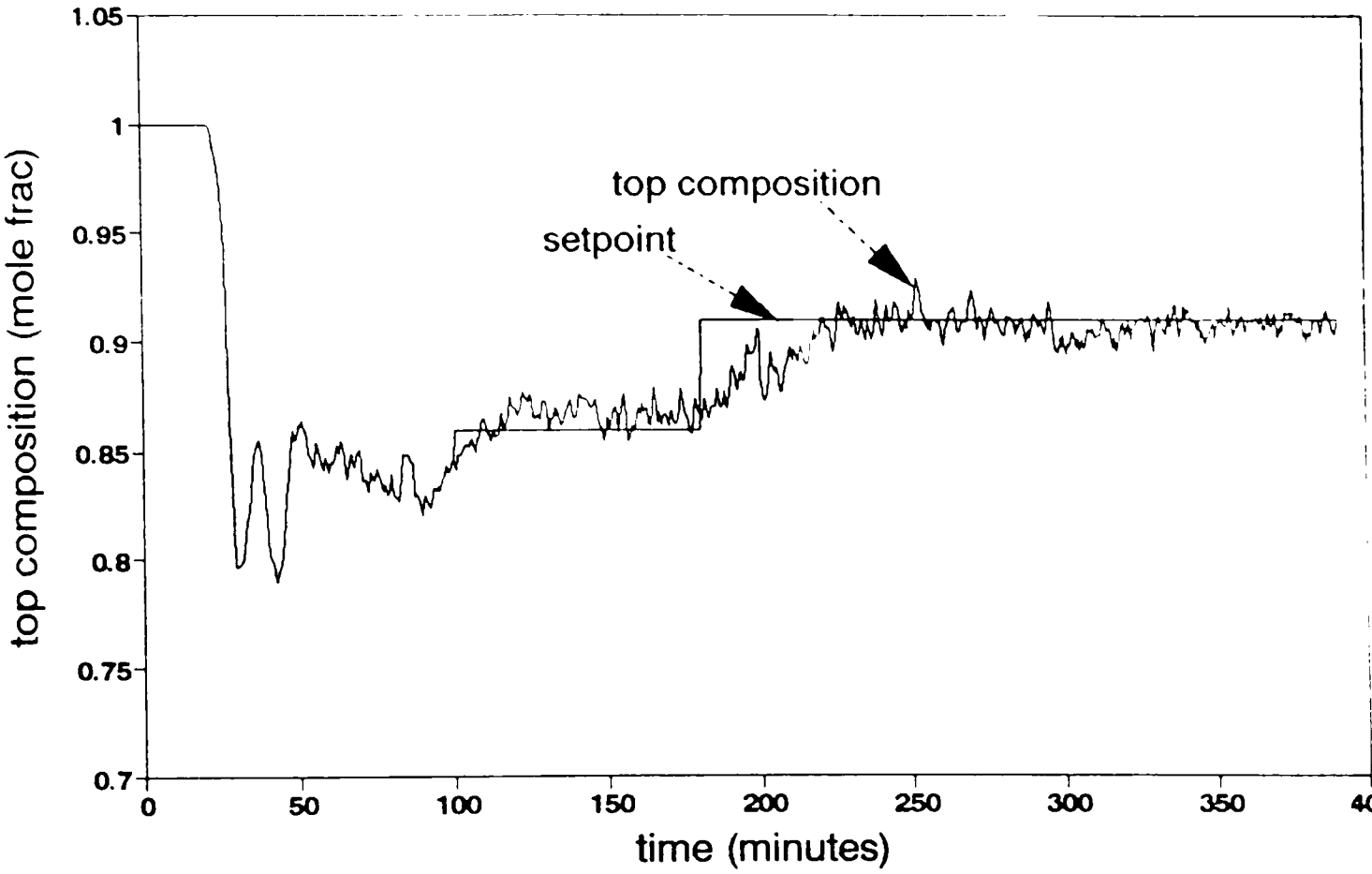

Figure 5.18. Setpoint tracking with neural network control in gain prediction mode (Case 1). (a) Top composition.

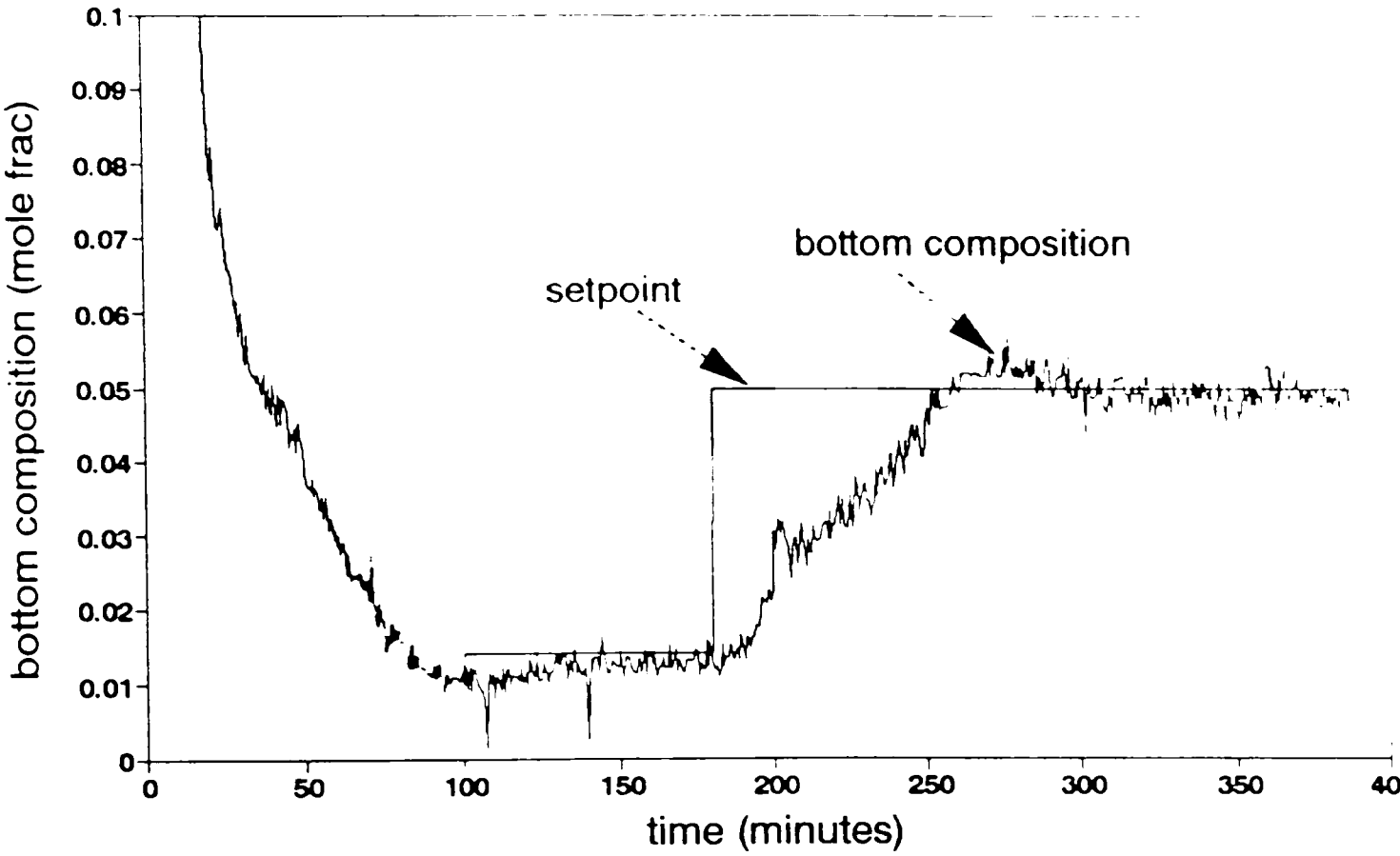

Figure 5.18. Continued. (b) Bottom composition.

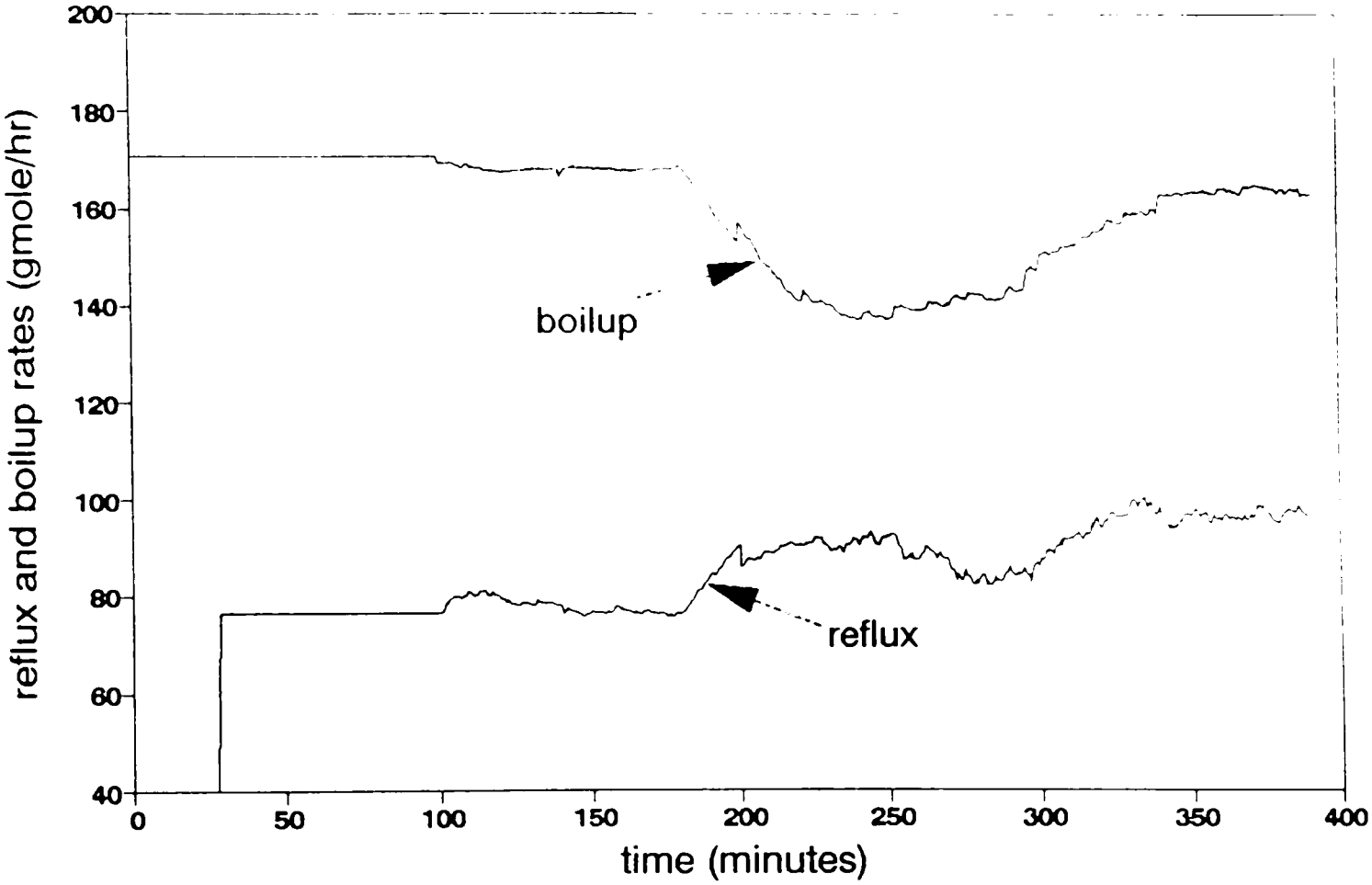

Figure 5.18. Continued. (c) Manipulated variables.

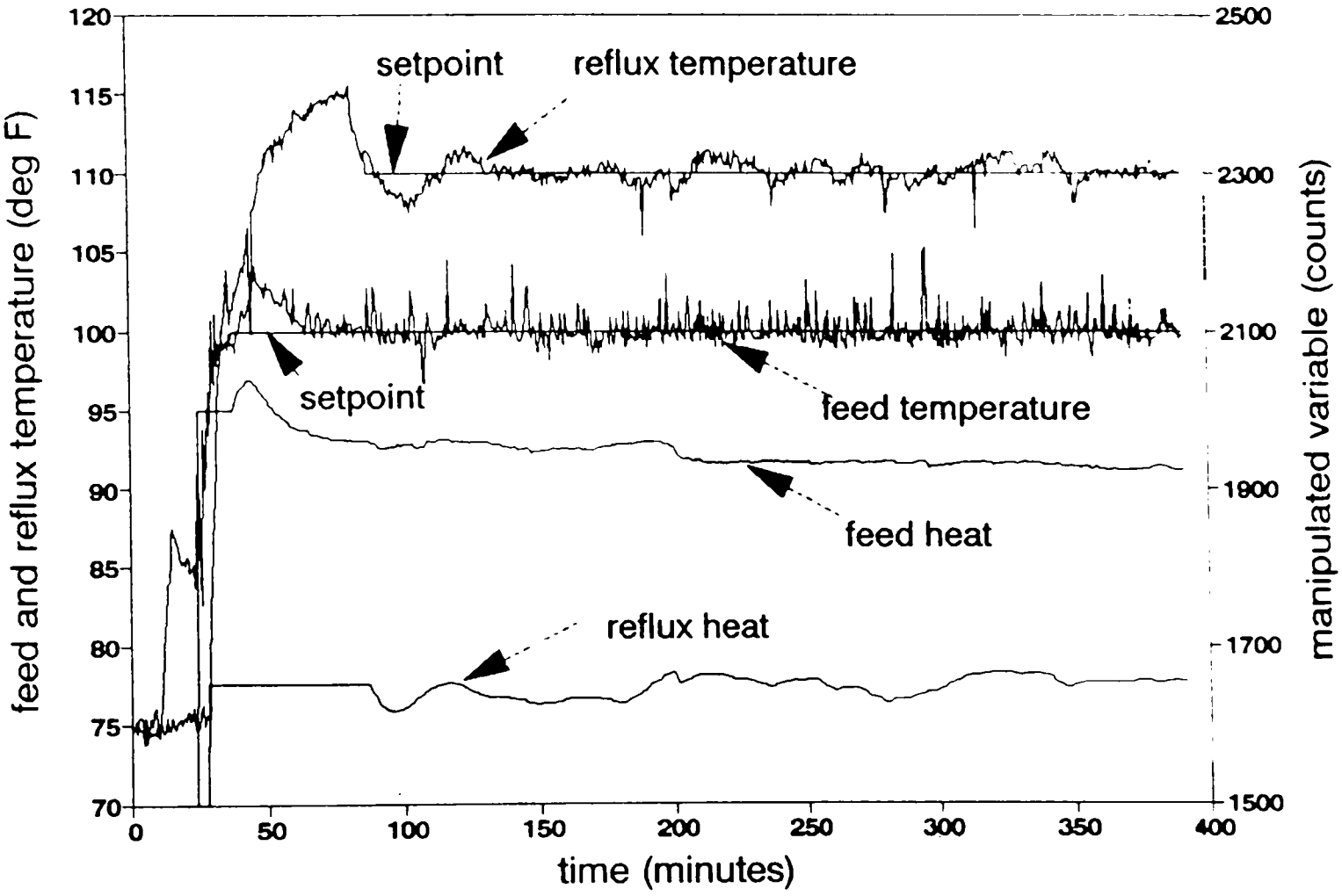

Figure 5.18. Continued. (d) Feed and reflux temperature control during dual composition control.

The manipulated variable action is shown in Figure 5.18(c). Immediately after the controllers are put into automatic mode, the manipulated variables start moving to maintain the process at the setpoints. As the setpoint changes are given, the boilup starts decreasing and the reflux starts increasing to bring the top and bottom compositions to their new setpoints. In this control strategy, the changes in the manipulated variables are calculated in an optimized sense to maintain the top and bottom compositions. This control approach is different from the control approach using the inverse of the steady-state-prediction method where the manipulated variables are calculated directly based on the steady-state target values of the compositions.

The four tuning parameters used for this controller are K_c^{top}, K_c^{bot} (Equation 4.8,4.9), α_x, and α_y (Equation 4.12, 4.13). The proportional constants, K_c^{top} and K_c^{bot}, are kept same (i.e., 1.1 and 1.1, respectively) as the previously described NN model-based inverse-of-state-prediction control aproach. The α_x and α_y are tuned on-line and found to produce reasonably good performance at 0.9 and 0.9, respectively. A value of $\alpha_x=1, \alpha_y=1$ would produce a purely proportional action, and $\alpha_x=0, \alpha_y=0$ would produce integral action only. The tuning ranges of α_x and α_y tried in different experimental runs are 0.85-0.95.

Figure 5.18(d) shows the control on the reflux and feed temperatures entering the column during this particular run. Control used the NN model-based inverse of the steady-state-prediction method already presented in section 4.1. Even with a constantly changing

reflux flowrate, this controller is able to keep the reflux temperature close to the setpoint of 110^0 F

5.2.3.2 Disturbance Rejection

The feed-composition disturbances are introduced according to Case 2 and Case 3 (Table 5.4) for the purpose of a comparative study. The detailed operating conditions during these experimental runs are shown in Tables 5.9 and 5.10. Figures 5.19(a) and 5.19(b) show the control results for a feed-composition disturbance from 20 mole% to 35 mole% methanol (+55% relative), introduced at about 125 minutes. With the introduction of this disturbance, the top and bottom compositions start deviating from their setpoints after about 10 minutes. The controller is able to bring back the compositions quickly (within the next 60 minutes) to their setpoints (90 mole% and 2.1 mole%, respectively). Figure 5.19(c) shows the response of the manipulated variables.

Figures 5.20(a) and 5.20(b) show the control results for a feed-composition disturbance from 30 mole% to 20 mole% (-40% relative) methanol, introduced at about 75 minutes. In this case, the controller is able to bring the compositions back to their setpoints (90 mole% and 2.5 mole%) within 100 minutes. Figure 5.20(c) shows the corresponding responses of the manipulated variables.

It can be observed that the magnitude of deviations in the top and bottom compositions (Figures 5.19 (a), (b) and 5.20 (a),(b)) are smaller than the results obtained in the inverse-of-the-state-prediction approach (Figures 5.15 (a), (b) and 5.16 (a), (b)). This deviation can be solely attributed to the nonstationary nature of the column. It is also

Table 5.9. Disturbance rejection with neural network control in gain prediction mode (Case 2)

Operating Characteristics	Initial Operating Conditions	Final Operating Conditions
Feed Rate (mols/hr.)	220.0	220.0
Feed Composition (mol % methanol)	20.0	35.0
Feed Temperature (deg F)	100.0	100.0
Reflux Rate (mols/hr.)	82.0	80.0
Reflux Temperature (deg F)	110.0	110.0
Vapor Boilup (mols/hr.)	150.0	170.0
Top Composition (mol % methanol)	90.0	90.0
Bottom Composition (mol % methanol)	2.1	2.1

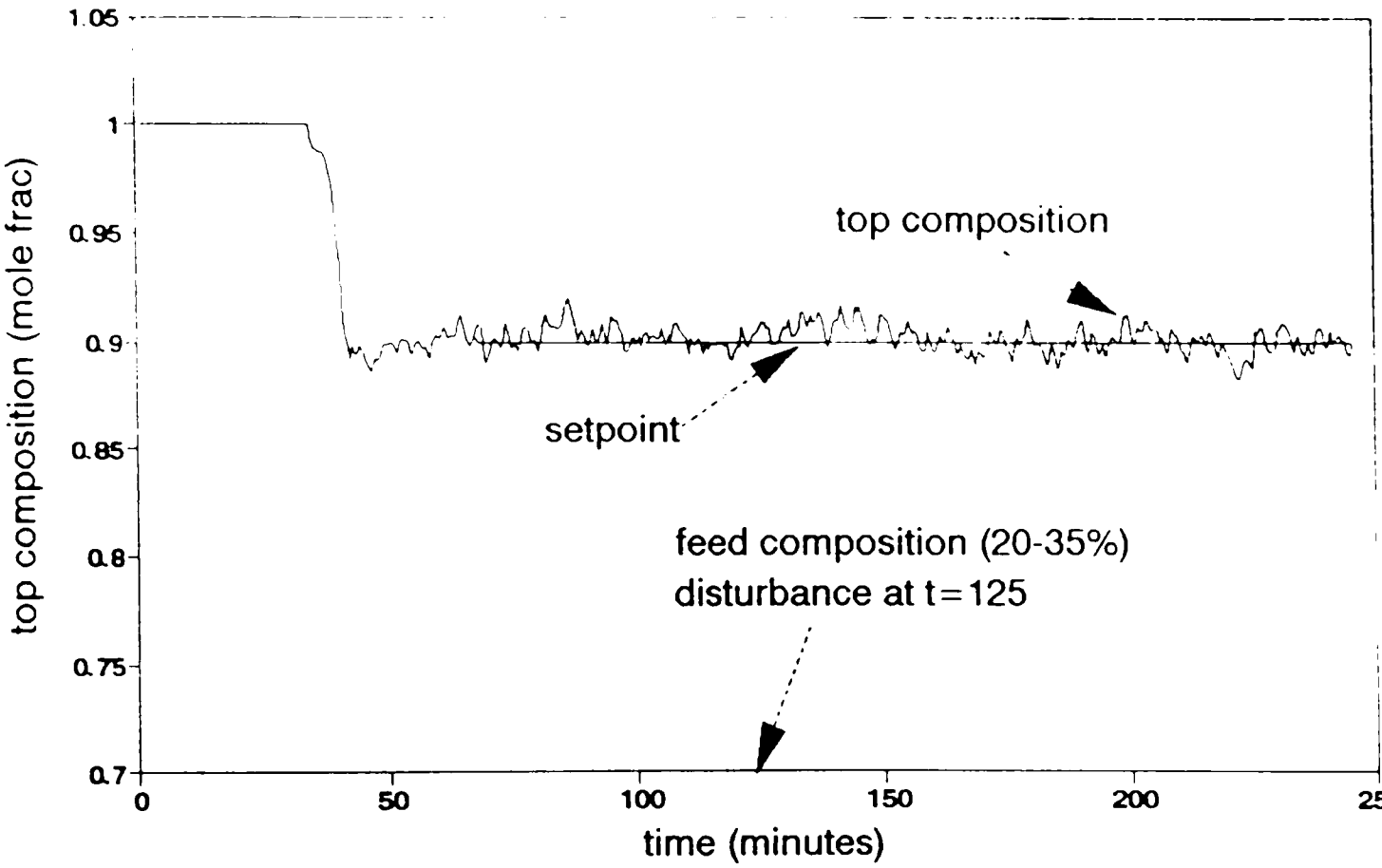

Figure 5.19. Disturbance rejection with neural network control in gain prediction mode (Case 2). (a) Top composition.

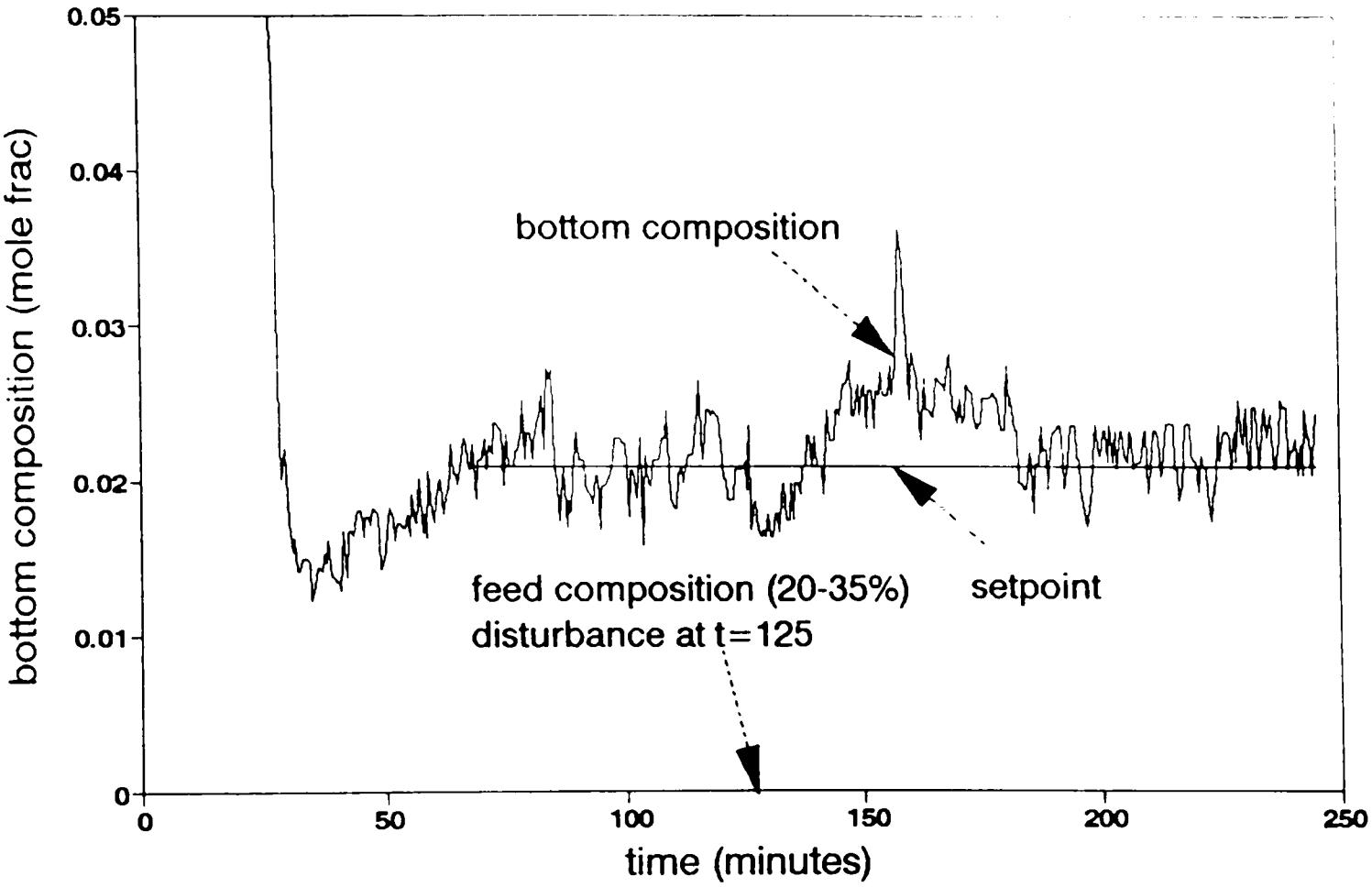

Figure 5.19. Continued. (b) Bottom composition.

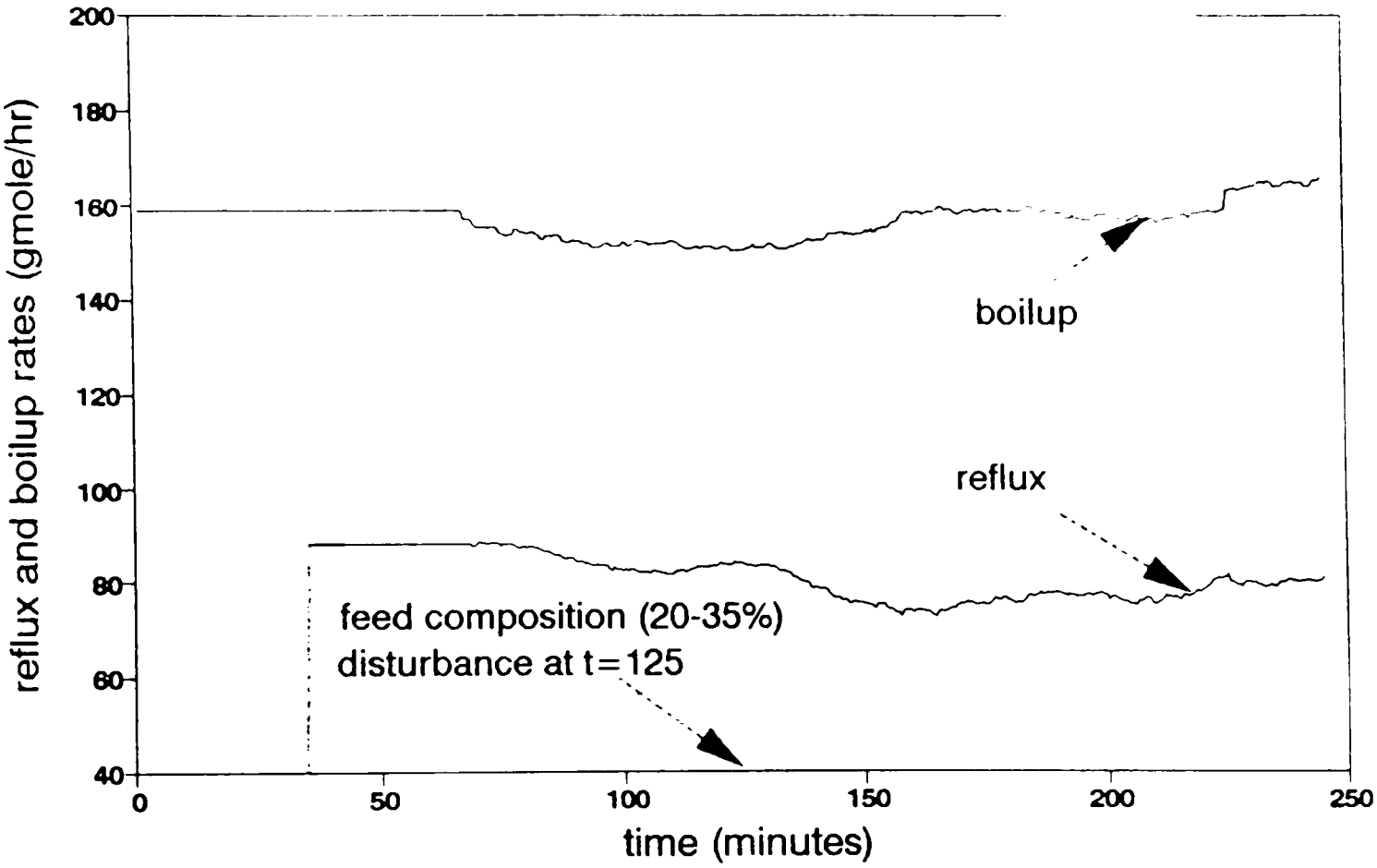

Figure 5.19. Continued. (c) Manipulated variables.

Table 5.10. Disturbance rejection with neural network control in gain prediction mode (Case 3)

Operating Characteristics	Initial Operating Conditions	Final Operating Conditions
Feed Rate (mols/hr.)	220.0	220.0
Feed Composition (mol % methanol)	30.0	20.0
Feed Temperature (deg F)	100.0	100.0
Reflux Rate (mols/hr.)	75.0	82.0
Reflux Temperature (deg F)	110.0	110.0
Vapor Boilup (mols/hr.)	155.0	160.0
Top Composition (mol % methanol)	90.0	90.0
Bottom Composition (mol % methanol)	2.5	2.5

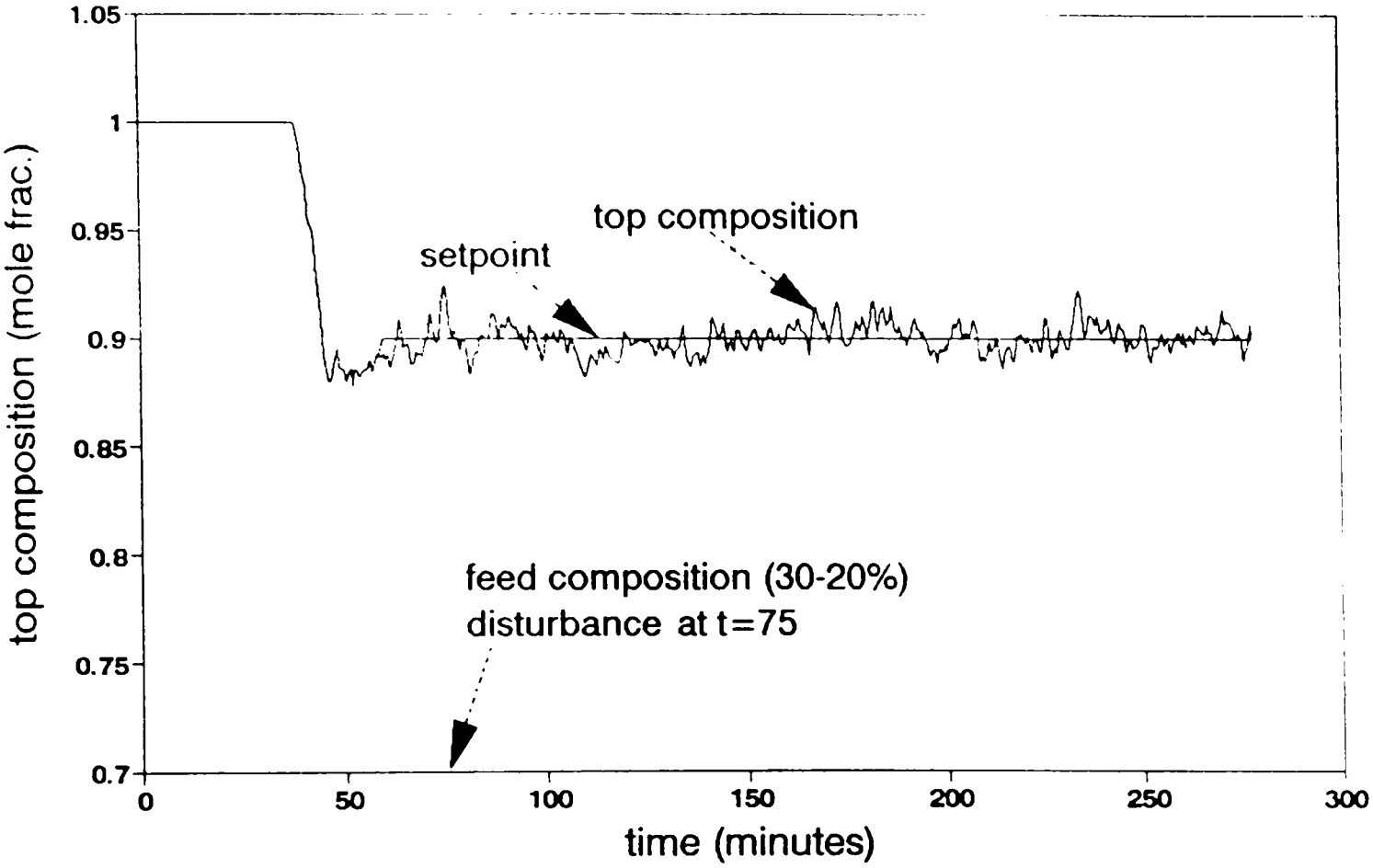

Figure 5.20. Disturbance rejection with neural network control in gain prediction mode (case 3). (a) Top composition.

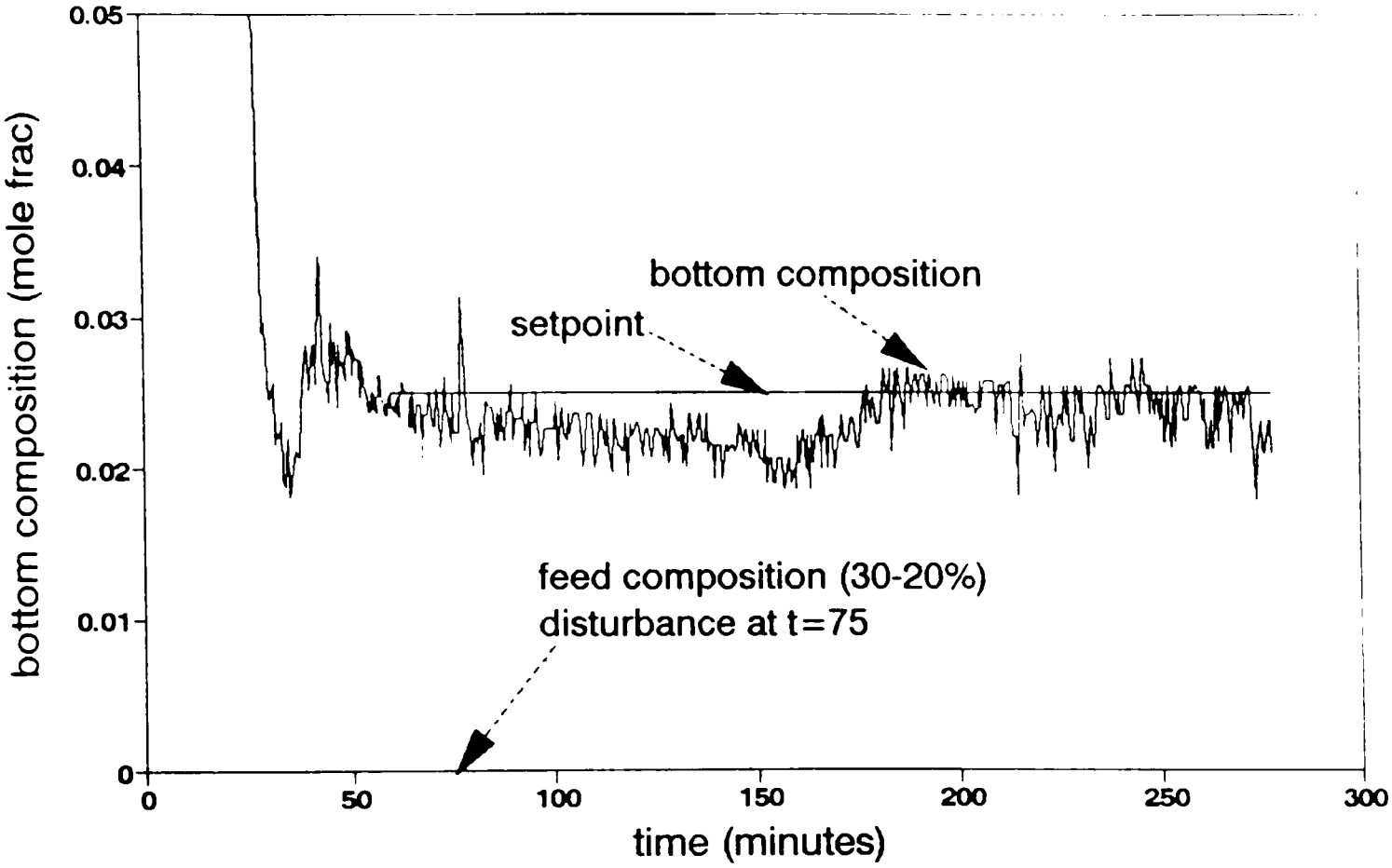

Figure 5.20. Continued. (b) Bottom Composition.

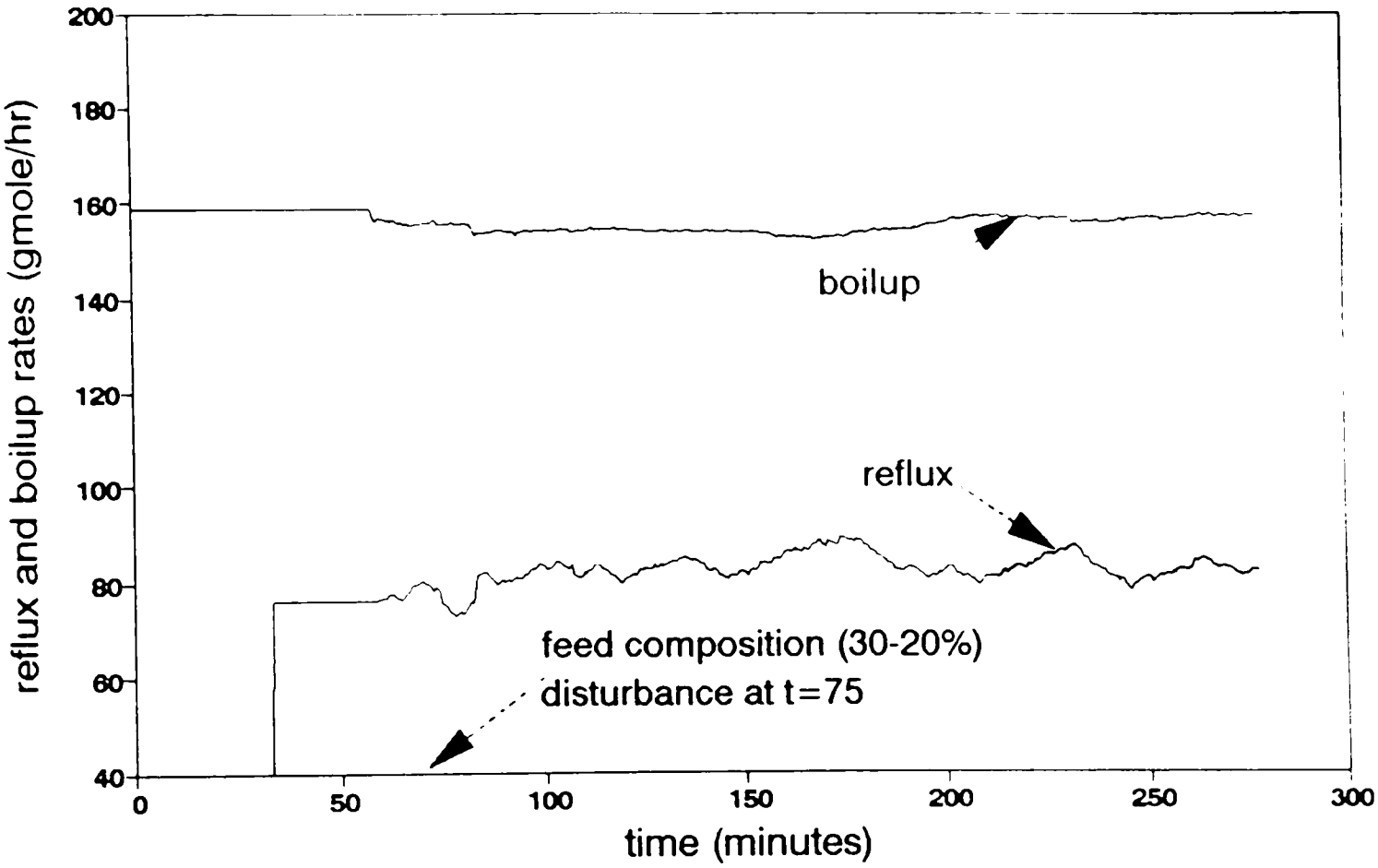

Figure 5.20. Continued. (c) Manipulated variables.

seen that the change in manipulated variable movements, particularly the reflux changes, are significantly more in the gain prediction mode, even though the composition deviations are less. This can also be due to the difference in tuning. However, no significant difference is observed in the change of manipulated variable movements in response to the setpoint changes.

5.2.4 Constrained Control of Distillation Column with NN Gain Prediction

In section 4.2, it is stated that the control strategy developed in this research based on the novel gain-prediction approach along with the Heuristic Random Optimizer has the ability to handle constraints. Simulation results verify this claim. However, experimental demonstration is also needed to verify its performance in a real-time situation. As any other real process, the present experimental system also possesses few operational constraints. The heater to the boiler has a maximum power limit. The reflux rate has a maximum limit corresponding to maximum vapor boilup. A minimum reflux rate has to be maintained for satisfactory operation of the distillation column. Therefore, the constraints are mainly on the manipulated variables.

The constrained control performance is tested by putting an upper limit of the vapor boilup close to the maximum power. In this experiment, an upper constraint for the boilup rate is set at 0.37 lbmoles/hr (i.e., $V < 0.37$ lbmoles/hr). The reflux is kept intentionally out of any feasible constraints.

Figures 5.21(a) and (b) show the result of the constraint control. A feed-composition disturbance (20 mole% to 50 mole% methanol) is introduced at 125 minutes.

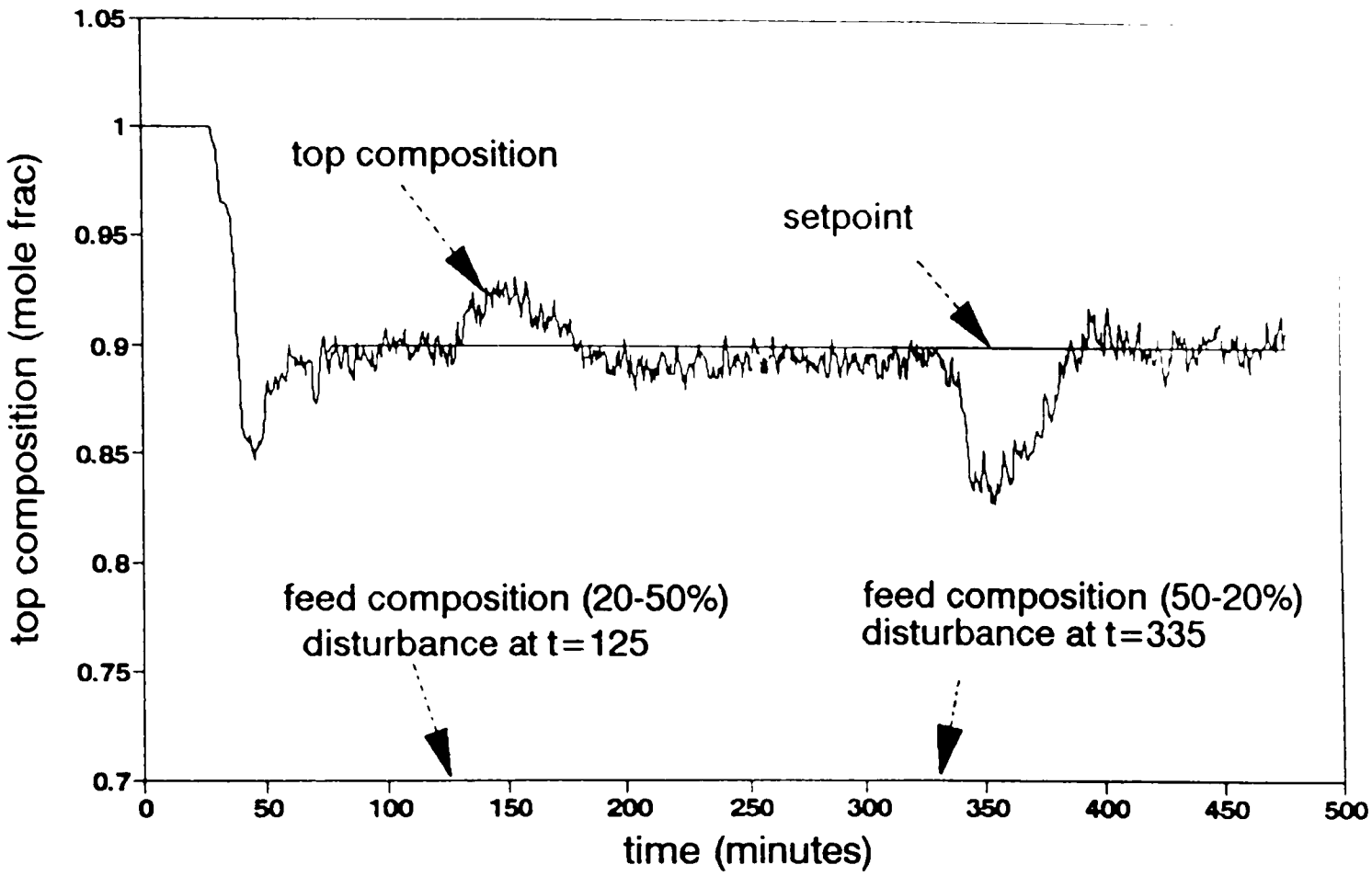

Figure 5.21. Constrained control with NN gain prediction using feed composition disturbance. (a) Top composition.

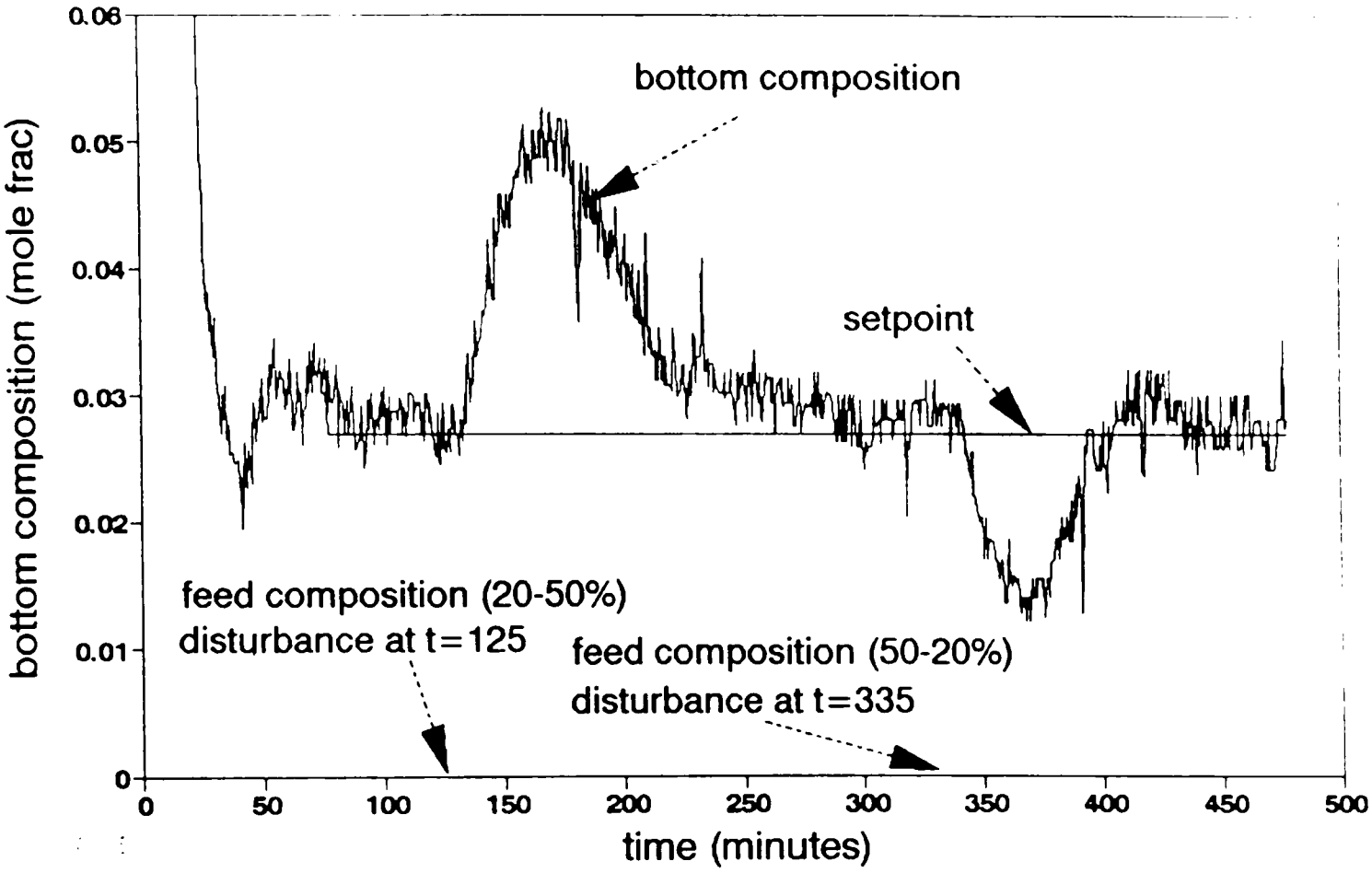

Figure 5.21. Continued. (b) Bottom composition.

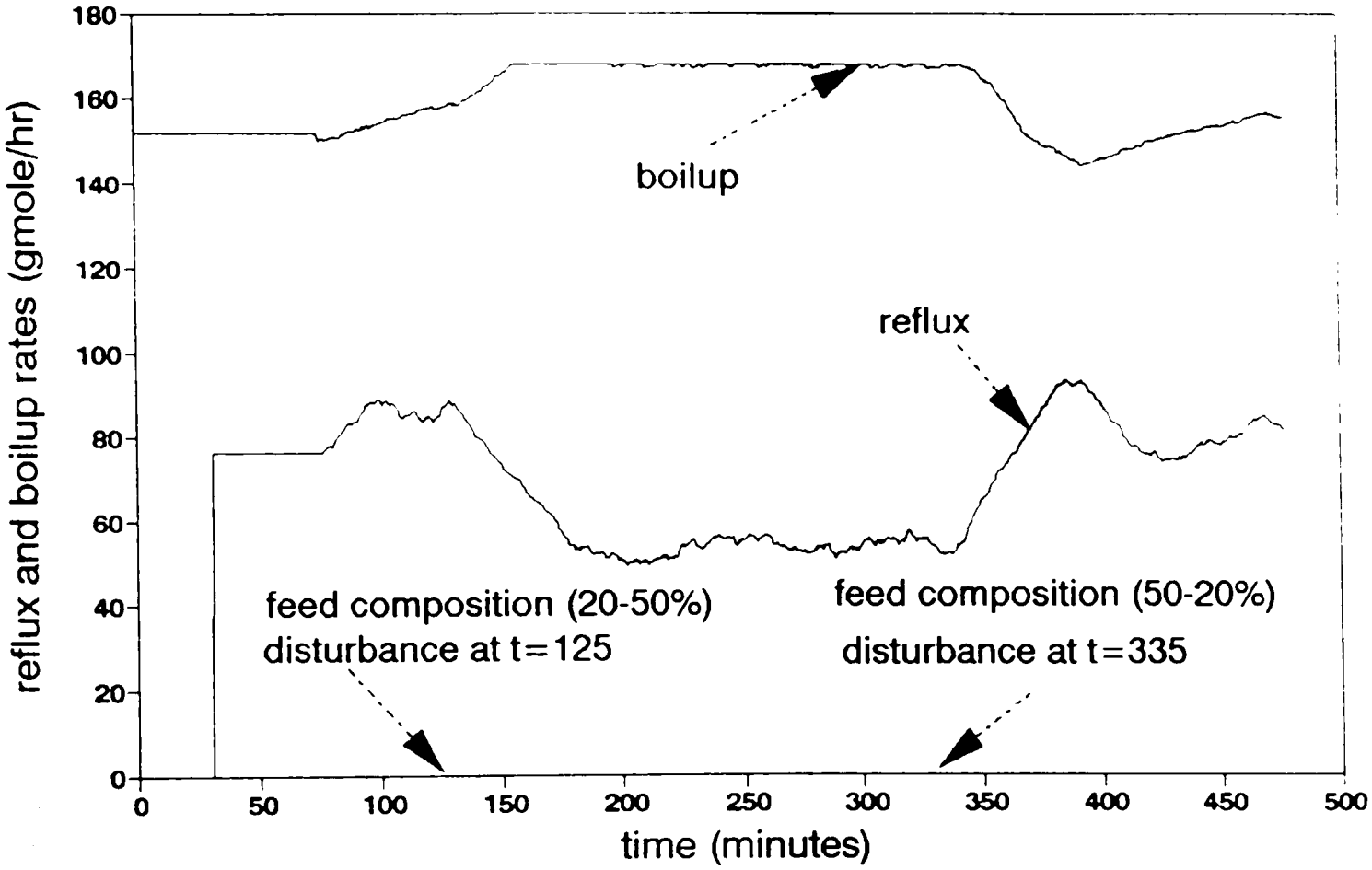

Figure 5.21. Continued. (c) Manipulated variables.

Both the top and bottom compositions are deviated higher than the setpoints. To keep the compositions at their setpoints, the boilup rate starts increasing and the refux rate starts decreasing. However, Figure 5.21(c) shows that the boilup hits the constraint at about 160 minutes and the reflux rate settles down to a value so as to keep the objective function (Equation 4.15) to a minimum. Similar to the simulation result (as shown in Figure 5.4(a)), it is observed that a negative deviation of the top composition from its setpoint and a positive deviation of the bottom composition from its setpoint are maintained when the boilup rate maintains the constraint. The controller is able to come out of the constraint when the feed-composition is changed back to 20% and eliminates the offsets in the top and bottom compositions. The controller also shows no delay or windup while coming out of the constraint.

Interestingly, this experimental run also shows the presence of nonlinearity in the process. It is known that a distillation column shows lower gain at high purity and the higher gain at low purity. Here, a positive feed-composition disturbance shows lower change at the top purity above 90 mole% (i.e., higher purity for the top), but higher change for the bottom purity above 2.7 mole % (i.e., lower purity for the bottom). An exactly opposite response is observed when the negative feed-composition disturbance is given at time t=335 minutes.

Table 5.11 shows a comprehensive evaluation of overall material balance and component material balance closures during the various experimental runs conducted in this study. The errors are calculated based on the duration of steady-state operation. The

Table 5.11. Material Balance Closure in Experiments

Experimental Figure Number	5.14	5.15	5.16	5.18	5.19	5.20	5.21
Period of Estimation (minutes)	60	60	30	120	60	60	30
Feed Flowrate (gmoles/hr)	220	220	220	220	220	220	220
Feed Composition (methanol mole %)	20	35	20	20	35	20	20
Average Distillate Flowrate (gmoles/hr)	30	55	42	34	58	38	42
Average Bottom Product Flowrate (gmoles/hr)	170	160	175	180	150	160	145
Top Composition (methanol mole %)	91	90	90	91	90	90	90
Bottom Composition (methanol mole %)	5	2	2.5	5	2	2.5	3
Overall Material Balance Error (%)	9.1	2.3	1.4	2.7	5.5	10.0	15.0
Component Material Balance Error (%) (Methanol)	18.6	31.5	4.2	9.2	28.3	13.2	4.2

average distillate flowrate, bottom product flowrate, top and bottom product compositions are also shown in this table.

5.2.5 Process Model Mismatch

Expectedly, perhaps performance of the model-based controller should largely depend on the validity of the process model. In this study, the neural network model is generated based on steady-state data sets derived from a simulator. The simulator has various idealizations and assumptions (as discussed in section 3.2.2) which differ from the real environment. The experimental distillation column also shows significant amount of nonstationary behavior. As a result, an absolute steady state cannot be achieved in this real process. However, (pseudo) steady state can be assumed when the process is under control and maintaining particular compositions. During this time, the values of the manipulated variables can be obtained based on a statistical average. Using this method, a comparison of steady-state compositions is obtained between the process and the model.

Figure 5.22(a) shows the difference in top compositions between the process and the simulator at various states. Similarly, Figure 5.22(b) shows the bottom composition differences. Unexpectedly, although the simulator shows significant deviations in terms of predicting states, the controller, based on the neural-network model (inverse-of-the-state-prediction mode) and the GMC law, is able to accommodate this mismatch and to perform well in servo and regulatory modes.

The state prediction is not good. The simulator should be rejected as a statistically valid model. However, control using the NN model trained on the simulator was good, as

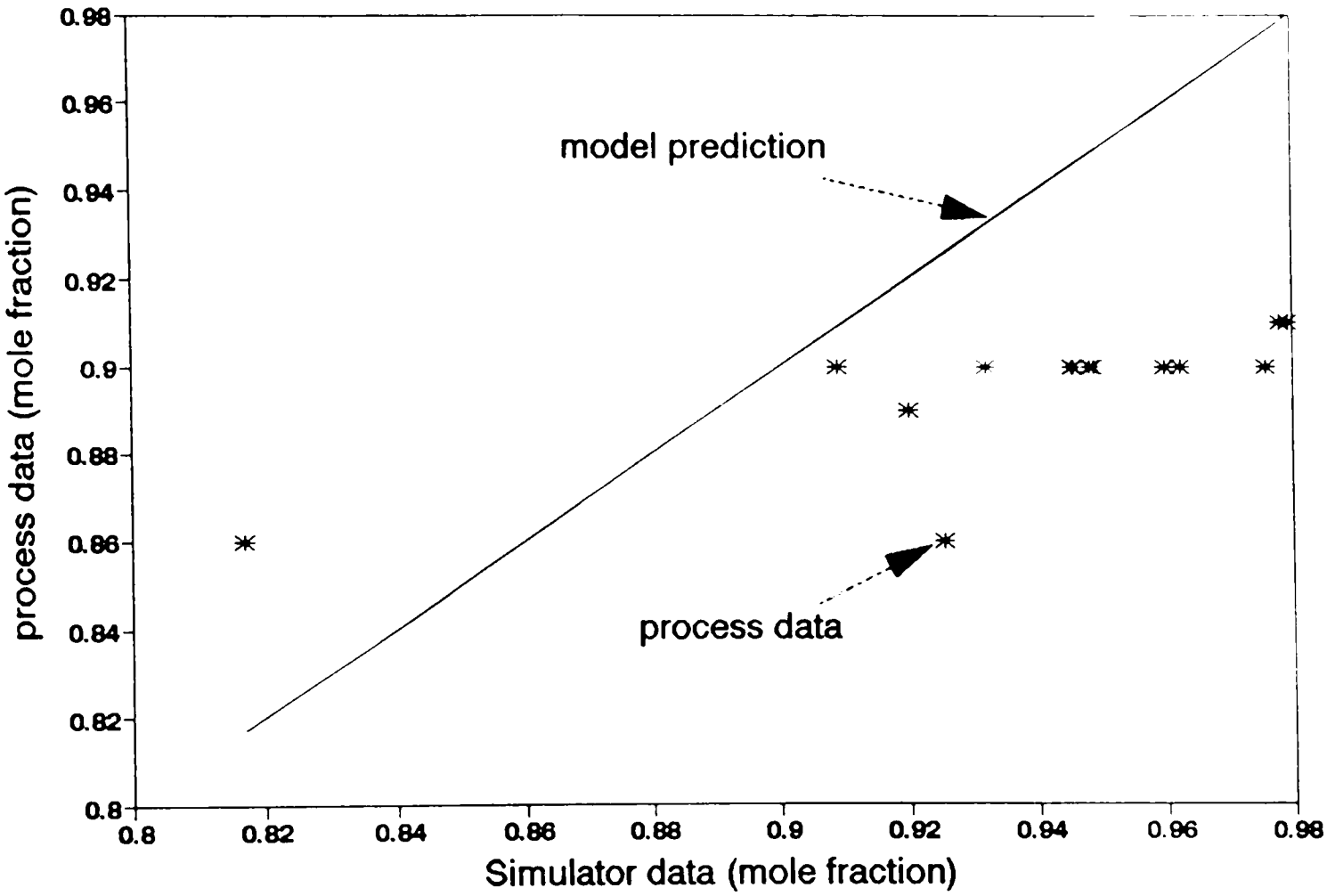

Figure 5.22. Process model mismatch. (a) Top composition.

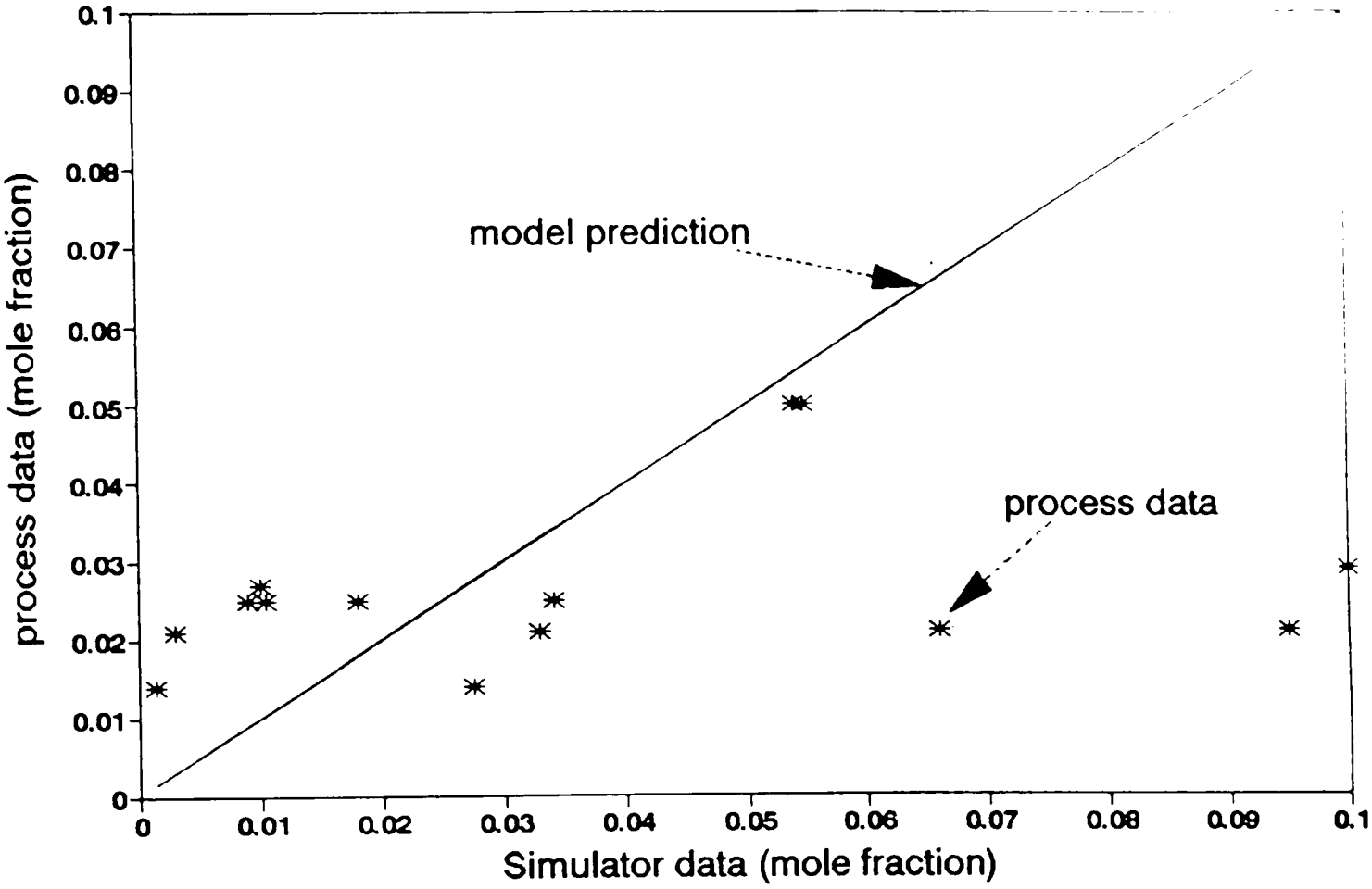

Figure 5.22. Continued. (b) Bottom composition.

the experimental results show. The result contradicts the normal expectation for good control and supports the conviction expressed earlier that the gain prediction is the key model feature which would indicate good control. Gain predictions have two components: magnitude and direction. While it is important that the magnitude of the change be approximate to the real process gain change, it is the direction which is more critical. If the model is able to point the right direction with a reasonably approximate magnitude of change, the model has the potential to make good control decisions. In this study, the amount of gain mismatch at various states was not determined, as it required large experimental steady-state data at a large (for this program) experimental cost.

5.2.6 ATV Results

ATV stands for Autotune Variation. This is a technique by which one can find the tuning parameters of a PI controller without making an extensive trial search in a multidimensional space. This method was originally developed by Astrom (1984) and has been described in the text by Luyben (1986). ATV method tries to find out the ultimate gain (K_u) and ultimate period (P_u) for sustained oscillation in the dependent variables in response to the manipulated variables. The tuning parameters are calculated from the K_u and P_u. The controllers are then subjectively detuned by an operator, using a common detuning factor on-line to achieve the subjective best tuning possible for the coupled system.

Figures 5.23(a) and 5.23(b) show the response of the process variables (top and bottom compositions, respectively) to changes in the manipulated variables. In this

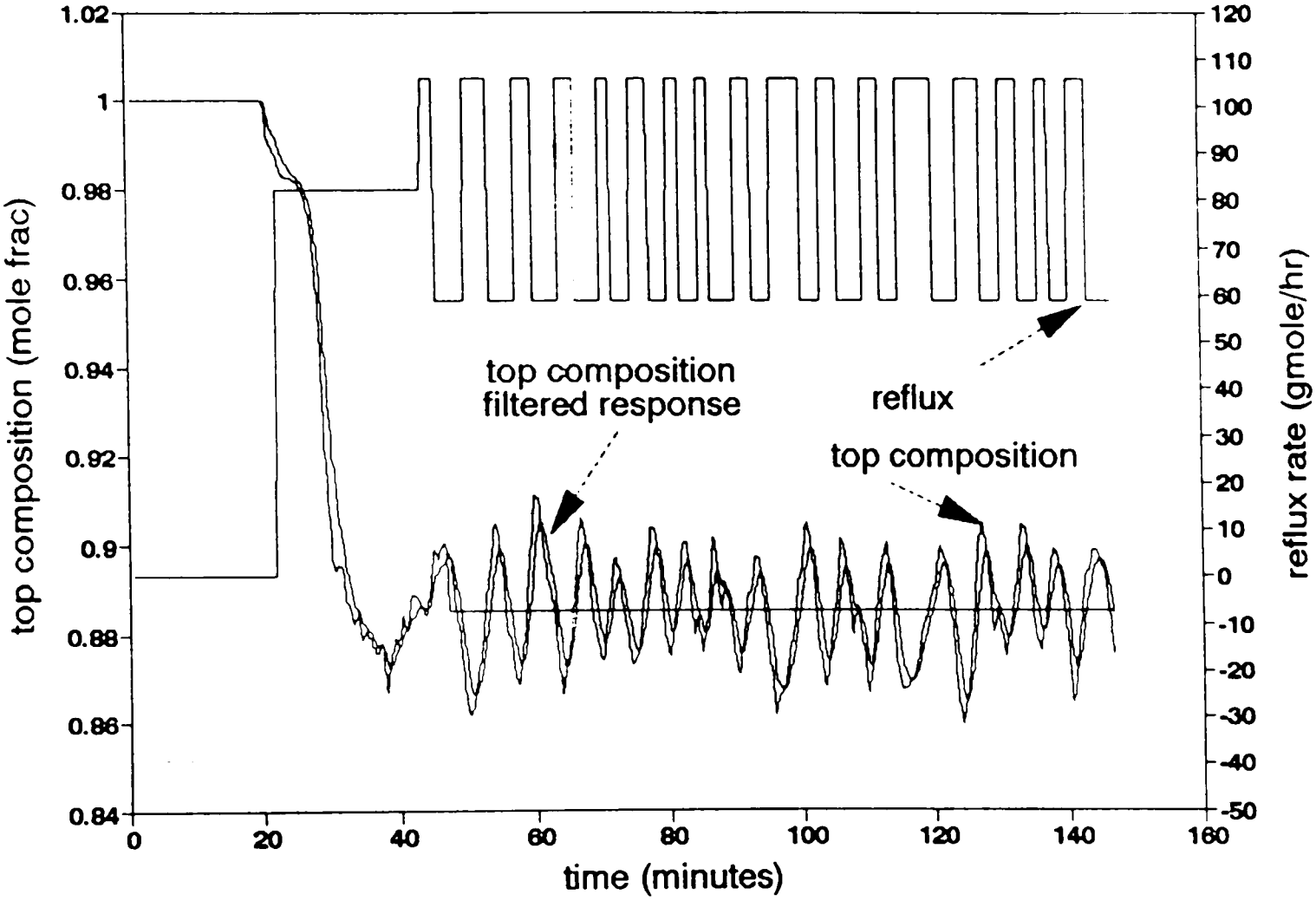

Figure 5.23. Auto tune variation relay feedback. (a) Top composition.

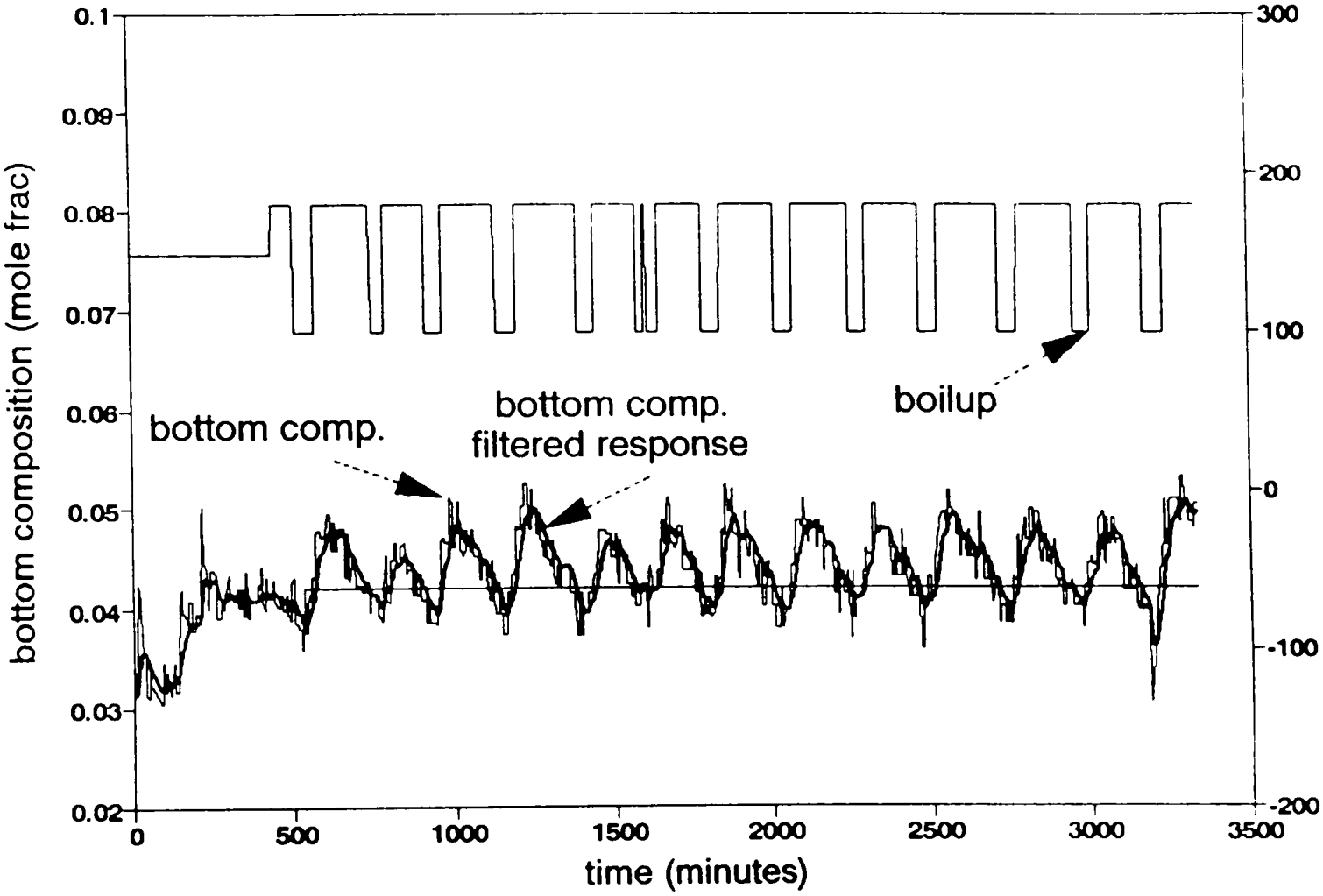

Figure 5.23. Continued. (b) Bottom composition.

method, a sustained step oscillation is created in the manipulated variable (200 counts for the reflux and 350 counts for the boilup) as shown in Figure 5.23 (a),(b) and is introduced as a feedback whenever the process variable crosses a particular setpoint (88.5% top composition in Figure 5.23(a) and 4.2% bottom composition in Figure 5.23(b)). The amplitude of the oscillation in the manipulated variable is called as relay height 'h'.

If the average amplitude of this oscillation in the process variable is 'd', the ultimate gain of the controller, K_u, can be calculated using the following equation.

$$K_u = \frac{4h}{\pi d} \tag{5.2}$$

The ultimate period, P_u, is the same as the period of oscillation. From Figures 5.23(a) and 5.23(b), K_u and P_u for the top and bottom compositions are found to be 20703 counts/mole fraction, 6.5 minutes and 99029 counts/mole fraction, 19.25 minutes, respectively.

Two different approaches for finding the tuning parameters are explored. One is based on the Tyreus-Luyben method and another based on the Ziegler-Nichols method. In the Tyreus-Luyben approach, the proportional constant and the integral constant are calculated from the following equations.

$$K_c^{TL} = K_u / 3.22 \tag{5.3}$$

$$T_i^{TL} = 2.2 * P_u \tag{5.4}$$

Then, the top and bottom control loops are detuned simultaneously using a single detuning factor, F_{DT} and described as follows.

$$K_c = K_c^{TL} / F_{DT} \tag{5.5}$$

$$T_i = T_i^{TL} * F_{DT} \tag{5.6}$$

Figures 5.24(a) and 5.24(b) show the results of dual-composition control using a detuning factor of 3.0 and Tyreus-Luyben tuning. The bottom composition is found to take much less time to cross the setpoint in comparison to other previously studied controller (15-20 minutes instead of 80-100 minutes). The controller is unable to eliminate the offset in either top or bottom compositions. A larger detuning factor would make the controller more sluggish and would, thereby, increase the offset. A smaller detuning factor would create a larger overshoot, and the process would go beyond the operational limits.

The Ziegler-Nichols method takes a similar approach, but considers bigger integral actions as shown below.

$$K_c^{ZN} = 0.45 * K_u \tag{5.7}$$

$$T_i^{ZN} = 0.83 * P_u \tag{5.8}$$

Figures 5.25(a) and 5.25(b) show the results using the Ziegler-Nichols method with a detuning factor of 4.5. It can be observed that the higher integral action is able to eliminate the offset in the top composition. However, there is a sustained offset and large overshoot in the bottom composition. The bottom composition control loop requires more integral action but less proportional. It is concluded that a straightforward ATV tuning may not always give the best tuning parameters but can be used for initial estimates for tuning the controller online and heuristically.

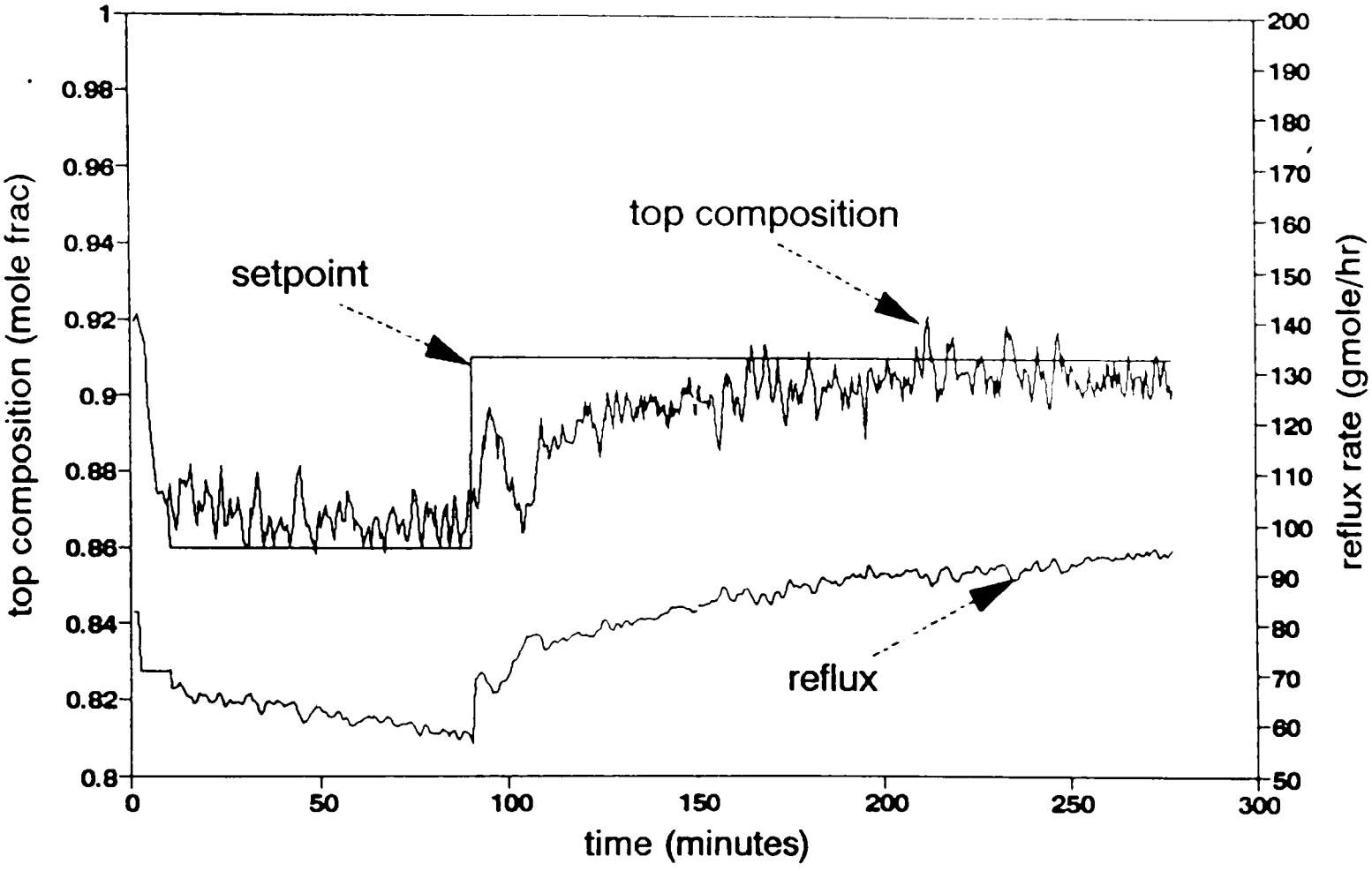

Figure 5.24. PI control with ATV (Tyerus-Luyben with DTF=3.0).
(a) Top composition.

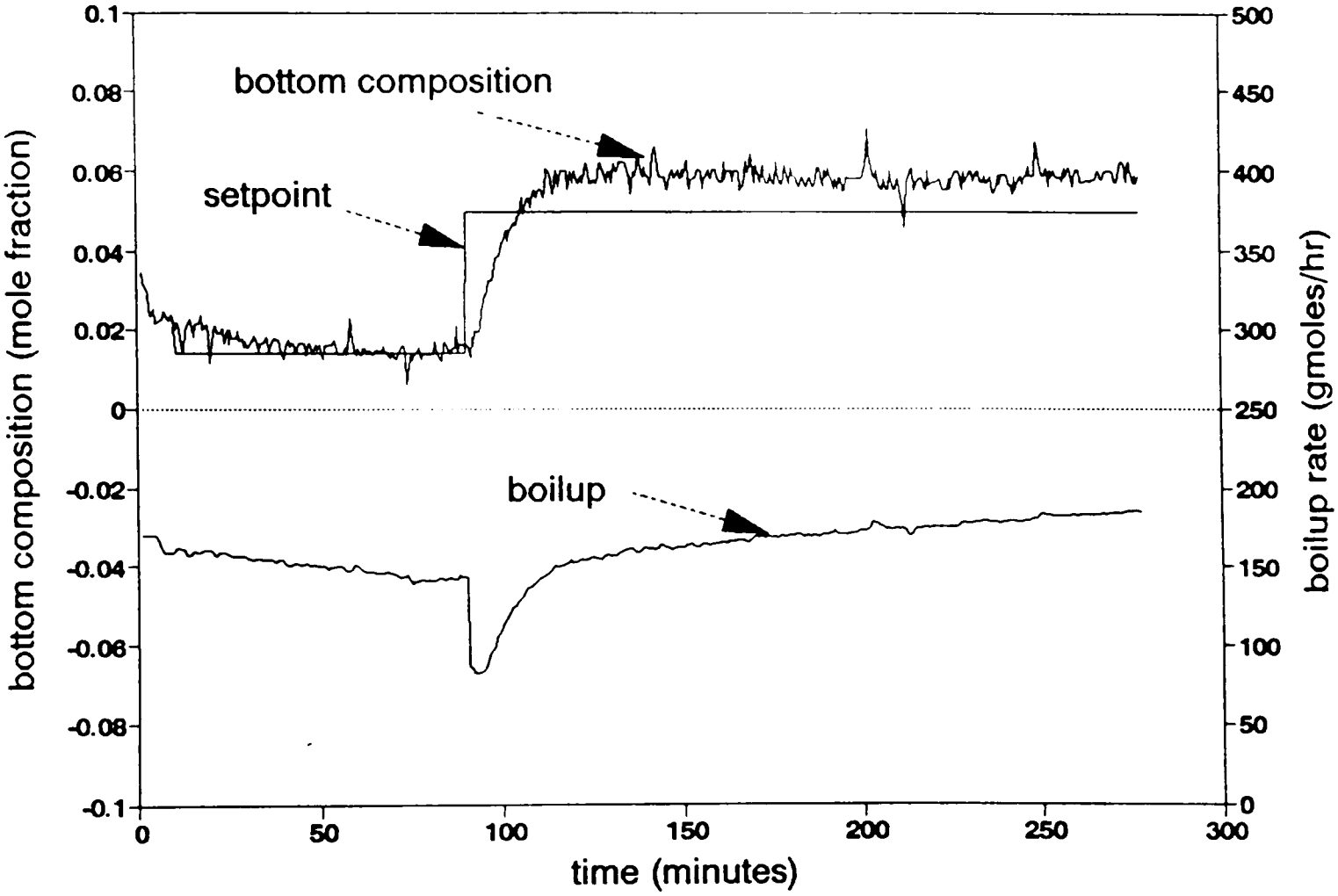

Figure 5.24. Continued. (c) Bottom composition.

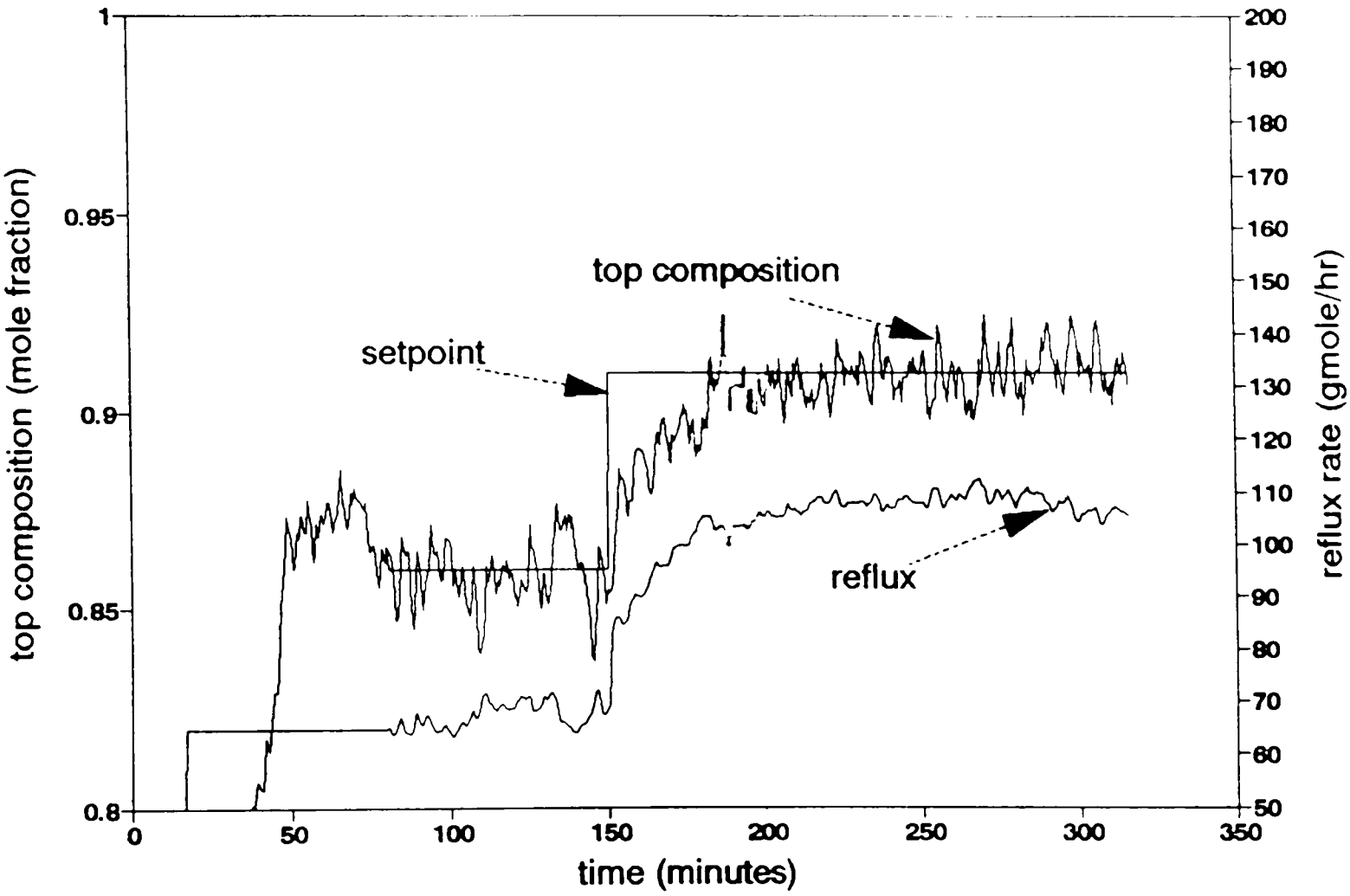

Figure 5.25. PI control with ATV (Ziegler-Nichols with DTF = 4.5).
(a) Top composition.

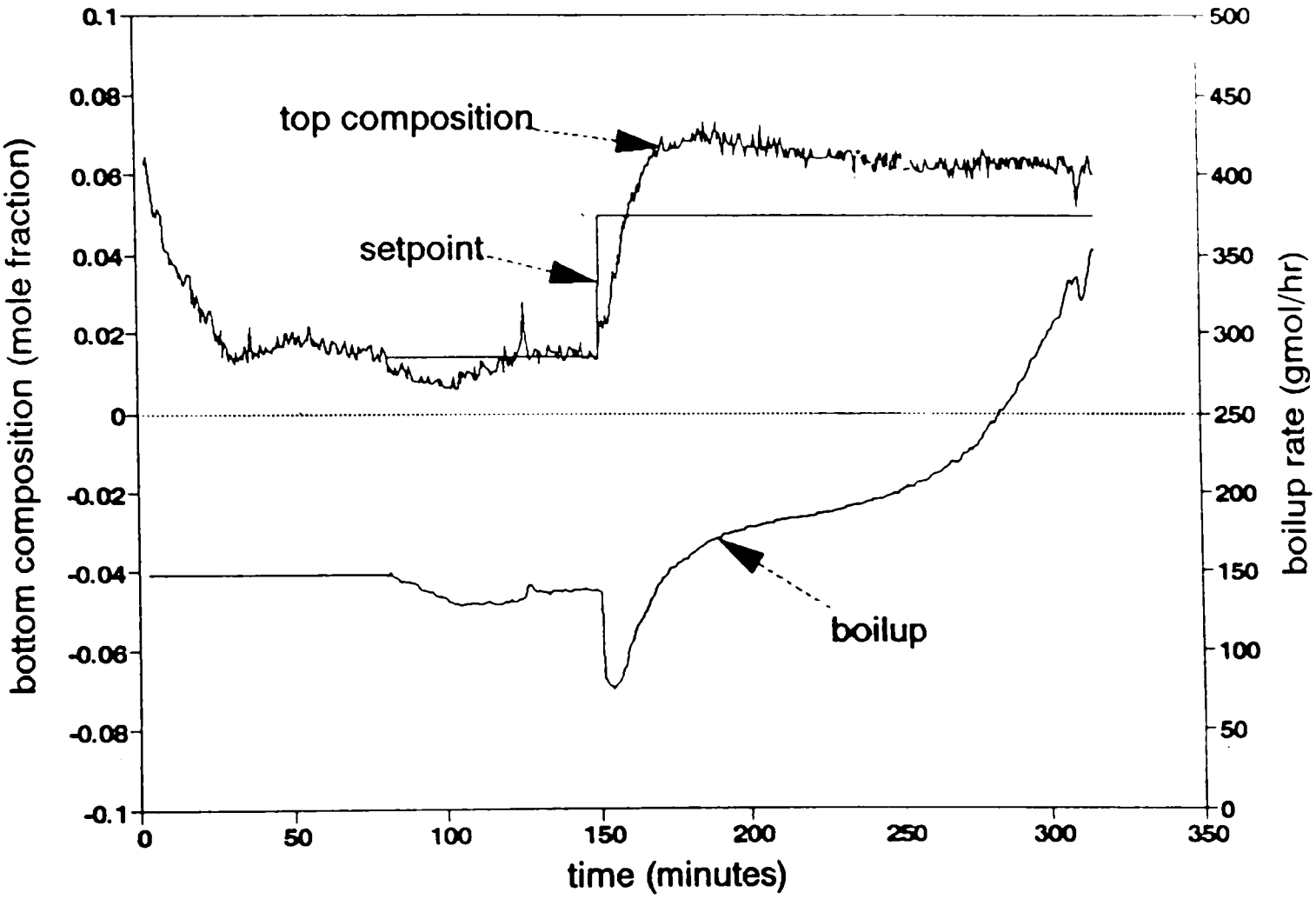

Figure 5.25. Continued. (b) Bottom composition.

CHAPTER VI

COMPARISON OF CONTROL RESULTS

The criteria for a fair comparison of different control strategies must include not only the resulting control performance, but several other issues, such as:

1. Process knowledge required of the control engineer,
2. Modeling ease,
3. Implementation ease,
4. Tuning ease,
5. Constraint handling ability,
6. Operator training,
7. Economics.

The following section describes the performance comparison made between various advanced controllers, viz. PMBC, [DMC]^{TM}, Advanced Classical Controller (ACC), Neural-Network Model-Based Controller using Inverse-of-State Prediction and Neural-Network Model-Based Controller using Gain Prediction and Optimization. Section 6.2 discusses some of the other issues important for controller comparison studies.

6.1 Performance Comparison

Table 6.1 shows a quantitative comparison of the performance of all controllers. The terms ISE, IAE and manipulated variable move are defined as follows.

Table 6.1. Quantitative Comparison of Controller Performance

Control Type	Setpoint Tracking				Disturbance Rejection					
					feed composition, 20-35 %			feed composition, 30-20 %		
Perfor -mance Criteria	Over-shoot (mol fr)	Rise-time (min.)	IAE (mol fr. min.)	Manip. Variable Move (gmol/hr)	ISE (mol fr. mol fr. min.)	Max. Dev. (mol fr.)	Manip. Variable Move (gmol/hr)	ISE (mol fr. mol fr. min.)	Max. Dev. (mol fr.)	Manip. Variable Move (gmol/hr)
Top ACC	0.013	28	1.2	V=150	0.007	0.015	V=140	0.007	0.007	V=160
Bot	0.003	87	0.9	R=340	0.0002	0.003	R=180	0.0002	0.002	R= 220
Top [DMC]™	0.014	17	1.1	V=110	0.009	0.020	V=60	0.009	0.007	V=55
Bot	0.007	24	0.5	R=100	0.0005	0.004	R=100	0.0005	0.004	R=120
Top PMBC	0.010	31	0.9	V=70	0.008	0.007	V=70	0.008	0.015	V= 60
Bot	0.002	70	1.1	R=90	0.0004	0.003	R=150	0.0004	0.003	R= 50
Top $NN_{inv\ of\ state}$	0.010	45	1.2	V=130	0.019	0.020	V=40	0.013	0.026	V=40
Bot	0.005	75	2.2	R=140	0.0035	0.011	R=45	0.0004	0.010	R=65
Top NN_{gain}	0.009	40	1.3	V=95	0.005	0.018	V=70	0.006	0.018	V=40
Bot	0.005	70	1.5	R=119	0.0014	0.007	R=70	0.0012	0.007	R=90

$$\text{Integral of the squared error (ISE)} = \sum_{t=0}^{2hr} e^2(t) \tag{6.1}$$

$$\text{Integral of the absolute value of the error (IAE)} = \sum_{t=0}^{2hr} |e(t)| \tag{6.2}$$

$$\text{Manipulated Variable Move} = \sum_{t=0}^{2hr} \Delta u(t) \tag{6.3}$$

where $e(t) = y_{sp}(t) - y(t)$ is the deviation (error) of the process variable from the desired setpoint and $\Delta u(t)$ is the change in manipulated variable action taken from the previous control action.

The [DMC]™ controller result is taken from the MS thesis of Amit Gupta (1994). [DMC]™ controller was configured for a four independent variables (feed flowrate, feed composition, reflux flowrate and reboiler heat input), and two dependent variables (methanol composition in the top and bottom products) system. A time-series model was developed from the Dynamic Matrix Identification ([DMI]™) program. Following DMCC protocol, the process tests required for the identification of the model were performed over a 96-hr period for step changes in the four independent variables. A steady-state time of 180 min was identified based on the response of the slowest settling variable (bottom composition). A 60-coefficient [DMI]™ model was used. Since one coefficient must be provided for each calculation of the controller, the [DMC]™ controller model was executed every 3 min. However, data was recorded each minute. Tuning of the [DMC]™ controller required specifying two tuning parameters for each dependent variable. These parameters a move suppression factor and an equal concern error. A simulation program,

part of the [DMC]™ control software, was used to determine initial tuning values. This simulation program assumes that the [DMI]™ model is a perfect representation of the process and conveniently allows various control studies to be performed for different tuning parameters. The initial values were subsequently fine-tuned on-line to subjectively improve the setpoint tracking and disturbance rejection control performance.

The Advanced Classical Controller (ACC) has also been studied by Gupta (Gupta, 1994) on the present distillation column. In all studies, tray compositions are inferred from the tray temperatures. Following the method of Moore (1992), tray 1 (counting from the bottom) and tray 5 were chosen as the locations for the bottom composition and top composition control, respectively. The control structure was used as cascade. A master controller infered the top product composition from tray 6, compared that value to the composition setpoint, and outputs a temperature setpoint to the slave controller. The slave controller compared the tray-5 temperature with this setpoint and manipulated the reflux flowrate. Bottoms control was similar. Feedforward control (standard lead-lag) was used to compensate for feed flowrate and composition changes. The models generated by the [DMI]™ analysis were used to calculate the transfer functions, and the feedforward correction was added to the reflux flowrate and the reboiler heat duty. A velocity mode algorithm was used for each of the PI controllers. The controller execution frequency was fixed at 5 sec. The initial tuning parameters were calculated following the method by Smith and Corripio (Gupta, 1994) which specify a first-order response of the first-order process. The controller was fine-tuned on-line to give reasonably good responses to both setpoint tracking and disturbance rejection.

Pandit studied the performance of a PMBC controller (Pandit, 1991). Pandit's nonlinear PMBC model was a nonideal, nonlinear description of the process derived from the fundamental tray-to-tray mass and energy balances and thermodynamic equilibrium considerations. Two model parameters of the distillation column, tray efficiency and a bias to the vapor boilup, were updated on-line to account for the process-model mismatch at steady-state. The steady-state was identified using on-line standard deviations of the key variables and a component material-balance closure error. This nonlinear steady-state model was used alongwith the GMC. The GMC parameters were tuned on-line based on the operator's experience to produce a resonably good response.

The two NN model-based control results are obtained from this work. The quantitative performance values (ISE, IAE, etc., as in Table 6.1) for the ACC, [DMC]^{TM} and PMBC are estimated from the figures in Gupta's thesis and Pandit's dissertation.

In the setpoint tracking mode, all controllers take approximately the same time to initially reach the new top and bottom composition setpoints (i.e., risetime). The [DMC]^{TM} controller performs slightly more aggressively, showing minimum rise time (17 and 24 min for top and bottom compositions) but maximum overshoot (0.014 and 0.007 mole fraction for top and bottom compositions) in camparison to other controllers. The two neural-network controllers show very similar performance in terms of rise time and IAE with ACC and PMBC controllers in the setpoint-tracking mode. PMBC showed the least manipulated variable work.

All of these controllers are able to eliminate the offset in the top and bottom compositions practically without any overshoot. The Advanced Classical Controller

(ACC) took the maximum time (87 min) to track the new setpoint for the bottom composition. The ACC also showed little cycling around the new top composition setpoint. The ACC has a noise-like character to the manipulated variable response. The noise-like response in the manipulated variables is primarily due to the choice of the lowest control interval (5 sec) which is supported by the simplest computational algorithm.

Because of the smallest control interval, ACC shows the maximum movements in manipulated variables (V=150, R=340 gmoles/hr) over the period of 2 hr. Since the Process-Model-Based Controller (PMBC) considers a rigorous nonlinear process model to calculate the manipulated variable actions, the controller frequency was fixed at 3 min. The [DMC]^{TM} controller used a Dynamic Matrix Identification (DMI) model with 60 coefficients. The slowest settling variable, the bottom composition, took about 180 min to reach steady state. Since one coefficient must be provided for each calculation/execution of the controller, the [DMC]^{TM} controller action was implemented every 3 min. However, the neural-network model-based controllers can take care of a nonlinear model of the process and also compute the manipulated variables rapidly. As a result, the control interval for the neural-network model-based controllers is fixed at a half -minute. These differences in control-execution frequency, the field tuning choices of three independent operators and the changes in the column behavior over the 6 year span of the five control strategy study make it impossible to legitimately claim that there are any significant performance differences between the techniques via servo mode. All strategies performed well.

For the disturbance rejection cases, also, all five controller performances are judged equivalent. All controllers do a fairly good job of maintaining the top and bottom compositions at their setpoints. The [DMC]™, PMBC and the two neural network controllers , however, have a smoother response of the manipulated variables compared to the ACC. The slight variations in amount of maximum composition deviations and ISE are mainly due to the nonstationary behavior of the process and the difference in human judgement in finding the optimum tuning parameters. The variations in manipulated variable movements are mainly due to the difference in the choice of control interval. The lower the control interval, the higher are the manipulated variable movements.

It must be noted here, that [DMC]™, PMBC, ACC and NN model-based inverse-of-the-state-prediction controllers had feedforward corrections for disturbance rejection in addition to the feedback loop. The NN-based gain-prediction controller as implemented here only had feedback action. Since the process is slow to respond with the changes in the manipulated variables, feedforward correction does not produce a significant difference in controller performance. Table 6.2 summarizes qualitatively the results and advantages of the different controllers.

6.2 Other Issues

Model-based controllers have demonstrated economic advantages over the classical PID approaches, but these advantages are achieved at a price. The process

Table 6.2. Summary of Control Performance

Control Issues	ACC	PMBC	[DMC]™	$NN_{inv\ of\ state}$	NN_{gain}
Servo and Regulatory	Good control with noise like response of manipulated variables	Good control with smooth manipulated variables response	Good control with smooth manipulated variables response	Good Control with smooth manipulated variables response	Good Control with smooth manipulated variables response
Model Type	linear	nonlinear	linear	nonlinear	nonlinear
Constraint Handling Capabilities	no	yes	yes	no	yes
Computa-tional Time Required for Control	least (control interval used 5 seconds)	significant (control interval used 3 minutes)	moderate (control interval used 3 minutes)	moderate (control interval used half a minute)	moderate (control interval used half a minute)
Handling of Economic Issues	no	yes	yes	no	yes
Amount of Modeling Effort Required	least but extensive on-line tuning is involved	moderate and require rigorous mathematical modeling	moderate and require exten-sive process step tests	moderate and model can be built off-line using CAD packages	moderate and model can be built off-line using CAD packages
Handling of Ill-behaved Dynamics	no	no	yes	no	no

knowledge required of the control engineer is greater. The front-end model development cost includes either substantial process step tests or engineering effort or both. The PMBC control strategy requires the control engineer to have very good knowledge of the process in order to develop the fundamental differential equations describing the process behavior. The [DMC]™ controller requires the control engineer to have a good knowledge of the process from the process operation point of view. The operator must determine in consultation with plant personnel the relative importance of various variables to be included in the multivariable controller. Often additional or improved sensors are required. While simple model-based controllers can be implemented in some existing Distributed Control Systems, an additional computer is often required to solve large problems. One must keep in mind that controllers should be designed to achieve the maximum economic benefits from a plant. Capturing these benefits will often require a large controller to encompass all the pertinent economic calculations and process constraints.

The neural-network models can be developed from available CAD packages or from existing data sets stored in the plant. Significant process knowledge and effort is required for data reconciliation, training the data sets for the neural network controllers, choice of good data sets, and proper CAD feature selection..

A significant advantage of model-based controllers and model-predictive controllers over the PID controller is the ease of constraint handling. Industrial processes typically have constraints on the manipulated and controlled variables and sometimes on the maximum change of manipulated variables to avoid any large upset in the process. The [DMC]™ controller has built-in programs to handle constraints and economic

optimization. A separate control program was written by Pandit (1991) for the PMBC controller to handle constraints. The neural-network model-based controller using gain prediction approach and Heuristic Random Optimization (HRO, Li and Rhinehart, 1996) takes care of the constraint inherently and no separate computational effort (such as the penalty function method with Lagrangian multipliers) is required. PI controllers do not have any built-in constraint-handling capabilities, and separate programs incorporating override logic have to be developed for constraint control.

CHAPTER VII

CONCLUSIONS AND RECOMMENDATIONS

7.1 Conclusions

In this work, a novel strategy of neural-network model-based gain-prediction control with constraint-handling capabilities has been developed and successfully tested on a lab-scale distillation column separating a methanol-water mixture. This control strategy has proved to be very effective in setpoint tracking, disturbance rejection and constraint handling.

Another neural-network model-based control strategy using the inverse of the steady-state-prediction approach (developed and tested earlier on a simulator by Ramchandran) has been successfully implemented on the laboratory distillation column. This controller was tested for dual-composition control (top and bottom) and preheater temperature control (feed and reflux). When unconstrained, this controller produced similar performance to the gain-prediction approach in dual composition control mode. In preheater temperature control, the controller parameters (proportional and integral constants of GMC law) required no retuning with flowrate changes or state (temperature) changes. The control strategy has proved to be very reliable at the unconstrained state of the process.

No significant differences could be derived in terms of quantitative performance comparison of these two NN model-based control strategies with other industrially relevant advanced controllers (ACC, PMBC, [DMC]^{TM}) on the various experimental runs.

In the unconstrained mode, all five control strategies performed comparably with respect to control variable and manipulated variable actions. The benefit of the nonlinear features of the NN controllers was especially evident on the preheater temperature control. However, each controller can be differentiated from others in terms of their qualitative capabilities. The neural-network model-based gain-prediction controller and the [DMC]^{TM} controller were best for constraint handling.

7.2 Recommendations

Some work is possible on this system that would make this study more comprehensive. The following recommendations are made.

1. All control comparison were made in the low-to-moderate purity region (86% to 95% top composition). Comparison studies should be carried out in the high-purity regions also to ensure the robustness of the controllers at different operating regions. The column boilup capability needs to be increased to permit this evaluation.
2. Incorporation of methods to handle difficult dynamics (such as inverse response) in the developed NN model-based control strategies would make the controller robust from all perspectives.
3. Nonlinear Internal Model Control (NLIMC) will be a definite improvement over traditional PID controllers. Control studies using NLIMC should be done to make controller comparisons comprehensive.
4. Some changes in the experimental setup are desired. The experimental setup was originally designed for unit operations exercises by undergraduate students. The

column has occasionally shown the phenomenon of 'weeping' on the top tray. In this situation, the vapor flowrate is not high enough to keep the holdup on the top tray and small part of the liquid on the top tray weeps through the holes and falls onto the tray below, leading to a loss of the separation on the top tray. The addition of greater reboiler heater power, two or three more trays in the column, and taller weirs to increase the liquid holdup on each tray would give better-behaved column performance, suitable for advanced control studies.

BIBLIOGRAPHY

Åstrom, K. J., and McAvoy, T. J. "Intelligent Control," *J. Proc. Cont.*, Vol. 2(3), 1992, 115 -127.

Åstrom, K. J., and Hagglund, T. "Automatic Tuning of Simple Regulators with Specifications on Phase and Amplitude Margins," *Automatica*, Vol. 20, 1984, 645.

Barnard, E. "Optimization for Training Neural Networks," *IEEE Trans. on Neural Networks*, Vol. 3(2), 1992, 232-240.

Battiti, R. "Accelerated Back-propagation Learning: Two Optimization Methods," *Complex Syst.*, Vol. 3, 1989, 331-342.

Battiti, R. "First- and Second-Order Methods for learning: Between Steepest Descent and Newton's Method," *Neural Computation*, Vol. 4, 1992, 141-166.

Bhat, N. V., Minderman, P., McAvoy, T. J., and Wang, N. S. "Modeling Chemical Process Systems Via Neural Computation," *IEEE Cont. Syst. Mag.*, Vol. 10(3), 1990, 24-30.

Broyden, C. G., Dennis, J. E., and More, J. J. "On the Local and Superlinear Convergence of Quasi-Newton Methods," *J.I.M.A.*, Vol. 12, 1973, 223-246.

Brown M. W., Lee, P.L., Sullivan, G. R. and Zhou, W. "A Constrained Nonlinear Multivariable Control Algorithm," *AICHE Annual Meeting*, San Francisco (1989).

Cao, S., and Rhinehart, R. R. "A self-tuning filter," *J. Proc. Cont.*, Vol. 6,1996.

Cao, S., and Rhinehart, R. R. "An efficient method for on-line identification of steady-state," *J. Proc. Cont.*, Vol. 5(6), 1995, 363-374.

Chang, T. S., and Seborg D. E. "A Linear Programming Approach to Multivariable Feedback Control with Inequality Constraints," *Int J Control*, 1983, Vol. 37, 583.

Cott, B. J., Reilly, P. M., and Sullivan, G. R. "Selection Techniques for Process Model-Based Controllers," paper presented at *AIChE National Meeting*, spring,1985, Houston, TX.

Cutler, C. R., and Ramaker, B. L. "Dynamic Matrix Control - A Computer Control Algorithm," Paper No. S1b, *AICHE 86th National Meeting*, April 1979; also *Joint Automatic Control Conf. Proc.*, 1980, San Francisco, CA.

Cutler, C.R., and Hawkins, R. B. "Constrained Multivariable Control of a Hydrocracker Reactor," *Proceedings of the ACC Conference,* Minneapolis, MN, June 10-12, 1987.

Dutta, P., and Rhinehart, R. R. "Experimental Comparison of a Novel, Simple, Neural Network Controller and Linear Model Based Controllers," *Proceedings of the ACC Conference,* Seattle, WA, June 21-23, 1995.

Dutta, P., and Rhinehart R. R. "Measures That Indicate the Need for Dynamic Compensation When Steady-State Models are Used for Control," accepted, *ACC Conference*, 1997.

Eaton, J.W., and Rawlings, J. B. "Feedback Control of Chemical Processes Using On-Line Optimization Techniques," *Comp. and Chem. Eng.*, Vol. 14, 1990, 469-479.

Economou, C.G., Morari, M., and Plasson, B.O. "Intenal Model Control - Extension to Nonlinear Systems," *Ind. Eng. Chem. Process Des. Dev.*, 1986, Vol. 25, 403.

Ganguli, S., and Saraf, D. N. "Startup of a Distillation Column Using Nonlinear Analytical Model Predictive Control," *Ind. Eng. Chem. Res.*, Vol. 32, 1993, 1667-1675.

Garcia, C. E., and Morari, M. M. "Internal Model Control.- 1. A Unifying Review and Some New Results," *Ind. Eng. Chem. Process Des. Dev.*, Vol. 21, 1982, 308-323.

Garcia, C. E., and Morari, M. M. "Internal Model Control-2. Design Procedure for Multivariable Systems," *Ind. Eng. Chem. Process Des. Dev.*, Vol. 24(2), 1985a, 472.

Garcia, C. E., and Morari, M. M. "Internal Model Control-2. Multivariable Control Law Computation and Tuning Guidelines," *Ind. Eng. Chem. Process Des. Dev.*, Vol. 24(2), 1985b, 484.

Gupta, A. "Comparison of Advanced Control Techniques on a Lab-Scale Distillation Column," M.S. Thesis, Texas Tech University, Lubbock, TX, 1994.

Haggblom, K. E., and K. V. Waller, "Control Structures for Disturbance Rejection and Decoupling of Distillation," *AICHE J.*, Vol. 36, 1990, 1107.

Henley, E.J., and Seader, J.D. *Equilibrium-Stage Separation Operations in Chemical Engineering*, John Wiley, New York, 1981.

Himmel, C. D., May, G.S. "Advantages of Plasma Etch Modeling Using Neural Networks Over Statistical Techniques," *IEEE Transactions on Semiconductor Manufacturing*, Vol. 6(2), 1993, 103-111.

Hokanson, D. A., Brad G. H., and Johnston, J. H. "DMC Control of a Complex Refrigerated Fractionator," *ISA Meeting*, Philadelphia, Pennsylvania, October 22-27, 1989.

Hsiung, J. T., Suewatanakal, W., and Himmelblau, D. M. "Should Backpropagation be Replaced by a More Effective Optimization Algorithm?" *Proc. IJCNN*, Seattlle, WA, 1991.

Humphrey, J. L., Seibert, A. F., and Koort, R. A. "Separation Technologies-Advances and Priorities," *DOE Contract* AC0&-901D12920, February 1991.

Kollias, S., and Anaastassious, D. "Adaptive Training of Multilayer Neural Networks using a Least Squares Estimation Technique," *Proc. IEEE Intl. Conf. of Neural Networks* (2nd), Vol. 1, 1988, 383-390.

Kramer, M. A., and Leonard, J. A. "Diagnosis Using Backpropagation Neural Networks-Analysis and Criticism," *Comp. and Chem. Eng.*, Vol. 14(12), 1990, 1323- 1338.

Kung, S. Y., and Hwang, J. N. "An Algebraic Projection Analysis of Optimal Hidden Units Size and Learning Rates in Backpropagation Learning," *Proc. IEEE Intl. conf. of Neural Networks* (2nd), Vol. 1, 1988, 363-370.

Lee, P. L., and Sullivan, G. R. "Generic Model Control," *Comp. and Chem. Eng.*, Vol.12(6), 1988, 573-580.

Lee, P.L. (Ed.), *Nonlinear Process Control: Applications of Generic Model Control*, Springer-Verlag, New York.

Leonard, J. A., and Kramer, M. A. " Improvement of the Backpropagation Algorithm for Training Neural Networks," *Comp. and Chem. Eng.*, Vol. 14(3), 1990a, 337-341.

Li, J., and Rhinehart, R. R. "Heuristic Random Optimization," accepted, *J. Proc. Cont.*, 1996.

Little, D. L., and Edgar, T.F., *ACC Proceedings*,1986, June 18-20, Seattle, Washington, 3; 1356.

Luyben W. L., and Tures, B. D. "Control of a Binary Distillation Column with Sidestream Drawoff," *Ind. Eng. Chem. Proc. Des. Dev.*, Vol. 14, 1975, 291.

MacMurray, J., and Himmelblau, D. "Identification of a Packed Distillation Column for Control via Artificial Neural Networks," *Proc. Amer. Cont. Conf.*, San Francisco, CA,1993,1455-1459.

Mehra, R.K., and Mahmood, S. "Model Algorithmic Control" Chapter 15 in *Distillation Dynamics and Control* (ed. P.B. Despande), ISA, Research Triangle Park, NC, 1985.

Moore, C. F. "Selection of Controlled and Manipulated Variables," in *Practical Distillation Control,* McGraw Hill, New York, 1992.

Morari, M., and Skogsted, S. "LV - Control of a High Purity Distillation Column," *Chem. Eng. Sci.*, Vol. 43, 1988, 33.

Morari, M., and Skogsted, S. "Control Configurations Selection for Distillation Columns," AICHE J., Vol. 33, 1987, 1620.

Pandit, H.G., and Rhinehart, R. R. "Experimental Demonstration of Constrained Process Model-Based Control of a Nonideal Binary Distillation Column," *Proc. Amer. Cont. Conf.*, Chicago, IL, 1992, 630-631.

Pandit, H.G., and Rhinehart, R. R. "Experimental Demonstration of Nonlinear Model-Based Control of a Nonideal Binary Distillation Column," *Proc. Amer. Cont. Conf.*, Chicago, IL, 1992, 625-629.

Pandit, H.G. "Experimental Demonstration of Model-Based Control Techniques," Ph.D. Dissertation, Texas Tech University, Lubbock, TX, 1991.

Park, S. "The Application of an Optimized DMC Multivariable Controller to the PCC Catalytic Cracking Unit", *International Symposium Advanced Process Supervision and Real-Time Knowledged Based Control*, University of Newcastle upon Tyne, U.K., November, 1988.

Parker, D. B. "Optimal Algorithm for Adaptive Networks: Second Order Backpropagation, Second Order Direct Proapagation, and Second Order Hebbian Learning," *Proc. IEEE Conf. on Neural Networks,* Vol. 2, 1987, 593-600.

Peel, C., Willis, M. J., and Tham, M. T. "A Fast Procedure for the Training of Neural Networks," *J. Proc. Cont.*, Vol. 2(4), 1992, 205-211.

Poli, I., and Jones, R. D. "A Neural Network Model for Prediction," *J. Amer. Stat. Assn.*, Vol. 89(425), 1994, 117-121.

Pottman, M., and Seborg, D. E. "Identification of Nonlinear Processes Using Reciprocal Multiquadratic Functions," *J. Proc. Cont.*, Vol. 2(4), 1992, 189-203.

Press, W. H., Teukolsky, S. A., Vetterling, W. T., and Flannery, B. P. *Numerical Recipes in C, The Art of Scientific Computing*, 2nd Edition, Cambridge University Press, England, 1992, 683-688.

Ramchandran S., and Rhinehart R.R. "A Very Simple Structure For Neural Network Control of Distillation," *J. Proc. Cont*, 1994.

Ramchandran S. "Neural Network Model-Based Control of Distillation Columns," Ph. D. Dissertation, Texas Tech University, Lubbock, TX, 1994.

Rhinehart, R. R. "An On-line SPC- Based Trigger for Control Action," *Proceedings of the SPIE Micro electronic Manufacturing '94 Conference*, paper 2336-06, October 17-21, 1994, Austin, TX, 50-58.

Rhinehart, R. R. "A CUSUM Type On-line Filter," *Process Control and Quality*, Vol. 2, 1992, 169-176.

Ricker, N.L. "The Use of Quadratic Programming for Constrained Internal Model Control," *Ind Eng. Process Des Dev*, Vol. 24(4), 1985, 925.

Ricotti, L.P., Ragazzini, S., and Martinelli, G. "learning Word Stress in a Sub-Optimal Second Order Backpropagation Neural Networks," *Proc. IEEE Conf. on Neural Networks*, Vol.1, 1988, 355-361.

Rietman, E. A., and Lory, E.R. "Use of Neural Networks in Modeling Semiconductor Manufacturing Processes: An Example for plasma etch Modeling," *IEEE Transactions on Semiconductor Manufacturing*, Vol. 6(4), 1993, 343-347.

Riggs, J. B., Beauford, M., and Watts, J. "Using Tray-to-Tray Models for Distillation Control," in *Nonlinear Process Control: Applications of Generic Model Control*, Ed. Peter L. Lee, Springer-Verlag London Ltd., UK, 1993, 67-103.

Rouhani, R., and Mehra, R.K. "Model Algorithm Control (MAC); Basic Theoretical Properties," *Automatica*, Vol. 8(4), 1982, 401.

Sanchez, J. M., and Shah S. L. "Multivariable Adaptive Predictive Control of a Binary Distillation Column," *Automatica*, Vol. 20, 1984, 607.

Shinskey, F. G., *Distillation Control*, McGraw-Hill, New York, 1984.

Thibault, J., and Grandjean, B. P. A. "Neural Networks in Process Control - A Survey," in *Advanced Control of Chemical Processes*, Eds. K. Najim and E. Dufour, *IFAC Symposium Series* No. 8, 1992, 251-260.

Tran D., and Cutler C. R. "Dynamic Matrix Control on Benzene and Toluene Towers," *ISA Meeting,* Philadelphia, Pennsylvania, October 22-27, 1989.

Tyreus, B. D., and Luyben W. L. "Controlling Heat Integrated Distillation Column," *Ind. Eng. Chem. Proc. Des. Dev.*, Vol. 25, 1986, 762.

Venkatasubramanian, V., Vaidyanathan, R., and Yamamoto, Y. "Process Fault Detection and Diagnosis Using Neural Networks-1. Steady-State Processes," *Comp. and Chem. Eng.*, Vol. 14(7), 1990, 699-712.

Venkatasubramanian, V., and Chan. K. "A Neural Network Methodology for Process Fault Diagnosis," *AICHE J.*, Vol. 35, 1989, 1993-2005.

Watrous, R. L. "Learning Algorithms for Connections and Networks: Applied Gradient methods for Nonlinear Optimization," *Proc. IEEE Conf. on Neural Networks*, Vol. 2, 1987, 619-627.

Weigand, A. S., Huberman, B. A., and Rumelhart, D. E. "Predicting the Future: A Connectionist Approach," *Intl. J. Neural Systems*, Vol. 1(3), 1990, 193-209.

White, H. "Some Asymptotic Results for Backpropagation," *Proc. IEEE Conf. on Neural Networks*, Vol. 3, 1987, 261-266.

Willis, M. J., Di Massimo, C., Montague, G.A., Tham, M. T., and Morris, A. J. "Artificial Neural Network Based Predictive Control," in *Advanced Control of Chemical Processes,* Eds. K. Najim and E. Dufour, *IFAC Symposium Series* No. 8, 1992, 261-266.

Wood, R. K., and Berry, M. W. "Thermal Composition Control of a Binary Distillation Column," *Chem. Engg. Sci.*, Vol. 28, 1973, 1707.

APPENDIX A

PMBC, ACC AND [DMC]™ CONTROL RESULTS

The following figures describe the setpoint tracking (Case 1, Table 5.4) and disturbance rejection (Case 2 and Case 3, Table 5.4) results. The PMBC results are reproduced from the dissertation of Hemant Pandit (1992). The ACC and [DMC]™ results are reproduced from Gupta (1994).

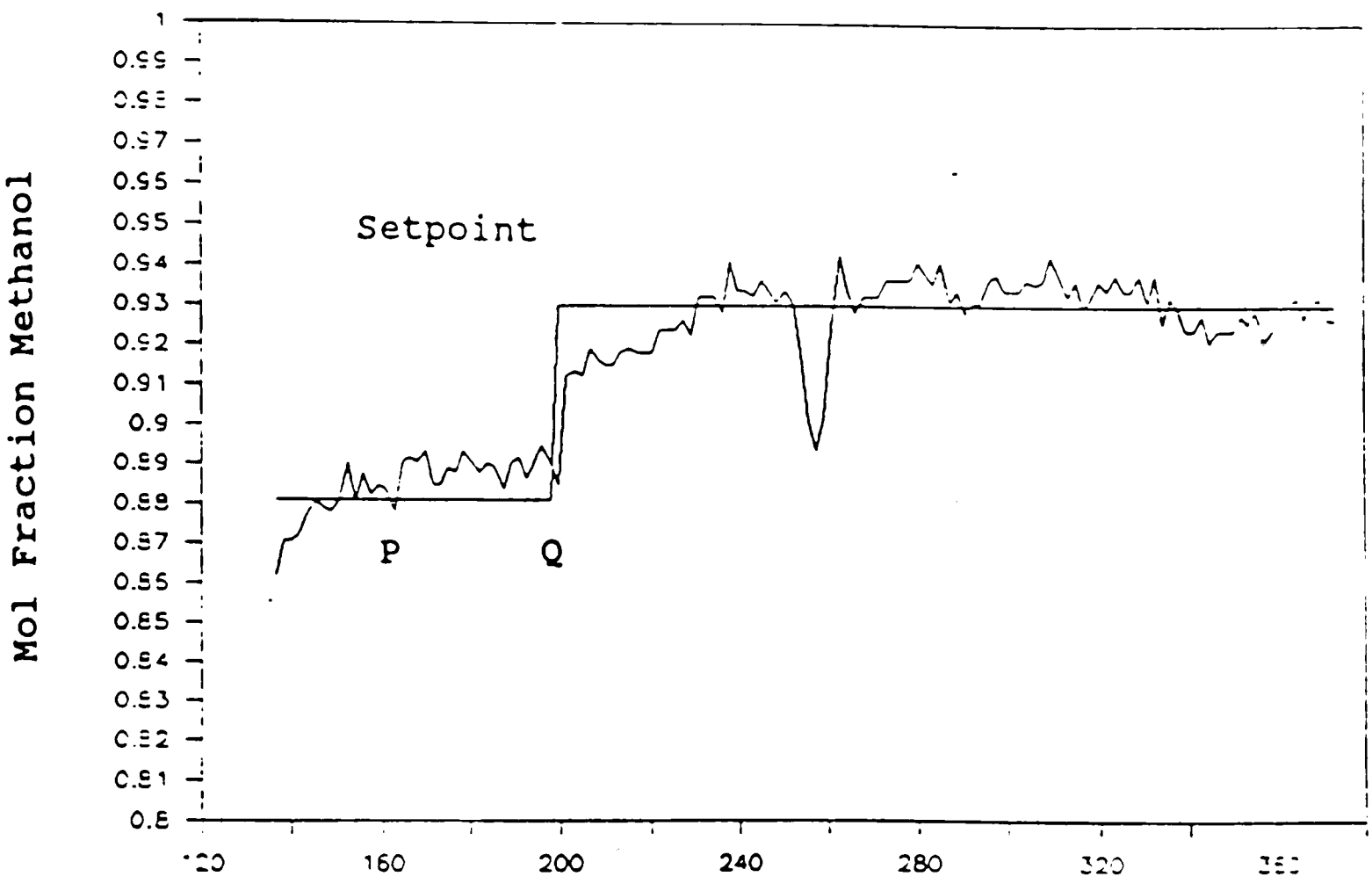

Setpoint Tracking : Top Composition
PMBC Controller (Hemant Pandit, 1992)

Figure A.1. PMBC controller Case 1 (Table 5.4).

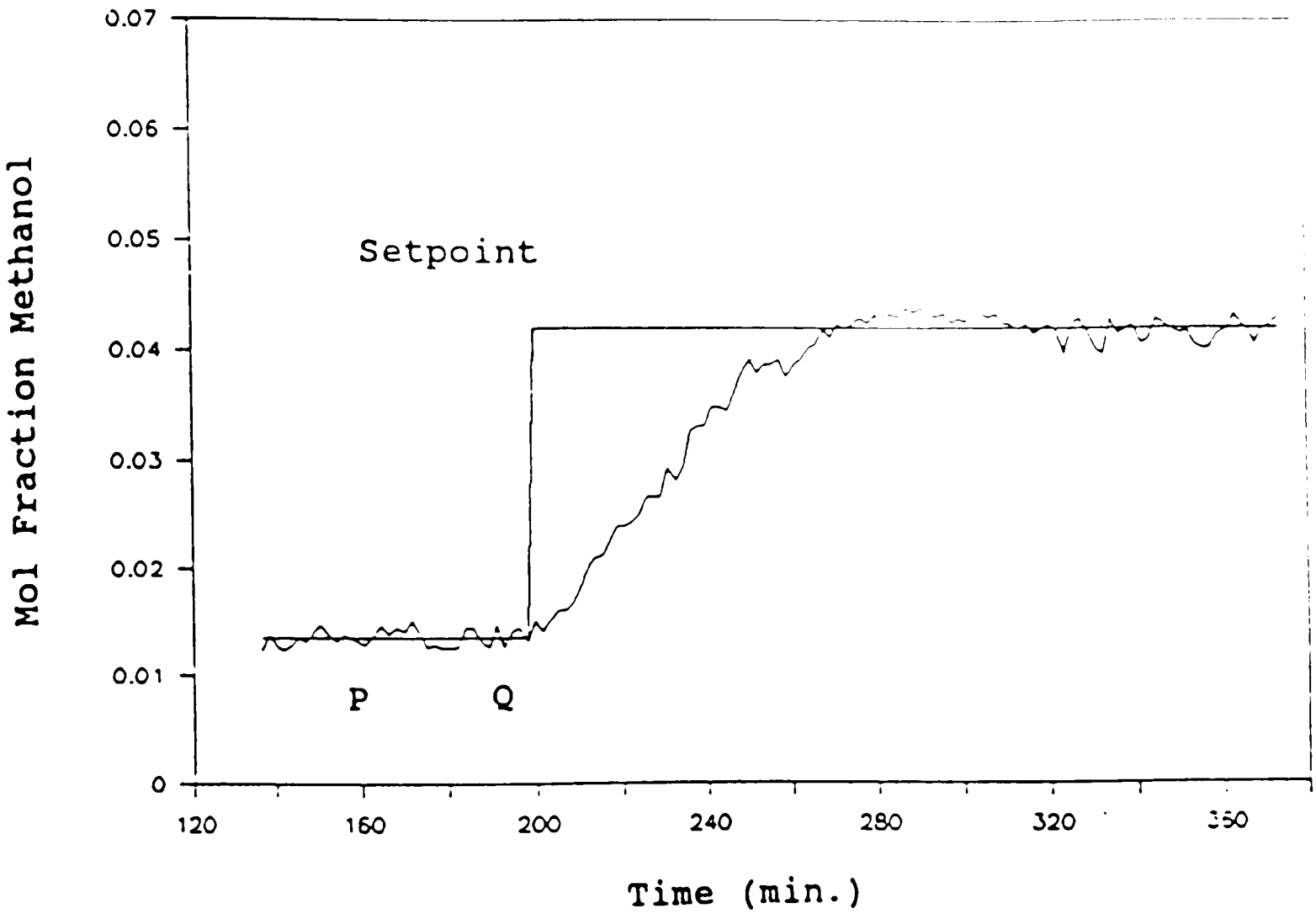

Setpoint Tracking (Contd.): Bottom Composition

Figure A.1. (b) (Contd.).

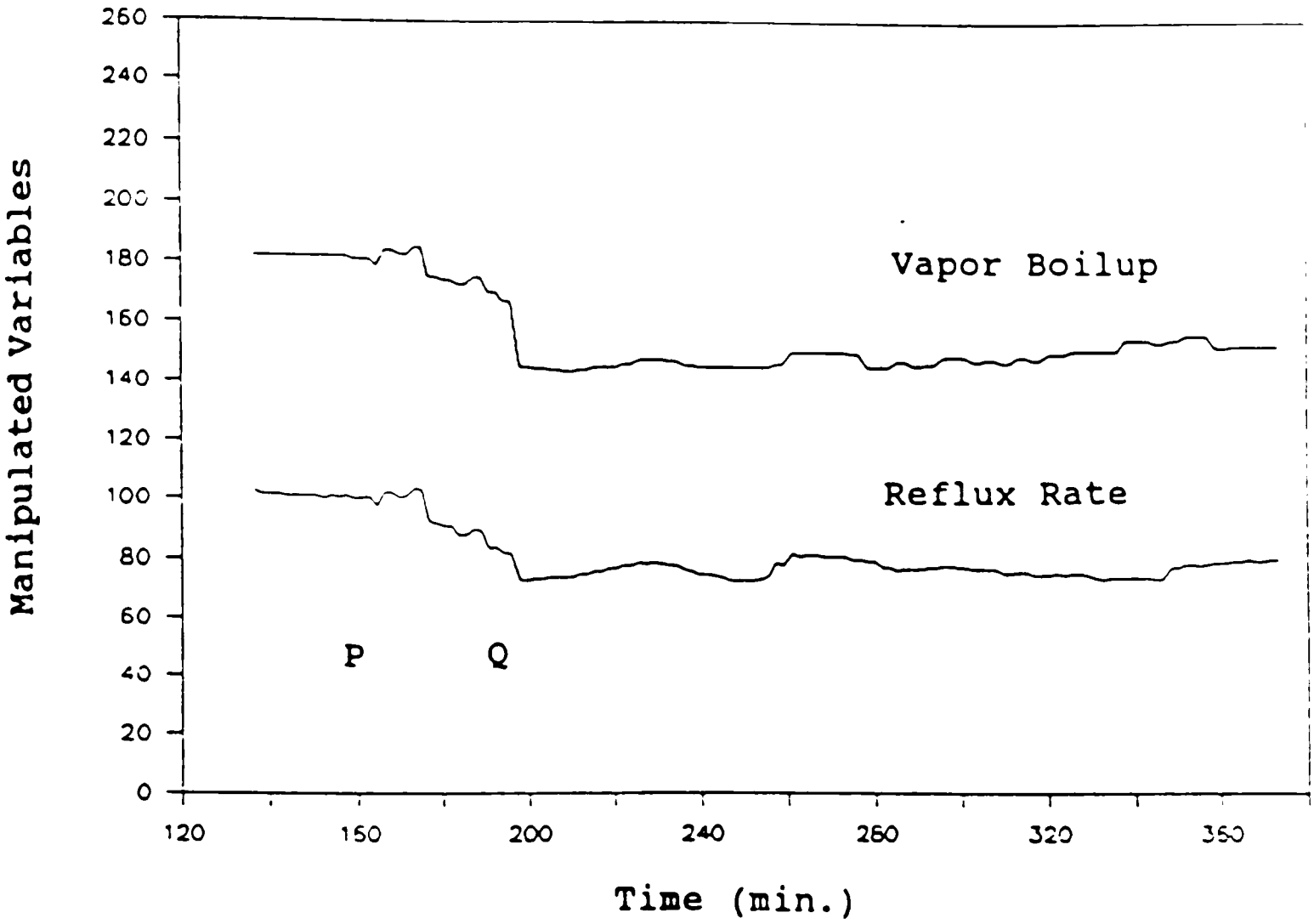

Setpoint Tracking (Contd.): Manipulated Variables

Figure A.1. (c) (Contd.).

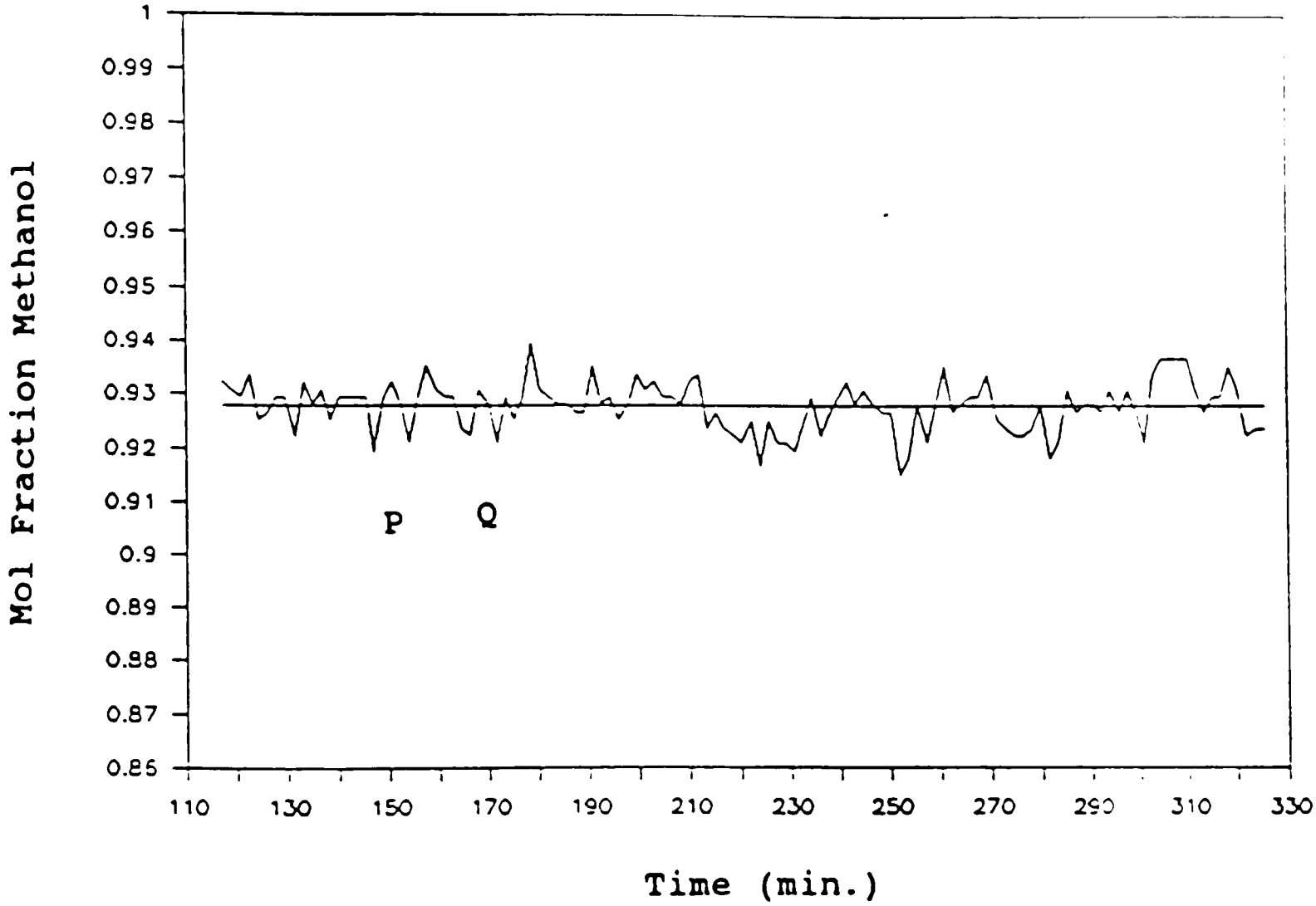

Disturbance Rejection : Top Composition
Feed Composition (20-35%) disturbance
PMBC Controller (Hemant Pandit, 1992)

Figure A.2. PMBC controller Case 2 (Table 5.4).

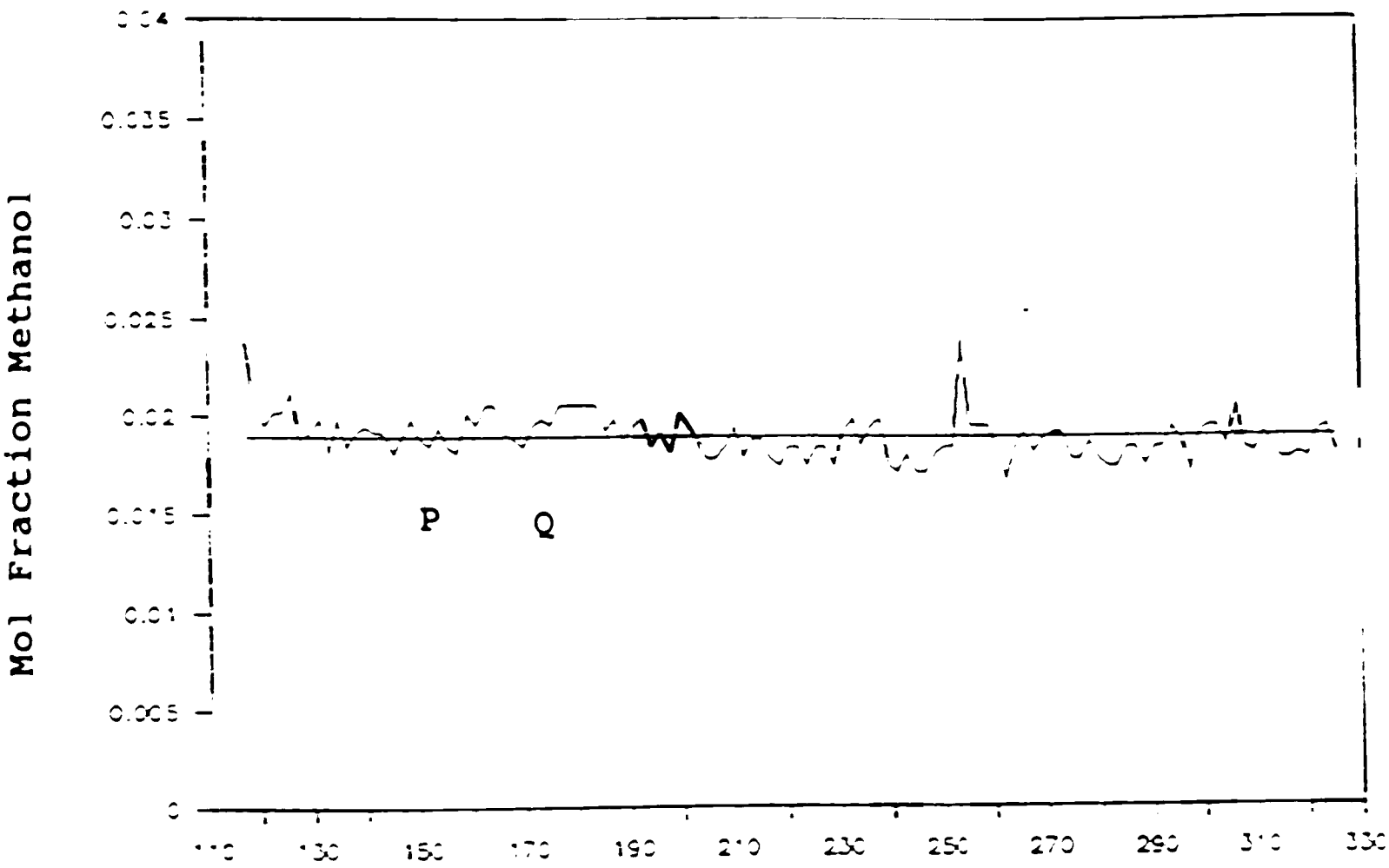

Disturbance Rejection (Contd.): Bottom Composition
Feed Composition (20-35% disturbance

Figure A.2 (b) (Contd.).

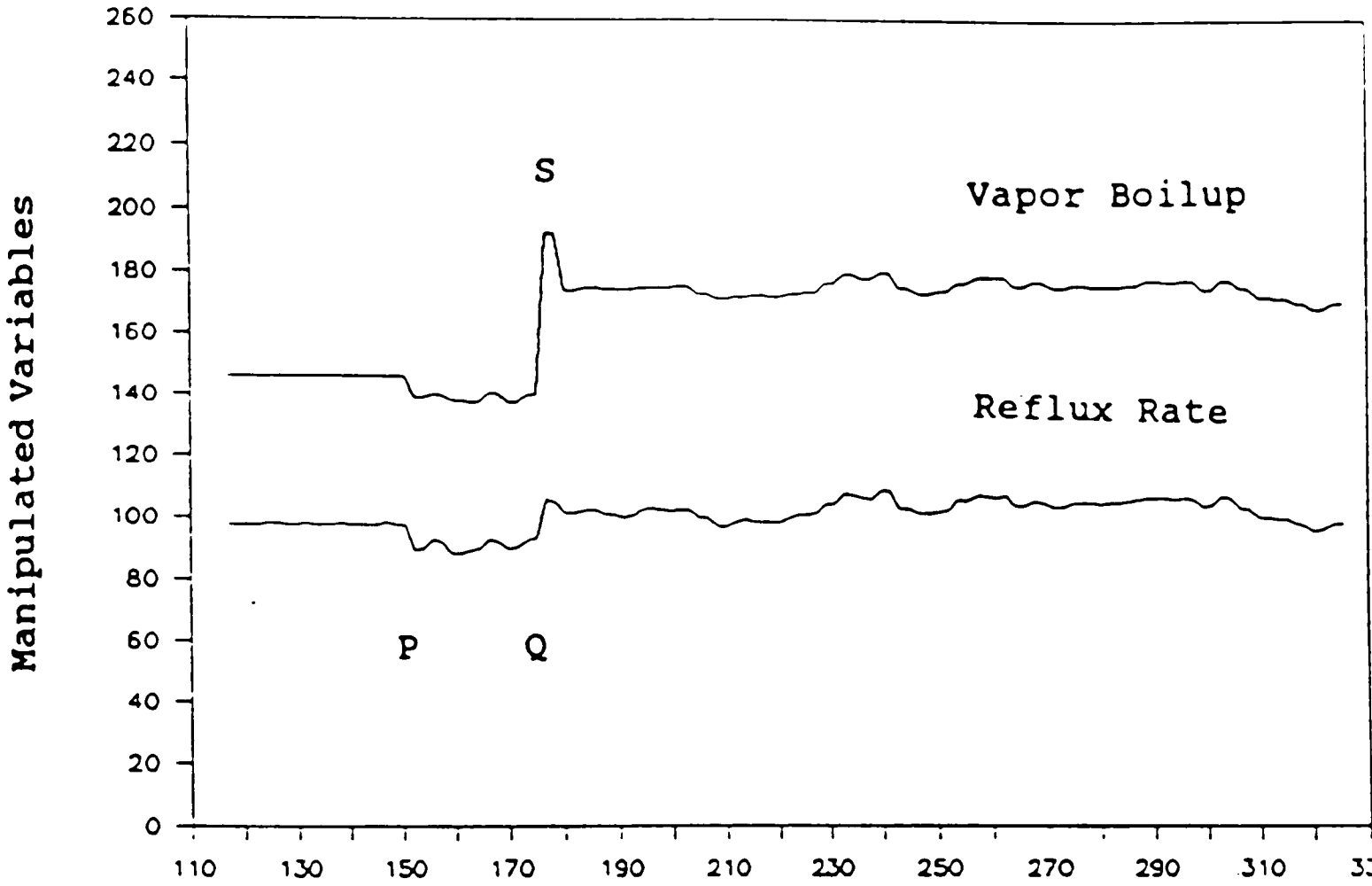

Disturbance Rejection (Contd.): Manipulated Variables
Feed Composition (20-35%) disturbance

Figure A.2. (c) (Contd.).

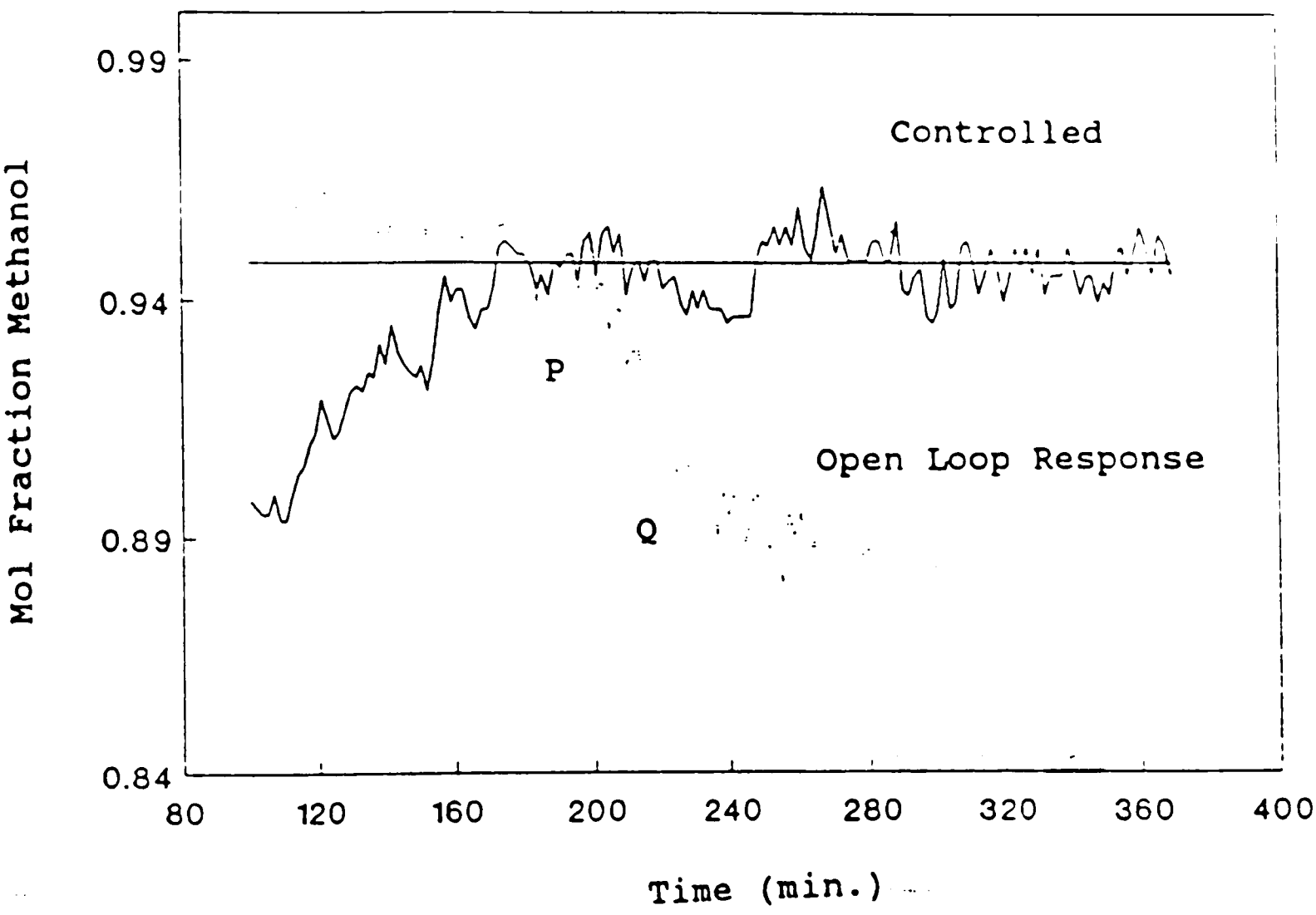

Disturbance Rejection : Top Composition
Feed Composition (30-20%. disturbance
PMBC Controller (Hemant Pandit, 1992)

Figure A.3. PMBC controller Case 3 (Table 5.4).

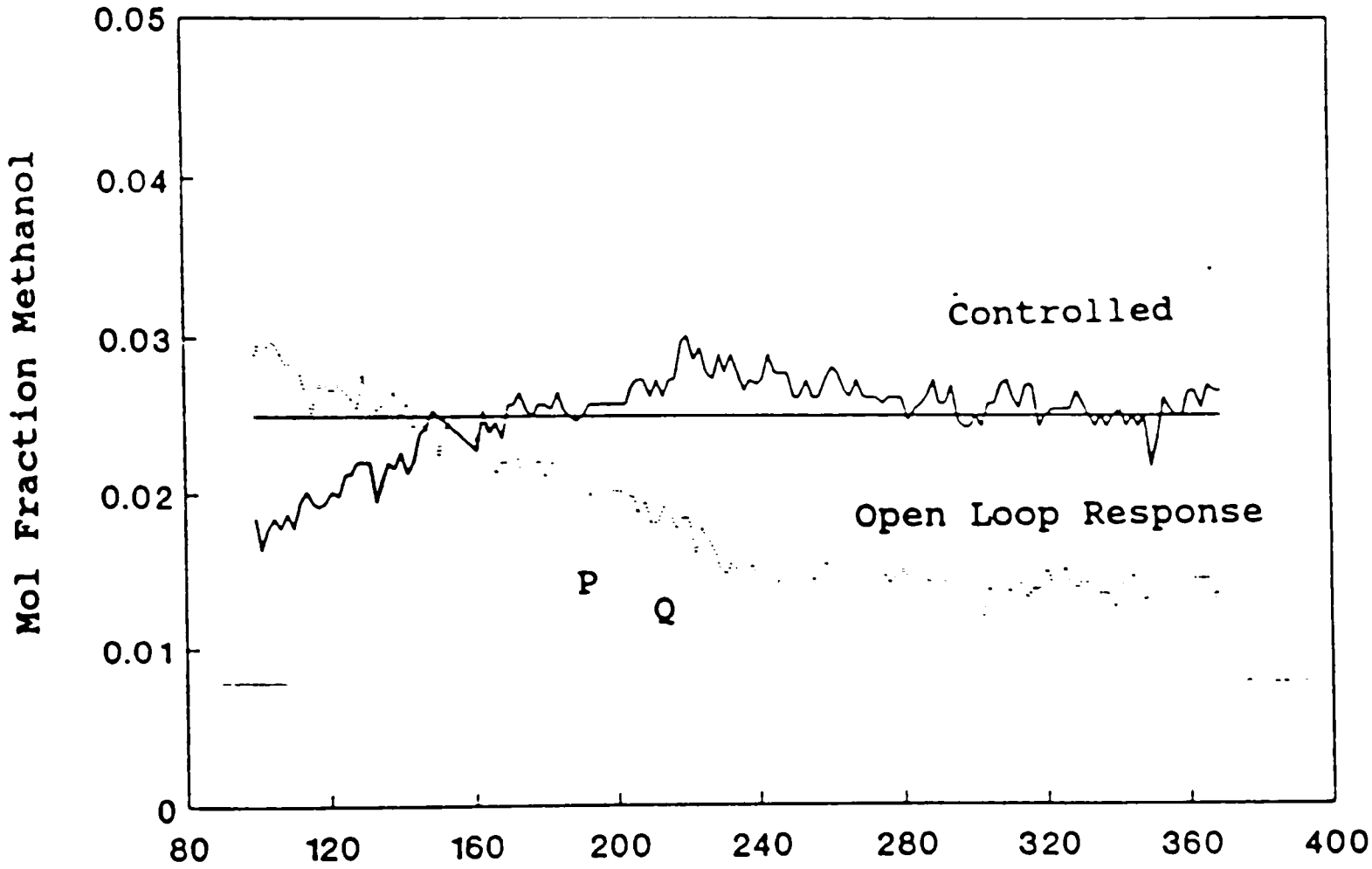

Disturbance Rejection (Contd.): Bottom Composition
Feed Composition (30-20%) disturbance

Figure A.3. (b) (Contd.).

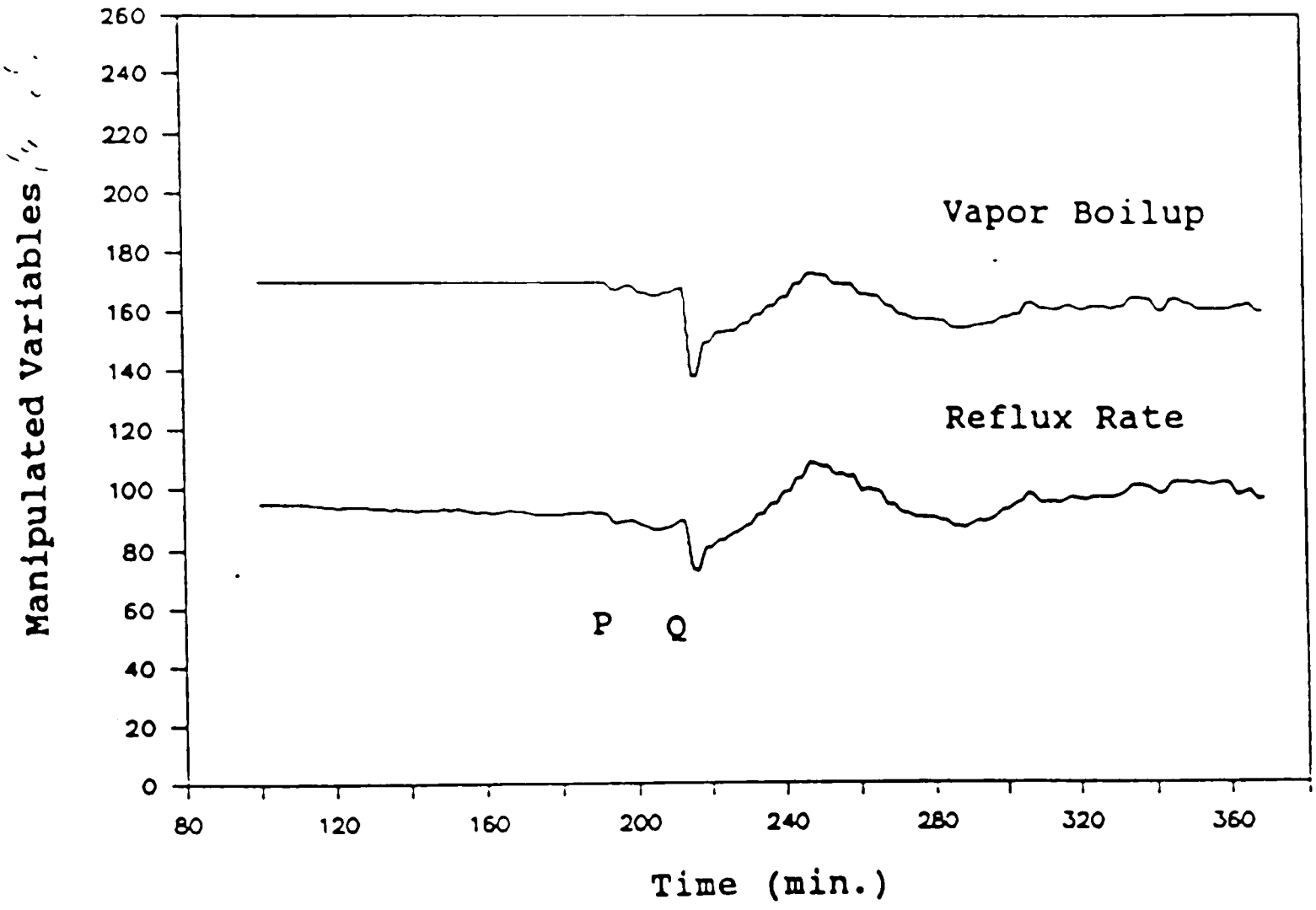

Disturbance Rejection (Contd.): Manipulated Variables
Feed Composition (30-20%) disturbance

Figure A.3. (c) (Contd.).

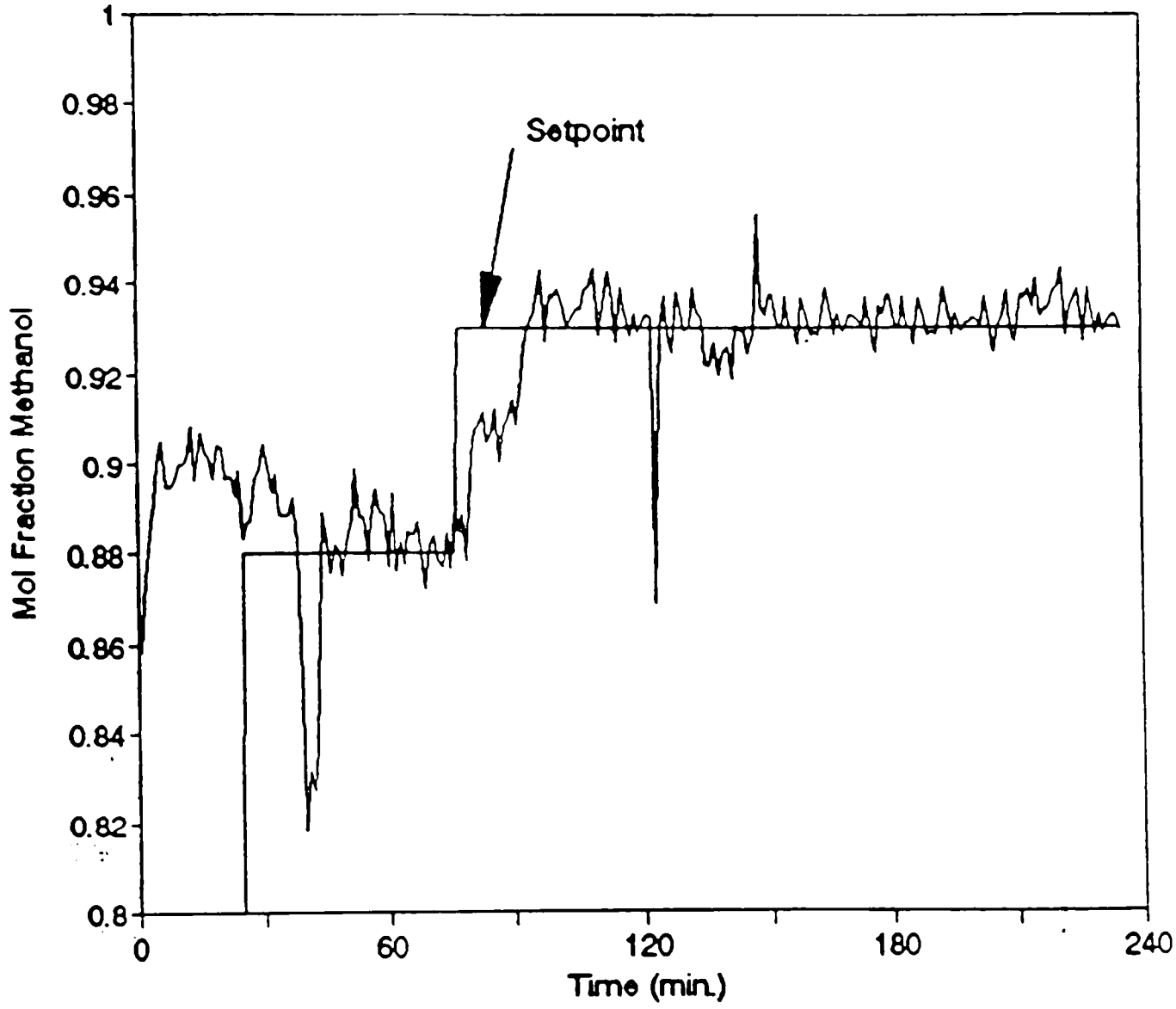

Setpoint Tracking : Top Composition
[DMC]™ Controller (Amit Gupta, 1994)

Figure A.4. [DMC]™ controller Case 1 (Table 5.4).

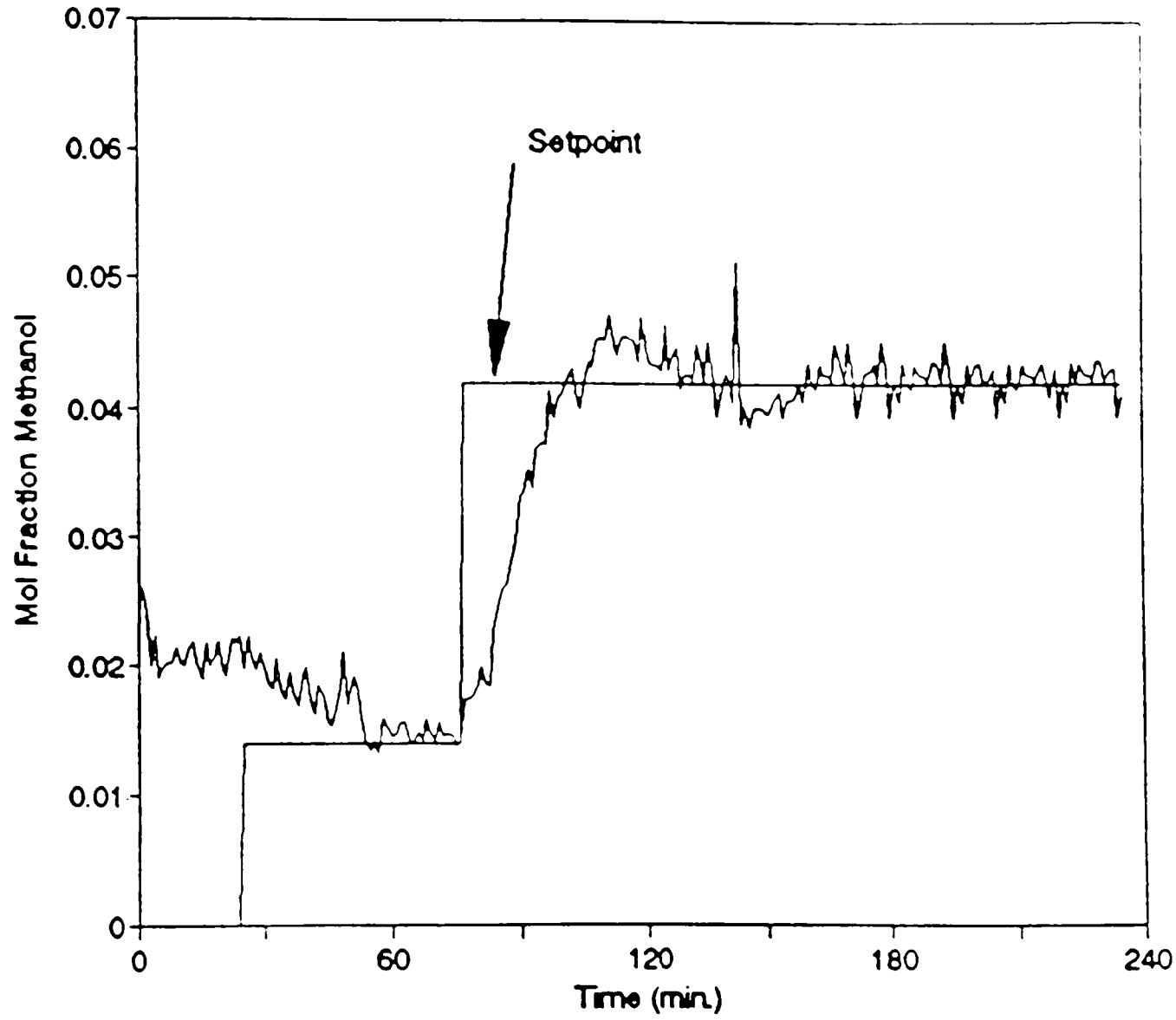

Setpoint Tracking (Contd.): Bottom Composition

Figure A.4. (b) (Contd.).

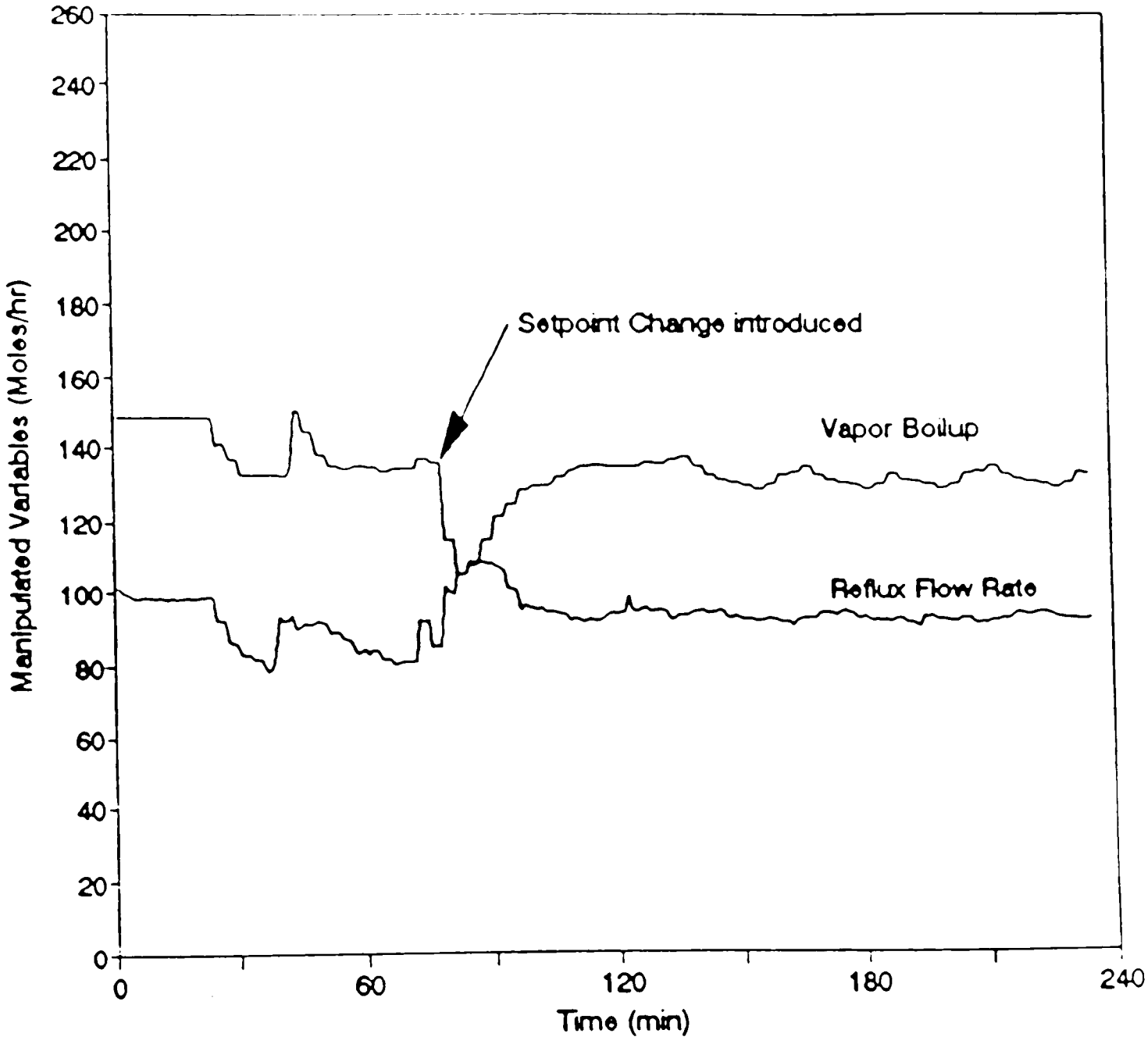

Setpoint Tracking (Contd.): Manipulated Variables

Figure A.4. (c) (Contd.).

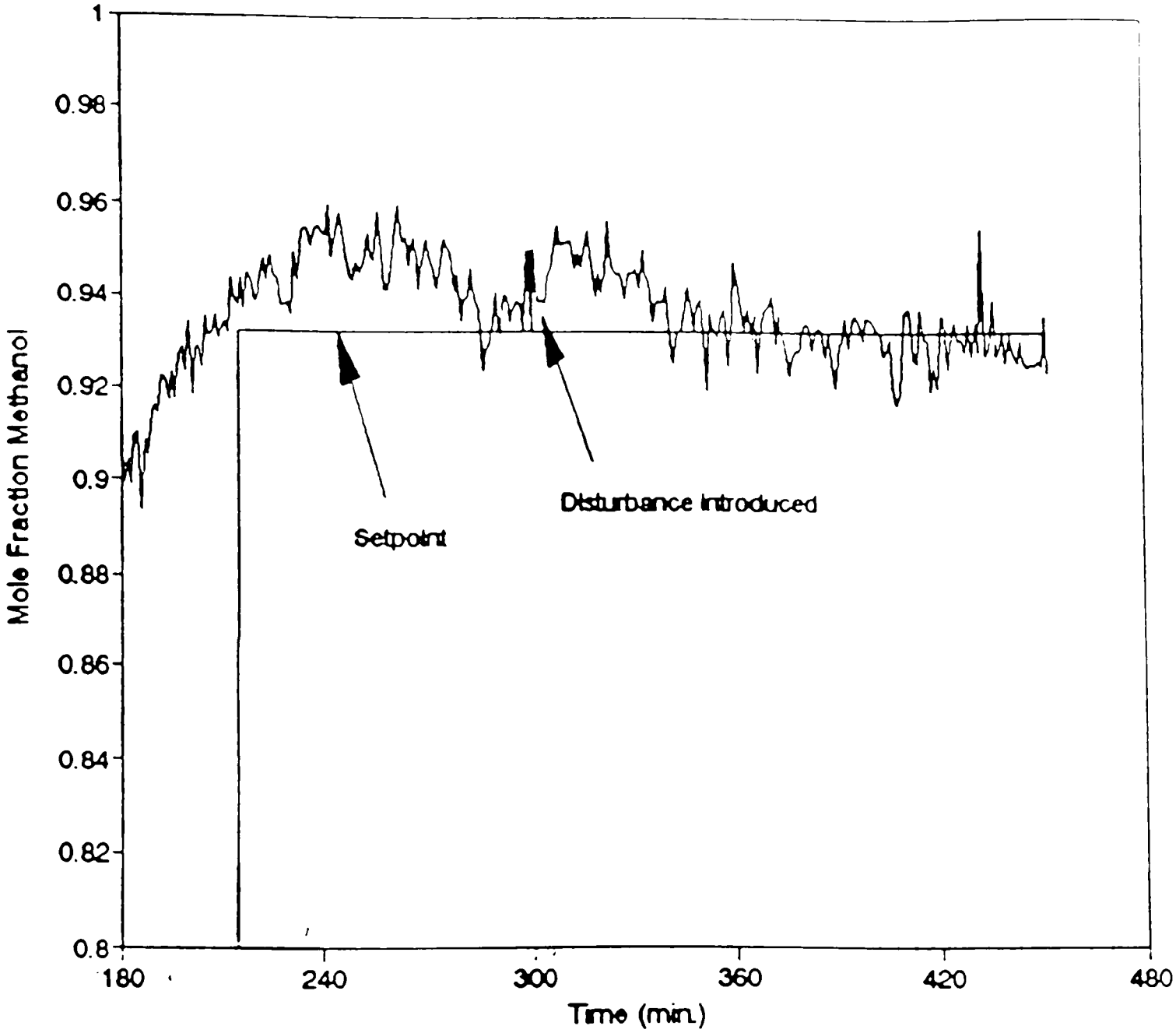

Disturbance Rejection : Top Composition
Feed Composition (20-35%) disturbance
[DMC]™ Controller (Amit Gupta, 1994)

Figure A.5. [DMC]™ controller Case 2 (Table 5.4).

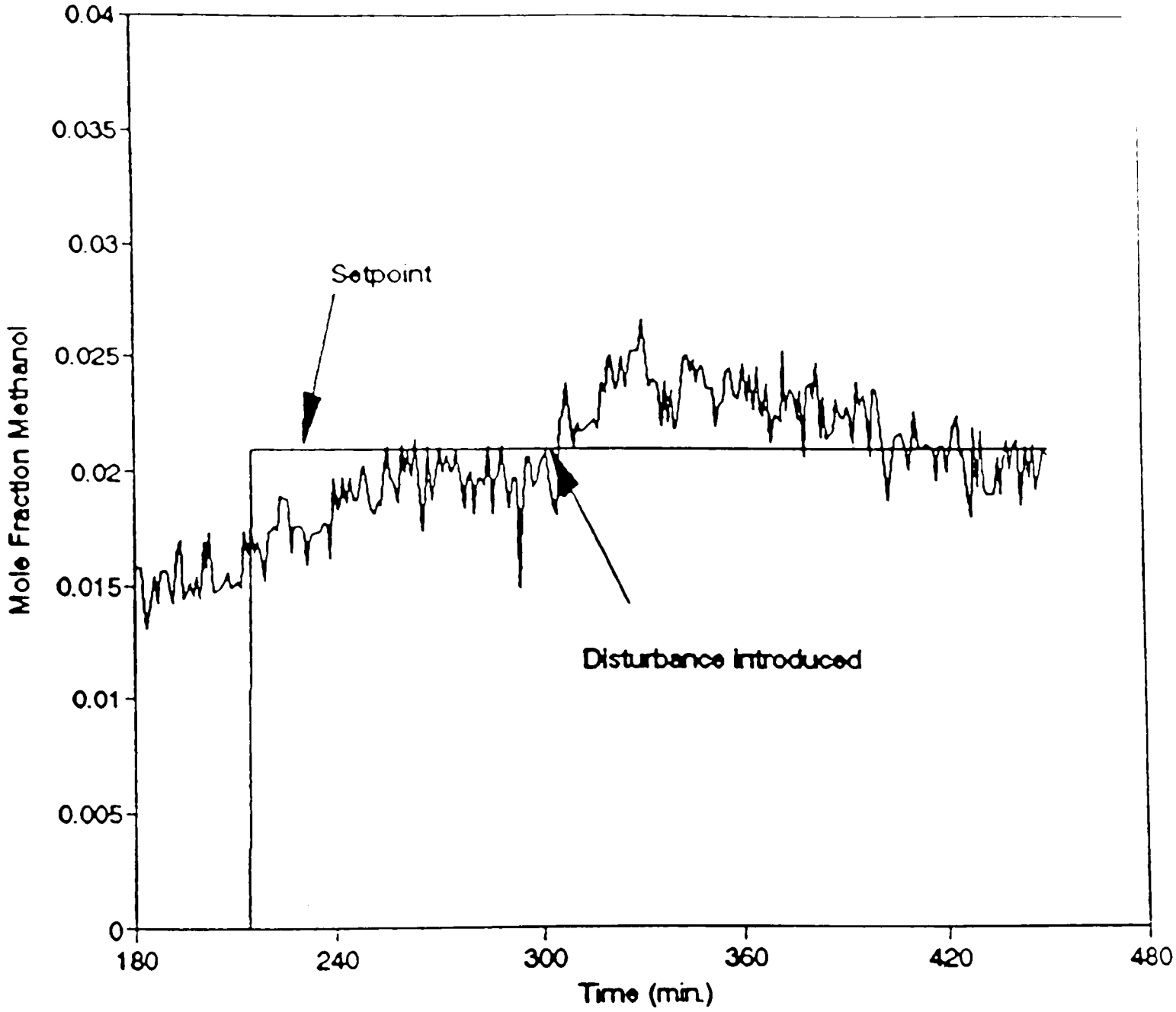

Disturbance Rejection · Bottom Composition
Feed Composition (20-35%) disturbance

Figure A.5. (b) (Contd.).

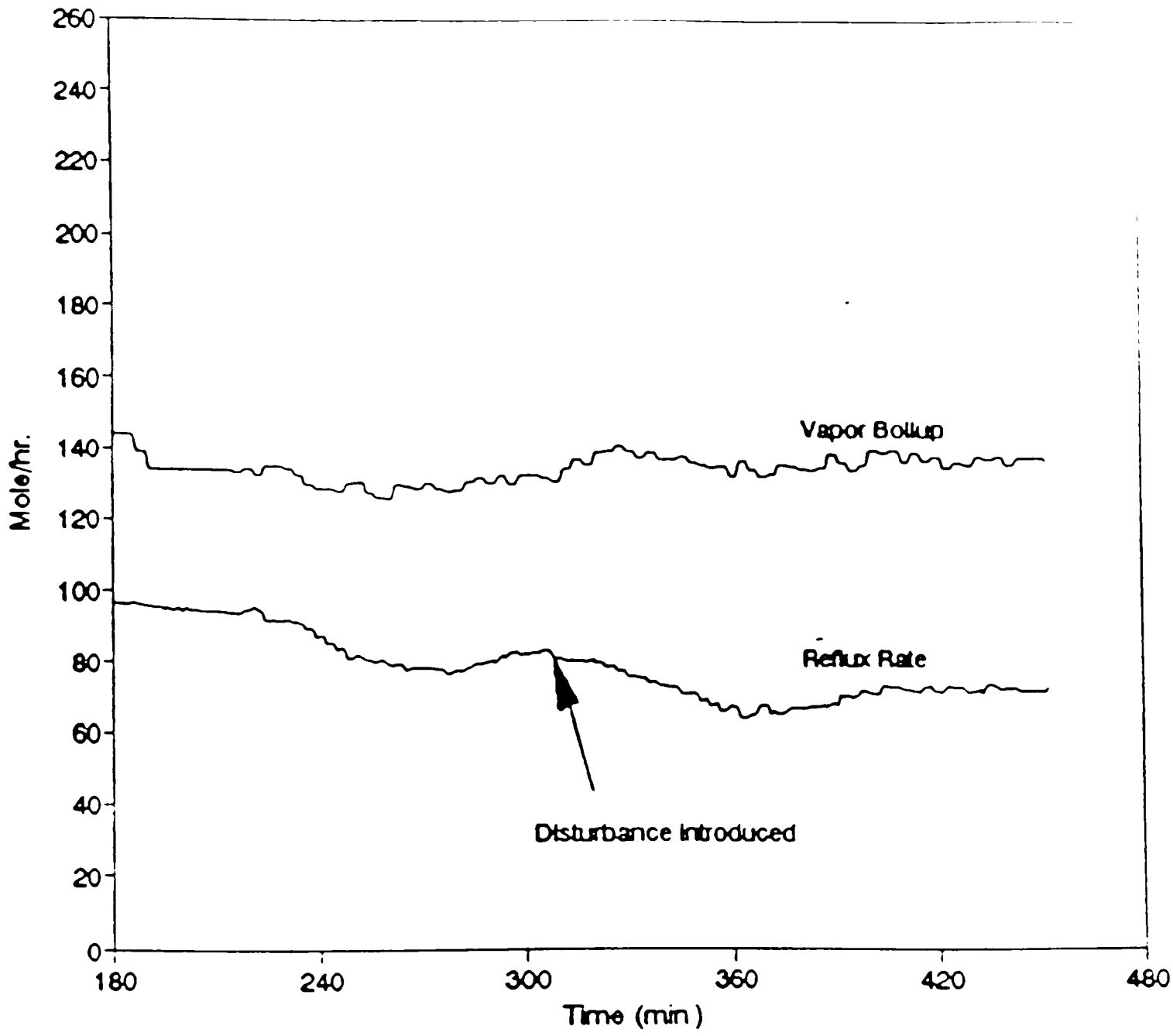

Disturbance Rejection (Contd.): Manipulated Variables
Feed Composition (20-35%) disturbance

Figure A.5. (c) (Contd.).

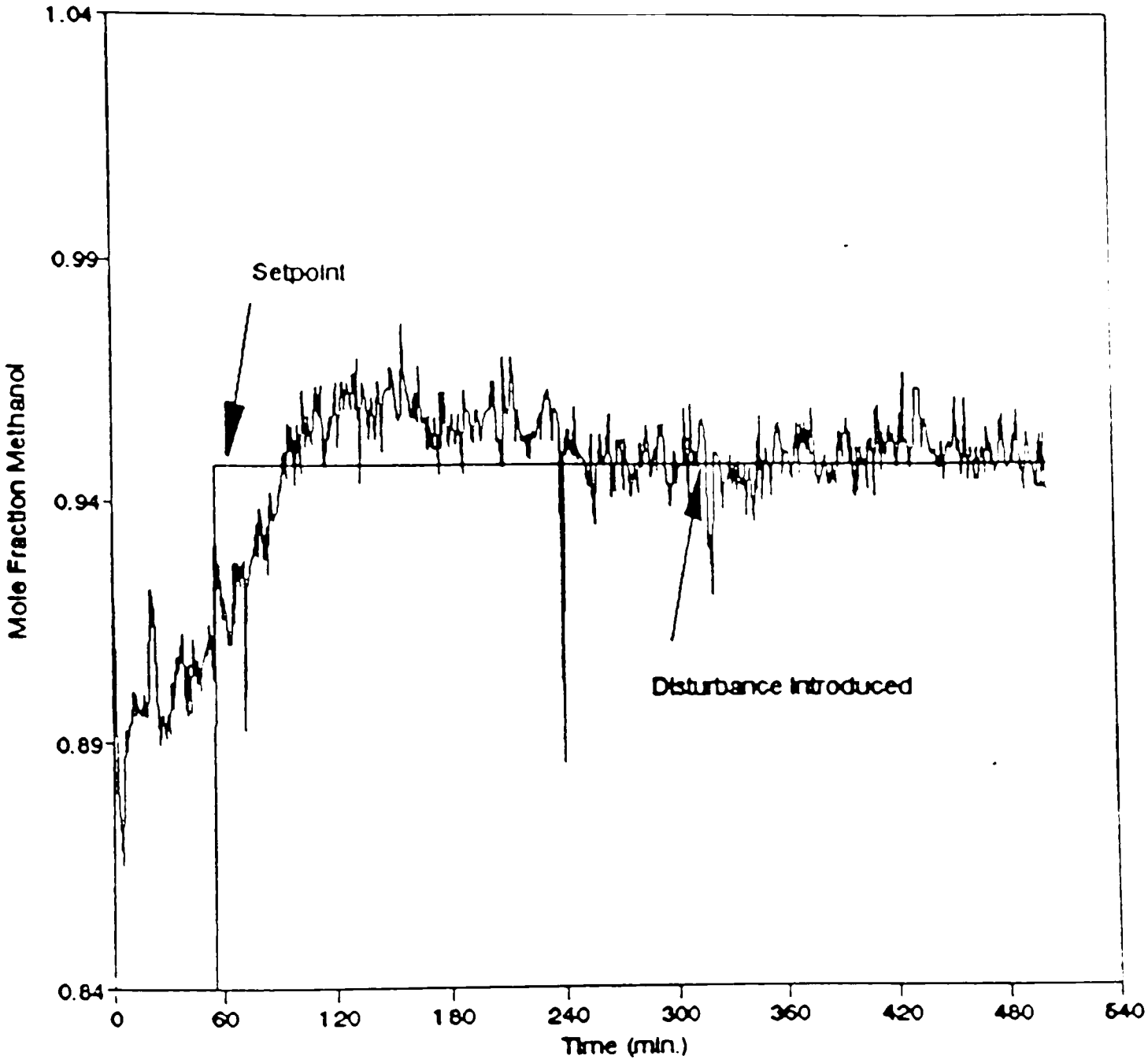

Disturbance Rejection : Top Composition
Feed Composition (30-20%) disturbance
[DMC]™ Controller (Amit Gupta, 1994)

Figure A.6. [DMC]™ controller Case 3 (Table 5.4).

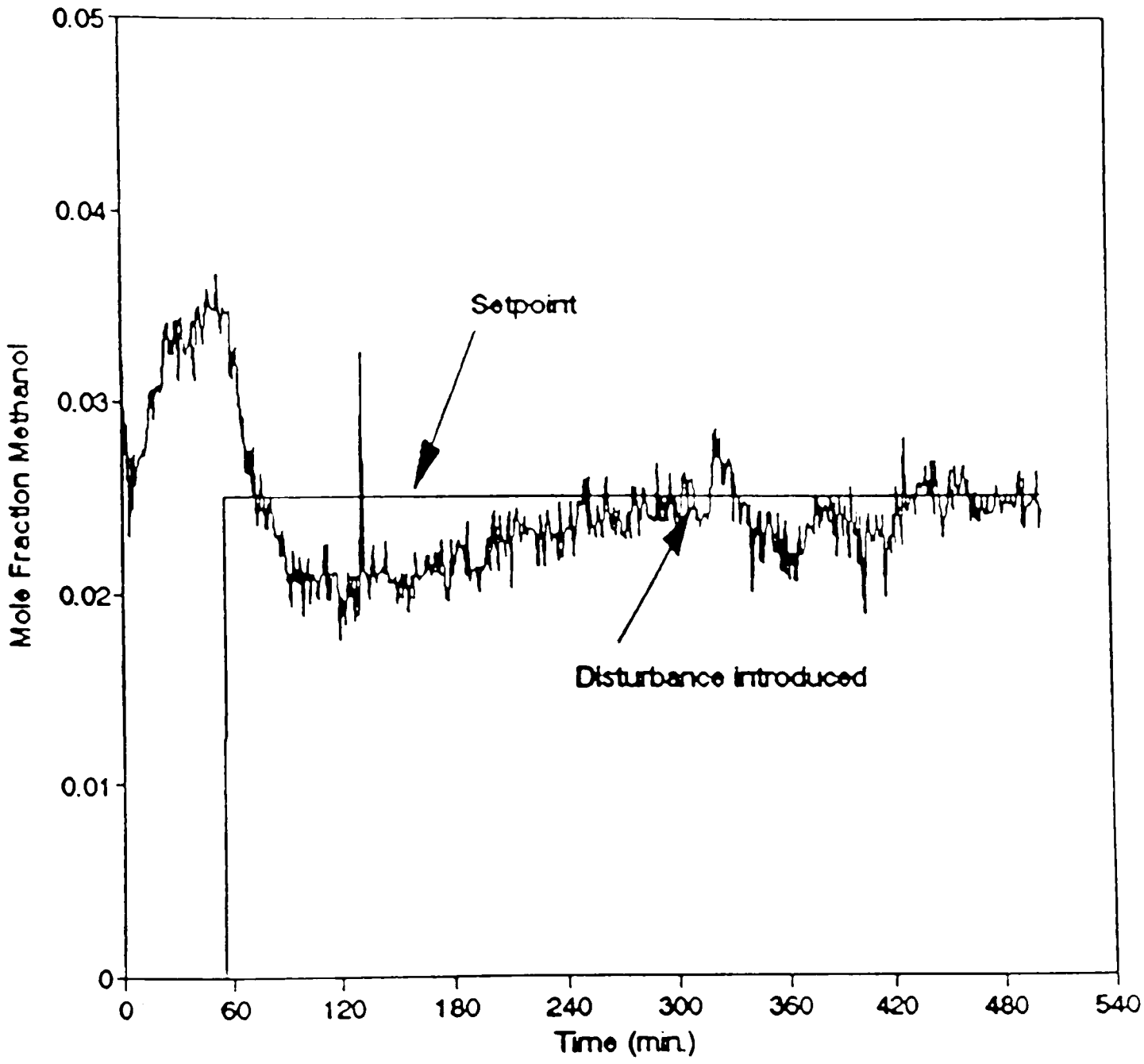

Disturbance Rejection Bottom Composition
Feed Composition (30-20%) disturbance

Figure A.6. (b) (Contd.).

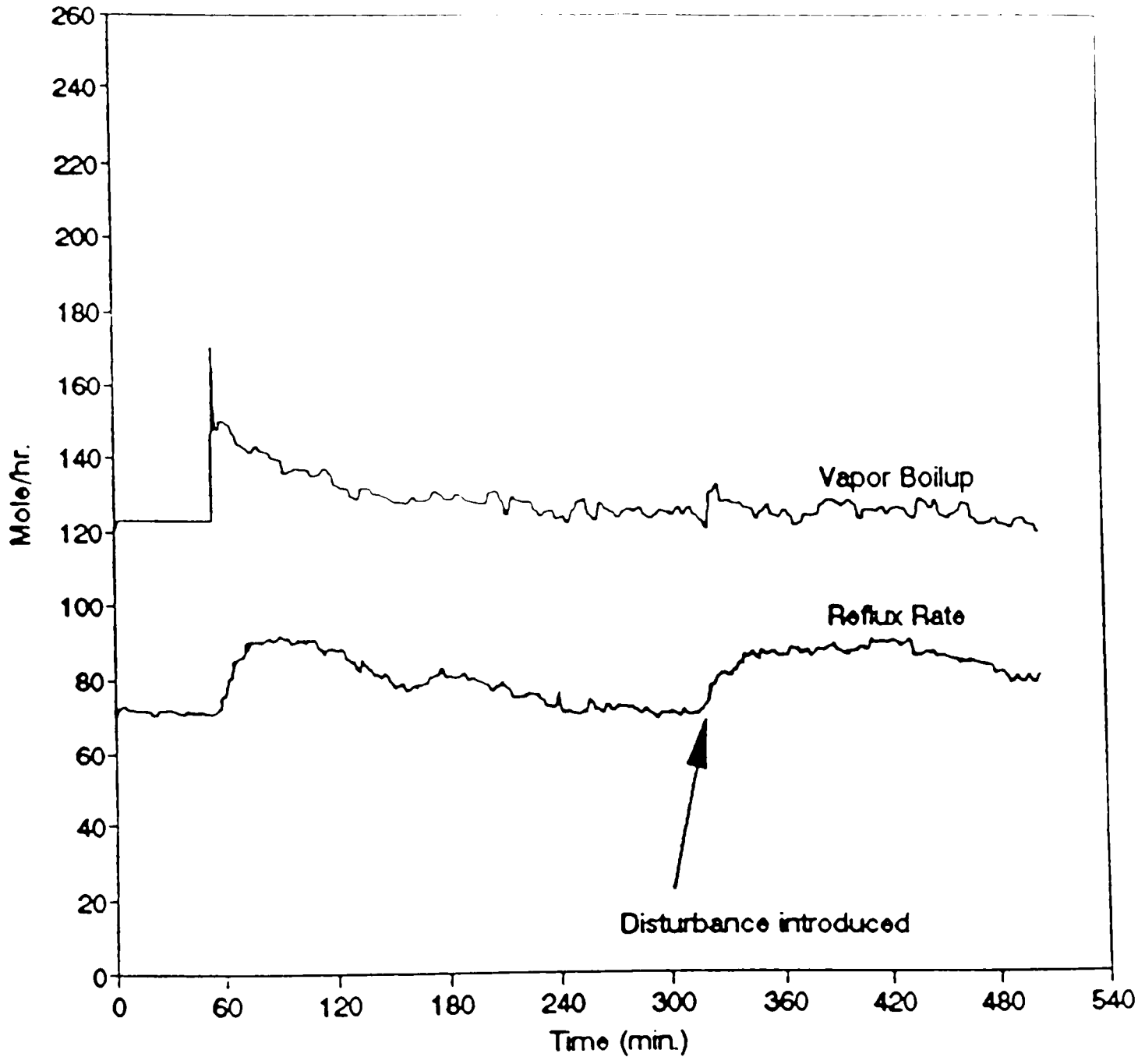

Disturbance Rejection (Contd.): Manipulated Variables
Feed Composition (30-20%) disturbance

Figure A.6. (c) (Contd.).

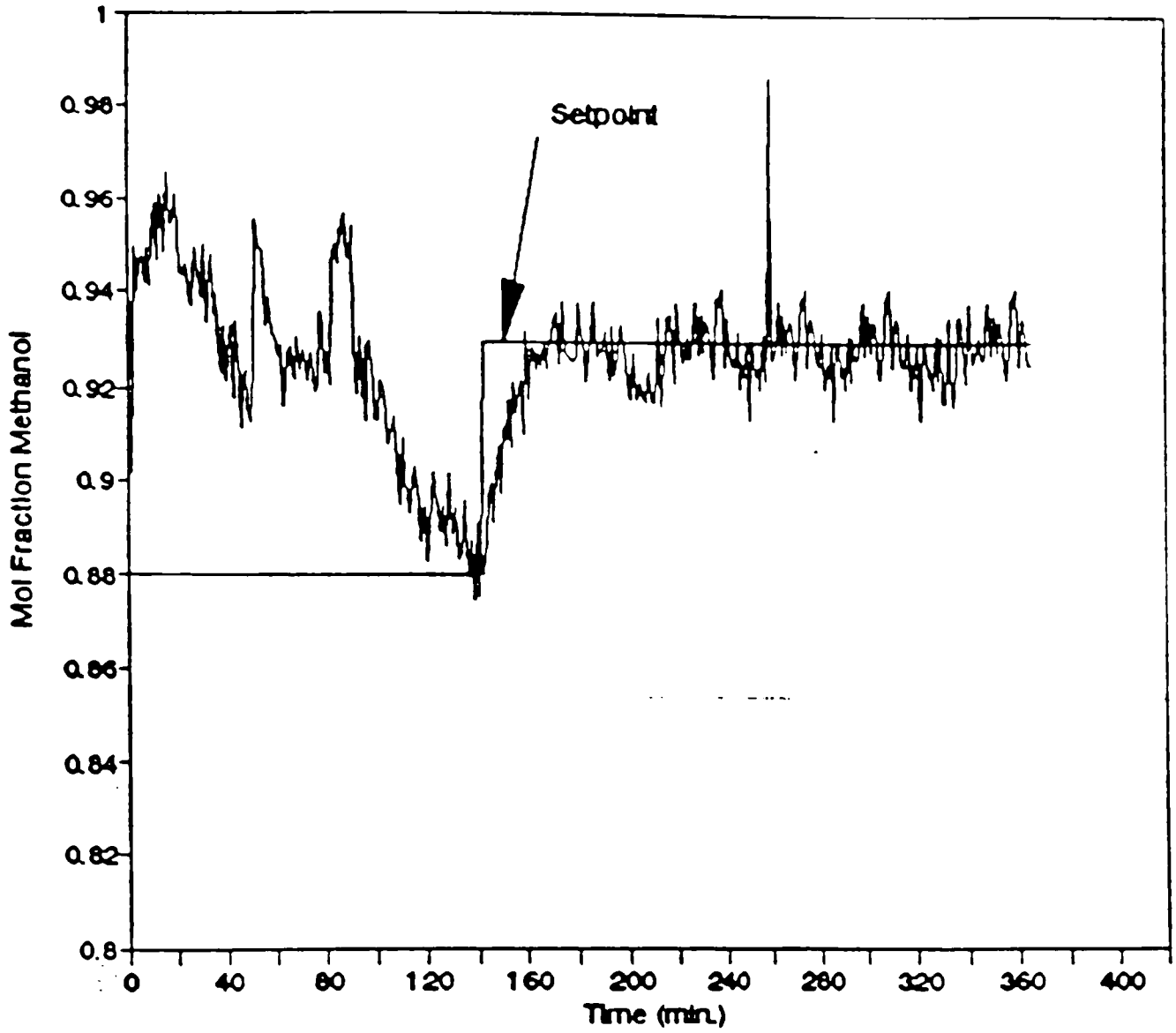

Setpoint Tracking : Top Composition
PI Controller (Amit Gupta, 1994)

Figure A.7. ACC controller Case 1 (Table 5.4).

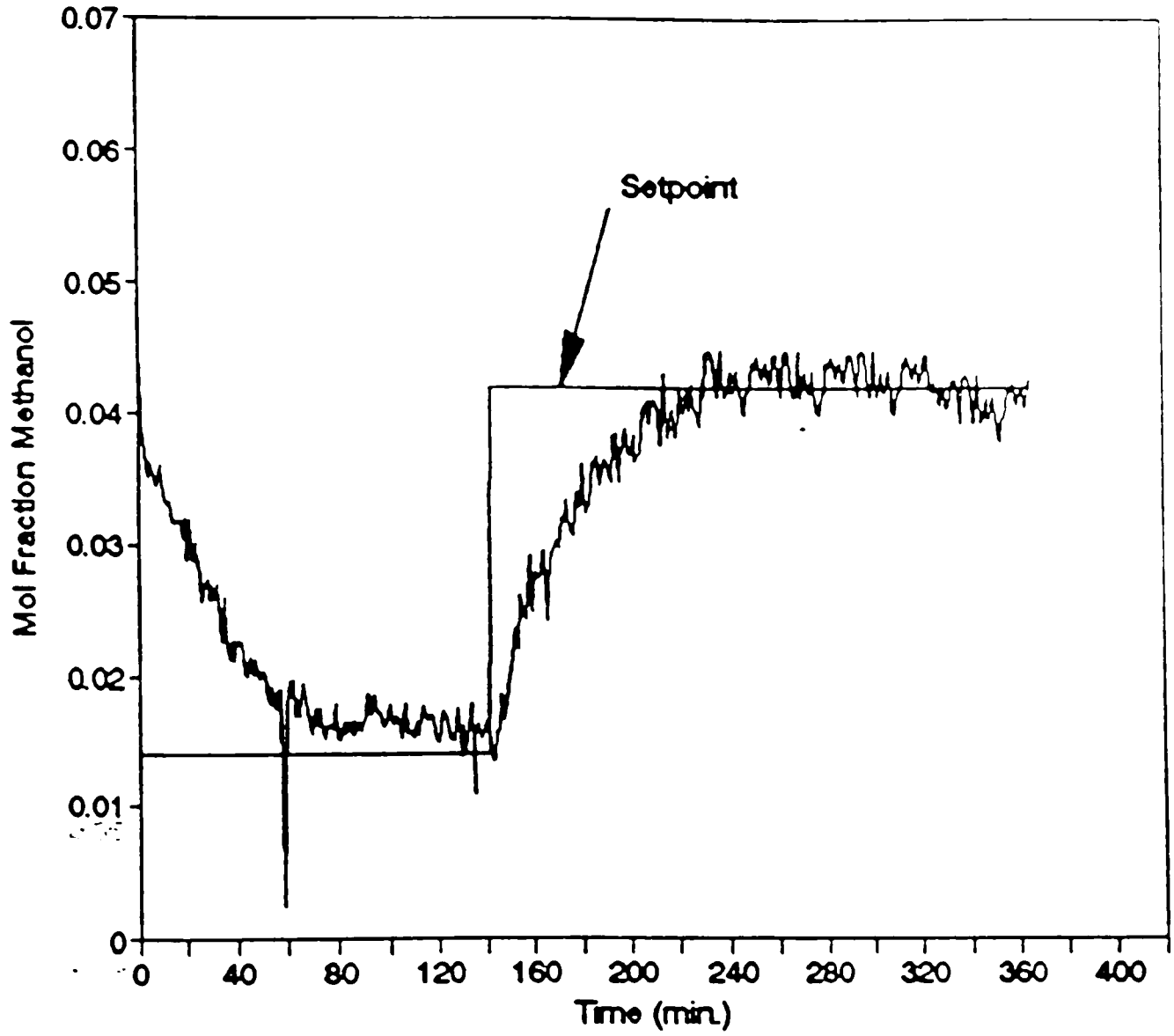

Setpoint Tracking (Contd.): Bottom Composition

Figure A.7. (b) (Contd.).

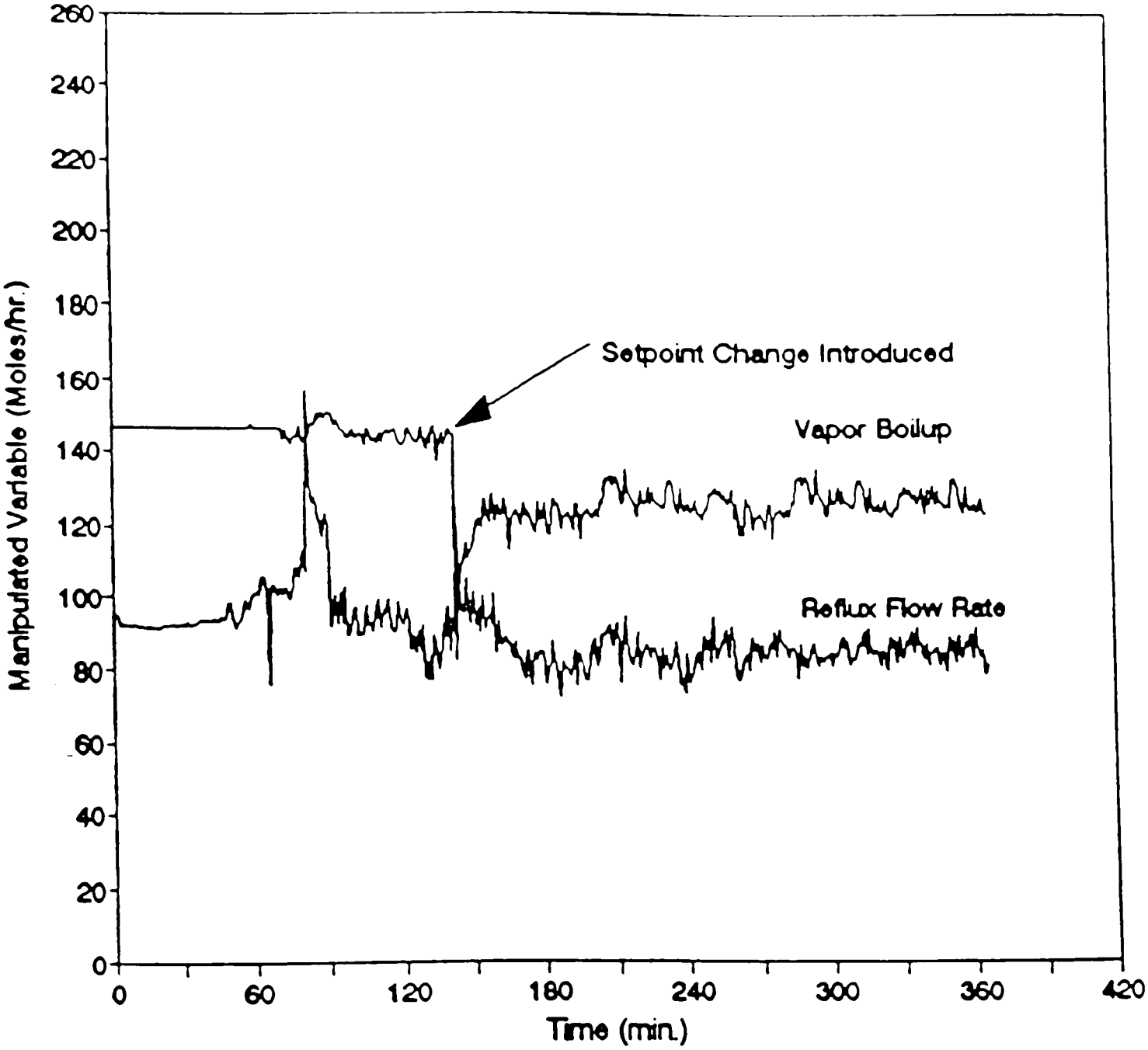

Setpoint Tracking (Contd.): Manipulated Variables

Figure A.7. (c) (Contd.).

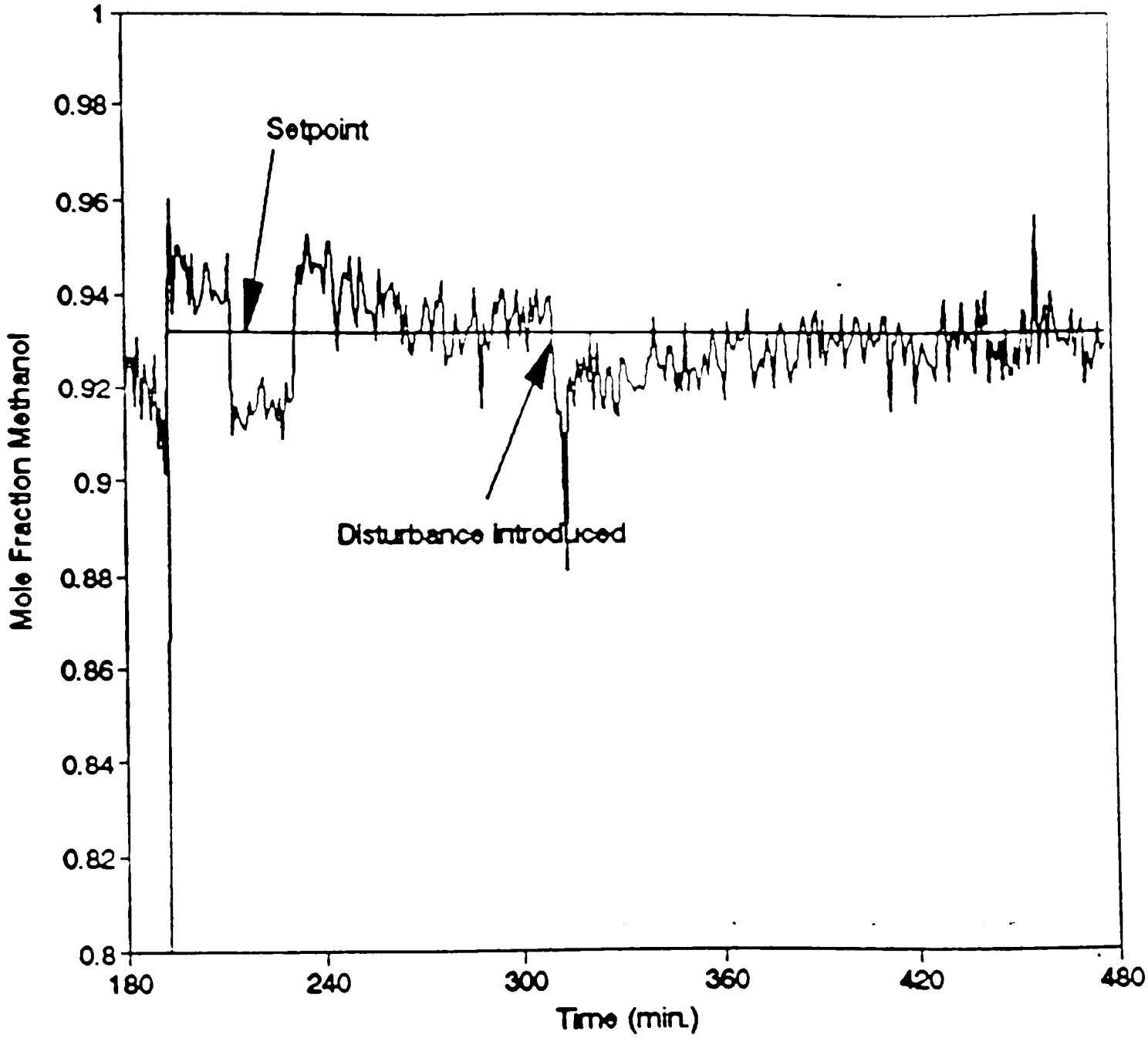

Disturbance Rejection : Top Composition
Feed Composition (20-35%) disturbance
PI Controller (Amit Gupta, 1994)

Figure A.8. ACC controller Case 2 (Table 5.4).

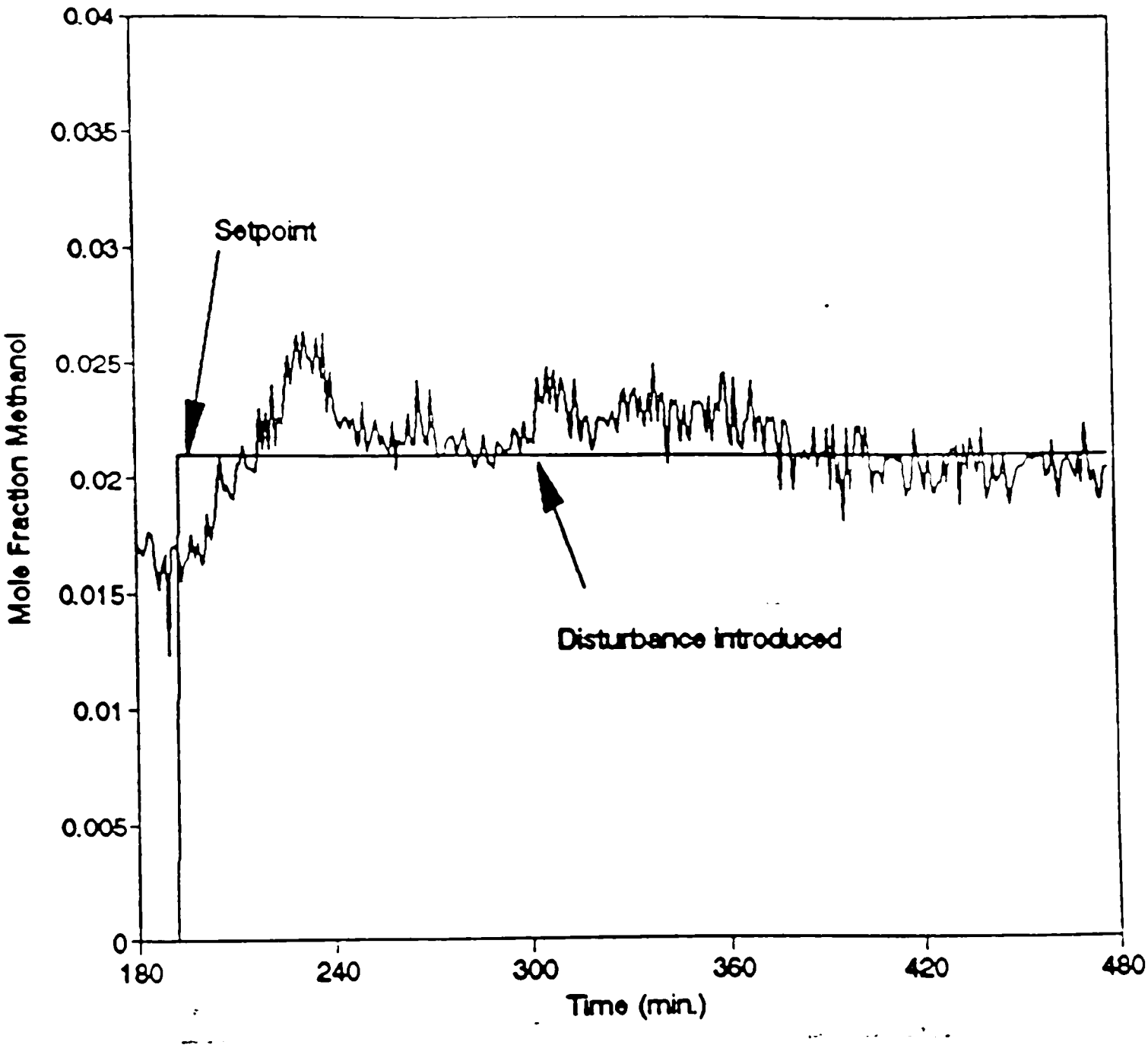

Disturbance Rejection : Bottom Composition
Feed Composition (20-35%) disturbance

Figure A.8. (b) (Contd.).

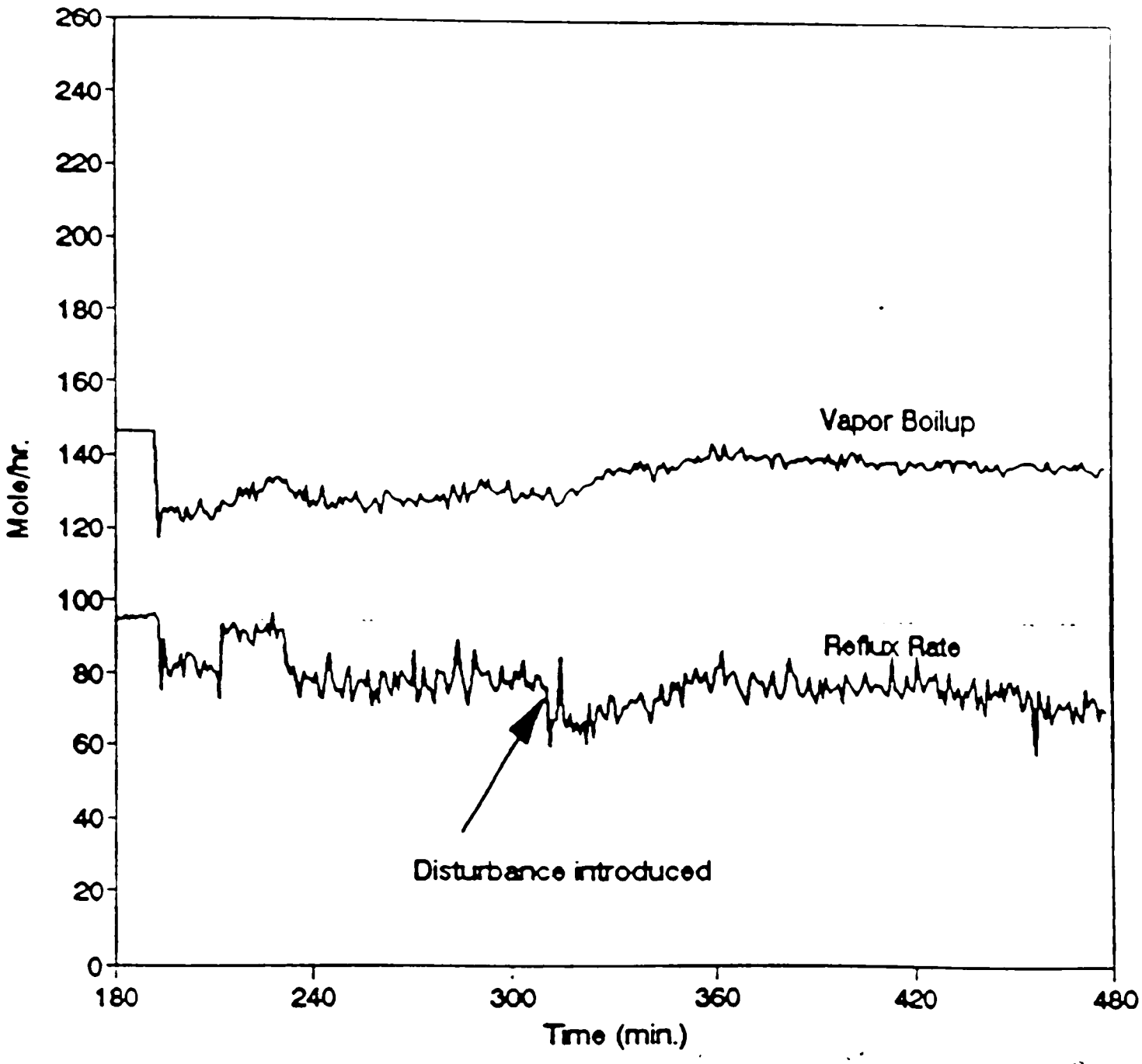

Disturbance Rejection : Manipulated Variables
Feed Composition (20-35%) disturbance

Figure A.8. (c) (Contd.).

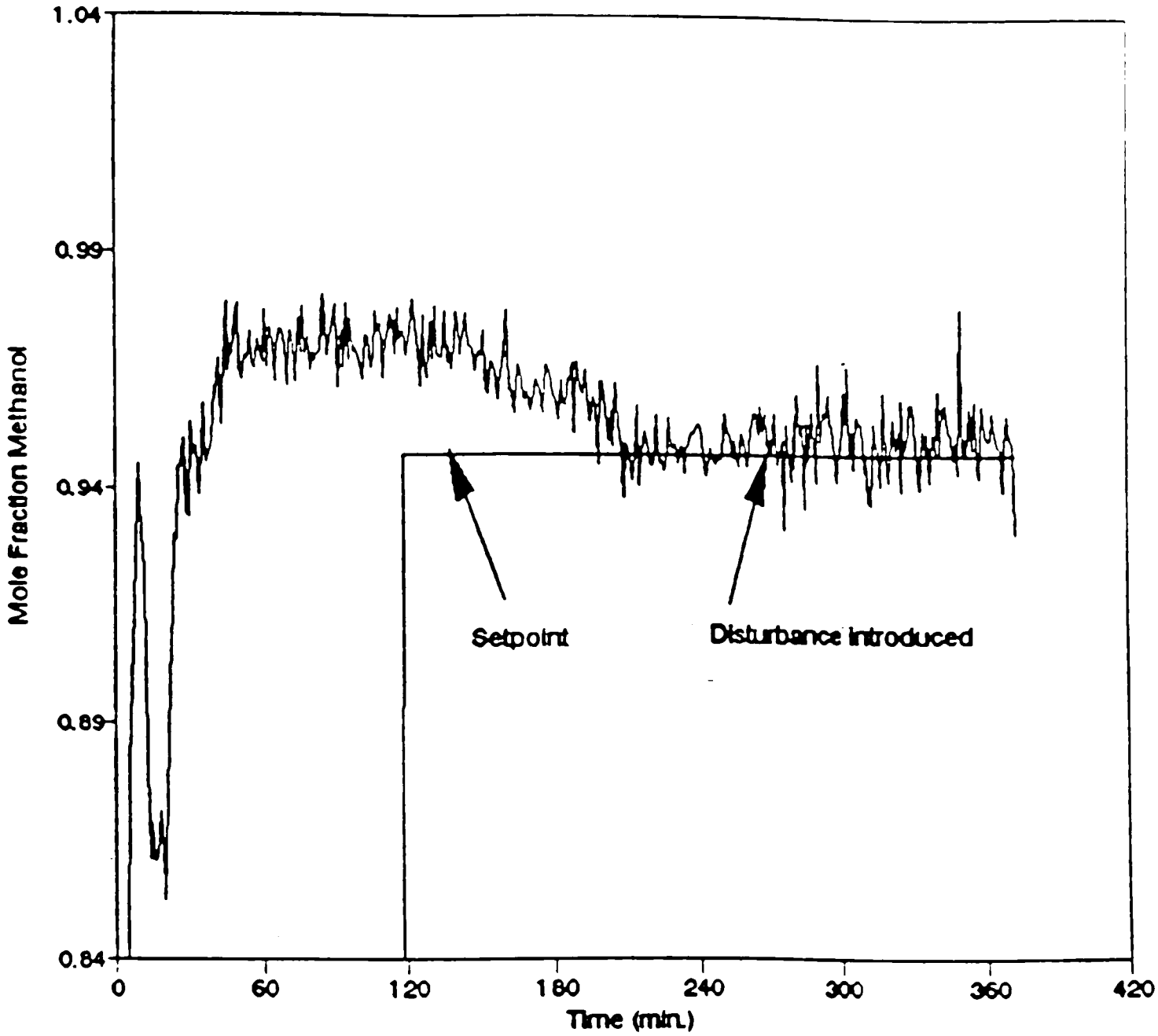

Disturbance Rejection : Top Composition
Feed Composition (30-20%) disturbance
PI Controller (Amit Gupta, 1994)

Figure A.9. ACC controller Case 3 (Table 5.4).

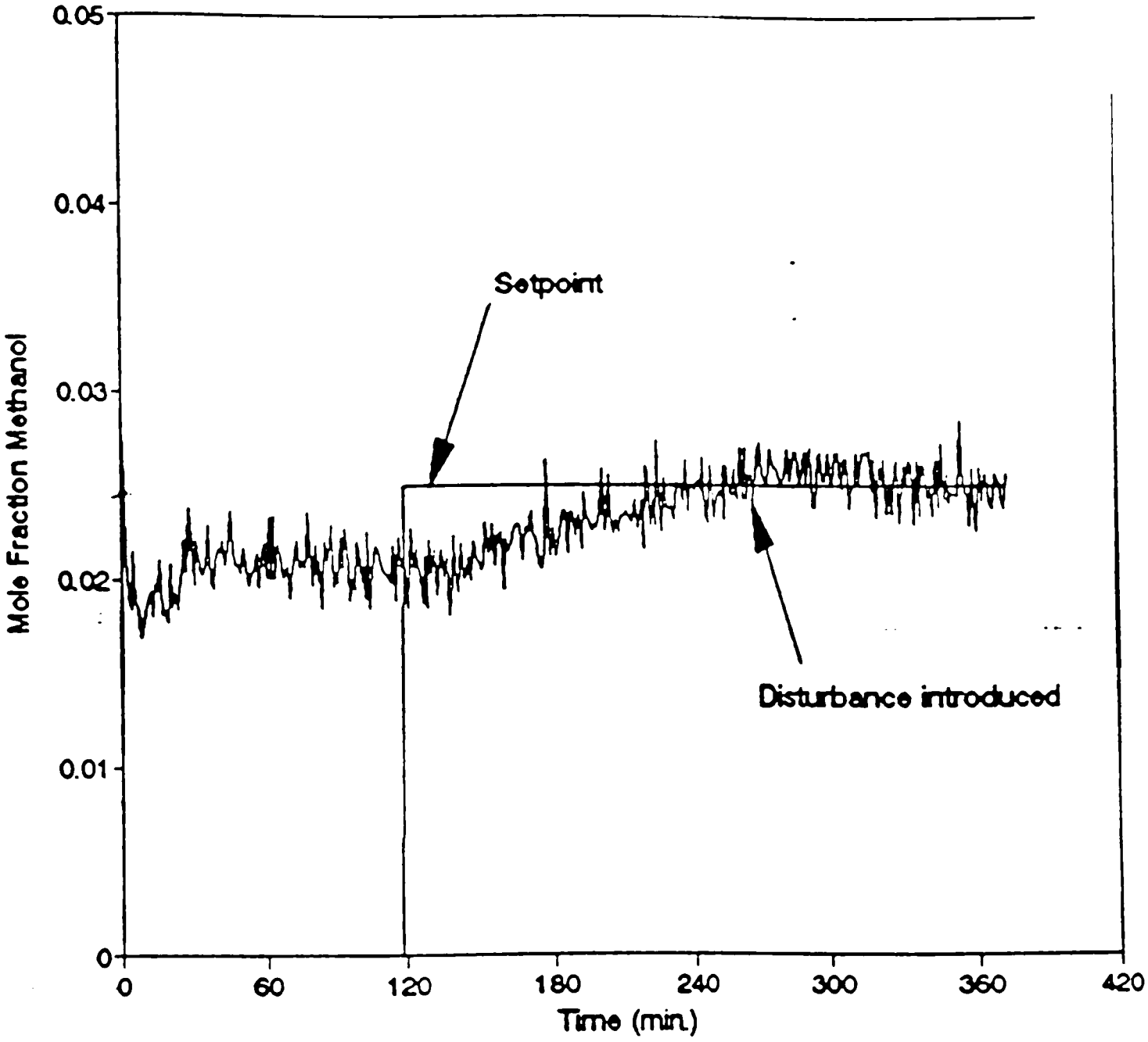

Disturbance Rejection : Bottom Composition
Feed Composition (30-20%) disturbance

Figure A.9. (b) (Contd.).

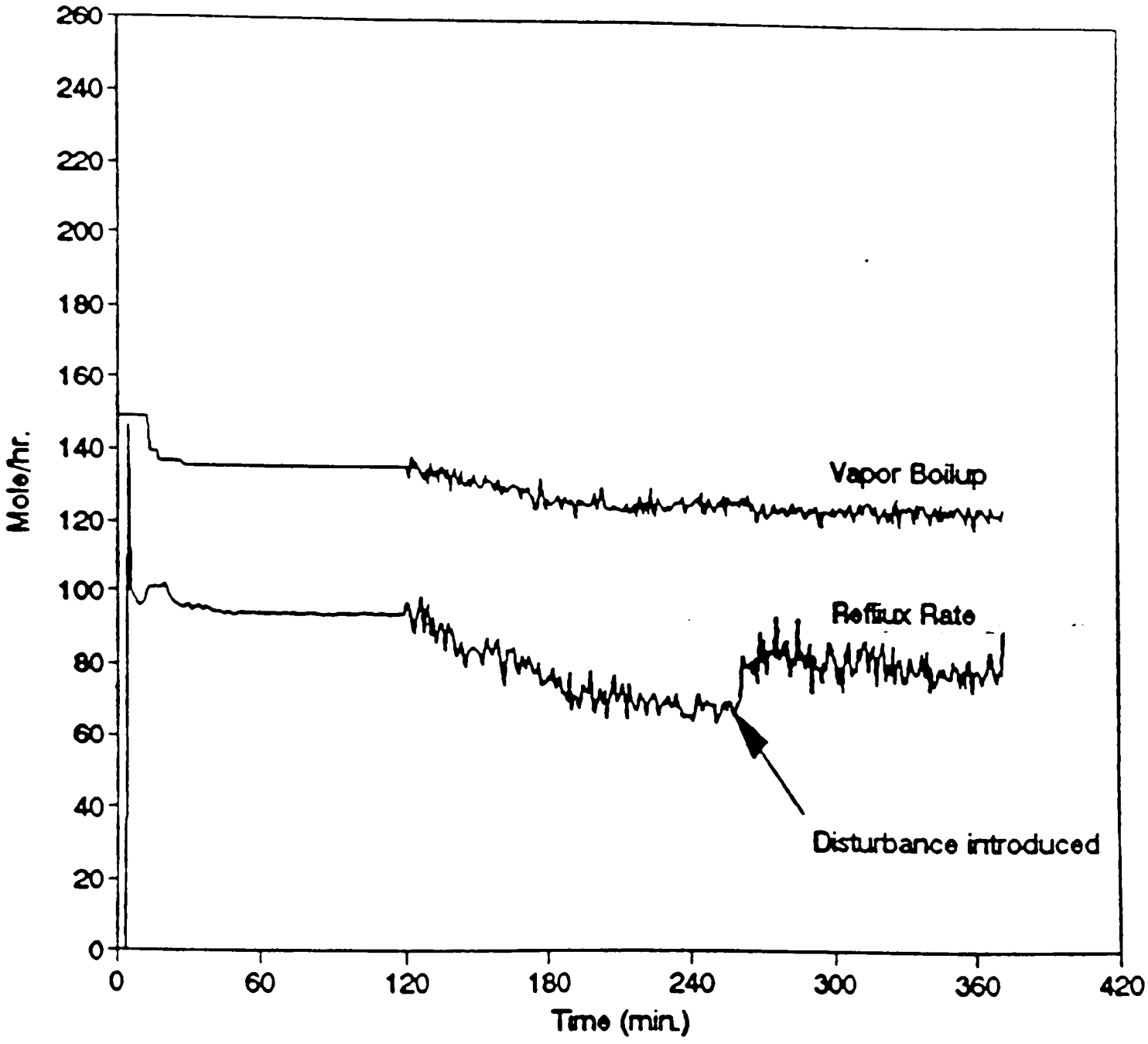

Disturbance Rejection : Manipulated Variables
Feed Composition (30-20%) disturbance

Figure A.9. (c) (Contd.).

APPENDIX B

INSTRUMENT CALIBRATION AND PROPERTY CORRELATION

B1. Reboiler Power Characteristic

The power characteristic of the reboiler is shown in Figure B.1. The following equation represents the fitted curve.

$$PW = 113.9336 - 16.4181(p) + 1.7196(p)^2 - 0.02218(p)^3 + 8.69e\text{-}5(p)^4 \qquad (B.1)$$

where PW is the power produced by the heater (watts) corresponds the percentage (p) of the full capacity.

The manipulated variable of the reboiler heater, calculated in count (as accepted by the KDAC system) can be correlated to the percentage (p) of the full capacity by the following equation.

$$\text{Boilup count} = 1300 + 16.0(p) \qquad (B.2)$$

B2. Enthalpy Correlation

The neural network model produces outputs for the vapor boilup in the units of lbmoles/hr. The theoretical heat required to generate the vapor boilup of the mixture can be correlated to the temperature by the following enthalpy equation (Chu et al., 1950).

$$\text{Methanol: } \lambda = 12681.53\left(1 - \left(\frac{T}{512.6}\right)\right)^{0.38}. \qquad (B.3)$$

$$\text{Water: } \lambda = 13469.36\left(1 - \left(\frac{T}{647.3}\right)\right)^{0.38}. \qquad (B.4)$$

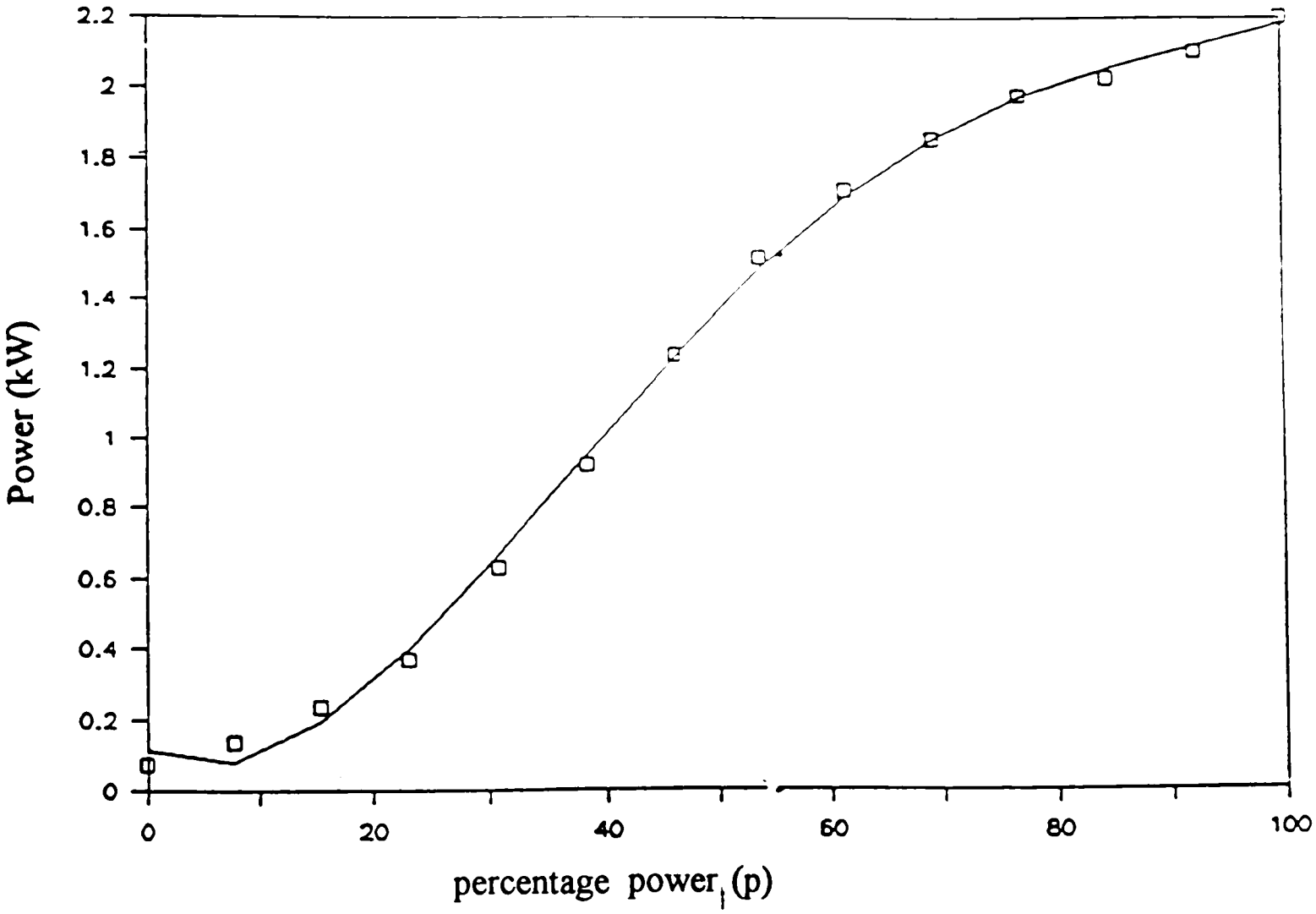

Figure B.1. Reboiler power characteristic.

where λ is the enthalpy in calories/gmole and T is the reboiler temperature (converted in degree kelvin) measured by KDAC system.

The enthalpy of the mixture, λ_{mix}, can be correlated to the pure component enthalpies by the following equation.

$$\lambda_{mix} = (\lambda.x)_{CH_3oH} + (\lambda.x)_{H_2o} \qquad (B.5)$$

where x is the stream composition.

A reverse relationship of Equation B.1 is used to calculate the required percentage power (%) from the amount of heat (converting calories to watts, PW) required to generate the vapor. The equation is shown below and a graphical comparison with equation B.1 is presented in Figure B.2.

$$(p) = 50.0 - 15.4663 * \log[\frac{3608}{(PW + 62.41)} - 1.569] \qquad (B.6)$$

B3. Reflux Pump Calibration

Reflux pump flowrate (with the piston gauge at 50%) is calibrated with the input signals (counts) in the operating region. Figure B.3 shows the result. A linear equation is found to produce a good fit and shown as below

$$\text{reflux flow (ml/min)} = (\text{reflux count} - 1049.3992)/12.6426 \qquad (B.7)$$

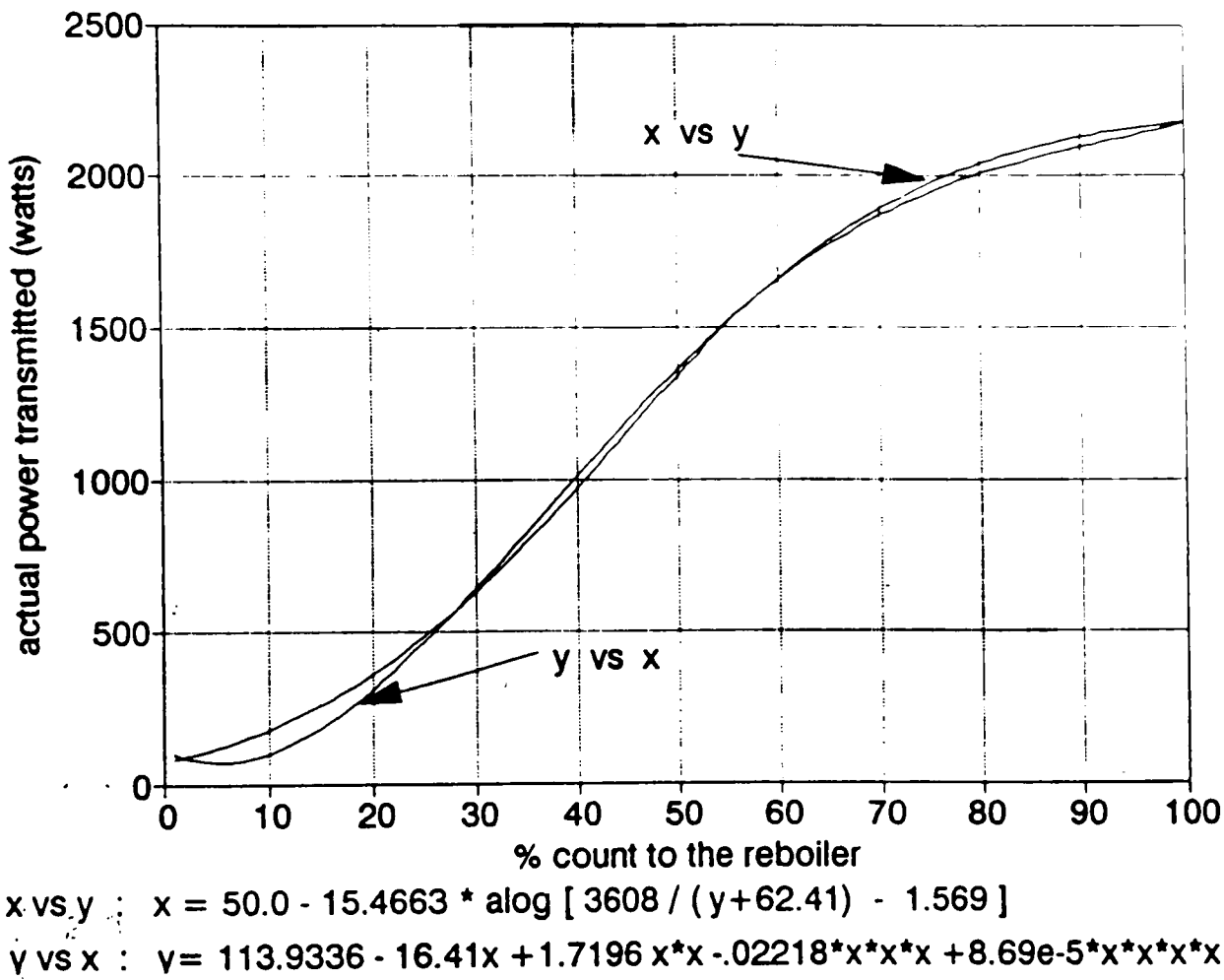

Figure B.2. Reverse power relationship.

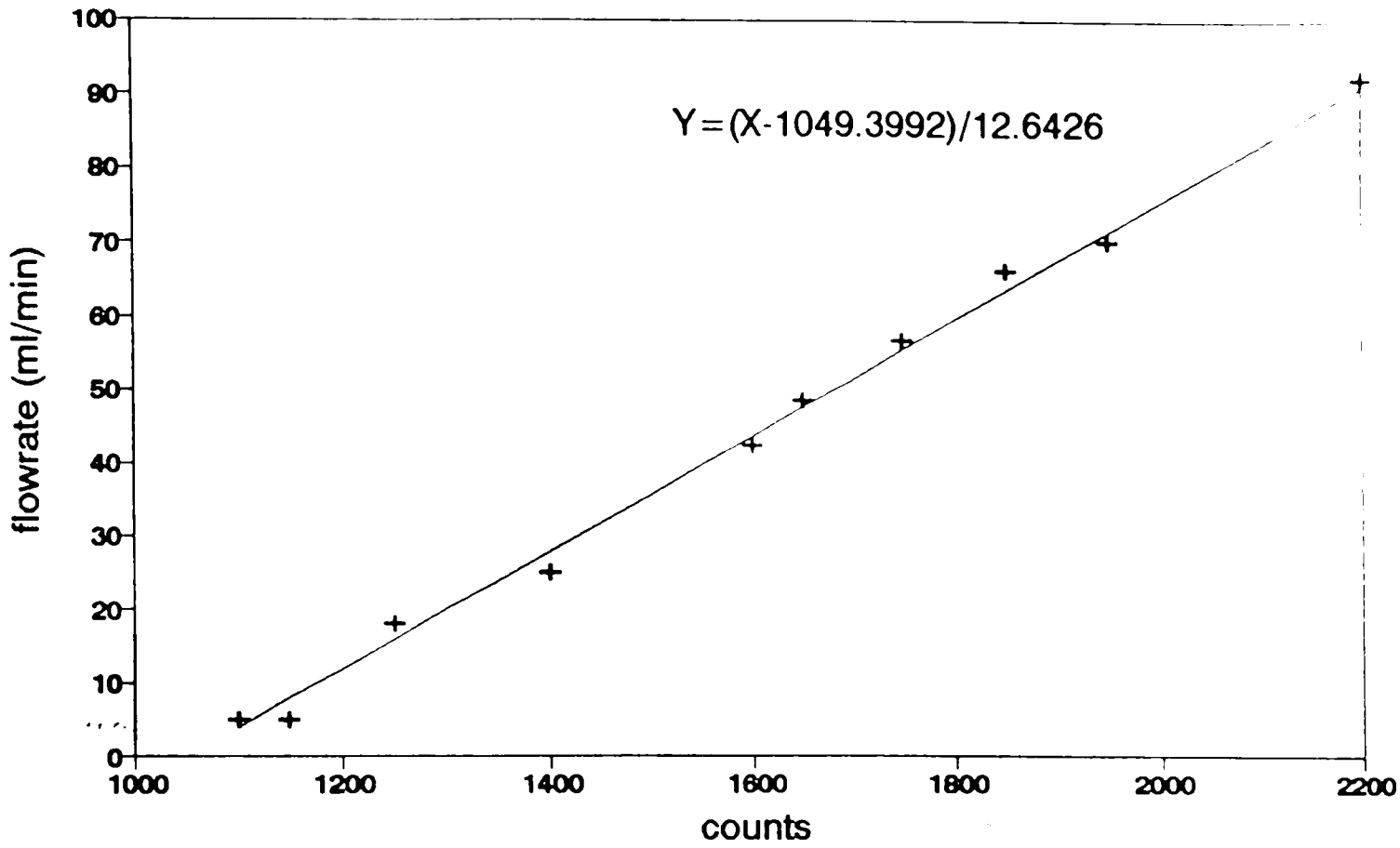

Figure B.3. Reflux pump calibration.

B4. Feed Pump Calibration

The feed pump is also calibrated in a similar way to reflux pump, and the fitted equation is shown below. Figure B.4 shows the linear fit.

feed flow (ml/min) = (feed count - 1034.728)/13.03244 (B.8)

B5. Composition Calibrations

The methanol-water equilibrium data obtained from literature (Henley and Seader, 1981) is fitted with polynomial of degree one and two for the top and bottom compositions. The temperature is assumed to be a good indicator of the composition because of the binary nature of the mixture and atmospheric pressure operation. In Lubbock, at 3200 ft above sea-level, the nominal atmospheric pressure is 13.9 psia (91 Kpa). The following empirical correlation is used to infer top and bottom compositions from the temperatures.

$$y = 2.66775 - 0.025919^{*} (T) \quad (B.9)$$

$$x = 3.814004 - 0.72428^{*}(T) + 0.000343^{*}(T)^{*}(T) \quad (B.10)$$

where T is the temperature in degrees Kelvin, y and x are the top and bottom compositions (mole fraction of methanol).

The compositions inferred from the temperature can also be tested off-line by using a refractometer available in the lab. A calibration of refractive index versus compositions is carried out and shown in Figure B.5.

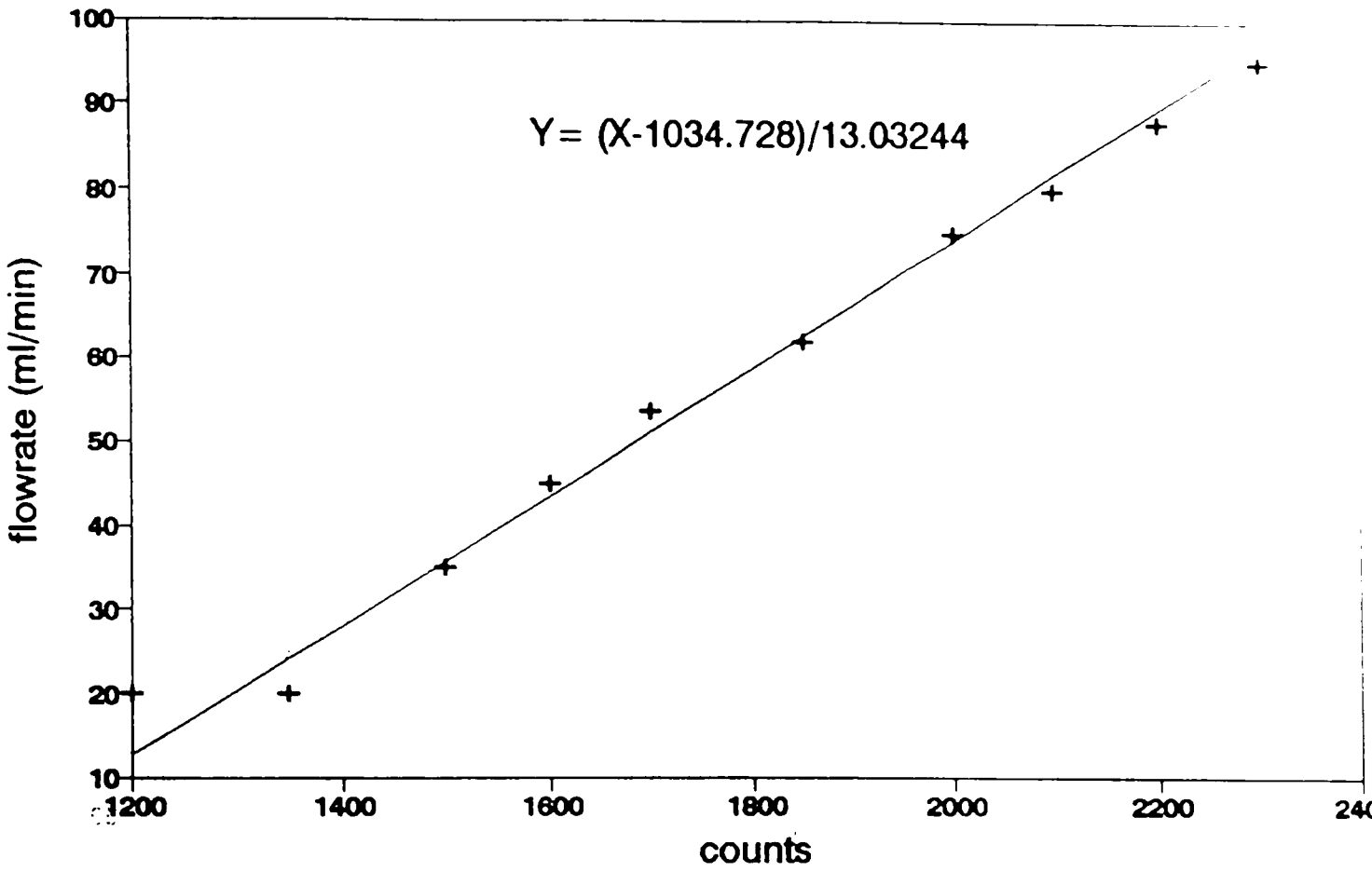

Figure B.4. Feed pump calibration.

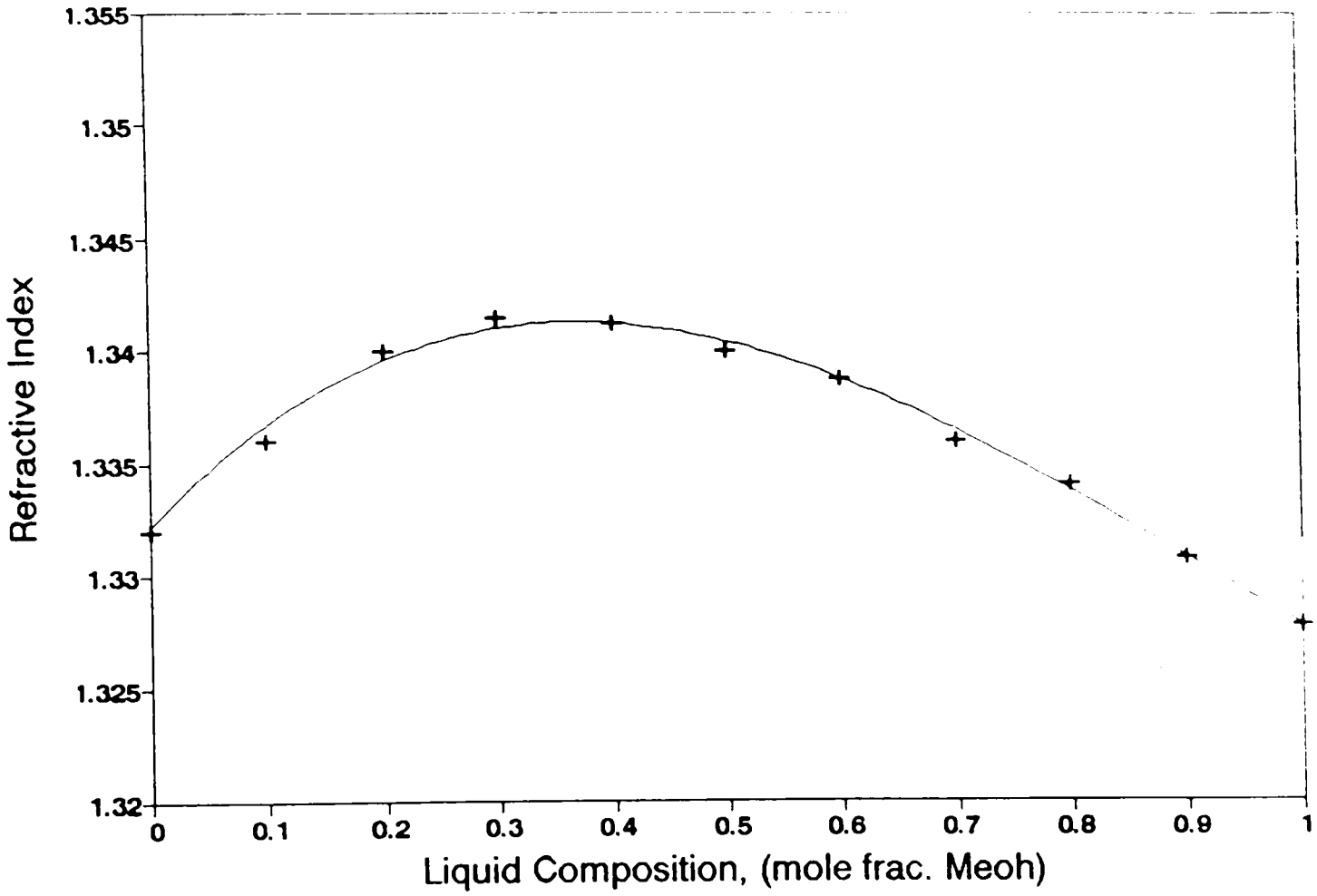

Figure B.5. Refractive index versus liquid composition (methanol-water mixture).

B6. Distillate and Bottom product flowrate

The Distillate flowrate is measured on-line using a differential transmitter. The following calibration equation shows a relationship between the count measured by the KDAC system and the flowrate in ml/min. Figure B.6 shows the linear fit.

flowrate = 0.035858 (count) - 83.7922 (B.11)

The bottom product flowrate is calibrated similarly, and the following equation is used. Figure B.7 shows the linear least square fit.

flowrate = 0.027854 (count) - 26.7254 (B.12)

The values of reflux flowrate, reboiler heat input, setpoint etc. can be keyed in directly and all the inputs and outputs are exhibited on the console. Figure B.8 shows a typical setup of the screen.

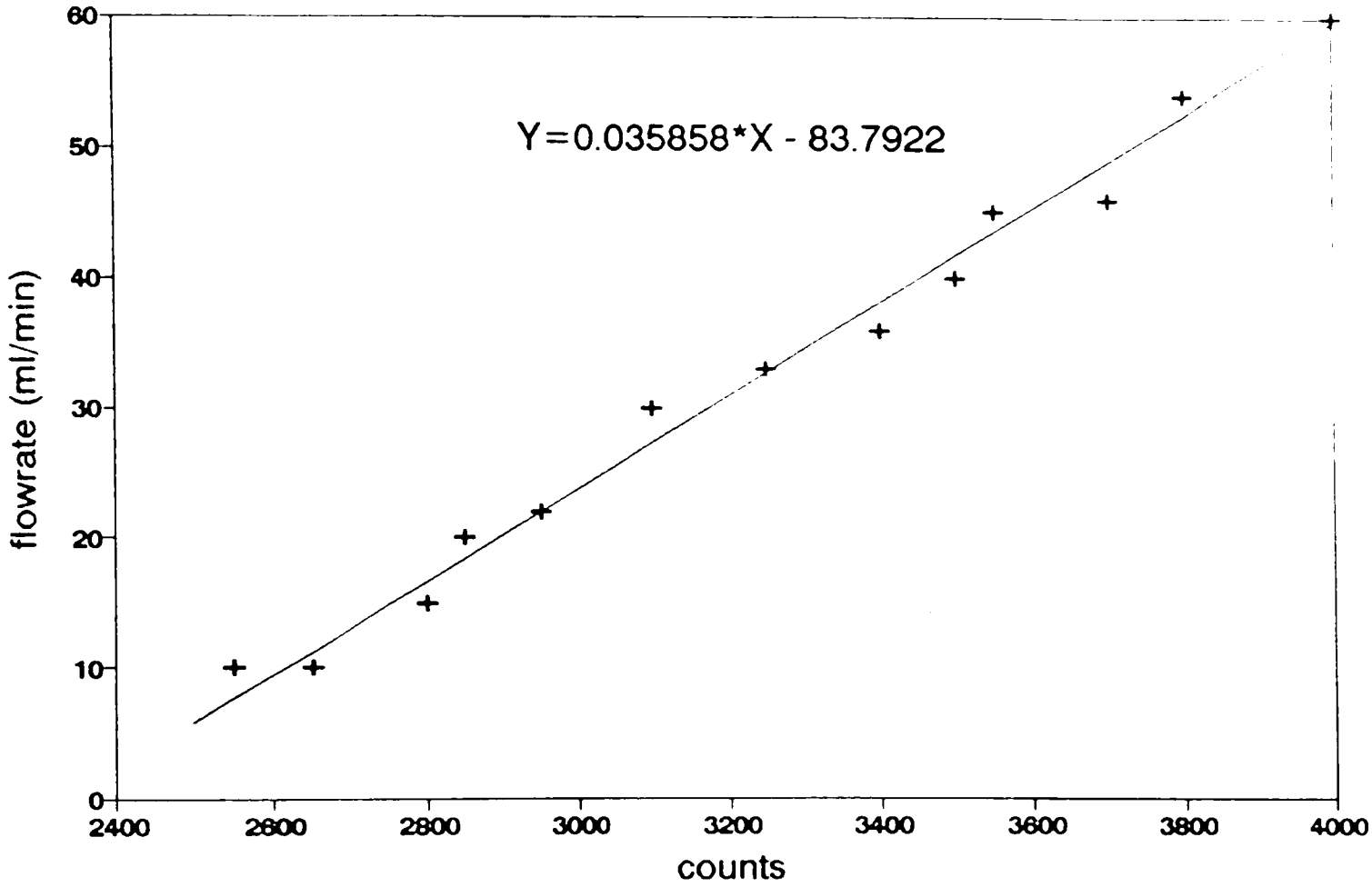

Figure B.6. Distillate flowrate calibration.

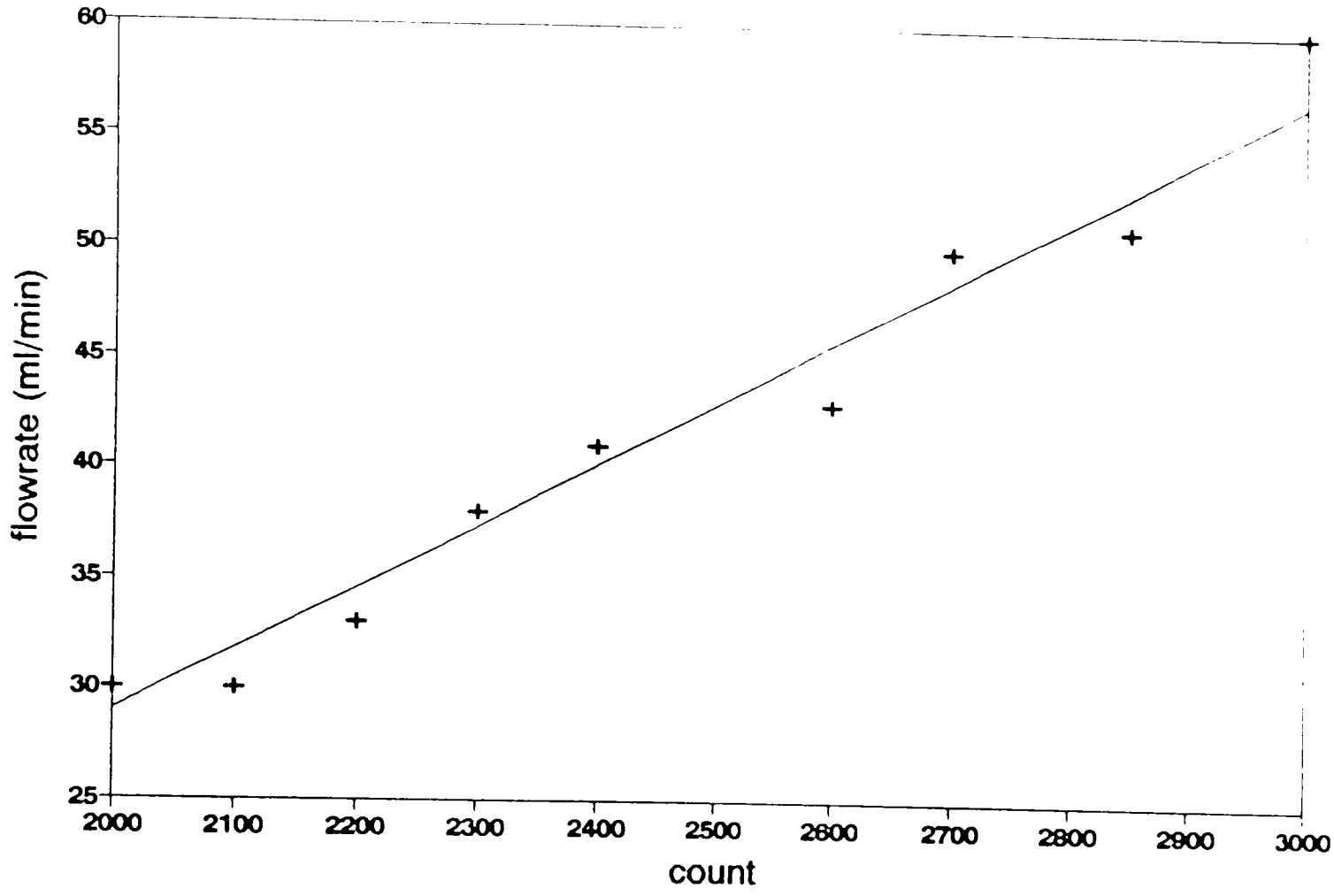

Figure B.7. Bottom flowrate calibration.

Started at 17:27:45 Current time 17:30:44 reading # 3

Temperatures F		Std dev	Controller	Setpoint	Value	
TRAY 1	198	0.2443	FEED PUMP	79.	79.00	ml/min
TRAY 2	186	1.5650	TOP COMPOSN...	0.9300	0.8642	mol fr
TRAY 3	176	0.4249	BOT COMPOSN...	0.0200	0.0353	mol fr
TRAY 4	158	0.6609	REFLUX HEAT ..	120.0	75.	temp,F
TRAY 5	158	0.6202	FEED HEAT	120.0	74.	temp,F
TRAY 6	157	1.2505	COOLING WATER.	0.875	1.64	gal/min
Water Out ...	66	0.62	TOP CONT MODE.	2.0		1=a,2=m
Water in	59	0.45	TOP CONT OUTPT	60.0000	157.9	ml/min
Cond.	100	1.38	TOP CONT GAIN.	180.0	2.0	
Feed	74	0.28	TOP CONT RESET	%2100.0	%2100.0	
Reflux	74	0.39	BOT CONT MODE.	2.0		1=a,2=m
Reboiler	201	0.4036	BOT CONT OUTPT	100.0000	198.0	%
Feed Compsn..	0		BOT CONT GAIN.	700.0	1.0	
FFWD Off			BOT CONT RESET	%2400.0	%2400.0	
D/P Cells - pressure or flow rate			Still heater.		100.00	%
Div. liquid level	6.8 in.		Dist. flow rate ..		41.7	ml/min
Boiler press.	0.0 in of H2O		cooling water rate		1.64	gal/min
Plate 6 press. ...	0.0 in of H2O		bottoms flow rate		0.0	ml/min
Divider press. ...	3.8 in of H2O		Reflux flow rate		60.00	ml/min

Figure B.8. Screen setup.

APPENDIX C

SOFTWARE

The following software is available with Dr. Russell Rhinehart, Professor in Chemical Engineering Department.

1. Neural Network Training Program (Marquardt-Levenberg Optimization),
2. Heuristic Random Optimization,
3. Simulator with Optimizer (Unconstrained and Constrained),
4. KDAC control program using NN inverse of a state prediction,
5. KDAC control program using NN gain prediction with HRO.